Diss ETH No. 9065

# BEDLOAD TRANSPORT CAPACITY OF SLURRY FLOWS AT STEEP SLOPES

A dissertation submitted to the

SWISS FEDERAL INSTITUTE OF TECHNOLOGY ZURICH

for the degree of

**Doctor of Technical Sciences**

presented by

**Dieter Rickenmann**

**Dipl. Bauing. ETH**

**born October 11, 1958**

**citizen of Zumikon (ZH)**
**and Horben (TG)**

accepted on the recommendation of

**Prof. Dr. D. Vischer, examiner**

**Prof. Dr. T. Dracos, co-examiner**

**Dr. M. Jäggi, co-examiner**

1990

Leer - Vide - Empty

## Preface

This work was performed at the Laboratory of Hydraulics, Hydrology and Glaciology of the ETH Zürich. It forms part of a joint research project with the Swiss Federal Institute for Forest, Snow and Landscape Research (WSL). The study was financially supported by a research grant ("Schulratsmillion") of the Board of the Swiss Federal Institutes of Technology.

I would like to express my appreciation to the Director of the Laboratory, Prof. Dr. D. Vischer, for the support and encouragement and to Dr. M. Jäggi, head of the river engineering section, for the supervision and criticism of my work. I am grateful to Dr. T. Davies from New Zealand who helped setting up the project and reviewed parts of the manuscript. Thanks are also extended to J. Zeller from the WSL for his interest in the study.

Several people from the workshop helped operating the flume system; I acknowledge the effort of Rolf Wirz, Stefan Züst, Bruno Schmid and Gery Wanner. Thanks also go to Karl Salzmann and Andy Rohrer for the drawings and to Marc Lehmann for the revision of the english draft.

Finally I would like to mention the moral support that I received from my wife Regula during the work.

Dieter Rickenmann

Leer - Vide - Empty

CONTENTS

## Abstract

During a flood event in a steep torrent, sediment may be transported by relatively clear water, by a hyperconcentrated slurry or in the form of a (pulsing) debris flow. The objective of this study was to examine the effect of an increasing fluid density and viscosity on the bed load transport capacity of the flow.

A clay suspension was used to simulate the slurry consisting of water and fine particles. The suspension was recirculated in a steep flume; the maximum volume concentration of clay particles in the flow was 22%. The clay suspension showed a non-Newtonian rheologic behaviour; it was treated as a Bingham fluid. In one test series, the flow resistance of the clay suspension flows without any sediment transport was measured. By using an effective viscosity for the given flow conditions, the results could be successfully analysed with conventional Newtonian formulae. In a second test series, the equilibrium bed load transport rates of the clay suspension flows were determined for different flow conditions. With increasing fluid density, transport rates were observed to increase continuously, for the experimental conditions by as much as a factor of 3 as compared to the corresponding clear water flows. Viscosity effects were found to become important if the particle Reynolds number is smaller than about 10. Then the flow around the grains was laminar, and transport rates decreased again.

For the majority of the bed load transport tests, density effects were dominant and viscous effects were negligible. These experiments were analysed together with the steep flume data of Smart and Jäggi (1983). By adjusting the density factor, both data sets could be described by a bed load transport formula (based on the flow rate) similar to the one of Smart/Jäggi. By including also the comprehensive data set of Meyer-Peter and Müller (1948) in the analysis, it was shown that an alternative transport equation (based on the dimensionless shear stress) is of more general applicability; with this relationship, bed load transport rates can be predicted both for low and steep slope conditions.

At steeper slopes, the transported grains occupy a considerable part of the (mixture) flow depth, thus influencing the flow resistance analysis. Depending on the known or assumed parameters, two different calculation procedures are proposed to determine the unknown parameters of the flow of the grain-fluid mixture.

## Zusammenfassung

Im Verlaufe eines Hochwasserereignisses kann in einem Wildbach Geschiebe auf verschiedene Arten talwärts verfrachtet werden: Als Geschiebetrieb durch relativ klares Wasser, als murgangartiger Transport durch eine schlammartige Flüssigkeit sowie in Form eines Murgangs (mit einer Front). Ziel der vorliegenden Arbeit war es, den Einfluss von zunehmender Dichte und Zähigkeit der Flüssigkeit auf das Geschiebetransportvermögen zu untersuchen.

Mit einer Ton-Suspension wurde die schlammartige Flüssigkeit nachgebildet, die in Natur aus Wasser und Feinmaterial besteht. Die Suspension wurde in einer steilen Versuchsrinne rezirkuliert, mit einer maximalen Volumenkonzentration an Tonpartikeln von 22%. Die Ton-Suspension verhält sich wie eine nicht-Newton'sche Flüssigkeit; sie wurde als Bingham'sche Flüssigkeit behandelt. In einer ersten Versuchsserie wurde der Fliesswiderstand von tonhaltigen Abflüssen ohne Geschiebetransport gemessen. Eine Auswertung mit bekannten Newton'schen Formeln ist möglich, falls eine effektive Zähigkeit des Abflusses eingeführt wird. In einer zweiten Versuchsserie wurde die Geschiebetransportkapazität für veschiedene Abflussbedingungen der Ton-Suspension bestimmt. Es zeigte sich, dass die Transportraten mit steigender Flüssigkeitsdichte zunehmen. In den Versuchen betrug die Zunahme bis zu einem Faktor 3, im Vergleich zu den entsprechenden Reinwasserabflüssen. Ein Einfluss der Zähigkeit wurde für Versuche mit einer Korn-Reynolds-Zahl kleiner als etwa 10 festgestellt. In diesem Fall werden die Körner laminar umströmt, und die Transportraten nehmen wieder ab.

Für die Mehrheit der Geschiebetransportversuche waren die Dichteeffekte massgebend, während der Einfluss der Zähigkeitsänderung vernachlässigt werden konnte. Diese Versuche wurden zusammen mit denjenigen von Smart und Jäggi (1983) ausgewertet. Es resultierte eine Geschiebetransportformel (in Funktion des Abflusses) ähnlich der von Smart/Jäggi vorgeschlagenen, wobei der Dichtefaktor angepasst werden musste. In einem weiteren Auswertungsschritt wurden auch die umfangreichen Versuchsresultate von Meyer-Peter und Müller (1948) einbezogen. Dabei zeigte sich, dass eine Transportgleichung, die in Abhängigkeit der dimensionslosen Sohlenschubspannung formuliert wird, eine allgemeinere Gültigkeit aufweist; mit dieser Formel können Geschiebetransportraten sowohl für flache als auch für steile Gefälle berechnet werden.

Bei steileren Gefällen wird ein beträchtlicher Teil der (Gemisch-) Ablusstiefe von transportierten Körnern besetzt; dies muss bei der Bestimmung des Fliesswiderstandes berücksichtigt werden. Je nach Fragestellung werden zwei verschiedene Berechnungsverfahren vorgeschlagen, womit die unbekannten Abflussgrössen des Korn-Flüssigkeits-Gemisches bestimmt werden können.

**Résumé**

Lors d'une crue dans un torrent, le sédiment peut être transporté par de l'eau relativement claire, par un mélange eau-suspensions à très haute concentration ou encore sous forme d'une lave torrentielle (avec front de propagation). Le but de la présente étude était d'examiner l'influence d'un accroissement de la densité et de la viscosité du fluide sur la capacité de transport solide.

Le fluide d'aspect boueux, qui en nature est composé d'eau et de materiaux fins, a été simulé en laboratoire par une suspension argileuse. Cette suspension a été mise en circulation dans un canal à forte pente, la concentration maximale en volume des particules d'argile étant de 22%. La suspension argileuse présente les caractéristiques d'un fluide non-newtonien; elle a été traitée comme un fluide de Bingham. Dans une première série d'essais, la résistance à l'écoulement de la suspension argileuse a été mesurée, en l'absence de tout transport solide. Une analyse des résultats est possible sur la base des formules de Newton, si une viscosité effective de l'écoulement est introduite. Dans une deuxième série d'essais, la capacité de transport solide de la suspension argileuse a été déterminée pour différentes conditions d'écoulement. Il a été constaté que les quantités de sédiment transporté augmentent avec la densité du fluide. Dans les essais réalisés, cette augmentation a atteint un facteur 3 par rapport au transport solide observé en eau claire. Une influence significative de la viscosité n'est apparue que pour des nombres de Reynolds des particules (rapportés au diamètre du grain) inférieur à environ 10. L'écoulement autour des grains est alors laminaire et les quantités transportées décroissent à nouveau.

Pour la majorité des essais de transport solide, les effets dus à la densité se sont avérés déterminants, de telle sorte que l'influence de variations de la viscosité a été négligée. Ces essais ont été analysés en regard des essais de Smart et Jäggi (1983). Une formule de transport solide (en fonction de l'écoulement) semblable à celle de Smart et Jäggi a pu être proposée, après une adaptation du terme décrivant l'effet de densité. Une seconde analyse, incluant les nombreux résultats d'essai de Meyer-Peter et Müller (1948), a montré qu'une équation de transport, exprimée en fonction de la force d'entraînement adimensionelle, présentait un caractère plus général. A l'aide de cette relation, les quantités de sédiments transportés peuvent être calculées dans le cas d'un canal à faible ou à forte pente.

Aux fortes pentes, les grains du matériau transporté occupent une grande partie de la profondeur de l'écoulement (du mélange). Ce fait doit être pris en considération lors de la détermination de la résistance à l'écoulement. Selon la nature du problème à résoudre, deux processus de calcul différents permettant de déterminer les paramètres inconnus de l'écoulement du mélange fluide-matériau solide sont proposés.

**Riassunto**

Durante una piene in un torrente i sedimenti possono essere trasportati a valle in diverse maniere: come trasporto solido di fondo con l'acqua che resta relativamente limpida, come liquido fangoso, oppure come vera e propria colata di fango (con un fronte). Scopo del presente lavoro era di indagare l'influenza di una crescente densità e viscosità del liquido sulla capacità di trasporto solido.

Il liquido fangoso è stato riprodotto con una sospensione argillosa che in natura consiste di acqua e materiale fino. La sospensione, che raggiungeva una concentrazione volumetrica massima di argilla del 22%, veniva recircolata in un ripido canale. Tale sospensione si comporta come un liquido non newtoniano ed è stata trattata come un liquido definito secondo Bingham. In una prima serie di esperienze su modello si è misurata la resistenza idraulica della sospensione senza trasporto solido. L'analisi con le consuete formule secondo Newton è qui possibile se si tiene conto della viscosità effettiva del deflusso. In una seconda fase si è stabilita la capacità di trasporto solido per diverse condizioni di deflusso della sospensione. Si è potuto constatare come la capacità di trasporto aumenti con il crescere della densità del liquido che nelle esperienze raggiungeva un valore massimo di 3 volte superiore ad un corrispondente deflusso con acqua limpida. Una influenza della viscosità è stata riscontrata nelle esperienze dove il numero di Reynold della grana era minore di circa 10. In questo caso la corrente attorno ai grani è laminare e le quote di trasporto diminuiscono.

Per la maggior parte delle esperienze con trasporto solido gli effetti rilevanti erano dati dalla variazione delle densità, mentre l'influenza della variazione della viscosità era trascurabile. Queste esperienze sono state analizzate tenendo anche conto dei risultati delle precedenti ricerche svolte da Smart e Jäggi (1983). Il risultato è una formula che permette il calcolo del trasporto solido (in funzione del deflusso) simile a quella proposta da Smart e Jäggi, dove però il termine concernente la densità è stato adattato. In una fase successiva sono state considerate anche le ricerche più estese svolte da Meyer-Peter e Müller (1948), grazie alle quali si è potuto dimostrare che una formula per il calcolo del trasporto solido espressa in funzione della forza di trascinamento resa senza dimensioni può trovare applicazione generale indipendentemente dalla pendenza longitudinale.

Quando le pendenze longitudinali diventano ripide una porzione importante della profondità di deflusso viene occupata da grani comportando un cambiamento della resistenza idraulica. A seconda delle costellazioni richieste vengono proposti due diversi procedimenti con i quali è possibile stabilire le condizioni idrauliche di deflusso della miscela acqua-grani mancanti.

Photo 1: Example of clay suspension flow in the experimental flume (at slope of 5 %, flow rate of 10 L/s and 15 vol.% clay concentration). Note similarity to flow conditions in Photo 3.

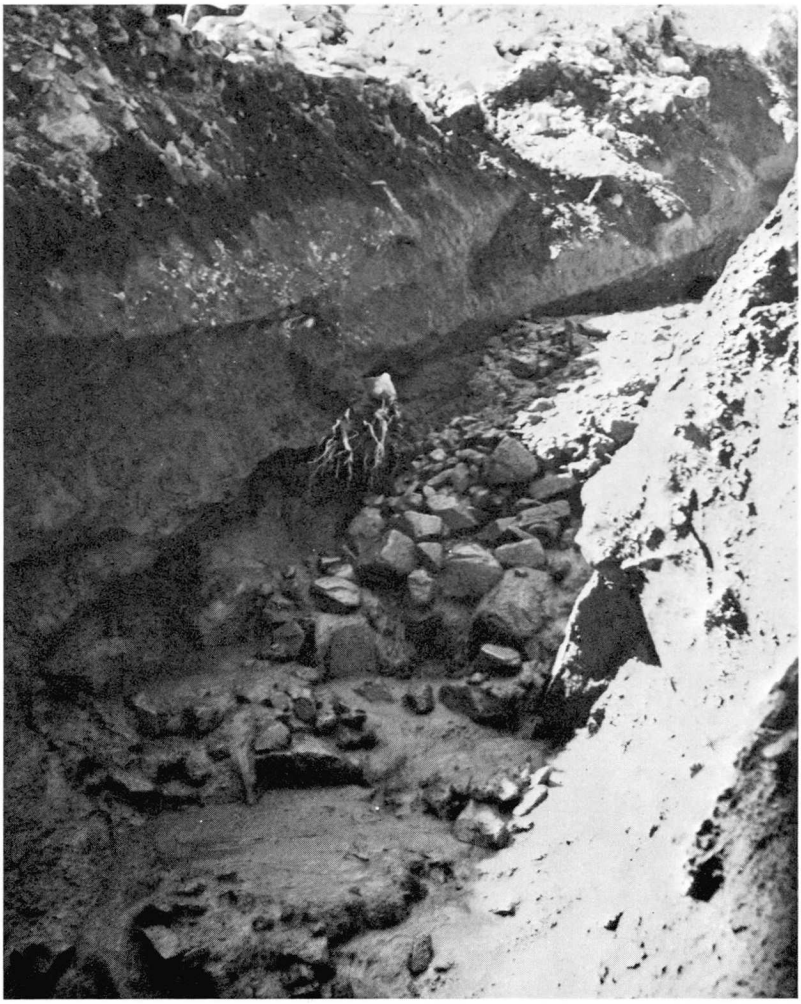

Photo 2: Front of debris wave moving down channel (about 3 m wide) at Wrightwood, California, 20 May 1969. There is fluid mud in the foreground, bouldery front in centre. (Photo reproduced from Johnson and Rodine, 1984, "Debris Flow", in Slope Instability [eds. D. Brunsen and D. Prior], reprinted by permission of Jon Wiley & Sons, Ltd.)

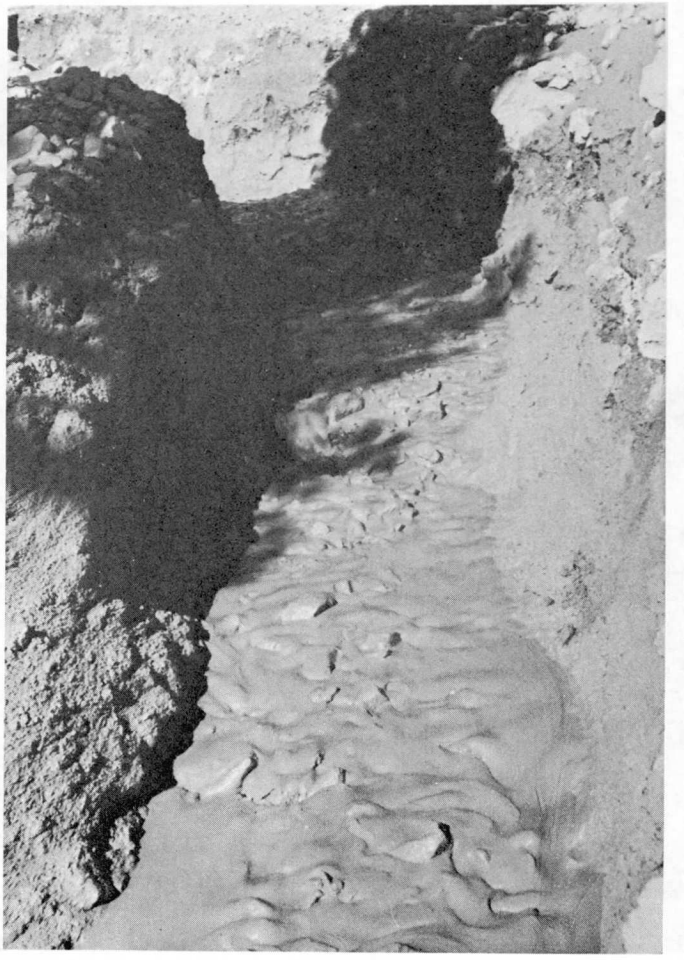

Photo 3: Steadily flowing debris about 10 m behind bouldery front shown in Photo 2. (Photo reproduced from Johnson and Rodine, 1984, "Debris Flow", in Slope Instability [eds. D. Brunsen and D. Prior], reprinted by permission of Jon Wiley & Sons, Ltd.) This situation represents similar flow conditions as simulated in the laboratory experiments.

# 1 INTRODUCTION

## 1.1 The term "debris flow"

Johnson's (1970) definition of a debris flow as a "gravity induced mass movement intermediate between landslide and waterflooding, with mechanical characteristics different from either of these processes" may be characteristic for the state of knowledge in this field. In a positive formulation, one could state that a "debris flow is the downslope movement of granular solids dispersed in a clay-water fluid and is known to be a significant sediment-transport process on land" (Hampton, 1975).

Other terms used for the same or a similar phenomenon include: mud(-rock)-flow, mud slide, earth flow, lahar, debris slide, debris avalanche, debris torrent, alpine mudflow and mountain debris flow. To some extent their use depends on the physical characteristics of a particular flow but sometimes they are also used synonynomously. Often the term "mudflow" refers more to flows containing mainly fine-grained earth material. A comprehensive collection of "mudflow" definitions is given in Naik (1983).

VanDine (1984) defined a debris torrent as "a mass movement that involves water-charged, predominantly coarse-grained inorganic and organic material flowing rapidly down a steep, confined, pre-existing channel" and suggested that this term should be preferred since "debris flow" can also refer to laterally unconfined flows.

Besides the fact that the mechanics of a debris flow are still poorly understood the variety of terms used for more or less the same phenomenon illustrates that there is also no generally accepted terminology and classification. It seems, however, that the term "debris flow" has been mostly used in the literature to refer to the phenomenon characterised by the above definitions and that it is probably the most widely accepted common expression.

## 1.2 Characteristics of debris flows

Probably the first comprehensive work on the topic dates back to 1910 when the Austrian engineer Stiny compiled a book entitled "Die Muren", which refers mainly to debris flows in the Alps. Excellent descriptions of the conditions of occurence, the flow characteristics, the physical properties and geomorphological aspects of debris flows are given in Costa (1984), Johnson and Rodine (1984), and Innes (1984). These reports also contain extensive literature reviews and present a good introduction into the subject.

Debris flows are often associated with heavy rainfall, saturated slopes, availability of loose material, steep channels and potentially disastrous effects in the fan area. As compared to "ordinary" floods in steep channels the flow behaviour and the physical properties of debris flows are distinctly different. While floods with minor sediment concentrations are in most cases treated as stationary and uniform flows, it is often observed that the front of a debris flow consists of a wave-shaped front part containing a lot of coarse boulders, possibly wood and comparativly little water while the preceding flow is more fluidic and less deep. It is also possible that a series of additional pulses follow the initial surge wave. Debris flow data suggests that such flows usually start at slopes steeper than 27% and that deposition occurs at valley or fan slopes steeper than 5% (Takahashi, 1981).

The flow depth of the front or a pulse can be up to 10 or 15 m, and the corresponding velocities are often in the range between 5 and 15 m/s. The bulk density of the mixture is usually larger than 1.4 $T/m^3$ and can reach values of about 2.4 $T/m^3$, which is possible due to the generally very wide grain size distribution of the transported sediment. Such a dense mixture can have viscosities several orders of magnitude higher than that of pure water. Viscometric measurements of debris flow materials show a non-Newtonian rheologic behaviour. It is not surprising, therefore, that debris flows are often observed to flow laminarly and that they have been said to show a similar flow behaviour to wet concrete.

## 1.3 The transition between "ordinary" floods and debris flows; Classification schemes

A rather comprehensive classification scheme considering various aspects of debris flows has been proposed by Kurdin (1973). According to this scheme the four following criteria are used: Nature of debris flow formation (mechanism of water and solids supply), rheological and flow characteristics, composition (relative proportion of water, fine and coarse material) and size of a debris flow event (eroded volumes, destructiveness). With regard to the flow behaviour the second and third items are mainly important. A similar classification is applied in China (Du et al., 1986).

Beverage and Culbertson (1964) made one of the first attempts to distinguish between different debris flow types according to the concentration of solids in the flow and to determine these limiting conditions. Since then a number of researchers have introduced similar classifications. A summary of the most common classification schemes based on sediment concentration is given by Bradley (1986) and is reproduced in Table 1.1. As is evident from the table there is not only some disagreement on the appropriate terms to be used but also on the delineation of the different flow types. According to O'Brien and Julien (1984) the maximum packing density of non-uniform silts, sands and gravels ranges from 67 to 88 percent by volume. This upper limit of approximately 90 percent solids by volume corresponds to a maximum mixture density of about 2.4 $T/m^3$.

Thus it seems that the use of the sediment concentration alone is not sufficient for a proper classification of different flow types. Pierson and Costa (1984, as indicated by Bradley, 1986) distinguish between streamflow and slurry flow according to whether the flow is Newtonian or non-Newtonian, and between slurry flow and granular flow, the limit beeing a function of particle size and gradation. According to Davies (1986, 1988), who reviewed numerous debris flow descriptions, basically three different types can be distinguished: Low density, steadily moving turbulent flows, carrying coarse particles as bed load only, the fluid consisting of a slurry of fine material (type 1); high density, laminar flows, coarse and fine particles being distributed uniformly over the depth, of unsteady nature with several pulses (type 2) or with only a

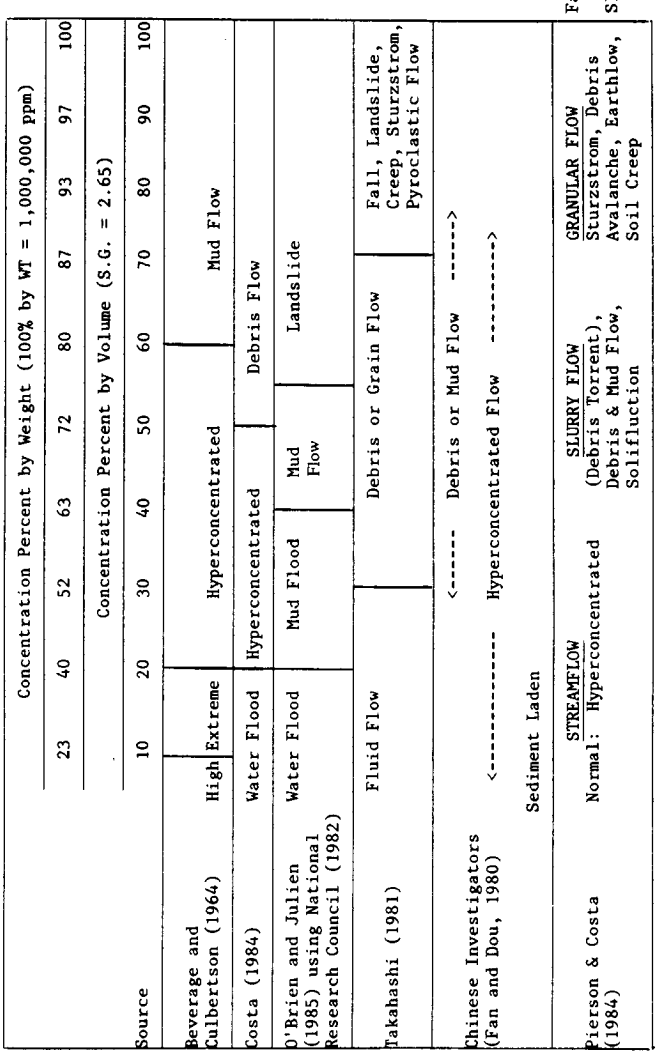


Table 1.1 : Classification of flows with high sediment concentrations, after Bradley (1986a).

single pulse (type 3). His classification scheme is reproduced in Table 1.2. The last two types have a higher viscosity than the first one, and a selective deposition of the coarser particles does not seem possible; because of greater flow depths and velocities their destructive power is considerable. As limiting density to distinguish between the steady and the unsteady type debris flow Davies proposed a density of about 1.6 to 1.8 T/m$^3$, which corresponds to a solids volume concentration of approximately 36 to 49%. He pointed out, however, that the transition seems to be rather abrupt if a particular flow changes from one type to the other. This abrupt transition is also reflected in deposits of either a "water flood" or a debris flow (Costa, 1984).

| Flow Type / Characteristic | 1 | 2 | 3 |
|---|---|---|---|
| Flow | Steady | Pulsing | Single pulse |
| Appearance | Turbulent | Laminar | Laminar |
| Sizes present above bed | Fine | Fine + coarse | Coarse + fine |
| Coarse load | At bed | Throughout depth | Throughout depth |
| Density | $\leq$ 1.6 T/m$^3$ | $\geq$ 1.8 T/m$^3$ | $\geq$ 1.8 T/m$^3$ |
| Viscosity | $\approx$10-100 x water | $\geq$1000 x water | $\geq$1000 x water |
| Velocity | Low; $\approx$ 2 m/s | High; $\approx$ 3-5m/s | High |
| Effect on bed | Depositional | Very erosive | Very erosive |

Table 1.2 : Debris flow characteristics, after Davies (1988).

Chinese researchers (Du et al., 1986) use a similar classification based on fluid and kinematic properties. They make a distinction between low-viscous and viscous debris flows. Their transition region lies in the density range of 1.8 to 2.0 T/m$^3$, and it is associated with rapidly increasing viscosity parameters in this range. Possibly due to the fact that Chinese debris flows consist mainly of fine material, their limiting values are higher than Davies' (1988) values. A similar separation into rapid turbulent and quasilaminar (structural) mud-streams is also proposed by Soviet researchers (Syanozhetsky et al., 1973).

In Japan Takahashi's debris flow models are widely accepted. Mainly based on flow characteristics and composition, Takahashi (1987) suggested a fourfold subdivision of the general term debris or mud flow: Stony debris flows only have a minor content of water and of fine material. Muddy debris flows or turbulent mudflows consist predominantly of smaller particles, and large scale turbulence is present due to randomly moving clusters of particles. A third case is a mixture of a stony debris flow in the near-bed layers with a turbulent mud flow prevailing in the upper layers. In an immature debris flow particles move basically as an intense bed load while the upper layer contains only very few grains.

## 1.4 Objective of the study

Debris flows primarily occur on steep slopes and can obviously have an enormous erosive power and transport capacity. In the past, studies on sediment transport in rivers and flumes were limited to bedslopes up to a few percent. It is only recently that interest on sediment transport processes in steep channels has grown. However, it is very difficult to measure sediment transport rates in torrents in the field, and only a few experimental studies have been carried out in steep flumes. Such studies, including flume slopes in excess of 10%, were performed by Mizuyama (1977), Mizuyama and Shimohigashi (1985), and Smart and Jaeggi (1983).

The transporting fluid used in these flume tests was clear water. It is likely that in torrents, already under "ordinary" flood conditions, considerable amounts of fine material are transported in suspension if the geology and the flood history allow so. However, it is difficult to predict how the increasing density and viscosity of the fluid influence the flow behaviour and the sediment transport rates if the flow changes from an "ordinary" flood to a low density debris flow (type 1 of Davies' classification). Therefore it was decided to carry out a series of steep flume tests using a clay suspension to represent the fine slurry of a debris flow, and to measure the flow resistance and the sediment transport capacity for various clay concentrations. Since the experiments of Smart and Jaeggi (1983) were performed at the same hydraulic laboratory they could serve as a reference condition for the clear water case.

Based on the various proposed classification schemes it can be concluded that the transition from the steady (type 1) to the unsteady (type 2 or 3) debris flow should occur at a mixture density in the range of 1.6 to 2.0 $T/m^3$, probably depending also on flow conditions. Calculated bed load concentrations (by volume) for the Smart/Jaeggi tests are as high as 33% for the same gravel material as was to be used in the new experiments. In preliminary tests clay suspensions with (volume) concentrations up to 20% and more were successfully recirculated in a small flume. From this information it could be estimated that bulk densities in the critical transition range should be reached with the planned experimental arrangement. Thus it seemed possible that unsteady flow would develop as a result of a natural flow instability in this critical density range.

To study the flow behaviour of debris flow surges an experimental investigation was performed by Davies (1988) at the same hydraulic laboratory using a conveyor belt flume where the bed moves upstream and the - in reality unsteady - front remains stationary with respect to the side walls and the observer.

In this study, the term "debris flow" is restricted to the unsteady, pulsing flows (type 2 and 3 of Davies' (1988) classification), while the steady flows (type 1) are referred to as slurry flows or hyperconcentrated flows with sediment transport.

Photo 2 (p. 13) shows a typical front of a debris flow. The flow conditions examined in the present study are illustrated by Photos 1 (p. 12) and 3 (p. 14).

# 2 LITERATURE REVIEW

## 2.1 Approaches to explain the mechanics of debris flows

### 2.1.1 General remarks

There are many countries that have to face problems due to the occurence of debris flows which can impose a constant threat to certain regions. Debris flows have long been known in mountainous regions in the Alps, in the Soviet Union, in Japan, in the Rocky Mountain areas of North America and in other places of the world.

Research on debris flows and related problems started in the 1960-ties, especially in Japan and in the United States. It began probably around the same period in China although many of their studies were only published in English towards 1980. Papers from Russian scientists appeared from time to time but it seems difficult to get a comprehensive picture of their research activities. In Austria it is primarily engineers that have been concerned with this topic, and their interest was mainly focussed on technical and practical aspects of planning countermeasures against debris flow events. Recently some Canadian researchers have also summarized approaches to determine the flow characteristics, with special regard to mitigation of debris flow hazard.

Topics of debris flow research cover various aspects such as: Mechanisms of formation and initiation; mechanics and rheological characteristics of motion, including fluid related and grain flow models; geologic analysis of deposits and determination of catchment characteristics and geomorphological aspects; and development of models for prediction of debris flow events and of (rough) rules for the design of torrent control projects.

A very concise review on the state of the art in modelling the motion of a debris flow was made by Iverson and Denlinger (1987). As a first approximation, the debris flow mass can be separated into a fluid matrix, consisting of water and the fine material, and the coarser particles. It is then assumed that the slurry with the fines behaves like a

pseudo-homogeneous fluid that carries along the coarse fraction. There are two main problems connected with this approach: Which is the limiting particle size that delinates the fine from the coarse particles, and what is the relative importance of grain-grain contacts and of fluid-grain interactions with respect to the total energy dissipation ?

In the past, two principally different debris flow theories have been developped. The viscoplastic model was applied independently by Yano and Daido (1965) and by Johnson (1965) to flows containing a lot of fine material in a viscous slurry, and is based on the approach by Bingham (1922) to describe a particular type of non-Newtonian flow. To treat the granular-type debris flows that consist mainly of coarser particles and only have little water, Takahashi (1978, 1980) proposed a set of equations based on the concept of dispersive grain stresses introduced by Bagnold (1954).

More recently attempts have been made to incorporate both fluid effects and grain-grain interactions in one single model (Ward and O'Brien, 1981; O'Brien and Julien, 1984; Chen, 1983,1986a,1988a,b). However, these theories have not yet been tested sufficiently with experimental data because it is very difficult also in the laboratory to examine the grain and fluid processes in detail.

### 2.1.2 **Fluid related models**

Suspensions of fine particles show a trend towards non-Newtonian rheological behaviour, the effect becoming more pronounced with increasing conentration. The fluid viscosity is no longer a constant but depends on the velocity gradient dv/dy (shear rate) in the flow. The rheological behaviour can be determined for example with a viscometer where the shear stress $\tau$ is measured as a function of the applied shear rate, for laminar flow conditions.

According to Brauer (1971), the most commonly used approaches to describe a non-Newtonian viscous fluid are the power law model of Ostwald and De Waele, the Prandtl-Eyring model and the Bingham model. The power law relation is given as:

$$\tau = A \left(\frac{dv}{dy}\right)^n \qquad (2.1)$$

where A is an empirical constant, v is the local fluid velocity, y is the coordinate perpendicular to the flow direction, and n an empirical constant called the fluid index. The Bingham model is written as:

$$\tau = \tau_B + \eta_B(\frac{dv}{dy}) \tag{2.2}$$

where $\tau_B$ is the Bingham (yield) stress and $\eta_B$ the Bingham viscosity. The apparent viscosity, being defined analogous to the viscosity of a Newtonian fluid, is given for a Bingham fluid as:

$$\eta_a = \frac{\tau_B}{dv/dy} + \eta_B \tag{2.3}$$

The reological behaviour of fluids that can be characterised with these approaches is depicted in Fig. 2.1. In the treatment of hyperconcetrated flows or of the viscous slurry of debris flows it is primarily the Bingham model and sometimes the power law relation that are commonly used. Debris flows have been modelled as Bingham fluids, dilatant fluids, or as viscoplastic fluids.

Viscous non-Newtonian fluids are usually divided into three categories: Pseudoplastic fluids, described by the power law model having an exponent $n<1$, and Bingham fluids both show a shear-thinning effect, which means that the viscosity decreases with increasing shear rate. Dilatant fluids, having an exponent $n>1$ in the power law model, on the other hand show a shear-thickening effect, the viscosity increasing with increasing applied shear. For $n=1$ the power law model is equal to the Newtonian relation, with K being equal to the Newtonian viscosity. It is interesting that both for power law fluids with $n<1$ and for Bingham fluids a certain minimum shear stress is required for the flow to start.

It should be noted that these models refer to ideal fluids. In reality many fluids show a behaviour that is described by more than only one model, depending on the shear range of interest. And even within a limited range of shear rates, the use of a particular model is often an approximation to the true rheologic behaviour.

Yano and Daido (1965) made rheological measurements and determined velocity profiles of a clay suspension of various concentrations flowing in an open channel. They showed that both the pseudoplastic and the

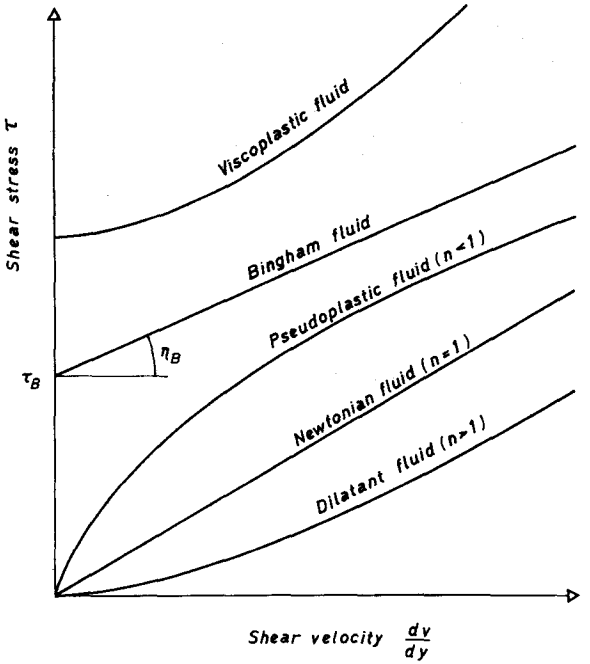


Fig. 2.1 : Rheological models for non-Newtonian viscous fluids.

Bingham model can be used to analyse the flow behaviour. D.G. Thomas (1963a) performed pipe flow experiments with different fine material suspensions including a kaoline slurry. In the analysis he compared various rheological models and concluded that the use of a more complex model than the Bingham approach is not justified. Johnson (1965), based on laboratory tests and observations of natural debris flows, proposed a modified Bingham model, the so called Coulomb-viscous model:

$$\tau = c' + p_n \tan\alpha_s + \eta_B\left(\frac{dv}{dy}\right) \qquad (2.4)$$

where c' is the cohesion, $p_n$ is the normal stress and $\alpha_s$ is the static angle of internal friction. In the case of dilute suspensions or if there are only smaller grain sizes present in the flow, the first two terms of equ. (2.4) may be replaced by a single shear strength parameter, becoming equal to the Bingham yield stress $\tau_B$. The Bingham model or a modified form thereof have been extensively used in the United

States (Johnson and Rodine, 1984; Naik, 1983) and in China (Cheng, 1986b) to explain many aspects of debris flows.

Since the Bingham model appeared adequate to describe the clay suspension used in the experimental work the rheology and the flow resistance of a Bingham fluid is treated in more detail in section 2.2 .

### 2.1.3 Grain flow models

In a fundamental work Bagnold (1954) studied the dynamics of grain dispersions. In his experiments he sheared neutrally buoyant wax spheres in a Newtonian fluid in an annular space between two concentric cylinders. By measuring the torque necessary to shear the grain dispersion, he could determine the solids shear stress T as a function of the applied shear rate for various grain concentrations. Since the flow depth normal to the shear plane was confined, the dilation of the moving grain mass caused a normal dispersive pressure P, which was also recorded. He found that this dispersive pressure P is proportional to the shear stress T acting between different grain layers. The proportionality factor can be termed dynamic friction angle $\alpha$, and the relation is written as:

$$T = P \tan\alpha \tag{2.5}$$

Depending on grain size, grain concentration, fluid viscosity and flow conditions, Bagnold (1954) distinguished two different flow regimes where $\alpha$ is approximately constant. If grain inertia dominates the flow behaviour $\tan\alpha$ was found to be about 0.75, and about 0.32 if the fluid viscosity is predominant. In the first case the resistive shear stress is mainly due to grain to grain contacts while in the second case it is primarily the interaction between the grains and the fluid that determines the flow behaviour. To separate the two flow regimes a dimensionless grain flow parameter G is given by Bagnold (1956) as:

$$G^2 = \frac{\sigma d^2 T}{\lambda \eta^2} \tag{2.6}$$

where $\sigma$ is the grain density, d the grain diameter, $\eta$ the dynamic fluid viscosity, and $\lambda$ the linear grain concentration which can be expressed

in terms of the solids volume concentration $C_s$ and the maximum possible packing concentration $C_*$ as:

$$\lambda = \frac{1}{(C_*/C_s)^{1/3}-1} \tag{2.7}$$

Grain shearing will be inertial if $G^2>1500$ and macroviscous if $G^2<100$; in the transition region both grain to grain and grain to fluid interactions are important. Bagnold (1954) showed that the dimensionless grain number G is analogous to the particle Reynolds number $Re^*$ defined as:

$$Re^* = \frac{d(T/\lambda\sigma)^{1/2}}{\eta/\sigma} \quad \text{for the inertial case} \tag{2.8}$$

and

$$Re^* = \frac{d(\tau/\rho)^{1/2}}{\eta/\rho} \quad \text{for the macroviscous case} \tag{2.9}$$

where $\rho$ is the fluid density. In terms of $Re^*$ the transition region lies between 55 and 10. For volume grain concentrations $C_s<57\%$ ($\lambda<12$) in his experiments, Bagnold (1954) determined two empirical relations to express the solid transmitted shear stress T:

$$T = a_i\sigma(\lambda d)^2(du/dy)^2\sin\alpha \quad \text{for the inertial case} \tag{2.10}$$

and

$$T = a_v\lambda^{3/2}(du/dy)\sin\alpha \quad \text{for the macroviscous case} \tag{2.11}$$

where $a_i$ and $a_v$ are empirical constants, u denotes the local grain velocity, and du/dy is the velocity gradient normal to the shear plane.

Bagnold (1956) noted that in his experiments for $\lambda < 22$ grain shearing became possible and then the dispersion behaved like a granular paste. He found that a residual shear stress at zero shear rate only existed for $\lambda > 14$. He termed this concentration value the "fluid" limit below which the grain dispersion would behave like a Newtonian fluid. For natural, reasonably rounded uniform bed material these $\lambda$-values correspond to volume concentrations of 57% and 52%. At the "fluid" limit ($\lambda$=14, $C_s$=52%) Bagnold found that the overall shear stress should be at least 100 times greater than the fluid shear due to viscous forces only. He could not determine the residual fluid shear stress due to turbulence (as modified by the presence of grains) but he stated that this effect

seems to become less and less important with increasing grain concentration.

Based on Bagnolds (1954) concept of dispersive pressure, Takahashi (1978) developed a set of equations to describe the flow of a concentrated grain-water mixture in a wide open channel. In his theoretical analysis he considered two different cases which he verified by experiments. In a steep flume he simulated the formation of a bore front by adding an abrupt water supply over a nearly saturated, erodible gravel bed. In one case the movement of the front asymptotically reached a quasi-steady state because the scouring depth of the bed remained limited. In the other case, at very steep flume slopes, he observed a progressive erosion of the bed and a continuous growth of the bore front, while the front velocity remained almost constant. Having determined the experimental constants, the grain concentration, the propagation velocity, and the mixture depth could be calculated by the theoretical relationships. For the given experimental conditions the formation of a quasi-steady state front which reaches an equilibrium grain concentration should theoretically occur in the slope range between 26% and 42%, while the bore front is supposed to continuously grow on slopes steeper than 42%.

Takahashi (1980) extended his analysis to describe the experimentally observed longitudinal profile of the snout for the quasy steady-state case where no bed erosion occurred beneath the snout. Additional tests with a non-uniform bed material showed a tendency for the velocity profile to become more uniform with the wider grain size distribution. He observed an accumulation of the coarser particles at the front which he attributed to the larger dispersive pressure associated with the coarser particles, driving them to the flow surface that moves faster than the lower layers.

For a stony type debris flow in the inertial regime where the momentum exchange is mainly due to grain contacts and the role of the interstitial fluid can be neglected, Takahashi (1978) obtained a relation for the vertical velocity distribution of a quasi-steadily moving front as:

$$u = \frac{2}{3d} \left(\frac{g \sin\beta}{a_i \sin\alpha} \left(C_s + (1-C_s)\frac{\rho}{\sigma}\right)\right)^{1/2} \left(\left(\frac{C_*}{C_s}\right)^{1/3} - 1\right) \left(h^{3/2} - (h-y)^{3/2}\right) \quad (2.12)$$

where $\beta$ is the slope angle, g the acceleration due to gravity, h the (mixture) flow depth and the vertical coordinate y is measured from the bed upwards. Takahashi (1987) later modified his approach to account for a nonuniform grain distribution over the depth. The velocity distribution calculated with this new model matches his experimental results better than his first model assuming a constant concentration, and it also agrees fairly well with experimental data of Tsubaki et al. (1982).

The effect of clay in the interstitial fluid is discussed by Takahashi (1980) to suggest that most debris flows are in Bagnold's inertial regime. He estimated the yield strength $\tau_B$ and the apparent viscosity by formulae taking into account size and concentration of the clay particles, and concluded that the effect of these parameters would be negligible in real debris flows. However, as shown below, the presence of silt and fine sand - in addition to the clay - in the fluid matrix can increase the apparent viscosity by several orders of magnitudes. In fact, Davies (1985, 1988) put forward the hypothesis that the unsteady, pulsing behaviour of debris flows is associated with the macroviscous and not the inertial flow regime.

According to Iverson and Denlinger (1987) the main deficiencies of Takahashi's theory are the neglection of dynamic effects of the interstitial fluid matrix and the assumption (in Takahashi's first model) that the solid particles are uniformly dispersed throughout the flow depth. They claim that this latter assumption leads to a mathematical overdeterminacy in that his theory basicly requires four equations having only three unknowns. Other restrictions are the assumption of an average grain size to represent an often very nonuniform material and the fact that a yield strength cannot be predicted by the dilatant fluid model (Naik, 1983). In spite of these limitations Takahashi's model has been applied in Japan with some success to treat granular type debris flows.

### 2.1.4 Other theories

Davies (1988) suggested that his type 1 flows (s. section 1.3) probably do not differ fundamentally from ordinary streamflow. Conventional flow resistance and sediment transport formulae may still apply although they might have to be modified to account for the changed density and

viscosity of the slurry. He expected that the single-pulse, unsteady (type 3) flows can be at least partly explained by Takahashi's (1978, 1980) theory.

Based on the analysis of existing debris flow descriptions Davies (1988) offered a new hypothesis concerning the occurrence of the multiple-pulse, unsteady (type 2) flows. He proposed that macroviscous flow (Bagnold's grain flow number $G^2$ being less than 100) is a necessary condition for the more or less uniform distribution of the coarser grains over the flow depth and for the onset of several pulses in large debris flow. According to Bagnold (1955) the increase of the shear stress in a macroviscous flow of high grain concentration leads to a decrease of the transport capacity of the flow. Since a selective deposition of larger grains is not possible in a macroviscous flow the decrease in the transport rate must be achieved by a decrease in the mean flow velocity. This, in turn, can bring about an instability of the flow, in that slower moving, deeper reaches begin to form and develop into surges. The initial increase in shear stress may be due to a change in flow depth, slope or grain concentration.

Assuming typical values for the slurry density, the flow depth, the grain size, the grain concentration, and the bed slope of a hypothetical debris flow, Davies (1988) calculated the necessary apparent viscosity $\eta_a$ of the slurry for macroviscous flow with equ. (2.6) to be about 5000 times that of water. In view of the measured rheological parameters of real debris flow slurries by Chinese researchers, this requirement does not seem to be unrealistic.

Ward and O'Brien (1981) also suggested that debris flows can occur in Bagnold's macroviscous, transitional or inertial regime, and simulated flows in the three regimes in flume experiments. To separate between the different regimes, they proposed to use the particle Reynolds number as defined by equs. (2.8) and (2.9), with limiting values as given by Bagnold. They presume that in actual debris flows mainly three types of resistive stresses are important. While in the macroviscous regime viscous stresses dominate and the flow appears to be laminar, turbulent and dispersive stresses should dominate in the inertial regime. Defining the turbulent shear stress according to Prandtl's mixing length concept, they expressed the total shear stress $\tau'$ in the inertial regime as:

$$\tau' = a_1 \sigma (\lambda d)^2 \sin\alpha (\frac{du}{dy})^2 + \rho (\kappa' y)^2 (\frac{dv}{dy})^2 \qquad (2.13)$$

where $\kappa'$ is the von Karman constant as modified by the presence of grains. Assuming that the particles and the fluid move with the same velocity, they integrated equ. (2.13) to obtain the vertical velocity distribution.

A similar approach was proposed by Takahashi (1987) to analyse his *muddy debris flows (or turbulent mud flows, s. section 1.3)*, but he suggested to use the mixture density instead of the fluid density in the turbulent shear stress term. A comparison between the obtained velocity distribution with equ. (2.12) and experimental data showed that the effects of turbulent mixing become more important for lower solids concentrations $C_s$ and higher relative depths h/d.

O'Brien and Julien (1984) stated that the energy dissipation in a debris flow is mainly caused by viscous, turbulent, dispersive and yield shear stresses. Their relative importance is a function of fluid and grain properties. To account for all these effects a general equation for the total shear stress is proposed as:

$$\tau' = \tau_B + \eta_B (\frac{dv}{dy}) + C_1 (\frac{du}{dy})^2 + \ldots \qquad (2.14)$$

where $C_1$ is a variable that depends on depth, concentration, sediment size and boundary roughness. The first and second term of equ. (2.14) contain yield and viscous stress and represent the Bingham model; the effect of turbulent and dispersive stresses are combined in the third term because they both depend on the shear gradient squared and because it is difficult to separate them in debris flows. By using a rotational viscometer O'Brien and Julien measured the rheological properties of the fluid matrix of actual debris flow deposits for various sediment concentrations, and determined values for $\tau_B$, $\eta_B$ and $C_1$. However, in conventional viscometers only sediment-water mixtures with relatively small grain sizes can be sheared, and thus dispersive stresses caused by coarser grains are not included in the analysis. As indicated by the dots in equ. (2.14) and pointed out by O'Brien and Julien this relation is still a simplification of the complex processes in a debris flow, and they noted that more experimental research is especially required to determine possible values of the paramter $C_1$.

Chen (1986a, 1988a,b) noted that Bagnold's model and also Takahashi's extension thereof have major constraints in modelling real debris flows. On the one hand Bagnold's formulation is strictly valid only for the fully dynamic state because in the transition to a quasy-static state the grain stress relation should not only contain a rate-dependent but also a rate-independent part, including cohesion. On the other hand the assumption of constant concentration and pressure over the flow depth is also too restrictive. Releasing the latter constraint, Chen (1988b) proposed that a normal stress relation should be solved simultanously with the conventionally used shear stress versus shear rate relation to obtain the velocity and pressure distribution for uniform debris flow. He termed his model the generalized viscoplastic fluid model, and the constitutive equations are given as (Chen, 1988b):

$$T_{yx} = c' \cos\alpha' + p \sin\alpha' + \mu_1 (\frac{du}{dy})^n \tag{2.15}$$

and

$$T_{yy} = -p + \mu_2 (\frac{du}{dy})^n \tag{2.16}$$

where $T_{yx}$,$T_{yy}$ denote the total shear and normal stresses, respectively, x is the coordinate in flow direction, p the pressure, $\alpha'$ can be the dynamic or the "static" angle of internal friction, and $\mu_1$ and $\mu_2$ are the consistency and cross-consistency indices, respectively. By expressing the relative viscosity $\eta_r=\eta_s/\eta_w$ of the suspension with a theoretical relation given by Krieger and Dougherty (1959):

$$\eta_r = (1 - KC_s)^{-B/K} \tag{2.17}$$

Chen (1988b) came to the following equation for $\mu_1$ and $\mu_2$:

$$\mu_j = a_j \sigma^{n-1} d^{2(n-1)} \eta_w^{2-n} C_*^{-B'/K} (1-KC_s)^{-B'/K} \tag{2.18}$$

where j=1,2, $a_j$ are numerical constants, $\eta_w$ is the dynamic viscosity of water, B' the "intrinsic" viscosity (shown to be close to Einstein's value of 2.5 in his theoretical equation for the relative viscosity of dilute suspensions, $\eta/\eta_w=1+B'C_s$), and K is a factor accounting for the interaction of the colliding particles (usually taken as $K=1/C_*$).

Chen (1988a) noted that the first two terms of equ. (2.15) represent a soil yield stress which might become negligible if a flow is in the fully dynamic range. The value of the flow behaviour index n can vary

from 1 (macroviscous regime) to 2 (inertial regime) or possibly assume a higher value. For the assumption of a constant grain concentration over the depth, Chen (1988a) showed that Bagnold's (1954) model is a particular case of the generalized viscoplastic fluid model (for the fully dynamic state and with $B'/K = 0$). Chen (1988b) obtained analytical solutions for the velocity distribution in the macroviscous flow regime (n=1), with which he could illustrate the influence of the parameter $B'/K$. Chinese researchers have found (Chen, 1986b) that the value of $B'/K$ should increase with increasing fine sediment concentration, thereby, according to Chen's model, decreasing the velocity gradient near the bed. Numerical solutions (Chen, 1988b) for the inertial flow regime (n=2) with $B'/K \neq 0$ show good agreement with experimental velocity profiles of Takahashi (1980) and Tsubaki et al. (1982). While the theoretical determination of the parameter $B'/K$ is relatively easy, assumptions are usually required for the value of the flow behaviour index n and for a relation between density and pressure.

Recent studies in the field of granular flow experiments and modelling are summarised by Iverson and Denlinger (1987). Extensive work has been done to study the behaviour of dry granular flows. It is found that generally grain collisions are inelastic which means that energy is dissipated during this process. Both translational and rotational energy can be exchanged during the grain contacts. In experiments performed by Drake and Shreve (1986, as described by Iverson and Denlinger, 1987) it could be observed that the particle fluctuation energy mainly originated from direct interactions of grains with the bed and that both the particle concentration and the frequency of collisions decreased with height above the bed. At the higher flow depths particles followed more irregular paths while near the bed they tended to flow parallel to the bed and occasionally formed densely packed clusters. Iverson and Denlinger presume that the random interactions of a relatively small number of grains (as compared to the flow depth) possibly results in a random macroscopic flow behaviour. Dissipation of fluctuation energy from the boundary into the flow is expected to occur over a shorter distance in the case of inelastic collisions such as for clay aggregates as compared to flows with hard quartz grains. This statement is somewhat contradictory to Chen's (1988b) model which predicts that the near bed shear zone should increase with increasing fine sediment concentration.

As to the role of an intergranular fluid matrix, Iverson and Denlinger (1987) report that during a collision the fluid will be pressurized and squeezed out of the gap between the grains, thus forming a cushion that dampens the collision of the solids. If grain collisions are mainly inelastic this fluid "cushioning" may lead to a reduced energy dissipation and thus increase the mobility of the flow. There are mixture theories that allow for large deformations and varying concentrations and contacts of particles and that include viscous drag effects arising from the relative movement of an interstitial fluid. However, according to Iverson and Denlinger, effects of inertial solid-fluid interactions, of pore-scale pressure fluctuations and of nonuniform particle size distributions have not been treated so far in a comprehensive theory.

## 2.2 Rheology and flow of hyperconcentrated suspensions

### 2.2.1 Rheological properties

In debris flow modelling it is often assumed that the finer particles (e.g. smaller than 1 mm) and the water form a fluid matrix which carries along the coarser particles or interact with them (Iverson and Denlinger, 1987; Davies, 1988). Many experimental studies have been made to determine the changed fluid properties of hyperconcentrated suspensions and the effect on the flow behaviour.

Naik (1983) summarised the factors that affect the rheological properties of a debris flow :

- concentration of solids
- clay content
- type of clay
- absolute size of the solid material
- size distribution of clay, silt, sand, and gravel fractions
- characteristics of clastic materials, such as shape, size and density
- packing arrangement
- proportions of fine-grained material to coarse clastic material such as rocks and boulders

- electro-chemical characteristics of the liquid phase

This list illustrates that it is difficult to develop theoretical equations to predict the rheological properties of natural grain materials. Therefore the main approaches to treat hyperconcentrated flows are based on an experimental determination of the rheological behaviour. The term hyperconcentrated flow or suspension is used here in the sense of water-sediment mixtures containing predominantly fine grains that are more or less uniformly dispersed within the flow.

A comprehensive review of theoretical relations to predict the change in viscosity as a function of increasing particle concentration and other factors is given by Naik (1983). To determine the viscosity of a suspension, $\eta_s$, at low concentrations of spherical grains A. Einstein (1906, cited by Naik, 1983) proposed the equation:

$$\eta_s = \eta(1 + 2.5C_s) \tag{2.19}$$

where $\eta$ is the viscosity of the suspending medium. According to Naik this formula should only be used up to volume concentrations $C_s \approx 0.01$. Above this concentration level hydrodynamic interactions between particles become important, and empirical and theoretical equations have been proposed to express the relative viscosity $\eta_r = \eta_s/\eta$ as a function of the ratio $C_s/C_*$, termed the reduced volume fraction. A comparison of a theoretical equation of Ackerman and Shen (1979) with experimental data shows good agreement over a wide range of reduced volume fractions from 0 to about 0.95 where the relative viscosity of the dispersion attained values of approximately 200. Ackerman and Shen's analysis showed that the grain size distribution should also affect the relative viscosity, and according to Moshev (1979) this is particularly important for bimodal dispersions, which are indeed often found in deposits of debris flows. Theoretical models that account for the effects of wide grain size distributions would be very complex. It has been shown, however, both by Moshev and by Ackermann and Shen that dispersions containing several discrete particle sizes which differ at least by a factor of ten can be analyzed by successively determining the relative viscosity of the fluid system including first only the smallest and then the next larger particle size. Naik (1983) proposed to apply this procedure to actual debris flow materials by dividing the wide grain size distribution into several discrete size classes.

In a debris flow the fluid matrix consisting of a suspension of fine particles is an important factor in causing a yield strength and non-Newtonian flow behaviour. To examine this aspect Naik (1983) measured the rheological properties of a clay suspension and velocity profiles in an open channel. Clay suspensions are generally considered to be purely viscous time-independent fluids, and the Bingham model has been shown appropriate to treat the flow behaviour at higher shear rates. Naik proposed to use a theoretical relation developed by D.G. Thomas (1961) to predict the Bingham parameters:

$$\tau_B = K_1 C_f^3 \tag{2.20}$$

and $$\eta_B = \eta_w \exp(K_2 C_f) \tag{2.21}$$

where $C_f$ is the volume concentration of fine particles, and $K_1$ is a dimensional and $K_2$ a dimensionless constant for a given particle type, depending on grain size and shape. According to D.G. Thomas (1963a) the above equations are valid up to fine material volume concentrations $C_f$ between 0.2 and 0.3; for higher concentrations the flow behaviour will change from shear-thinning (pseudoplastic) to shear-thickening (dilatant flow). Based on the assumption that the approach of Ackerman and Shen (1979) can also be used for grain dispersions in a Bingham fluid, Naik (1983) developed rather complex theoretical relations to predict the Bingham yield stress and the Bingham viscosity for such a dispersion. His equations show good agreement with measured Bingham parameters of Mills (1983) for uniform dispersions of spherical glass beads sheared in a clay slurry. When applied to dispersions of crushed quartz sand and coarse particles from Mount St. Helens mudflow deposits, the predicted rheological parameters deviated from the measured ones, probably due to the effect of irregular particle shape.

Wan (1982) measured the Bingham parameters for a kaoline and a bentonite clay suspension and determined the following empirical relation for the Bingham yield stress:

$$\tau_B = K_3 C_f^3 \tag{2.22}$$

where $K_3$ is a dimensional constant. It is interesting that this equation shows the same dependence on concentration as the theoretical formula

(equ. 2.20) given by D.G. Thomas (1961). For the kaoline suspension Wan presented also a relation for the Bingham viscosity:

$$\eta_B = K_4 + K_5 c_f^{1.68} \tag{2.23}$$

where $K_4$, $K_5$ are dimensional constants. Wan made further maesurements for a bentonite slurry containing sand particles up to 0.21 mm and found that both $\tau_B$ and $\eta_B$ increase more strongly with concentration above a total volume concentration (including clay and sand) of approximately 30%.

O'Brien and Julien (1986) noted that in previous studies in which the Bingham model was used to analyse the flow of hyperconcentrated suspensions (e.g. Thomas, 1963a,b; Wan, 1982; Mills, 1983) the rheological parameters were determined from measurements in the high shear rate region (dv/dy > 100 1/s). They claim that in natural debris flows and hyperconcentrated sediment flows representative shear rates are of the order of 5 to 50 1/s. Therefore the effective Bingham yield stress would be smaller than values obtained from backextrapolating high shear rate measurements, whereas larger values result for the Bingham viscosity. To determine the Bingham parameters for ten different natural soils they used a special viscometer in which they could shear a fluid containing sand particles up to 0.5 mm. Their empirical relations for $\tau_B$ and $\eta_B$ determined in the low shear rate region are given as:

$$\tau_B = K_6 \exp(K_7 C_f) \tag{2.24}$$

$$\eta_B = K_8 \exp(K_9 C_f) \tag{2.25}$$

It can be seen that the relation for the Bingham viscosity (equ. 2.25) is similar to the theoretical equation (2.21) given by D.G. Thomas (1961). O'Brien and Julien measured the Bingham parameters also for sand-clay mixtures. For a clay volume concentration of 6 % and sand particles up to 0.25 mm the Bingham viscosity increased rapidly with concentration above a total volume concentration of about 20 %, while for a natural soil containing sand particles up to 0.5 mm a rapid increase occurred at total volume concentrations above about 50 %.

Chen (1986b) summarised Chinese concepts of modeling hyperconcentrated streamflow and noted that the Bingham approach is very widely

used in China. Many empirical expressions have been developed to estimate the Bingham yield stress. Fei (1981) proposed the following equations:

$$\tau_B = K_{10} C_{sfw} C_f^{1.73} \qquad \text{for } C_f < 0.106\, C_{sfw}^{-0.462} \tag{2.26a}$$

$$\tau_B = K_{11} C_{sfw}^{2.23} C_f^{4.33} \qquad \text{for } C_f > 0.106\, C_{sfw}^{-0.462} \tag{2.26b}$$

where $C_{sfw}$ denotes the weight concentration of fine particles smaller than 0.025 mm. According to the above relations the influence of the total particle concentration by volume $C_f$ on the yield stress is the bigger the higher is the amount of fine particles. For example, if $C_{sfw}$= 0.1 then the critical total concentration $C_f$ is 31 %, and if $C_{sfw}$= 0.2 then $C_f$ is 22 % above which there is a rapid increase of the Bingham yield stress $\tau_B$ with increasing total concentration. Fei (1981, 1983) also found that $\tau_B$ should depend on a critical sediment concentration $C_{fm}$ at which all free water is extracted (bound by cohesive particles), $C_{fm}$ being mainly a function of particles finer than 0.01 mm. Tang (1981) further introduced a cohesion and a geometry index to calculate $\tau_B$ and his relation showed good agreement with field data from the Yellow River. Kang and Zhang (1980) analysed numerous samples of debris flow material from a particular torrent and they found a breakpoint in the $\tau_B$ vs. $C_f$ relation at a critical concentration of C≈40 % and in the $\eta_B$ vs. $C_f$ relation at a value of $C_f$≈45 %. Chen (1986b) concluded that at lower concentrations $\tau_B$ varies mainly with $C_f$ and the amount of colloidal particles while at higher concentrations the internal friction between colliding particles becomes important.

As to the Bingham viscosity Chu (1983) proposed an equation similar to the one given by Einstein (equ. 2.19):

$$\eta_B = \eta_w(1 - 2.5K_{12}C_f) \tag{2.27}$$

where the term $K_{12}C_f$ is equal to the concentration of sediment plus bound water. Chu further suggested another relation which can be written as:

$$\eta_B = \eta_w\left(1 - \frac{C_f}{C_*}\right)^{-2.5} \tag{2.28}$$

Fei (1983) modified equ. (2.28) and developed two separate forms the use of which depends on the presence of particles finer than 0.01 mm. Chen (1986b) noted that equ. (2.28) is similar in form to the theoretical equation for the relative viscosity proposed by Krieger and Dougherty (1959), equ. (2.17), and that a similar empirical relation was found by McTigue (1982). Again it appears that the Bingham viscosity is not only a function of the total concentration but also of the sediment composition and the grain size distribution.

Shen and Xie (1985) measured the Bingham properties of fine slurries containing sand particles up to 0.5 mm in diameter. They suggested to apply equations similar to (2.24) and (2.28), and it is interesting that they used a two step procedure analogous to that proposed by Naik (1983). First they calculated Bingham yield stress and viscosity for the fine slurry having only particles smaller than 0.01 mm. Knowing the rheological properties of this "new" fluid matrix they then computed the Bingham parameters for the whole slurry including the coarser particles.

Summary

From the above discussion it can be concluded that no unique relation has been found to express either the Bingham yield stress or the Bingham viscosity as a function of concentration and material parameters. Empirical equations have been proposed that are similar to formulas developed on a theoretical basis. Viscometric measurements of grain dispersions with different size classes show that the Bingham parameters tend to increase more rapidly with concentration above a certain critical value of the total volume concentration, which appears to lie somewhere in the range of 20% to 50%. This distinct change may be related to the increasing influence of internal friction at higher grain concentrations (Chen, 1986b).

### 2.2.2 Flow resistance of a Bingham fluid

#### 2.2.2.1 Definitions

Naik (1983) reviewed theoretical approaches to treat the flow of a Bingham fluid and stated that the flow resistance should be a function of the following dimensionless parameters:

$$f = Fn\ (k_s/h,\ Fr,\ Re_B,\ Y_f) \tag{2.29}$$

where $k_s$ denotes the equivalent sand roughness and $k_s/h$ is termed the relative roughness, and where the following definitions are used:

$$f = \frac{8\tau_o}{\rho V^2} \quad : \text{ Darcy-Weissbach friction factor} \tag{2.30}$$

$$Fr = \frac{V}{(gh)^{1/2}} \quad : \text{ Froude number} \tag{2.31}$$

$$Re_B = \frac{4Vh\rho}{\eta_B} \quad : \text{ Bingham Reynolds number} \tag{2.32}$$

$$Y_f = \frac{2\tau_B}{\rho V^2} \quad : \text{ Yield factor} \tag{2.33}$$

where $\tau_o = \rho ghJ$ is the shear stress at the bed, J is the slope ($=\tan\beta$) and V is the mean cross-sectional velocity. The yield factor can also be replaced by the Hedstroem Number He which is given as:

$$He = \frac{\rho\tau_B(4h)^2}{\eta_B^2} \quad : \text{ Hedstroem number} \tag{2.34}$$

and the relation between $Y_f$, He and $Re_B$ is:

$$Y_f = \frac{2He}{Re_B^2} \tag{2.35}$$

High values of $Y_f$ or He indicate increasing non-Newtonian characteristic of the flow.

2.2.2.2 Laminar flow

By integrating the Bingham equation (2.2) for laminar flow in a wide open channel the velocity distribution over the depth is obtained as:

$$v = \frac{\rho gJ(h^2-y'^2)}{2\eta_B} - \frac{\tau_B(h-y')}{\eta_B} \tag{2.36}$$

where y' is measured downwards from the flow surface. From this equation the mean velocity can be calculated as:

$$V = \frac{h\tau_o}{3\eta_B}\left[1 - 1.5\frac{\tau_B}{\tau_o} + 0.5\left(\frac{\tau_B}{\tau_o}\right)^3\right] \qquad (2.37)$$

These results are confirmed by the equations given by Howard (1963) and Kozicki and Tiu (1967). If the last term in equ. (2.37) is neglected and the stress ratio $a' = \tau_B/\tau_o$ is smaller than 0.5 this leads to an error in the mean velocity that is smaller than 6.3 %. The simplified relation can be expressed as:

$$\tau_o = 1.5\tau_B + \eta_B\frac{3V}{h} \qquad (2.38)$$

Combining equ. (2.37) with equs. (2.30), (2.32) and (2.34) a friction factor relationship in terms of f, $Re_B$ and He is found as:

$$\frac{1}{Re_B} = \frac{f}{96} - \frac{He}{8Re_B^2} + \frac{8}{3f^2}\left(\frac{He}{Re_B^2}\right)^3 \qquad (2.39)$$

The use of equ. (2.39) allows the friction factor to be plotted against the Bingham Reynolds number, with the Hedstroem number as an additional parameter.

Kozicki and Tiu (1967) considered the steady, uniform, laminar flow of non-Newtonian fluids in straight open channels of arbitrary cross sections. For different non-Newtonian flow models they developed a general method to predict the flow rate and the maximum velocity. Their equations for the Bingham model are somewhat more elaborate than the ones given above, in that they include two cross-sectional shape parameters a and b; for a rectangular channel a and b are a function of the aspect ratio $A_s$=W/h, where W is the width of the channel. From the equation for the mean velocity given by Kozicki and Tiu, Naik (1983) developed a relation between f, $Re_B$ and He similar to equ. (2.39) but including the shape parameters a and b.

Johnson (1970) presented a numerical method to compute the velocity and shear stress distribution for the laminar flow of a Bingham fluid in a rectangular channel. He also showed that the existence of dead regions at the corners becomes important for narrow channels (low aspect ratio).

D.G. Thomas (1963a) used the Bingham model to analyse pipe flow experiments with non-Newtonian suspensions. He stated that besides the use of an f-$Re_B$-He relation another, equally satisfactory method to predict

the laminar friction loss is the introduction of an effective visocity $\mu_e$ which allows the conventional Newtonian relation f = 16/Re (for laminar pipe flow) to be used. This method was first proposed by Caldwell and Babbitt (1941), and the definition of $\mu_e$ is similar to the apparent viscosity $\eta_a$ except that the former is used for mean flow values. Considering the simplified equ. (2.38) for open channel flow, the bed shear stress $\tau_o$ can be plotted as a function of the shear rate term 3V/h, and then an effective viscosity $\mu_{e2}$ is obtained as:

$$\mu_{e2} = \eta_B + \frac{\tau_B h}{2V} \tag{2.40}$$

or, if $\mu'_{e2}$ is calculated from equ. (2.37) instead of equ. (2.38) :

$$\mu'_{e2} = \eta_B \; / \; [1 - 1.5(\frac{\tau_B}{\tau_o}) + 0.5(\frac{\tau_B}{\tau_o})^3] \tag{2.41}$$

Now a conventional friction factor diagram can be used if the corresponding Reynolds number $Re_2$ is defined as:

$$Re_2 = \frac{4Vh\rho}{\mu_{e2}} \tag{2.42a}$$

or $$Re_2 = \frac{4Vh\rho}{\mu'_{e2}} \tag{2.42b}$$

Quian et al. (1980) performed flume experiments with a muddy slurry and showed that their data in the laminar flow region can be represented equally well by an f-$Re_B$-He and an f-$Re_2$ plot. In the latter diagram the data points lie close to the theoretical relation f = 96/$Re_2$. Zhang et al. (1980) carried out similar open channel tests in flumes with different cross sections. They presented their results in an f vs. $Re_2$ plot and found the relation f = $A_m/Re_2$ for the laminar flow region, where $A_m$ is 84 for the rectangular and the U-shaped and 74 for the trapezoidal cross section. Wan (1982) measured the flow resistance of a bentonite suspension in a closed rectangular channel (30 cm wide and 20 cm high), and in an f vs. $Re_2$ diagram the data points lie rather close to the line f = 96/$Re_2$.

2.2.2.3 Laminar-turbulent transition

Following the approach of Hanks (1963), who developed a criterion for the laminar-turbulent transition of a Bingham fluid flowing in a pipe, Naik (1983) established a similar criterion for open channel flow. His proposed relations are given as:

$$\frac{a'_c}{(1-a'_c)^3} = \frac{He}{48'000} \tag{2.43}$$

$$Re_{B,c} = \frac{He}{12a'_c}\,(1 - 1.5a'_c + 0.5a'^3_c) \tag{2.44}$$

where the subscript c denotes the critical conditions at transition, and according to Naik the "constant" 48'000 may vary between 24'000 and 96 000, analogous to the critical Reynolds number in the Newtonian case being in the range of 2'000 to 8'000. Naik found quite good agreement between the equs. (2.43) and (2.44) and his experimental data obtained from flume tests with a kaoline suspension. His data covered Hedstroem numbers He up to $2 \cdot 10^6$ and stress ratios $a'_c$ up to 0.75. Hanks (1963) in his analysis, however, had found good agreement between theory and experiments only for $He < 10^5$ or $a'_c < 0.55$.

As an alternative the laminar-turbulent transition can be detected on a conventional f vs. Re plot when a suitable Reynolds number is defined, as for example by using $Re_2$ given by equ. (2.42a). In experimental studies with a clay suspension or a fine slurry, values for the critical Reynolds number $Re_{2,c}$ at transition were found to be between 3'000 ... 5'000 (Quian et al., 1980), 4'000 ... 5'000 (Zhang et al., 1980), 4'000 ... 6'000 (Wan, 1982, covered flume) and 6'000 ... 8'000 (Cao et al., 1983, including field data). For his pipe flow data, Thomas (1963a) gave a critical Reynolds number of about 2'100, defined analogous to $Re_2$ using an effective viscosity. According to Straub et al. (1958), who collected flume data on the laminar and turbulent flow of Newtonian fluids, the lower critical Reynolds number seems to depend to some extent on the channel shape and is generally larger than for pipe flow. They also concluded that the cross-sectional shape is quite important in rough laminar open channel flow.

2.2.2.4 Smooth and rough turbulent flow

The velocity distribution in turbulent open channel flow of a Newtonian fluid is usually described by a loagrithmic relation (Yalin, 1977):

$$\frac{v}{v_*} = \frac{1}{\chi} \ln\frac{y}{k_s} + B_s \qquad (2.45)$$

with $B_s = 2.5 \ln(Re_k^*) + 5.5$ if $Re_k^* <\simeq 5$ (2.46)

or $B_s = 8.5$ if $Re_k^* >\simeq 70$ (2.47)

where the roughness Reynolds number $Re_k^*$ is defined as $Re_k^* = v_* k_s \rho/\mu$. The value $Re_k^* \simeq 5$ is the upper limit of the hydraulically smooth turbulent flow (or regime), and $Re_k^* \simeq 70$ is the lower limit of the fully developed turbulent or rough turbulent flow (or regime); in between these values the flow is in the transitional regime. Fig. 2.2 (taken from Yalin, 1977, his Fig. 2.5) illustrates how the value of $B_s$ varies with $Re_k^*$ for the experimental data obtained by Nikuradse.

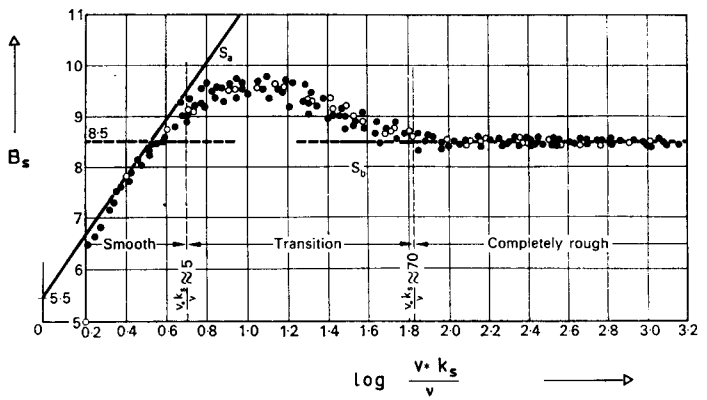


Fig. 2.2 : Variation of $B_s$ with roughness Reynolds number $Re_k^*$ (after Yalin, 1977).

D.G. Thomas (1963b) performed pipe flow experiments with titania, kaoline and thorium oxide suspensions. He correlated his data for smooth

turbulent flow with a modified Blasius equation using the Bingham Reynolds number $Re_B$. If the Bingham yield stress $\tau_B$ was less than 23.9 N/m² the values of the friction factor f tended to approach those for Newtonian flows with increasing $Re_B$, but for $\tau_B$ > 23.9 N/m² f tended to diverge from the Newtonian value with increasing $Re_B$.

Hanks and Dadia (1971) developed a sophisticated theoretical analysis for turbulent flow of a Bingham fluid in smooth pipes. They introduced a paramter $B_t$, which is to be determined from experiments, representing the effect of the boundary in damping the turbulence. Naik (1983) adapted this theory for smooth turbulent open channel flow of a Bingham fluid. He found from his experiments with a kaoline slurry that for values of the yield factor $Y_f$ smaller than 0.001 the flow is essentially Newtonian (and $B_t$ assumes its Newtonian value), and for $Y_f$>0.001 the flow behaviour shows increasing non-Newtonian character (and $B_t$ increases linearly with $Y_f$). His theoretical predictions were confirmed by experimental data. In Fig. 2.3 a friction factor diagram computed by Naik is shown. According to the theory the friction factor can be higher or lower than in Newtonian flow, depending on the values of the Bingham Reynolds number and Hedstroem number. For increasing values of $Re_B$ the friction factor approaches the Newtonian value. This confirms one of D.G. Thomas' (1963b) observations, and it seems that in Naiks tests $\tau_B$ was always smaller than Thomas' critical value of 23.9 N/m².

Gupta and Mishra (1974) showed that the conventional f vs. Re relationship for Newtonian flow is also valid for pipe flow of a Bingham fluid. Both Wan (1982) for his covered flume tests with a kaoline suspension and Zhang et al. (1980) for their open channel experiments with fine slurries presented their data on a f vs. $Re_2$ plot (using the effective viscosity $\mu_{e2}$ ). There is a smooth transition on their diagrams from the clear water data to the hyperconcentrated data points indicating that such a representation is possible not only in the laminar but also in the smooth turbulent region. From pipe and open channel flow experiments with a clay suspension, Yano and Daido (1965) concluded that the conventional Newtonian relations can be used if a suitable Reynolds number is defined, which is however given in their analysis by a more complex expression than the one for $Re_2$.

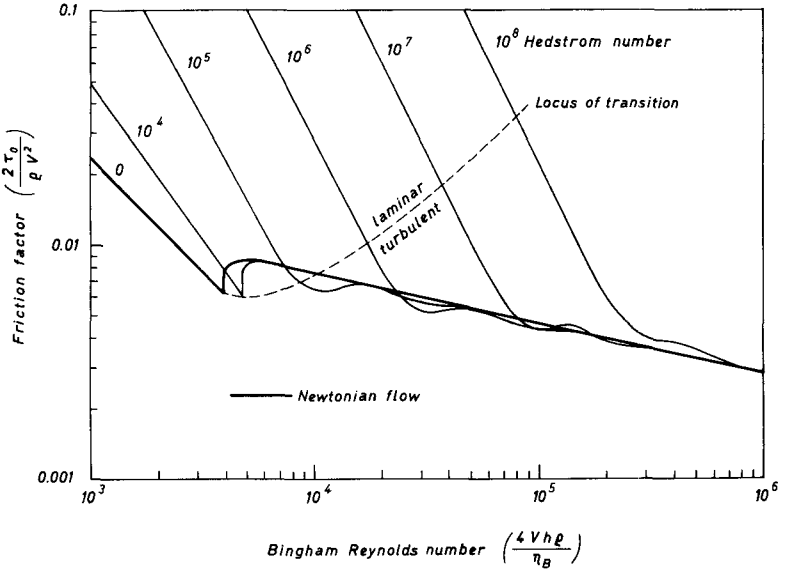


Fig. 2.3 : Friction factor diagram for a Bingham fluid as given by Naik (1983); it was produced from the Bingham relations for laminar flow and for smooth turbulent flow (with Naik's approach), and also shows the limiting line separating the laminar and turbulent flow regime. (Note that f is defined here as $2\tau_o/\rho V^2$ which is different from the definition in equ. (2.30) used in this study.)

Torrance (1963) conducted experiments with pseudoplastic fluids in smooth and rough pipes. His flow resistance equations can be given for Bingham fluids (fluid index n=1) as:

$$\frac{1}{\sqrt{f}} = A_1 \log(1-a') + A_2 \log(Re_B\sqrt{f}) - A_3 \quad \text{for smooth pipes} \quad (2.48)$$

$$\frac{1}{\sqrt{f}} = A_4 \log\left(\frac{R}{k_s}\right) + A_5 \quad \text{for rough pipes} \quad (2.49)$$

where $A_1$, $A_2$, $A_3$, $A_4$ and $A_5$ are constants and R is the hydraulic radius.

Yang and Zhao (1983) performed experiments with hyperconentrated slurries in a rough flume and developed the following equations:

$$\frac{1}{\sqrt{f}} = 2\log\left(\frac{R}{k_s}\right) + A_6 - A_7\log\left(Re^*_{k,B}\right) \quad \text{for the transitional regime} \tag{2.50}$$

$$\frac{1}{\sqrt{f}} = 2\log\left(\frac{R}{k_s}\right) + A_8 \quad \text{for the rough turbulent regime} \tag{2.51}$$

where the constants $A_6$, $A_7$, $A_8$ depend on the roughness characteristics, and $Re^*_{k,B}$ is the roughness Reynolds number defined with the Bingham viscosity: $Re^*_{k,B} = v_* k_s \rho/\eta_B$. It may be noted that these experiments included flume slopes of 10 % and 20 % whereas all other open channel studies mentioned here were limited to bed slopes of a few percent.

If a suitable Reynolds number is defined, as for example $Re_2$ (equ. 2.42), one could also imagine that the universal Colebrook equation, valid both in turbulent smooth and rough flow, may be used. According to Henderson (1966) it is expressed for open channel flow as:

$$\frac{1}{\sqrt{f}} = -2\log\left(\frac{k_s}{12R} + \frac{2.5}{Re\sqrt{f}}\right) \tag{2.52}$$

where the Reynolds number is defined as $Re = 4VR\rho/\eta_w$. For flow in the fully rough regime (large Re), this formula becomes identical to the Nikuradse equation:

$$\frac{1}{\sqrt{f}} = 2\log\left(\frac{12R}{k_s}\right) \tag{2.53}$$

As there is only little information available on turbulent flow of a Bingham fluid in rough pipes or open channels, Naik (1983) developed a theory for such flows in open channels. He assumed that the Bingham Reynolds number is large so that the laminar shear stress due to the Bingham viscosity $\eta_B$ can be neglected in comparison to the turbulent shear stress. His equation can be given as:

$$\frac{1}{\sqrt{f}} = 0.88(1-a')\left[A_o + \ln\left(\frac{R}{k_s}\right)\right] \tag{2.54}$$

$$\text{with} \quad A_o = \ln\left[\left(\frac{30h}{R}\right) \exp\left(-1 - \frac{(A_s+2)h^2}{4A_{cs}}\right)\right] \tag{2.55}$$

where $A_s$ is a shape factor (depending on the depth to width ratio) and $A_{cs}$ is the area of the flow cross section. Naik compared measured mean velocities for the flow of a kaoline suspension over a rough bed (made

of a wire screen with a thickness of 3 mm) with theoretically predicted values by equs. (2.54) and (2.55); he found good agreement between measured and calculated velocities.

To distinguish between hyraulically smooth, transitional and rough turbulent flow of a Bingham fluid, Naik (1983) suggested to use a modified roughness Reynolds number which is also a function of the yield/ wall stress ratio a':

$$Re_k^{*'} = v_* k_s \rho(1-a')/\eta_B \qquad (2.56)$$

If, however, the effective viscosity $\mu_{e2}$ can be successfully used to define a flow Reynolds number $Re_2$ one may expect that also the particle Reynolds number can be suitably expressed with $\mu_{e2}$:

$$Re_2^* = v_* d\ \rho/\mu_{e2} \qquad (2.57)$$

2.2.2.5 Summary

It is interesting that both equations proposed for hyperconcentrated flow in the rough turbulent regime, equs. (2.49) and (2.51), are independent of any viscosity or yield stress parameter and are in fact similar in form to the Newtonian relation (2.53).

To determine the flow resistance of a hydrodynamically smooth turbulent or a laminar flow two alternative methods may be valid: Either using new relationships developed for Bingham fluids where f is a function of $Re_B$ and He, or defining an effective (representative) viscosity $Re_2$ and applying conventional formulae for Newtonian fluids.

### 2.2.3 Flow and fluid characteristics

D.G. Thomas (1963b) pointed out that the use of Newtonian friction factor relations (by defining a suitable Reynolds number) for non-Newtonian flow may be a too simplified approach. For it implies that the scale and intensity of turbulence in a non-Newtonian system is essentially the same as in Newtonian fluids provided there is a Reynolds

number similarity. There seems to be a general agreement that with increasing non-Newtonian behaviour the turbulence characteristics of the flow must be damped in some way.

The velocity profile in turbulent flow is generally divided into three zones: The laminar sublayer, the transition zone and the turbulent core. Dodge and Metzner (1959) presented a generalised power law model for the velocity distribution of pseudoplastic fluids and concluded that the turbulent resistance law is very similar to the Newtonian friction factor relation. According to Gust (1976), the existence of a Newtonian flow structure is suggested by mean flow measurements in the logarithmic part of the turbulent boundary layer of cohesive sediment suspensions which behave like a Bingham fluid.

Richardson and Julien (1986) stated that large scale turbulence may still be present in hyperconcentrated flow while small scale turbulence may be rapidly damped. This is in agreement with van Rijn's (1983) conclusion that turbulent fluid diffusivity is reduced in such flows. Both van Riin and Richardson and Julien report that the effect of high sediment concentrations on the von Karman constant $\kappa$ is not yet clear. The change of a wake strength coefficient with increasing near bed concentration of fines was used by Parker and Coleman (1986) to predict changes in flow depth, velocity and resistance. Julien and Lau (1988) theoretically concluded that the wake strength coefficient may still remain the same as for clear water flow if the concentration of fine sediment is uniform over the depth. They claim that Parker and Coleman mistakenly assumed a decrease of the drag coefficient in dilute suspensions and questionned their predicted changes in flow parameters.

Bradley (1986) noted that in natural streams turbulent stresses control the flow behaviour and the sediment transport for fine material concentrations up to 20 % by volume. However, this limiting concentration can be much smaller for highly viscous clay suspensions (as for example with bentonite clay). Quian et al. (1980) gave a limiting concentration of 15 to 20 % for hyperconcentrated flows. Fan and Dou (1980) concluded from measurements that in hydrodynamically rough flow the fluctuation energy remains strong within the boundary layer and that the friction factor is close to the value for clear water flow.

Bed forms may change with increasing fine sediment concentration (Simons et al., 1963) and thus influence the flow resistance. The effect of hyperconcentrated flows on bed forms seems however uncertain (Bradley, 1986). In the upper flow regime grain roughness is mainly important, and it seems unlikely that "small-scale" bed forms would develop with high suspended sediment concentrations.

With increasing values of the Bingham parameters $\tau_B$ and $\eta_B$ the (effective) viscosity of the fluid matrix also increases. This leads to an increase in the thickness of the laminar sublayer (Gust, 1976; Woo, 1985; Ashida et al., 1987) as well as to a decrease in the fall velocity (Thomas, 1963a; Wan, 1982; Woo 1985).

For a suspension with a fine sediment concentration of 20 % by volume, Bradley (1986) calculated a reduced fall velocity according to D.G. Thomas' (1963a) method to be about 30 % of its clear water value. Wan (1982) used a more sophisticated approach to determine the settling velocity in a Bingham fluid. He measured the fall velocity W of different particles in a clay suspension of various concentrations and determined the universal Reynolds number $Re_1$ as well as the drag coefficient $C_D$ given by Ansley and Smith (1967):

$$Re_1 = \frac{\rho W^2}{\eta_B W/d + \tau_B \pi/24} \tag{2.58}$$

$$C_D = \frac{4}{3} \frac{(\sigma-\rho)gd}{\rho W^2} \tag{2.59}$$

Wan plotted his data in a $C_D$ vs. $Re_1$ diagram, which shows his points to lie close to a line for natural sand settling in a Newtonian fluid. Wan balanced the integral of the drag force due to the yield stress over a sphere surface, given as $\tau_B \pi^2 d^2 7/8$ by Ansley and Smith, with the submerged weight of a spherical particle, $\pi d^3(\sigma-\rho)g/6$, to obtain the critical Bingham yield stress $\tau_{B,c}$ at non-settling conditions:

$$\tau_{B,c} = 0.067(\sigma-\rho)gd \tag{2.60}$$

Wan experimentally verified this non-settling criterion for gravel particles, glass and lead balls up to 1.66 cm in bentonite suspensions of different concentrations.

## 2.3 Sediment transport

### 2.3.1 Sediment transport in hyperconcentrated flow

#### 2.3.1.1 Effect of combined increase in fluid density and viscosity

The effects of high concentrations of fine material in suspension on the fluid and flow properties are discussed in section 2.2. If the fine material is uniformly distributed over the flow depth then the suspension can be considered as a pseudo-homogeneous fluid having both an increased density and viscosity as compared to clear water. While the increase in fluid density obviously reduces the submerged weight of transported (coarser) particles, the effect of a changed viscosity on the mechanics of sediment transport is more complex.

Beverage and Culbertson (1964) observed from field data that the sand concentration increased in hyperconcentrated flows with increasing amounts of fine material in suspension. They concluded that water and fine material act as lubricants and that the decreased fall velocity helps to keep coarser material in suspension by less turbulence as compared to clear water flows. Colby (1964) developed an empirical method to calculate the increase in sediment transport rates as a function of suspended sediment concentration and flow depth. His correction factor, giving the increase in transport as compared to a corresponding clear water flow, can be as high as 100, with a mean value of about 10, and is based on field data (Rio Puerco, New Mexico) as well as flume data (Simons et al., 1963) covering fine material concentrations $C_f$ up to 8.7 %. To compute the correction curves he included the effect of reduced fall velocities. Bradley (1986a) reported field data from the Mount St. Helens mudflow. In this case no bed load discharges were measured. For the hyperconcentrated (turbulent) flows suspended sediment transport rates increased by about a factor of 10 as compared to clear water flow, and for the laminar mud flows the transport rates were even another order of magnitude higher.

Only a limited number of flume studies have been performed to consider the effect of a suspension of cohesive sediments on the sediment transport capacity of the flow. Simons et al. (1963) conducted flume

experiments with a bentonite clay suspension. The maximum clay concentration $C_f$ was 2.3% at which the apparent viscosity (which they did however not define) was increased by a factor of about 4 and the fall velocity reduced by a factor of about 2 as compared to clear water. The bed material used in the sediment transport tests had a fall diameter of 0.47 mm and 0.54 mm. Increasing clay concentrations resulted in the following effects: For the lower flow regime, with ripples and dunes as bed forms, they noted a stabilization of the bed and a decrease in the flow resistance. The transported bed material (bed load and suspended load) decreased in flows over a dune bed, which they attributed to a reduced fluid shear due to a smaller f-value. In the upper flow regime (plane bed, standing waves, antidunes) they observed an increase in flow resistance as well as in the sediment transport rate. They plotted their data in terms of dimensionless transport and shear parameters similar to those given by Bagnold (1956):

$$\Phi_{*t} = \frac{q_t}{b\,[(s-1)g\cos\beta d_m^3]^{1/2}} \tag{2.61}$$

and $$\theta_* = [(\theta-\theta_c)\theta^{1/2}]^{2/3} \tag{2.62}$$

with $$\theta = \frac{\tau_o}{\rho g(s-1)d_m} \tag{2.63}$$

where $q_t$ is the volumetric transport rate per unit width of bed load and suspended load, $d_m$ refers to the mean grain size of the transported material, b is a constant for a given bed material and can be related to $d_m$, $\theta$ denotes the dimensionless bed shear stress, and $\theta_c$ is the critical value of $\theta$ at initiation of motion. In the $\Phi_{*t}$ vs. $\theta_*$ plot of Simons' et al. there is much less scatter of the data points if the fine sediment (clay) is not included in the calculation of $\Phi_{*t}$.

Kikkawa and Fukuoka (1969) performed flume experiments using very fine sand as washload and sand of 0.18 mm mean diameter as bed material. With increasing washload concentrations they observed increasing bed material transport rates both for lower and upper regime flows. With regard to bed forms they noted a change from dunes to a flat bed and from a flat bed to antidunes when the washload concentration in the flow was increased.

Wan (1982) recirculated a bentonite suspension with increasing concentrations $C_f$ up to 0.97% in a covered, rectangular flume, and used cylindric plastic particles of 3.45 mm volumetric diameter as bed material. The change in the grain-fluid density ratio s was negligibly small; at the maximum clay concentration the Bingham viscosity $\eta_B$ was about 4 cps. and the Bingham yield stress $\tau_B$ about 0.56 N/m². For an assumed shear rate of approximately 20 1/s, this would result in an effective viscosity $\mu_{e2}$ of about 30 cps. (or 30 times that of water). Wan plotted his sediment transport data in terms of the dimensionless parameters $\Phi_t$ and $\theta$, with:

$$\Phi_t = q_t/[(s-1)gd_m^3]^{1/2} \qquad (2.64)$$

but noted that most of the transported bed material moved as bed load. As compared to the corresponding clear water flows the $\Phi_t$ values for the bentonite suspension runs were lower if $\theta \lesssim 0.4$ and higher if $\theta \gtrsim 0.4$. Wan calculated bed load transport rates for his experimental conditions with the formula of Engelund and Fredsoe (1976), including some adjustements: He took into account the effect of a Bingham fluid (i.e. his bentonite suspension) on the drag coefficient using equs. (2.58) and (2.59); and he used a new relation to determine the dimensionless shear stress $\theta_c$ for incipient motion of a particle in a Bingham fluid (s. section 2.2.3). After having corrected some of his measured transport rates for particles that moved in suspension he found fair agreement between calculated and measured values. The results indicate that, compared to clear water flow, the bed load transport rates were smaller in the bentonite suspension, especially in the low flow intensity region (due to a larger $\theta_c$-value); $\Phi_B$ was reduced by about 20% at the highest clay concentration ($C_f$ = 97%), at a shear stress $\theta$ = 1.0. The suspended load, on the other hand, is supposed to be larger due to the reduced fall velocity. As a result, the total sediment transport rate in a clay suspension flow would be smaller in the low flow intensity region and larger in the high flow intensity region, as compared to clear water flow.

With respect to bed forms Wan observed that dunes are lower and smoother in the bentonite flows and that the transition to a flat bed occurred at lower flow intensities than in clear water flow. Wan only presented flow resistance data for runs with a fixed bed and no sediment transport; the data points were plotted in a f vs. $Re_2$ diagram, and they

showed a similar behaviour as with a Newtonian fluid (s. also section 2.2.2). It may be noted that by using plastic particles with a density of 1.29 g/cm³, the density factor (s-1) was only about 14% of the value for quartz grains in water, and that the transport rates calculated with the dimensionless sediment transport formula of Engelund and Fredsoe agreed fairly well with the measured ones.

Wan and Song (1987) conducted flume experiments with a clay suspension and using PVC particles with densities of 1.27 and 1.34 g/cm³ as bed material. They measured flow and sediment parameters and found that the total transport rate (bed load and suspended load) of the plastic particles increased with increasing clay concentration. They plotted the concentration of the transported PVC particles as a function of the flow intensity parameter $V^3/(gR_bW)$, where $R_b$ is the hydraulic radius corrected for side wall influence. If the fall velocity was calculated according to Ansley and Smith (equ. 2.58 and 2.59), the flume data of Wan and Song for the turbulent flow runs followed more or less a straight line on a log-log plot. For the laminar flow runs they observed higher bed material transport concentrations than in turbulent flow but the dependence on the flow intensity parameter (shown in a plot using the fall velocity in clear water) was much weaker. The difference in sediment transport capacity between the laminar and turbulent runs was very pronounced (several orders of magnitude) at low flow intensities ($V^3/(gR_bW) \approx 1$), whereas at higher flow intensities ($V^3/(gR_bW) \approx 10$) there was almost no difference.

Bradley (1986) conducted flume experiments with a bentonite clay suspension of different concentrations up to $C_f = 3.1\%$, at which the fluid viscosity was about 870 times larger than that of water. He measured (total) sediment transport rates using sand of 0.18 mm mean diameter as bed material. At a bentonite concentration $C_f = 2.2\%$ the fall velocity of this sand was reduced by about a factor of 2. As bed forms he observed both dunes and plane beds. In general sediment transport rates over plane beds were an order of magnitude larger than those over dunes, for the same fluid discharge. For the plane bed case the turbulent bentonite suspension flows transported about 3 to 5 times as much bed material as did the corresponding clear water flows. Two runs at the highest clay concentrations were in the laminar flow regime, one having dunes and the other a plane bed; the sediment transport capacity was increased by about a factor of 10 as compared to the turbulent

hyperconcentrated flows (with the same fluid discharge). No clear and significant change in flow resistance was found for the turbulent flows as compared to the clear water flows, but for the laminar flows f increased considerably. Bradley noted that a fluidized layer of bed material was in motion in the plane bed laminar flow run; this layer was about 25 grain diameters thick.

Woo (1985) made a theoretical study on sediment transport in hyperconcentrated flows. He considered the effect of fine suspended material on bed material transport rates by applying a modified form of the Einstein (1950) sediment transport equation to the flume data of Simons et al. (1963). Woo included three modifications to the Einstein formula: Use of the measured average channel velocity instead of a calculated one; a correction factor for laminar flow effects which is related to the particle Reynolds number (Einstein and Chien, 1953); and a correction to the von Karman "constant" (Einstein and Abdel-Aal, 1972), which is used for the suspended load calculations. He compared calculated bed load discharges obtained with the original and the modified Einstein equation for the flow conditions of the experiments of Simons et al. (they measured only total bed material concentrations). These calculations showed almost no difference in the results. Theoretical considerations led Woo to the conclusion that a decrease in the density factor (s-1) will increase the bed load discharge, and an increase in fluid density generally will decrease the bed load discharge. He stated that for the flow conditions of the Simons' et al. experiments these effects seem to have counterbalanced each other. Woo further concluded that the increase in total bed material transport in a clay suspension must be mainly due to an increase in the suspended bed material discharge. He calculated the total bed material discharge and found that by accounting for the changed density and viscosity in the Einstein equation, the measured discharges of Simons et al. can be slightly better predicted than without this adjustment. Woo also computed the total bed material discharges with Yang's (1979) equation but he only found a marginal improvement over the calculated discharges with the Einstein equation.

2.3.1.2 Effect of change only in grain-fluid density ratio

Woo's (1985) considerations are limited to the experimental range of the Simons et al. (1963) flume data for which the highest clay concentration was 2.3%. Bradley (1986) theoretically examined the effect of increased fluid density for a fine suspended sediment concentration of 20.1%. He found that the Meyer-Peter and Müller (1948) equation predicts an increase in bed load discharge by a factor of 1.67, and the Einstein (1950) equation an increase by a factor of 1.51. In the calculations with the latter formula Bradley also accounted for the decreased fall velocity of the transported particles.

Shields (1936) performed sediment transport experiments using water and particles of different densities. The specific densities s (= $\sigma/\rho$) varied from 1.06 up to 4.25. His bed load transport equation can be written as:

$$q_B = \frac{10qJ(\tau_o-\tau_c)}{\sigma(s-1)^2 d_m} \tag{2.65}$$

where $q_B$ is the volumetric bed load transport rate per unit width, q is the volumetric water discharge per unit width, and $\tau_c$ is the critical shear stress at incipient motion. It may be noted that the density factor (s-1) in equ. (2.65) appears with an exponent of 2 and not in a linear form like in many bed load transport equations.

Mizuyama and Shimohigashi (1985) made steep flume tests to study the effect of fine material in suspension on bed load transport. For a slope range between about 10 and 20 %, with pearl-clay as fine sediment and sand with $d_m$ = 1.9 mm as bed material they found the following relationship to be valid:

$$q_B = A' \; q \; S^2 \; \frac{1}{(s-1)^2} \tag{2.66}$$

where A'= 20 for clear water and A'= 25 for the experiments with the fine sediment suspension. They also performed some tests with flyash (being somewhat coarser than the pearl-clay) as fine sediment; in a plot in terms of the dimensionless parameters $\Phi_B$ and $\theta$ the flyash data points lie close to comparative points from clear water tests. As compared to the pearl-clay experiments (performed with a movable bed), the transport

rates with the flyash suspension are about twice as high, because they were obtained from tests with a fixed, rough bed (Mizuyama, 1988). The viscosity of the fine material suspensions was not determined but Mizuyama (1988) estimated that it only slightly increased with increasing concentration.

Chee (1988) reported on flume tests on the washout of a gravel dam under a constant water discharge. In the experiments the density ratio s was varied between 2.65 and 4.50 by using particles with different specific weights; the initial downstream slope of the dam was fixed between 33% and 45%. Chee determined a dimensionless equation in which the ratio $q_B/q$ depends, among other parameters, on the factor $1/(s-1)^2$.

Meyer-Peter and Müller (1948) performed bed load transport experiments and also included some runs using particles lighter (coal) and heavier (baryt) than ordinary quartz grains. Their flume data is given in Smart and Jäggi (1983), and the highest measured $\Phi_B$ value was 0.46. In a simplified form, the Meyer-Peter/Müller bed load formula can be expressed as (Yalin, 1977):

$$\Phi_B = 8(\theta-\theta_c)^{1.5} \tag{2.67}$$

where $\Phi_B$ is defined with $q_B$:

$$\Phi_B = q_B/[(s-1)gd_m^3]^{1/2} \tag{2.68}$$

Another flume study on sediment transport using particles of different densities was carried out by Luque and van Beek (1976). Using water as transporting fluid, the density ratio s covered a range from 1.34 up to 4.58. The experiments were made in a closed rectangular channel, and the slope of the movable bed was varied between 0° and 22°, one objective being to study the iniation of motion at steep slopes. Measured bed load transport rates were correlated in terms of the dimensionless parameters $\Phi_B$ and $\theta$ to yield:

$$\Phi_B = 5.7(\theta-\theta_c)^{1.5} \tag{2.69}$$

The highest measured value of $\Phi_B$ was about 0.08. Equ. (2.69) can be rearranged as:

$$q_B = \frac{5.7}{(s-1)g} \left(\frac{\tau_o - \tau_c}{\rho}\right)^{1.5} \tag{2.70}$$

As compared to equ. (2.65) from Shields there is only a linear dependence on the density factor (s-1) in equ. (2.70). Luque and van Beek also measured the average particle velocity of single grains, $U_b$, at relatively low shear intensities and found the following empirical relation:

$$U_b = 11.5(v^* - 0.7v_c^*) \tag{2.71}$$

where $v_c^*$ denotes the shear velocity at initiation of motion. A similar equation for the mean speed of bed load grains was theoretically derived by Bridge and Dominic (1984) (s. section 2.3.2, equ. 2.98). According to equ. (2.71) the particle velocity may depend on the density ratio s only via $v_c^*$, and if the above relation is also valid at higher shear intensities then $U_b$ must ultimately become independent of s. Yalin (1977) concluded that s is not an important variable for the uniform motion of grains which is approximately the case for grains flowing "en masse", but that s can not be neglected if the individual, irregular motion of a saltating grain is considered.

It is interesting that in the dimensionless form of both equs. (2.69) and (2.67) $\Phi_B$ is only a function of $\theta$ and $\theta_c$, and that density effects within the given experimental ranges can be accounted via the dependence of the dimensionless parameters on the factor (s-1).

This fact is also illustrated in Fig. 2.4 (s. page 49), taken from Yalin (1977), where bed load transport data from various sources are shown on a log-log plot of $\Phi_B$ vs. $\theta$ including particles heavier and lighter than ordinary quartz grains. In this plot only the Wilson (1966) data points for nylon particles in water (s = 1.138), covering a range of $\theta$ values between 1 and about 3.2, are located apart from the general trend defined by the rest of the data. From the limited data it seems that only at higher shear stresses the effect of the density ratio s becomes noticable. Considering the weight of the moving layer and its average velocity, Yalin (1977) theoretically developed a bed load transport equation in which $\Phi_B$ is given as funtion of $\theta$, $\theta_c$, and s:

$$\Phi_B = 0.635\ \theta^{0.5}\ m\ [1 - \frac{1}{zm}\ln(1+zm)] \tag{2.72}$$

with $m = (\theta/\theta_c) - 1$ (2.73)

and $z = 2.45\theta^{0.5}/s^{0.4}$ (2.74)

A check of Yalin's equation was made for one of Wilson's data points using $\theta = 2.3$, $\theta_c = 0.05$, and $s = 2.68$ (for sand) or $s = 1.14$ (for nylon), respectively. While Yalin's equ. (2.72) predicts a slightly smaller transport rate for the sand case, the measured $\Phi_B$ value (at $\theta = 2.3$) for sand is about 2.4 times higher than that for nylon.

Wang and Zhang (1987) presented a new bed load transport equation that is based on a probabilistic approach similar to the concept of Einstein's formula. The bedload transport rate in their equation is proportional to the probability of detachment, the average jump length and height, and the average grain velocity. They showed that both the jump characteristics and the grain velocity also depend on the density ratio s. They plotted their equation in terms of the dimensionless parameters $\Phi_B$ and $\theta$, presenting three curves for different density ratios s, together with selected flume data mainly taken from Yalin (1977), s. Fig. 2.4, covering a range of $\Phi_B$ from 0.001 up to 100 and of $\theta$ from 0.04 up to about 5. For a given shear rate $\theta$ larger than about 0.1 their equation predicts decreasing $\Phi_B$ values for decresing density ratios. Most of the flume data shown in the plot is for the transport of quartz grains in water but some data from Wilson (1966) for nylon particles (with s=1.138) in the higher shear intensity region ($\theta \approx 1$ to 3.2) seems to support the equation of Wang and Zhang also for s values smaller than 2.68. For $\theta$ values below about 0.1 the influence of s on $\Phi_B$ appears to be negligible. Thus their theory does not contradict the data for particles of different densities obtained by Luque and van Beek (1976) and by Meyer-Peter and Müller (1948) (since only a few data points of the Swiss investigators have $\theta$ values above 0.1, with a maximum of 0.25). However, the prediction of smaller dimensionless transport rates with decreasing s values at high shear stresses is not in agreement with Yalin's equ. (2.72), which predicts larger $\Phi_B$ values.

Low (1989) conducted a large number of experiments with lightweight sediments to investigate the effect of the the density ratio s on bed load transport rates. He used cylindrical plastic particles with various amounts of lead inside them to obtain s values between 1.17 and 2.46. Based on dimensional analysis and a regression of his experimental

results he found that the bed load transport rate should be related to the ratio of the shear velocity to the grain fall velocity; he proposed the equation:

$$q_B = 110 \frac{v^{*2} d}{W^5} \tag{2.75}$$

where $q_B$ is in [$m^3/s.m$], $v^*$ in [m/s], d in [m] and W in [m/s]. He incorporated an expression by Rubey (1933), in which the fall velocity is proportional to the factor $[gd(s-1)]^{0.5}$ for his experimental conditions. Then he obtained the relationship $\Phi_B = \Theta^3$, which is identical to the Einstein-Brown (Henderson, 1966) formula.

Low also compared his measured transport rates graphically with those predicted by different bed load transport equations; these included the formulae of Shields (equ. 2.65), of Meyer-Peter and Müller (equ. 2.67), of Bagnold (equ. 2.97) with the constant b = 4.25, of Yalin (equ. 2.72), and of Smart and Jäggi (equ. 2.83). It is interesting that with all the considered equations there was no systematic grouping of the data points belonging to a given density ratio s, except for the equation of Smart and Jäggi. Thus it appears that the first four formulae adequatly account for a change in the grain-fluid density ratio. Low performed a regression analysis in terms of the parameters used by Smart and Jäggi, and he proposed that their equation (2.83) should be multiplied on the right hand side by a factor of $(s-1)^{-0.5}$, in order to better account for a change in s.

### 2.3.1.3 Effect of increase in fluid viscosity, laminar flow

Willi (1965) studied the erosion of a gravel bed with time at steep slopes. He considered the effect of a change in the eddy viscosity $\nu'$ which is often defined as $\nu' = l^2 |dv/dy|$ (where l is Prandtl's mixing length), thus being analogous to the laminar kinematic viscosity $\nu$; the total shear stress can then be expressed as:

$$\tau = \rho \frac{dv}{dy} (\nu + \nu') \tag{2.76}$$

Using a relationship between the von Karman konstant $\kappa$ and the grain concentration developed by Einstein and Chien (1955), Willi found that the bed load transport rate $q_B$ should be proportional to $1/\sqrt{\nu'}$. He also

calculated $\nu'$ from his measurements and concluded from a regression analysis that in his measurements there was a much weaker dependence, i.e. $q_B$ was found to be proportional to $1/\nu'^{0.05}$.

Hong et al. (1984) examined the effect of a water temperature change from 30° C to near 0° C on the transport of sand in an open channel. For the given temperature variation the viscosity of water was varied by a factor of 2.5. For their flat bed runs they found only a slight increase in the bed friction factor but an increase in the bed layer discharge concentration by about a factor of 3 for the highest viscosity increase. The results of the individual runs are, however, not directly comparable because the experiments were conducted so as to maintain approximately a constant depth while the energy slope was higher for the lower temperature runs (Lau, 1987). Furthermore, Woo (1985) questionned the increase in the bed layer discharge on account of the uncertain definition of the reference concentration which Hong et al. used to distinguish between bed load and suspended load.

With regard to bed load transport Yalin (1977) stated that with decreasing Reynolds number the average distance travelled by individual particles is reduced. Both Davies and Samad (1978) and Coleman (1967) performed flume experiments concerning the fluid dynamic lift force on a particle near the bed at low Reynolds numbers. The results of both studies indicate negative lift force coefficients if the particle Reynolds number is less than 5, or (as an alternative criterion) if the laminar sublayer is larger than the particle size.

For bed load transport in turbulent flow Bagnold (1956) found that the grain concentration at the bed, $C_o$, reached a maximum of about 0.53 if $\theta \geq \approx 0.4$. From theoretical considerations, on the other hand, he calculated $C_o$ to be about 0.3 for bed load transport in laminar flow at $\theta = 2$. These findings may suggest that the bed load transport rate could be greater in turbulent flow than in laminar flow at the same dimensionless shear stress. In experiments with a very low particle-fluid density difference ($\sigma-\rho = 0.004$) in a closed rectangular channel, Bagnold (1955) observed that with increasing grain concentration turbulence was more and more suppressed; near the bed $C_o$ decreased from its maximum value in turbulent flow while the grain concentration at the top of the flow increased. At a mean concentration of $C_s \approx 0.35$ the flow was completely laminar and the grains were dispersed uniformly over the flow depth.

Later Bagnold (1973) stated that bed load transport by saltation can also occur in laminar flow and must therefore be a different process from that of the turbulent transport of suspended solids. Bridge and Dominic (1984) concluded that turbulence modifies the saltation trajectories, especially at the higher flow stages, and that the fluid-transmitted shear stresses become more important at higher shear velocities; this implies that bed load transport should be different in laminar and turbulent flow. Yalin and Karahan (1979) described that grains of the uppermost layer are dragged in laminar flows in the form of a "grain carpet", which is similar to Bradley's (1986) description of a moving "fluidized layer" near the bed.

#### 2.3.1.4 Hydraulic transport of solids in pipes

In section 2.3.2 it is shown that the experimental and theoretical derivation of a bed load transport formula for turbulent pipe flow by Wilson (1966, 1984, 1986) resulted in similar equations as the ones commonly used for open channel flows. Therefore the findings from pipe flow experiments may also be relevant for the prediction of the sediment transport behaviour in an open flume under similar flow conditions.

Brühl (1976) reported on a study in which he examined the effect of a slurry of fines on the hydraulic transport of sand in a pipe. According to his literature survey, previous studies indicated partly contradictory effects. He found with preliminary experiments that the pressure gradient, $\Delta H/L$, for the transport of sand in a bentonite slurry was reduced at lower velocities but increased at higher velocities, as compared to the case with clear water as carrier fluid. The reduction of the pressure gradient was the more pronounced, the finer was the slurry material and the larger was the sand concentration.

Brühl performed main tests with very fine limestone and quarzit particles (because they are chemically less reactive than bentonite clay). The limestone and quarzit slurries showed a slightly plastic (Bingham type) behaviour; a linear dependence of the viscosity on the slurry concentration was observed up to $C_f \approx 13$ % (where the maximum viscosity was about 3 cps.). In the presentation of the results for different slurry concentrations, the change in pressure losses were plotted as a function of the mean fluid velocity. The conditions at the critical deposit velocity (below which sand starts to settle out of the

flow) are probably most similar to equilibrium transport conditions in an open channel flow. It is noted that most sand particles moved in the layers near the bottom of the pipe, and in some cases there was a stationary deposit layer. For the transport of sand with a mean diameter of about 0.35 mm, Brühl found that the reduction in the pressure gradient at critical conditions increased with increasing fine material concentration. Again a larger reduction resulted for higher sand concentrations. This means that for a given bed slope in open channel flow, the sediment transport capacity should increase under the above conditions, if the pipe flow results are transferable.

A few other findings of Brühl's study may also be of interest. Experiments with a coarser sand of about 1.0 mm mean diameter indicated a somewhat smaller reduction in the pressure gradient for the transport in a slurry of fines. For the 0.35 mm sand, a reduction of $\Delta H/L$ was observed for the tests with a velocity V smaller than 4.5 m/s. For the tests with V = 5.0 m/s, however, $\Delta H/L$ was larger than for the clear water case.

Brühl concluded that main effect of the slurry of fines is to make the flow more homogeneous, which was also confirmed by measured velocity profiles. He attributed this homogenizing effect to the increased densitiy and viscosity of the fluid, resulting in decreased settling velocities W of the coarser particles. For the sand of 1.0 mm this reduction in W was less pronounced than for the smaller sand. The higher is the slurry concentration, the larger are the particles which make up the new homogenoeous fluid and which should no longer be looked at as "transported" sediment. At high velocities the transport mode is largely homogeneous also without any fine particles.

Brühl used existing methods, i.e. the approach of Durand and the one of Führböter, to calculate the $\Delta H/L$ values for his experimental conditions. He modified the density dependent parameters in these calculation procedures, and he also accounted for the reduced settling velocities in the fine material slurry. Thus he obtained much better predictions of the measured values than if he used the settling velocities in clear water. This too confirmed his hypothesis that the change in W is at least partly responsible for the change in the pressure gradient $\Delta H/L$.

A.D. Thomas (1979a,b) performed experiments to find the critical deposit velocity $V_d$ and the gradient at depsosition $J_d$ for the hydraulic transport of solids in pipes. He used both fluids and particles of different densities such that the density ratio s varied between 2.04 and 9.71 while the fluid viscosity differed as much as by a factor of 70. For large pipe sizes and for the case that the particle size d was larger than the thickness of the laminar sublayer $\delta$, he suggested to use the following equations given by Wilson and Judge (1976):

$$J_d = K_1 g\rho(s-1) \tag{2.77}$$

$$V_d = [2.0 + 0.3\log\frac{d}{DC_D}]\ [2gD(s-1)]^{1/2} \tag{2.78}$$

where D is the pipe diameter and $K_1$ is a constant. It can be seen that $V_d$, which can be looked at as an index of the transport capacity of the flow, is only affected by the fluid viscosity via the drag coefficient $C_D$. An increase in $C_D$ will result in a slight decrease in $V_d$, implying an increase in sediment transport capacity. However, the influence is only weak in equ. (2.78), as there is a logarithmic dependence on $C_D$. The opposite effect is predicted by equs. (2.77) and (2.78) as a result of a change in the density factor (s-1): The smaller is the density difference between the fluid and the transported solids, the higher will be the transport capacity of the flow.

For the other case, if $d \lesssim \delta$ and for solids concentrations $C_s$ up to about 20%, A.D. Thomas (1979a,b) developed semi-empirical expressions for the critical conditions at deposition, now denoted by $V_d^*$, and for $J_d^*$, respectively, as:

$$V_d^* = 1.1[g\eta(s-1)/\rho]^{1/3} \tag{2.79}$$

and

$$J_d^* = 4.4[1+C_s(s-1)][g\eta(s-1)/\rho]^{2/3}\rho/D \tag{2.80}$$

From these two equations it can be concluded that the higher the fluid viscosity the lower the transport capacity of the flow will be in the pipe. Obviously the influence of the fluid viscosity is larger for the case $d \lesssim \delta$ than for $d \gtrsim \delta$. A.D. Thomas (1979a) further showed that by combining the theories for the two cases he could improve the prediction

results for the cases where the particle size was close to the thickness of the laminar sublayer.

A.D. Thomas (1979b) also reported on experiments carried out in pipes under laminar flow conditions, where coarse particles were transported mainly in the sliding bed. He found that the pressure gradient required to prevent deposition will always be greater than in turbulent flow, implying a decrease in transport capacity in laminar flow.

Many experiments were carried out by Lanzendorf (1984) to study the motion of solid particles in a pipe at conditions where the thickness of the laminar sublayer is of the order of the grain diameter d. He studied the movement of isolated cylindrical particles along the smooth bottom of the pipe and found that the ratio of the particle to the local fluid velocity decreased with an increase in the relative thickness $\delta/d$ of the laminar sublayer. This again suggests that the transport capacity may be expected to decrease with increasing fluid viscosity, for otherwise constant flow conditions.

2.3.1.5 Summary

There seems to be general agreement that in turbulent hyperconcentrated flows the suspended load transport rates increase with increasing fine material concentration; this was concluded from field observations (Beverage and Culbertson, 1964; Bradley, 1986), from laboratory experiments (upper regime tests of Simons et al., 1963; Kikkawa and Fukuoka, 1969; Wan, 1982; Bradley, 1986; Wan and Song, 1987), and from theoretical considerations (Woo, 1985). What regards the effect on bed load transport rates, an increase in $q_B$ due to a decrease of the density factor (s-1) is predicted from experimental results by Shields (1936), by Meyer-Peter and Müller (1948) and by Luque and van Beek (1976), and from theoretical considerations by Yalin (1977) and by Woo (1985). However, Wan and Song's (1987) theory predicts a decrease in $\Phi_B$ for decreasing s values at higher shear stresses ($\theta \geq \approx 0.1$). Low (1989) found that many bed load transport formulae adequatly account for a change in the density ratio s, but that the Smart and Jäggi (1983) equation should be modified. Information on the effect of an increasing viscosity alone on $q_B$ in open channel flow is less conclusive (Hong et al., 1984; Woo, 1985; Lau, 1987). Wan (1982) concluded from his experiments that $\Phi_B$ was smaller in the bentonite suspension flows than

in the corresponding clear water flows, particularly in the low flow intensity region.

Results from pipe flow experiments indicate the following trends for the hydraulic transport of solids (at conditions that are probably similar to equilibrium bed load transport in flumes) in a slurry of fines: An increase in transport rates will result for the case where the thickness of the laminar sublayer is (still) smaller than the representative grain size, but a decrease can be expected if the flow is in the hydrodynamically smooth regime (Brühl, 1976; A.D. Thomas, 1979a,b). An increase in the thickness of the laminar sublayer (without any change in the density ratio s) will probably lead to a decrease in the transport rate of particles along the bottom of a pipe (Lanzendorf, 1984).

There is not yet much information available on sediment transport in laminar flow. In their experiments, both Wan and Song (1987) and Bradley (1986) observed an increase in the total bed material discharge; in Bradley's study the transport rates in laminar flow were about an order of magnitude higher than in the corresponding turbulent flow (with the same fluid discharge). Pipe flow tests reported by A.D. Thomas (1979b) may suggest that the bed load transport rates decrease in laminar flow, assuming that bed load is the predominant mode of transport at a velocity slightly above depositional conditions. Negative lift forces for particles near the bed (Coleman, 1967; Davies and Samad, 1978) and theoretical considerations by Bagnold (1956) seem also to indicate that bed load transport should be smaller in laminar flow than in turbulent flow.

### 2.3.2 Bed load transport at steep slopes and high shear stresses

It is only recently that interest on sediment transport problems has also focussed on steep streams. A limited number of laboratory studies have been made to study the bed load transport in steep flumes. But there is almost no field data available since it is very difficult to measure transport rates of coarse material in steep streams.

Smart and Jäggi (1983) performed flume experiments including slopes from 3 to 20 % and using gravel-sand mixtures as bed material. The mean

grain size $d_m$ was 4.2 and 10.5 mm for the two relatively uniform materials, while $d_m$ was 2.0 and 4.3 mm for the two materials with a wide grain size distribution. Their measured dimensionless transport rates $\Phi_B$ ranged from 0.13 up to 83. In the analysis of their experiments they also included the extensive data set of the Meyer-Peter/Müller experiments (given in Smart and Jäggi, 1983) which cover the low intensity transport region including flume slopes between 0.04 and 2%. A regression analysis of these two data sets resulted in the following bed load transport formula:

$$q_B = \frac{4}{(s-1)} \left(\frac{d_{90}}{d_{30}}\right)^{0.2} S^{1.6} \, q \, \left(1 - \frac{\theta_c}{\theta_m}\right) \tag{2.81}$$

where $d_{90}$ and $d_{30}$ are characteristic grain sizes, than which 90 % and 30 %, respectively, of the material by weight is finer. At high transport rates the sediment in motion occupied a significant part of the mixture flow depth $H_m$ which is then larger than the fictitious fluid (water) flow depth $H_f$ (=q/V). For this increase in flow depth Smart and Jäggi found an empirical relation as a function of slope and dimensionless transport rate:

$$H_f/H_m = 1 - 1.41 \, S^{1.14} \, \Phi_B^{0.18} \tag{2.82}$$

A transport formula in terms of the well-known dimensionless parameters can also be derived from equ. (2.81):

$$\Phi_B = 4 \left(\frac{d_{90}}{d_{30}}\right)^{0.2} S^{0.6} \, c \, \theta_m^{0.5} \, (\theta_m - \theta_c) \, \frac{\theta_f}{\theta_m} \tag{2.83}$$

where c is a flow resistance coefficient defined as $c = V/v^*$, $v^*$ and $\theta_m$ are to be calculated with the (corrected) mixture depth $h_{r,m}$, while $\theta_f$ should be determined with the (corrected) fictitious fluid depth $h_{r,f}$. Equ. (2.83) differs from their corresponding form given in Smart and Jäggi (1983) and in Smart (1984), where the factor $\theta_f/\theta_m$ had not been considered. Thus equ. (2.83) overpredicts the transport rates at the steeper slopes (high transport rates). A reinterpretation of their data and a discussion of the applied sidewall procedure is given in chapter 4.

Mizuyama (1977) carried out similar sediment transport tests with flume slopes up to 20 % and presented the following bed load transport equation for flow over a plane bed:

$$\Phi_B = \frac{12-24\sqrt{S}}{\cos\beta}\,\theta^{(1.5-\sqrt{S})}\,[1-k^2\frac{\theta_c}{\theta}][1-k(\frac{\theta_c}{\theta})^{1/2}] \qquad (2.84)$$

where k is a function of the slope.

Takahashi (1987) compared bed load transport formulae with several data sets from steep flume experiments. He slightly modified an equation developed by Ashida, Takahashi and Mizuyama in order to achieve better agreement also with the flume data of Smart and Jäggi, and proposed the following version of Mizuyama's equation:

$$\Phi_B = \frac{1+5\tan\beta}{\cos\beta}\,(\frac{8}{f})^{0.5}\theta^{1.5}[1-k'^2\frac{\theta_c}{\theta}][1-k'(\frac{\theta_c}{\theta})^{1/2}] \qquad (2.85)$$

where k' is also a function of the slope. It is not clear, however, whether $\theta$ is defined with $h_w$ or $h_m$ in equ. (2.84) and (2.85).

Daido (1983) also reported on bed load transport tests in steep channels. Based on experimental data including flume slopes up to 10 % and on theoretical considerations about the average transportation velocity and the mean thickness of the transported sediment layer he gave the following equation:

$$\Phi_B = B_2\theta^{1.5}(1 - \frac{\theta_c}{\theta})^{1.5} \qquad (2.86)$$

where $B_2$ is a proportionality constant that may be a function of the slope, the ratio $\theta_c/\theta$, the relative depth h/d, and the Froude number $Fr = V/(gh)^{0.5}$. For his experimental conditions Daido found $B_2 = 3.7$.

From data of Japanese steep flume tests that cover a slope range between 5 % and 25 %, and for conditions where $\theta$ is much larger than $\theta_c$, Mizuyama (1981) proposed a rather simple equation:

$$\frac{q_B}{q} = 5.5\,S^2 \qquad (2.87)$$

Ward (1986) collected available data on sediment transport in steep flumes. In addition to the 77 measurements of Smart and Jäggi he found another 46 observations with information on the ratio $q_B/q$, slope, median grain size, and gradation. A regression analysis resulted in a equation similar to (2.87) but including also grain size characteristics:

$$\frac{q_B}{q} = 7.16\ (d_{50})^{-0.25}\ (\frac{d_{90}}{d_{30}})^{0.2}\ S^2 \qquad (2.88)$$

where $d_{50}$ in [mm] is the characteristic grain size, than which 50% of material by weight is finer. The disadvantage of this formula is that it is not dimensionless on the right hand side, and thus application to a field situation seems questionable.

Takahashi (1987) introduced the term "immature" debris flow (s. also sec. 1.3) where the moving grain layer is in the domain of sediment gravity flow and the concentration over the whole thickness of the moving layer is approximately constant and equal to 0.4 $C_*$. It is different from a debris flow in that there is still a clear water layer above the moving sediment carrying almost no grains; and it is different from ordinary bed load by the fact that gravity rather than fluid shear is the main force acting on the grains. If an appropriate bed load transport and flow resistance formula is used, the limiting condition between ordinary bed load movement and an immature debris flow can be given in terms of the slope and a dimensionless water discharge $q^* = q/(g^{0.5}d^{1.5})$. Takahashi developed the following equation for immature debris flows; it is based on a part of the experimental data of Mizuyama, Smart and Jäggi, and Takahashi, and on observed grain velocity profiles:

$$\frac{q_B}{v^*\ d} = \frac{2}{3}\ \frac{4.2-0.3C_*}{\cos^2\beta(\tan\alpha-\tan\beta)^2}\ \theta^2\ (1 - \frac{\theta_c}{\theta})^2 \qquad (2.89)$$

Equ. (2.89) can be rearranged to give:

$$\Phi_B = \frac{2}{3}\ \frac{4.2-0.3C_*}{\cos^2\beta(\tan\alpha-\tan\beta)^2}\ \theta^{2.5}\ (1 - \frac{\theta_c}{\theta})^2 \qquad (2.89b)$$

From Takahashi's plot of the various debris flow types in a diagram of S vs. q* it can be seen that immature debris flows generally occur at

higher slopes and higher discharges q* than ordinary bed load transport flows. It appears from equ. (2.89b) that under these conditions $\Phi_B$ should depend more strongly on $\theta$ than under ordinary bed load transport conditions.

Wilson (1966) intended to study the bed load transport of fine bed material at high shear stresses. Previous flume data only covered $\Phi_B$ values up to about 10 and $\theta$ values up to about 1. He performed bed load transport tests with sand of 0.7 mm diameter in a pipe, because it was easier to achieve high shear stress conditions in a pressurized conduit. He measured $\Phi_B$ values up to 280 and $\theta$ values up to 8.4. This still seems to be the only comprehensive data set on bed load transport at such high shear intensities. From a correlation of his experimental results Wilson (1966, 1986) found the empirical relationship:

$$q_B = \frac{12}{g(s-1)} \left(\frac{\tau_o - \tau_c}{\rho}\right)^{1.5} \tag{2.90}$$

where $\tau_o$ is the shear stress at the surface of the deposit, corrected for ripple drag. It is evident that equ. (2.90) is basically similar to the Meyer-Peter/Müller formula, equ. (2.67), except that the constant is 12 instead of 8, which might be due to the fact that the equations are valid in different shear intensity regions and/or for different flow conditions. Fig. 2.4 (taken from Yalin, 1977) shows the experimental range covered by various studies on bed load transport including those of Wilson and Meyer-Peter/Müller.

Wilson (1984,1986) also made a theoretical analysis of bed load transport in turbulent pipe flow. From measured concentration profiles of coarse particle slurries he assumed a linear concentration distribution across the transported layer. Together with considerations on the grain velocity gradient and the thickness of the sheared layer he obtained the following theoretical equation:

$$q_B = \frac{1.51}{g(s-1)\kappa \tan\alpha} \left(\frac{\tau_o}{\rho}\right)^{1.5} \tag{2.91}$$

At high shear stresses $\tau_c$ is negligible in comparison to $\tau_o$. Wilson (1986) assumed $\kappa = 0.4$ and $\tan\alpha = 0.32$ (Bagnold's "inertial" value) which gives $1.51/(\kappa\tan\alpha) = 11.8$. It is interesting that equ. (2.91) is

very similar in form to the empirical equ. (2.90), and that - with the above assumptions - also the numerical constants are almost the same.

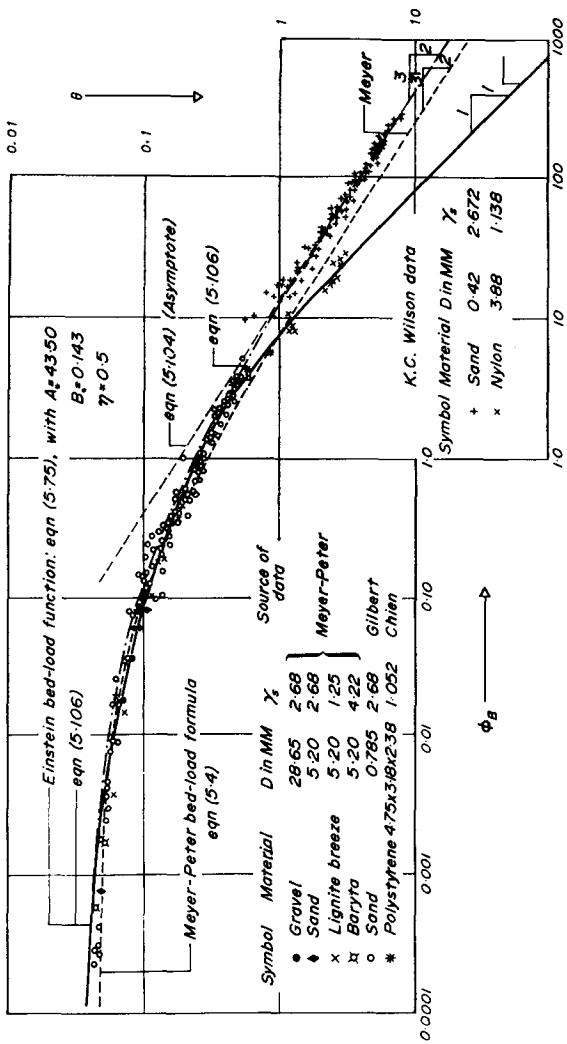


Fig. 2.4 : Comparison of bed load transport formulae with experimental data, after Yalin (1977).

Before reviewing selected sediment transport formulas Yalin (1977) presented theoretical considerations based on dimensional analysis. The following set of characteristic parameters may be used to define the two-phase motion of cohesionless granular material of specified geometry in a fluid:

$$\rho,\ \mu,\ \sigma,\ d,\ h,\ v^*,\ g(\sigma-\rho) \tag{2.92}$$

Choosing the seven independent parameters indicated in (2.92) and selecting d, $\sigma$, and $g(\sigma-\rho)$ as basic quantities, a general expression for sediment transport is obtained:

$$\Phi = \phi[g(s-1)d^3/\nu^2,\ \theta,\ h/d,\ s] \tag{2.93}$$

where $\nu = \mu/\rho$ is the kinematic viscosity of the fluid and $\phi$ is a function describing the dependence of $\Phi$ on the dimensionless parameters in the square brackets. The first term in the brackets is equal to $Re^*/\theta$ and reflects the influence of $\mu$; it has the advantage that it is independent of the flow stage.

From an inspection of the Meyer-Peter/Müller bed load transport formula, equ. (2.67), it can be shown (Yalin, 1977) that for very high shear intensities, i.e. $\theta >> \theta_c$, the following proportionality relation is obtained:

$$\Phi_B \sim \theta^{1.5} \tag{2.94}$$

or
$$i_B \sim \rho v_*^3 = \tau_o v_* \tag{2.95}$$

where $i_B$ is the bed load transport rate by immersed weight of solids per unit width.

Based on experimental data of both transport of quartz grains in water and in air, Bagnold (1956) developed a theory on bed load transport. His equation can be given as:

$$\Phi_{*B} = (\theta - \theta_c)\theta^{0.5} \tag{2.96}$$

where $\Phi_{*B} = q_B/b[g(s-1)d_m^3\cos\beta]^{1/2}$, $\theta = \theta/\cos\beta$ and $\theta_c = \theta_c/\cos\beta$. The factor $\cos\beta$ accounts for the reduction in shear resistance at higher bed

slopes. Yalin (1977) rederived Bagnold's equation in a shorter manner and obtained a slightly simplified version neglecting the influence of cosβ (which effect is smaller than 0.5% for slopes less than 10%):

$$\Phi_B = b(\theta - \theta_c)\theta^{0.5} \tag{2.97}$$

Yalin showed furthermore that for very high shear stresses equ. (2.97) ultimately results in the same proportionality relations (2.94) and (2.95) that he also had obtained from the Meyer-Peter/Müller formula. Bagnold (1956) found that extrapolated curves of the bed load portion of various sediment transport data on a log-log plot are asymptotic to the relation $\Phi_{*B} = 9 \cdot \theta^{3/2}$. In the same plot he also showed data of his experiments with a small density difference $(\sigma-\rho) = 0.004$; the transport of the light weight grains occurred in suspension but the data, including θ values up to about 4, plots parallel to the asymptotic relation for bed load transport.

Yalin (1977) also examined the bed load formula of Einstein (1950). For high shear stresses the original Einstein equation follows the proportionality relation $\Phi_B \sim \theta$. Yalin agreed on the principles of Einstein's formula but proposed some modifications in the details of its derivation. The modified version was then shown by Yalin to become asymptotic to $\Phi_B \sim \theta^{3/2}$ at high shear stresses, the same behaviour as demonstrated for the Meyer-Peter/Müller and the Bagnold formula.

In their theoretical development of a bed load transport equation Bridge and Dominic (1984) used an approach similar to the one of Bagnold (1956, 1973). They derived expressions for the mean velocity of the moving grains, $U_B$, and for the immersed weight of grains moving over a unit bed area, W', as:

$$U_B = a(v^* - v_c^*) \tag{2.98}$$

with $$a = \frac{1}{\kappa} \ln\left(\frac{y_n}{y_1}\right) \tag{2.99}$$

$$W' = (\tau_o - \tau_c)\tan\alpha \tag{2.100}$$

where $y_n$ is the distance of the effective fluid thrust from the boundary

and $y_1$ is the "roughness height". Combining equs. (2.98) and (2.100) yields:

$$\Phi_B = \frac{a}{\tan\alpha} (\sqrt{\theta} - \sqrt{\theta}_c)(\theta - \theta_c) \qquad (2.101)$$

For high shear stresses (i.e. $\theta >> \theta_c$) the proportionality relation $\Phi_B \sim \theta^{3/2}$ is obtained again. Bridge and Dominic theoretically discussed the influence of the parameters in equ. (2.99) on the value of 'a' and concluded that 'a' should increase for both fixed and mobile beds if the bed shear stress increases. They analyzed available data both on grain velocity and on sediment transport rates for lower and upper stage plane beds. They found the parameter 'a' to increase with transport stage (defined as $v^*-v^*_c$), which they attributed to increasing suspended sediment concentrations. $\tan\alpha$, on the other hand, was found to decrease with increasing bed load concentration, grain size and grain shear stress. The overall result is an increase in the value $(a/\tan\alpha)$ from lower stage plane beds (mean value 9.5) to upper stage plane beds (mean value 17.1). It may be interesting to note that in the Smart/Jäggi equation (2.83) for bed load transport on steep slopes there is the factor $cJ^{0.6}$ which is close to $cJ^{0.5} = Fr$; thus there seems to be a dependence of $\Phi_B$ upon the Froude number which varied in their experiments between approximately 1 and 3.

Hanes and Bowen (1985) theoretically developed a granular fluid model for intense bed load transport. They considered the moving grain layer to be composed of two zones: A region of collision dominated grain flow which they analyzed based on Bagnold's concept of dispersive stresses, and a saltation region where both grain and fluid stresses are important. They found that their theoretical equation for the total bed load transport can be fairly well approximated by a simple expression; Hanes (1986) later gave a corrected version as:

$$\Phi_B = 6\ \theta^{2.5} \qquad (2.102)$$

The theory of Hanes and Bowen allows to calculate $\Phi_B$ separately for the two bed load transport regions; they concluded that about 90 % of the total transport is contributed by the saltation zone.

Summary

From a limited number of flume experiments on bed load transport at slopes S steeper than about 10 %, it has been found that the ratio $q_B/q$ is proportional in first place to the factor $S^{1.6}$ (Smart and Jäggi, 1983) or to $S^2$ (Mizuyama, 1981; Ward, 1986).

Semi-theoretical considerations on bed load transport lead to the conclusion that - in terms of the conventional dimensionless parameters - the equation $\Phi_B = A\ \theta^{3/2}$ becomes a good approximation at high shear stresses (Bagnold, 1956; Yalin, 1977; Daido, 1983; Bridge and Dominic, 1984). This dependency is also confirmed from the analysis of hydraulic transport of solids in pipes (Wilson, 1984, 1986). For the case of an "immature" debris flow, where a grain layer starts to move as a whole, a relationship with the proportionality $\Phi_B \sim \theta^{2.5}$ has been proposed, based on experimental data (Takahashi, 1987). A theoretically developed granular fluid model also suggests that at very high transport stages the relationship $\Phi_B \sim \theta^{2.5}$ might be valid (Hanes and Bowen, 1985).

The studies of Smart and Jäggi (1983), Daido (1983) and Bridge and Dominic (1984) indicate that the bed load transport on steep slopes may further depend on flow conditions; experimental data suggests that the Froude number is an important parameter.

### 2.3.3 Initiation of Motion

Many studies about the beginning of sediment transport have confirmed in principle the well-known Shields (1936) curve (Yalin, 1977). In such a diagram the dimensionless shear stress at initiation of motion, $\theta_c$, is plotted against the particle Reynolds number, $Re^*$. The Shields curve shows the following characteristics: For $Re^* \geq \approx 400$ measured $\theta_c$ values vary between about 0.03 and 0.06, and often an average value of 0.05 is assumed; when the flow near the bed is the transitional regime between hydrodynamically rough and smooth flow, $\theta_c$ reaches a minimum at about $Re^* \approx 10$; below $Re^*$ of about 2 it has long been assumed that $\theta_c \approx 0.1/Re^*$ based on the few data points then available. Recently, some investigations have been made to study especially the incipient motion in the laminar boundary flow region (see below).

Slope effect and large relative roughness

For flows at steep slopes the calculation of $\theta_c$ has to be modified to account for changed gravity effects. Ashida and Bayazit (1973) introduced a new definition for the critical, dimensionless bed shear stress for incipient motion at steep slopes, $\theta_{sc}$:

$$\theta_{sc} = \frac{\theta_c}{\cos\beta\tan\alpha-(s/(s-1))\sin\beta} \tag{2.103}$$

Exactly the same definition was proposed by Mizuyama (1977) and by Daido (1983), and a similar one, neglecting the lift force influence, by Bathurst et al. (1982a). Ashida and Bayazit (1973) performed experiments on the initiation of motion in a steep flume at high relative roughness values d/h. They plotted their data in terms of $\theta_{sc}$ vs. d/h and showed that $\theta_{sc}$ increases from 0.04 for d/h $\leq\approx$ 0.4 to about 0.12 at d/h $\approx$ 1.7. However, in their experiments the values of d/h increased with increasing slope. Thus the increase in $\theta_{sc}$ seems to be mainly a slope effect appearing in the definition of $\theta_{sc}$, and the general trend in their plot may be due to spurious correlation because d/h is also a function of the slope.

An alternative way to express the critical, dimensionless bed shear stress for initiation of motion at steep slopes, $\theta_c'$, is to introduce a modification factor so that $\theta_c'$ can be compared directly to $\theta_c$ for low slope conditions. Based on a balance of moments acting on single grain on an inclined bed surface, Luque and van Beek (1976) suggested the equation:

$$\theta_c' = \theta_c \frac{\sin(\alpha-\beta)}{\sin\alpha} \tag{2.104}$$

They showed that the above equation represents their experimental data for slope angles $\beta$ = 12°, 18°, and 22°, if the angle of internal friction $\alpha$ was taken to be 47°. If the factor $\sin(\alpha-\beta)$ in equ. (2.104) is expanded, one obtains an equivalent formula, which was independently given by Stevens et al. (1976):

$$\theta_c' = \theta_c \cos\beta\left(1 - \frac{\tan\beta}{\tan\alpha}\right) \tag{2.105}$$

For example, if $\beta = 11.3°$ (S = 20 %) and $\alpha = 32°$ then $\theta_c$ is reduced according to equ. (2.104) or (2.105) by a factor of 0.67.

Ikeda et al. (1982) started from a force balance to calculate the reduction factor $\theta'_c/\theta_c$. They arrived at a rather complex equation which can be simplified if the lift force is assumed to be zero:

$$\theta'_c/\theta_c = (1 - \tan^2\beta/\tan^2\alpha)^{0.5}\cos\beta \qquad (2.106)$$

For the same example as given above ($\beta = 11.3°$, $\alpha = 32°$) the reduction factor is calculated by equ. (2.106) as 0.93. From their experimental data on the initiation of motion on side slopes and on plane level beds they concluded that the influence of the lift force can be neglected although inclusion of this effect results in a slightly lower prediction of $\theta_c$ or $\theta'_c$.

Low values of $Re^*$; $\theta_c$ in a Bingham fluid

Yalin and Karahan (1979) reported on an extension of the Shields' diagram by Mantz (1977) for the region $Re^* \lesssim 1$, for which the following relation is obtained based on new experimental data:

$$\theta_c = 0.1/Re^{*0.3} \qquad (2.107)$$

According to Yalin and Karahan it is not important for the initiation of motion whether the whole flow is laminar or in the hydraulically smooth region (with $\delta > d$) because the viscous flow near the bed is essentially the same if $\tau_o$ is also the same. But the conditions for the detachment of a grain are expected to be different for hydraulically transitional or rough turbulent flow as compared to laminar flow; for these two cases two different curves should exist for incipient motion. They performed experiments to determine $\theta_c$ both in laminar flows as well as in turbulent flows being inbetween the hydraulically smooth and rough regime. The experimental data seems to prove their hypothesis. For example at $Re^* \approx 6.5$, $\theta_c \approx 0.07$ for laminar flow and $\theta_c \approx 0.035$ for hydraulically transitional turbulent flow, while the two curves tend to approach each other for $Re^* \lesssim 1$. Similar experiments were carried out by Lin and Sun (1983) with a glycerol and water solution to determine $\theta_c$ in a viscous flow; they basically confirmed the existence of different curves for the incipient motion.

Daido (1971) proposed to use the shear stress ratio $a' = \tau_B/\tau_o$ as an additional parmater in calculating $\theta_c$ in a clay suspension (Bingham fluid). He showed theoretically that for $Re^* \lesssim 7$, $\theta_c$ should become larger with increasing non-Newtonian characteristic of the flow. For example if $a' = 0.5$, $\theta_c$ is increased by about a factor of 1.5 to 2.

In his study on the transport and the initiation of motion of plastic particles in a clay suspension, Wan (1982) theoretically developed a relation to express $\theta_c$ in a Bingham fluid flow:

$$\theta_c = 0.047 + K' \frac{7\pi}{2} \frac{\tau_B}{\rho g(s-1)d} \qquad (2.108)$$

He determined the constant $K' = 0.4$ from his experiments, which confirmed the linear dependence of $\theta_c$ on $\tau_B$. The highest measured value for $\theta_c$ was about 0.23. Wan did not indicate whether the flow in the corresponding experiments was laminar or turbulent, but the theoretical reasoning to obtain equ. (2.108) is based on the assumption of laminar flow. Similar to Daido's (1971) theory equ. (2.108) predicts an increase in $\theta_c$ with an increase of the Bingham yield stress $\tau_B$.

Critical flow discharge

Combining the Shields type criterion for initiation of motion with the Manning-Strickler flow resistance equation and a relation to characterise the grain roughness, Schoklitsch (1950) developed a formula for the critical flow rate (per unit width) at beginning of bed load transport, $q_{cr}$:

$$q_{cr} = 0.26\ (s-1)^{1.67}\ d_{40}^{1.5}\ S^{-1.17} \qquad (2.109)$$

where $d_{40}$ is to be used in [m] and $q_{cr}$ is in [$m^3$/s.m]. Equ. (2.109) is based on laboratory and field data. Bathurst et al. (1985b) proposed a non-dimensional version of Schoklitsch's equation. They examined a great number of experiments with regard to critical conditions at initiation of bed load transport. For a slope range $0.25\% \leq S \leq 20\%$ and for essentially uniform bed material, they introduced the equation:

$$q_{cr} = 0.15\ g^{0.5}\ d_{50}^{1.5}\ S^{-1.12} \qquad (2.110)$$

Equ. (2.110) may be modified to include a density factor (s-1), with the exponent given by equ. (2.109):

$$q_{cr} = 0.065\ (s-1)^{1.67}\ g^{0.5}\ d_{50}^{1.5}\ S^{-1.12} \qquad (2.111)$$

Whittaker and Jäggi (1986) performed experiments on the stability of block ramps, using rather uniform blocks at slopes between 5 % and 25 %. Based on similar considerations as above, they determined the following equation which defines the critical conditions at which the block ramp is beginning to be destroyed:

$$q_{cr} = 0.257\ (s-1)^{0.5}\ g^{0.5}\ d_{65}^{1.5}\ S^{-1.167} \qquad (2.112)$$

where $d_{65}$ is the characteristic grain size, than which 65 % of material by weight is finer. Retaining the same exponent of the density factor as in equ. (2.111), equ. (2.112) may be transformed into (using s=2.65):

$$q_{cr} = 0.143\ (s-1)^{1.67}\ g^{0.5}\ d_{65}^{1.5}\ S^{-1.167} \qquad (2.113)$$

By comparing equ. (2.113) with equ. (2.111) it can be concluded that the critical discharge predicted for the block ramp situation is roughly twice as high as for the beginning of bed load transport data which is the basis of the constant in equ. (2.110) and (2.111). The relative depths in the block ramp tests were in the range $0.5 < h/d_{65} < 5$, and thus they were possibly somewhat lower than in the flume situations analysed by Bathurst et al., but there may be other reasons for the different constant.

It is noted again that the formulae for the critical flow discharge were derived from the concept of a critical shear stress, and thus there is no basic difference in using one approach or the other.

# 3 EXPERIMENTS

## 3.1 Experimental program

As mentioned in section 1.4 the objective of the study was to determine the bed load transport capacity of a slurry flow in a channel at steep slopes. The muddy slurry flowing in a torrent was simulated in the laboratory by recirculating a clay suspension. Various amounts of clay were mixed into the water circuit in order to examine the effect of an increasing density and viscosity of the carrier fluid on the sediment transport capacity.

The flow behaviour and sediment transport characteristics were examined for five different clay concentration (or fluid density) levels; the highest concentration of the clay suspension was about 22 % by volume, for which the flume system could be reasonably well operated. For each concentration level two kinds of tests were performed. First the flow resistance was measured for flows of the clay suspension without sediment transport. This allowed to study the effect of the non-Newtonian rheological properties of the clay suspension on the flow behaviour, independent of any interference with transported sediment in a two phase flow. In a second step, both the bed load transport capacity of the clay suspension and the flow resistance of the fluid-gravel mixture were determined for each concentration level.

One objective of the study was to compare the new experiments with the results obtained by Smart and Jäggi (1983) who had used clear water as transporting fluid. It was decided to use the same sediment as the bed material No. IV of Smart and Jäggi. Thus their results could serve as reference conditions, being equal to the case of a suspension with 0% clay content (or a fluid with the density of water).

The flume slope, the fluid discharge and the fluid density (clay concentration) were set for each experimental run; together with the rheological properties they formed the independent parameters. The fluid velocity, the (mixture) flow depth and the equilibrium bed load transport rate were measured as dependent parameters.

## 3.2 Flume apparatus

Sediment transport tests in a steep flume had already been performed at the same hydraulic laboratory by Hänger (1979) and by Smart and Jäggi (1983). For the new tests with the objective of recirculating a clay sespension, the existing laboratory setup was slightly modified. A schematic sketch of the flume system is shown in Fig. 3.1.

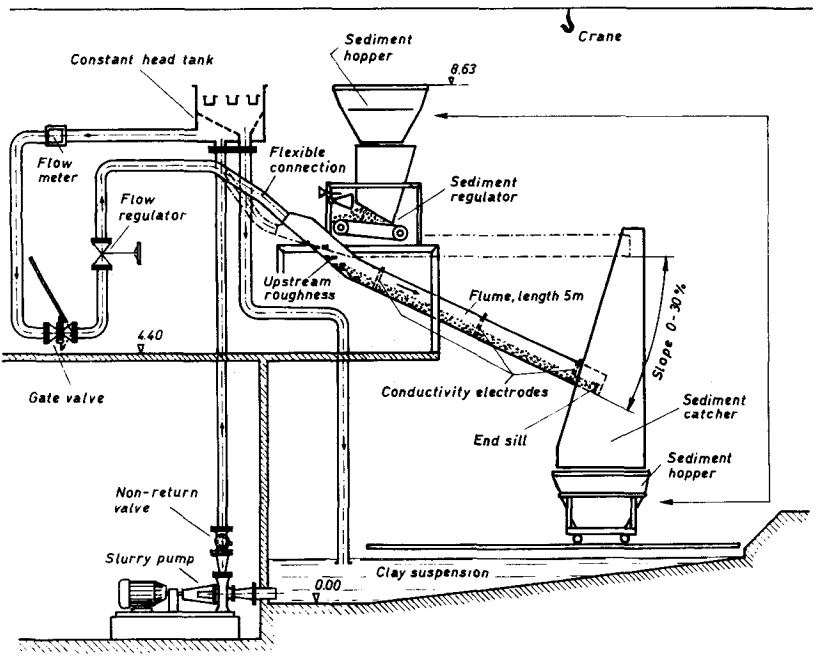


Fig. 3.1 : Schematic sketch of the flume system.

The water or clay suspension was recirculated in a independent fluid circuit. First a conventional water pump was used, but after having reached a certain concentration of the clay suspension (about 15 % by volume), a special slurry pump had to be installed. Settling of clay particles had to be expected during times when the pump was not operated. Therefore the volume of the sump was made as small as

possible, in order to limit the amount of added (dry) clay and to minimize concentration fluctuations after resuspension of settled clay particles. The overall volume of the circuit was about 10 $m^3$, including the sump, the constant head tank and the pipelines.

The flume had a usable length of 5 m, with a width of 20 cm and 40 cm high perspex side walls. The bed material consisted of relatively uniform gravel. It was fed from two pairs of exchangable sediment hoppers via a conveyor belt which discharged the gravel into the slightly steeper upstream portion of the flume. There roughness elements were installed in order to avoid scouring of the movable bed at the top of the flume. The movable bed was maintained by an end sill of adjustable height. The roughness elements consisted of three tooth-shaped metal ˜lates, fixed about 10 cm apart from each other across the bottom of the flume. They could be tilted at any angle against the flow, in order to adjust the upstream roughness as required by flow conditions.

Before performing a sediment transport test the desired flow rate was set by a regulating valve. Then a movable bed was built up by initially reducing both the sediment input and the flow rate, using a gate valve. This could be opened quickly to set the desired flow rate again; the sediment feeding rate was increased almost simultanously, so that initial scouring of the bed could be avoided.

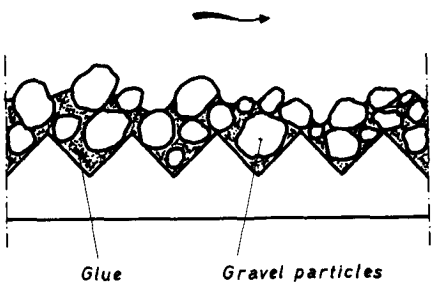


Fig. 3.2 : Longitudinal section of the fixed rough bed, made of gravel particles glued on a tooth-shaped PVC-plate.

In order to determine the flow resistance for the clay suspension alone, without any sediment transport but under similar roughness conditions, a fixed rough bed was mounted on the flume bottom. The fixed bed was made of gravel particles glued on a tooth-shaped PVC-plate (s. Fig. 3.2), so as to obtain a slightly irregular plane bed which is more like a natural bed than a completely plane bed. The grain size distribution of the gravel particles was the same as for the bed material used in the sediment transport tests (with $d_m$ = 10.0 mm, s. section 3.4).

## 3.3 Clay material and clay suspension

Since the fluid volume of the circuit was about 10 $m^3$ and some part of the added clay was "lost" (for the suspension) having settled out in dead zones of the system, several tons of clay were necessary to achieve a volume concentration of the flowing suspension of over 20 %. A clay called Opalit (brand name) was used for the experiments. It is commercially available in Switzerland, and is ground from the so called "Opalinuston". Opalit can serve as a sealing material in earth dams or other works. This type of clay had been previously used for hydraulic experiments by Abdel-Rahman (1963) and in soil mechanics research by H. Einstein (1966).

The grain size distribution curves for Opalit as given by the above two authors are shown in Fig. 3.3, and soil mechanical and mineralogical properties are listed in Table 3.1. The values given by H. Einstein and by Abdel-Rahman differ somewhat from each other. This could be due to either variations in the composition of the used Opalit or to different methods used in analyzing the samples. In this study, the particle density of the Opalit was taken as 2.65 $g/cm^3$.

Determination of the particle size distribution can be very difficult, and for certain clay types very differing results may be obtained (Grim, 1968). If the clay fraction of Opalit is determined with a more modern method than wet sedimentation, it is about 40% (Kahr, 1989). This value corresponds better with the overall mineral content for the clay groups given in Table 3.1.

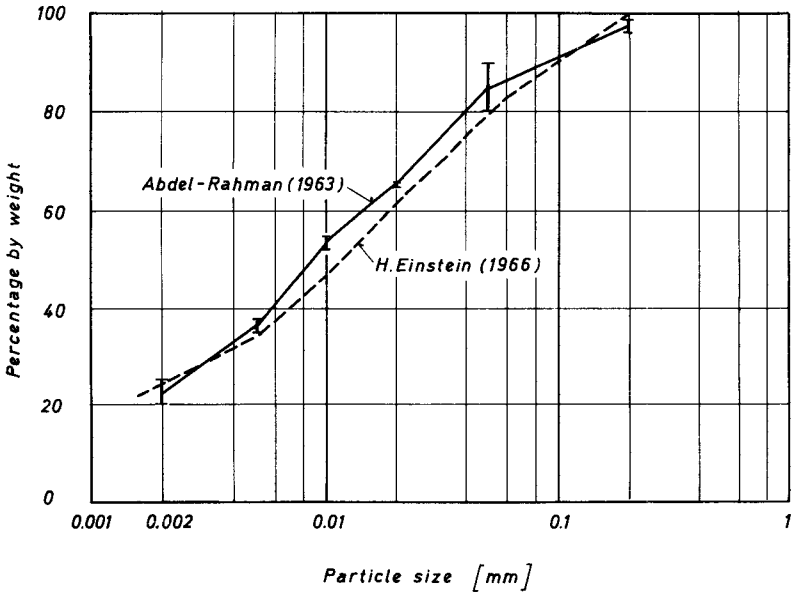


Fig. 3.3 : Grain size distribution curves for Opalit clay.

| Property: | H. Einstein (1966): | Abdel-Rahman (1963): |
|---|---|---|
| Liquid limit [%] | 47.3 | 41.0 - 43.0 |
| Plastic limit [%] | 16.6 | 18.0 - 19.5 |
| Plasticity index [%] | 30.7 | 23.0 - 23.5 |
| Particle density [g/cm³] | 2.71 | 2.60 - 2.65 |
| Clay fraction < 0.002mm [%] | 24.2 | 22.0 - 25.0 |
| Mineral content [%]: | | |
| Illite (Muskovite) | 20 - 25 | |
| Kaolinite | 20 - 25 | |
| Chlorite | 5 - 10 | |
| mixed-layer type clay | 5 - 10 | |
| Calcite | 10 | |
| Carbonate | | 6 |

Table 3.1 : Soil mechanical and mineralogical properties of Opalit clay.

The clay was added into the operating circuit via the conveyer belt of the sediment feeding machine. Thus the addition rate was regular and could be kept small, so that good mixing of the dry clay with the flow was obtained and no particle aggregation or clusters formed.

Once the pump had been started it took no longer than half an hour until the flow had established a new equilibrium between the resuspended particles and the ones still resting in the dead zones of the system; then the fluid density remained practically constant until the pump was shut off again. After a day or two of not operating the system, the density of the flowing clay suspension had decreased by a few tenths of a percent at the lower concentration levels, and up to a few percent at the higher concentreation levels. This change affected the rheological properties of the fluid only about as much as the uncertainty of the viscometric measurements. However, if one series of experiments for a given concentration level lasted more than about a week, or if the system was not operated for a similar period, the fluid density decreased by a greater amount, changing the rheological parameters $\tau_B$ and $\eta_B$ by more than 10 %.

It should be noted, however, that there was no experimental requirement to keep the Bingham parameters constant at a given clay concentration level, since they were measured separately for each experiment.

For the examined steep slopes, flow rates and relative roughnesses, and with the roughness conditions at the flume entrance, the turbulence intensities were found to be sufficient to result in a uniform concentration distribution of the suspended clay particles over the flow depth.

### 3.4 **Bed material**

One of the four bed materials used by Smart and Jäggi (1983) was also taken for this study. For experimental reasons their material no. IV was chosen. As it is the coarsest sediment mixture they had employed and comperatively uniform, the separation of the transported gravel in the downstream sediment hoppers from the clay suspension could be best achieved. The clay slurry is drained and separated from the grains in the hoppers through a plastic mesh on one side, with quadratic holes of

2 mm width. If a finer bed material with a wider grain size distribution had been used, drainage of the clay suspension would have become difficult or impossible already at lower clay concentrations than with the selected material. The grain size distribution of the material used is shown together with material no. IV of Smart and Jäggi in Fig. 3.4. They claimed that the slight variation in grain size distribution during the tests did not significantly affect the results.

Table 3.2 gives the characteristic diameters of the original mixtures of these two bed materials. The new mixture was made from the same, naturally river rounded grains that had been previously used by Smart and Jäggi and also by Hänger (1979). The specific density of the material had been determined by Hänger as 2680 kg/m³, and the angle of repose as 32.5°; these values were also adopted for this study.

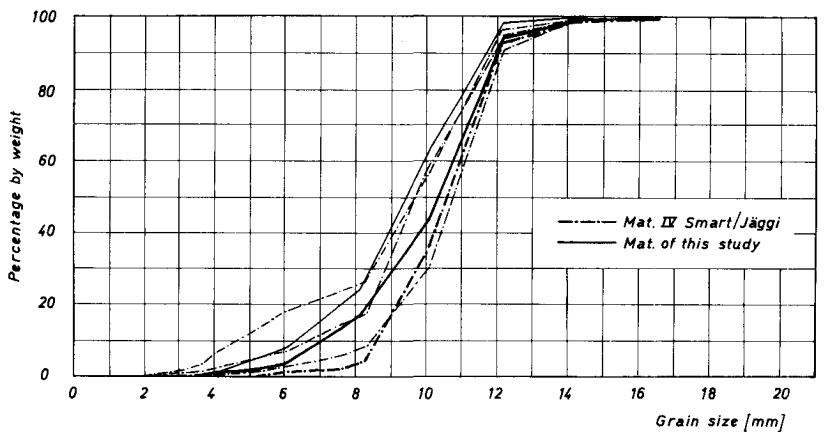


Fig. 3.4 : Grain size distribution curves of the bed material used in this study, in comparison with material no. IV of Smart and Jäggi (1983); the thick line refers to the original distribution, the thin lines represent samples taken during or after the tests.

| Material: | $d_m$ [mm] | $d_{90}$ [mm] | $d_{30}$ [mm] | $d_{90}/d_{30}$ |
|---|---|---|---|---|
| of this study | 10.0 | 12.0 | 8.7 | 1.38 |
| no. IV of Smart and Jäggi | 10.5 | 12.1 | 9.0 | 1.34 |

Table 3.2 : Grain size characteristics of bed material.

## 3.5 **Measuring methods**

### 3.5.1 **Slope**

The flume slope, which was preset before each test, was one of the independent parameters. It was measured by a spirit-level. The maximum error $\Delta S_B$ in the slope setting of the flume bottom was determined by levelling to be about $\pm 0.3$ % (absolute slope value).

At equilibrium transport conditions both the slope of the movable bed and the fluid surface slope should be approximately equal to the flume slope. The maximum deviation of the fluid surface slope from the flume slope was less than $\Delta S_F = \pm 0{,}4$ %. Thus the maximum, absolute deviation of the energy slope from the flume slope S amounts to $(\Delta S_B + \Delta S_F) \simeq \pm 0.7$ %. This results in a maximum relative error of $(\Delta S_B + \Delta S_F)/S = 0.10$ for a slope S = 7 % or of $(\Delta S_B + \Delta S_F)/S = 0.035$ for a slope S = 20 %.

### 3.5.2 **Fluid discharge**

A magnetic flow meter was used to monitor the fluid discharge. According to the manufacturer the relative accuracy of the instrument should be within $\pm 1$ % of the actual flow rate. Fluctuations of the fluid dis-

charge during a test were generally also less than ±1 %, as indicated by relatively slow changes in the reading.

However, at the two highest clay concentration levels the reading was observed to vary by as much as about 10 %. This might have been due to local and periodic clay accumulations in front of the plate of the regulating valve, influencing also the flow in the magnetic flow meter about 2 m upstream of the valve. Therefore the instrument was placed further upstream in a vertical part of the pipeline where no adverse effects due to deposited and partly consolidated clay material had to be expected. This measure, however, did reduce the fluctuations in the reading only partly, indicating that they probably originated in the head tank.

### 3.5.3 **Sediment discharge**

The sediment feeding rate could be controlled by regulating the speed of the conveyer belt, which is driven by rollers, and by adjusting a slot through which the gravel was discharched into the flume.

The sediment feeding machine was originally calibrated by Hänger. He determined the roller speed in function of the position of the regulating knob (s. Fig. 3.5). Having installed an additional regulating knob at a more convenient place, Hänger's function was checked by new measurements, which are also shown in Fig. 3.5. At the highest speeds the new points indicate a slight deviation from the original, straight line.

The result of the calibration for the bed material no. IV used both by Smart and Jäggi and by Hänger is given in Fig. 3.6.[1)] Because the gravel mixture of this study was slightly different from the original material no. IV, a few check measurements were made with the new mixture. The corresponding points are also shown in Fig. 3.6.

---

1) In the original Fig. 8 of Smart and Jaeggi the ordinate is incorrectly labelled "$G_B(s-1)$" instead of "$G_B(s-1)/s$" which represents the weight measured under water.

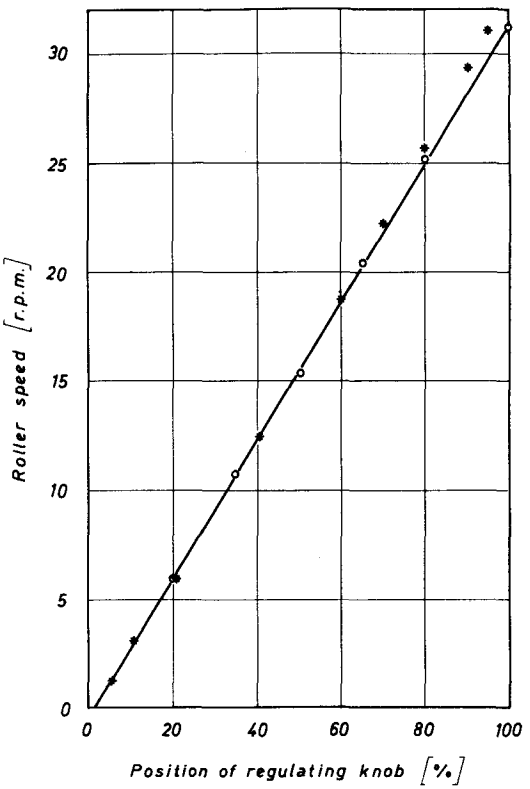


Fig. 3.5 : Relation between the position of the regulating knob and the roller speed (expressed in revolutions per minute) of the sediment feeding machine; the stars indicate control measurements.

Both Fig. 3.5 and 3.6 indicated that the original calibration curves could also be adopted for this study, if the position of the regulating knob would not exceed a value of 70 %. For the experiments of this study, the position of the regulating knob was in one case at 71 %, otherwise it was lower. The deviation of the control measurements from the originally calibrated feeding rates is estimated to be less than a few percent.

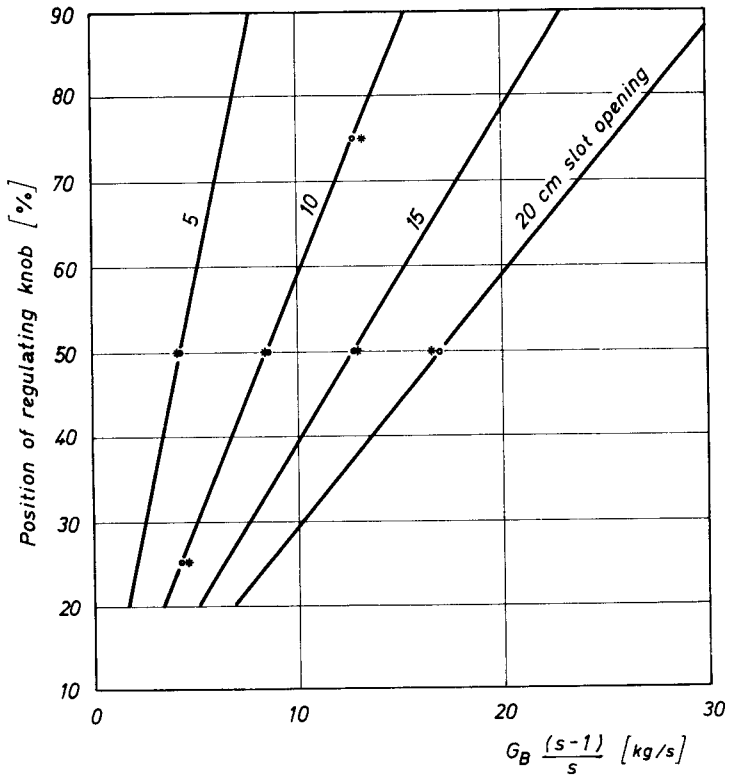


Fig. 3.6 : Resulting calibration lines of the sediment feeding system for bed material no. IV of Smart and Jäggi and of Hänger; the stars indicate control measurements of this study.

### 3.5.4 **Fluid velocity**

In a sediment transporting flow at steep slopes the solids occupy a considerable part of the flow cross-section; the heavier particles do not move with the same velocity as the carrier fluid except for debris flows. Therefore the fluid velocity cannot be determined from a knowledge of the mixture flow depth and the flow rate alone.

A method to measure the fluid velocity in such a two phase flow is the salt-velocity technique (see for example Davies and Jäggi, 1981). It was already employed by Smart and Jäggi (1983). Also in this study three pairs of electrodes were fixed on the flume walls (s.Fig. 3.7). By injecting a slug of salt solution the conductivity increase due to passage of the salt cloud can be recorded at each measuring cross-section. The conductivity readings were transmitted via an analog/digital converter to a personal computer where they were stored and analysed.

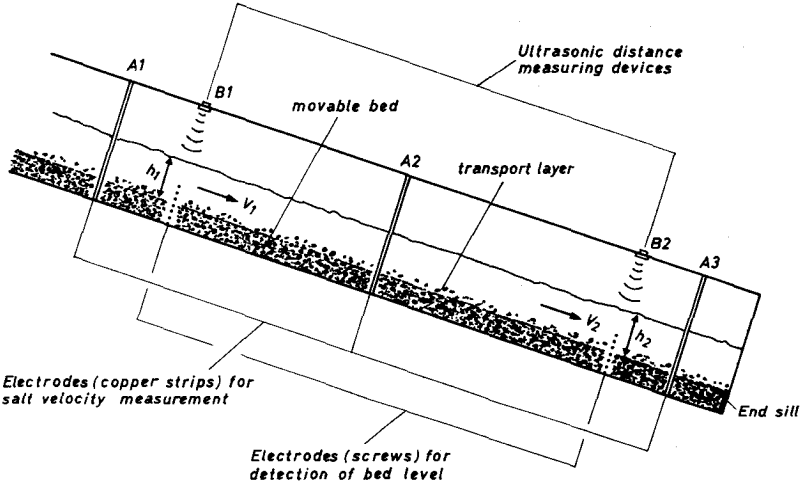


Fig. 3.7 : Measurement installations along experimental flume to monitor fluid velocity ($V_1$, $V_2$), fluid surface level and bed level ($h_1$ and $h_2$ are the mixture flow depths); A1, A2, A3 and B1, B2 refer to locations of measuring cross-sections.

Fig. 3.8 shows three different types of small tubes which were used for an optimal injection of the salt solution into the flow at the top of the flume. At the lower clay concentrations of the suspension the tracer was injected from a glass bottle, in which a higher pressure was produced manually. At higher clay concentrations above about $C_f \approx 10$ % this method did no longer provide sufficient mixing of the salt solution with the fluid. Therefore the glass bottle was replaced by a steel tank

which allowed to use higher pressures. With pressures between 1.5 and 2.5 bar the tracer could then be injected much faster too, and mixing was sufficient again.

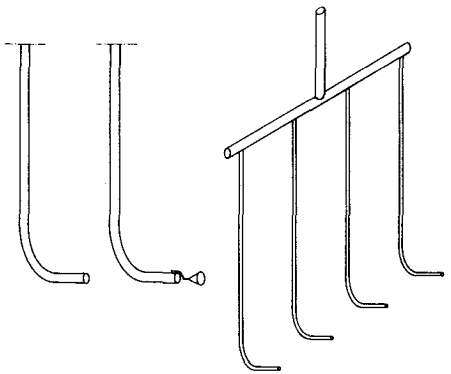

Fig. 3.8 : Three types of tubes used to inject the salt solution into the flowing clay suspension.

If the salt solution is well mixed with the flow, the recorded conductivity increase is representative for the whole measuring cross-section. Then the average fluid velocity can be calculated as the travelling time of the salt cloud between two cross-sections divided by the corresponding interdistance of the electrode pairs. Having installed three electrode pairs, the velocity in the upper and lower reach of the flume could be determined.

The sampling frequency of the conductivity readings was 33 Hz. This is clearly above the frequency of the fluid surface undulations, which were estimated to be between 1 and 10 Hz (with wave amplitudes of up to about 1 cm). An example of the conductivity readings is shown in Fig. 3.9.

The calculation of the travelling time of the salt cloud is illustrated in Fig. 3.10. The starting point ($t_A$) of the conductivity increase is generally clearly defined; the determination of an end point ($t_E$) may be more difficult because the tail of the curve can be quite long. To separate the base conductivity signal from the peak due to the

salt tracer, a base line had to be determined. Similar to the procedure of Smart and Jäggi, the mean value of all conductivity readings was calculated and multiplied by a certain factor which was found from experience. A moving average value was then used to compute the starting and end point of the passing salt cloud.

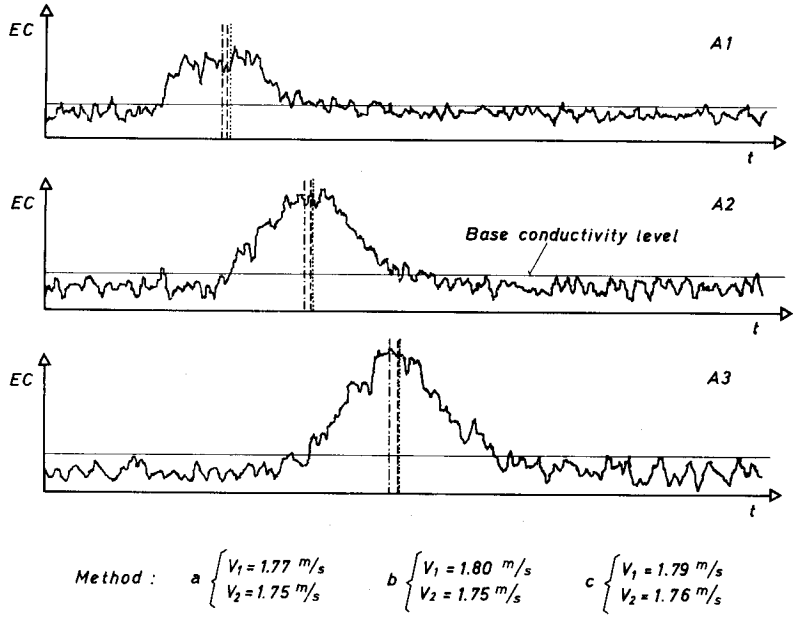


Fig. 3.9 : Example of salt velocity measurement. Conductivity readings (EC = electric conductivity) in function of time (t) are shown for the three measuring cross-sections (A1, A2 and A3). The average fluid velocity in the upper ($V_1$) and lower ($V_2$) flume reach was calculated by the three methods a, b, and c. (The experimental conditions for this run were: S = 20 %, Q = 10 L/s, $\rho$ = 1.08 g/cm$^3$; no sediment transport.)

Three different methods were employed to find a reference time which is representative for the passage of the tracer (s. Fig. 3.10). The first method (a) is the same as the one used by Smart and Jäggi,

determining the centroids of the whole area under the peak; Fig. 3.10a shows the line through the centroid defining the time $t_a$. With the second method (b) the reference time ($t_b$) is determined by the line dividing the area under the conductivity curve into two equal halves, s. Fig. 3.10b. The third method (c) is one described by Cao (1985): The reference time ($t_c$) is computed for the centroid of the shaded area in Fig. 3.10c; the shaded area is calculated via an intermediate conductivity value ($EC_{E'}$) which is a function of the difference between the base conductivity level ($EC_A$) and the peak conductivity level ($EC_P$).

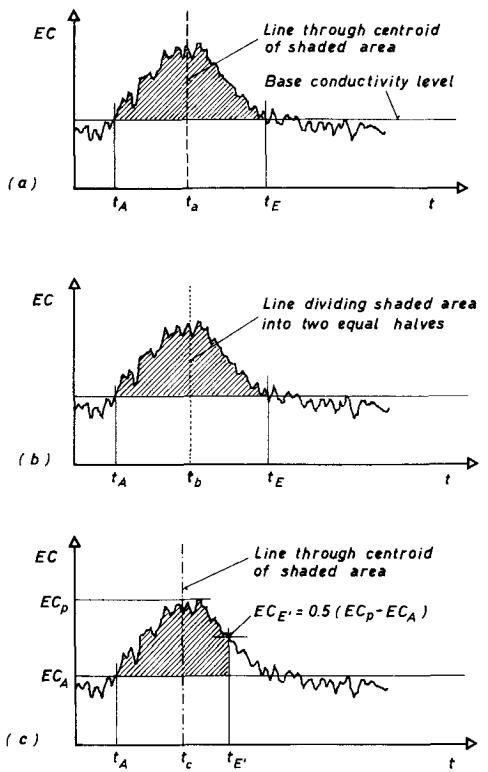


Fig. 3.10 : Three methods to determine the reference time ($t_a$, $t_b$, $t_c$) for calculating the travelling time of the salt cloud, using the salt velocity technique (EC = electric conductivity).

From a knowledge of the flow rate and the measured flow depth for a flow over the fixed bed without any sediment transport, the average fluid velocity could also be calculated; it is denoted by $V_h$. This allowed an independent check of the above three methods to be made; the corresponding velocities are refered to by $V_{mes}$. Fig. 3.11 shows the ratio $V_{mes}/V_h$ in function of the relative depth for all three methods.

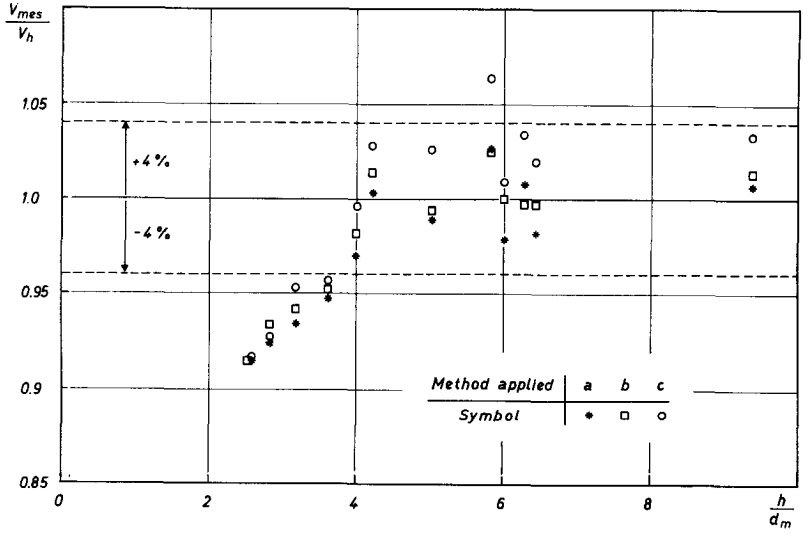


Fig. 3.11 : Ratio of velocity measured with salt tracer technique to the one obtained from the flow rate and flow depth measurement ($V_{mes}/V_h$), in function of the relative depth ($h/d_m$); the three different methods (a, b, c) are compared that were used to determine $V_{mes}$ from the conductivity readings.

It can be seen from Fig. 3.11 that the salt velocity technique tends to give too lower velocities than the depth-discharge method, for relative depths values less than about 4. (In the sediment transport tests

the values $h_m/d_m$ were always above 4, so that this peculiarity did not affect the corresponding velocity measurements.) A comparison of the three analyzing methods shows that method c seems to give slightly too high velocities while methods a and b yield comparable values. A very similar picture regarding the average velocities determined at lower relative depths was also obtained by Bathurst et al. (1984), s. Fig. 3.12. It is difficult to decide whether the salt-velocity technique or the depth-discharge method is more reliable in this region; the determination of the flow depth gets more uncertain and three-dimensional effects become more important with decreasing h/d values.

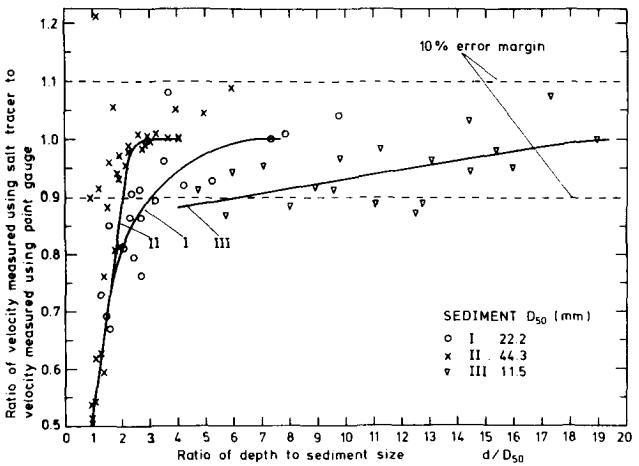


Fig. 3.12 : Figure taken from a study by Bathurst et al. (1984) showing the ratio of velocity using the salt tracer method to velocity measured using the point gauge method, in function of the ratio of depth to sediment size, $h/d_{50}$; data are for flows without sediment transport (sediment I, II and III) or with low rates of sediment transport (sediment III only); calibration curves (solid lines) were fitted by eye.

Because of the relatively strong fluctuations in the conductivity signal (s. Fig. 3.9), the velocities for the upper flume reach ($V_1$) and

for the lower reach ($V_2$) differed sometimes by more than 5 %. During the analysis it was decided to use only those measurements with $(V_1-V_2)/V_2 <$ 5 % for the determination of a mean value. The mean value for each test was generally determined from a minimum of 7 individual velocity measurements.

Having found that method (a) gave the largest number of useful measurements under all flow conditions, it was selected for the final analysis of the experiments.

Because of corrosion problems in the pipe system it was desirable not to use sodium chloride as tracer salt. Also, the applied salt should influence the rheological properties of the clay suspension as little as possible. One possible problem is that cations in the clay structure may be replaced by ions of the added salt. According to Grim (1968) the replacing power of $Na^+$ is much weaker than that for other common cations. It was therefore decided to use sodium acetate as tracer salt. A few viscometric measurements were carried out to check the effect of the added salt on the Bingham parameters of the clay suspension. The results indicated that the rheological parameters did not change noticably if the amount of sodium acetate was kept below about 20 % by weight of clay in the suspension.

### 3.5.5 **Flow depth**

Smart and Jäggi (1983) determined the mixture flow depth ($H_m$, s. Fig. 3.14) by visual observation of the flow through the perspex flume wall. By using a muddy clay suspension in this study, the motion of the grains could no longer be visually detected. Furthermore it was desirable to have an automatic recording and display of the flow depth on a personal computer, so as to have a faster and more accurate method to find the equilibrium transport conditions.

Two kinds of measurements were required: to record the fluid surface level and, in addition, to determine the bed level in the case of the sediment transport tests.

Two ultrasonic distance measuring devices were installed, one at an upstream and one at a downstream cross-section 3.5 m apart (s. Fig.

3.7). They were operated at a measuring frequency of about 30 Hz, which was found to be sufficient for fluctuations of fluid surface undulations with a frequency of about 1 to 10 Hz; the sampling frequency was about 40 Hz. The instruments gave a digital distance reading with a resolution of 1 mm. The air temperature was recorded before each series of measurements, and a numerical correction was applied for the change of sound velocity with temperature. The fluid surface level was measured during five to seven seconds, before an average value was displayed and stored on the computer.

In the case of tests without any sediment transport, the flow depth (H) could then be determined. The bed level of the fixed rough bed was taken as the mean elevation of the roughness elements (grains) above the flume bottom (s. Fig. 3) at the measuring cross-sections (B1 and B2, s. Fig. 3.7). For a fluid flow over the fixed rough bed, the standard deviation of repetitive fluid surface measurements (determined as an average value over 5 second periods) was generally less than 0.5 mm which gives an idea of how reproducible these measurements were. The maximum amplitude of the surface undulations was about ±1 cm.

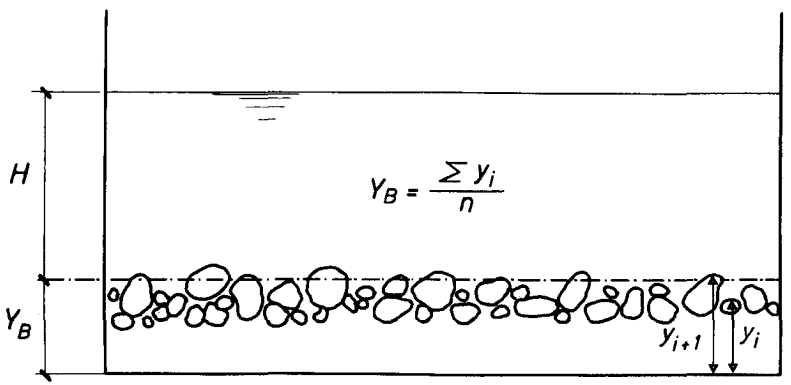


Fig. 3.13 : Scematic sketch of flume cross-section illustrating the method to determine the level of the fixed rough bed.

In the sediment transport tests the thickness of the erodible but not moving grain layer in the flume depends mainly on the height of the end sill and to some extent also on the flow conditions. The bed level was defined as the height above the flume bottom where the largest gradient in grain velocity over depth could be detected. In transport tests with clear water as a carrier fluid, it was observed that a rather marked boundary exists between fast moving grains of the bed load transport zone and the almost stationary gravel particles in the bottom layer underneath.

The following technique was employed to detect the bed level: At the same two measuring cross-sections (B1 and B2) where the ultrasonic devices were installed, a number of "point" electrodes (screws) were fixed at different levels above the flume bottom on both side walls, each successive level (screw) being 5 mm higher (s. Fig. 3.14). During a

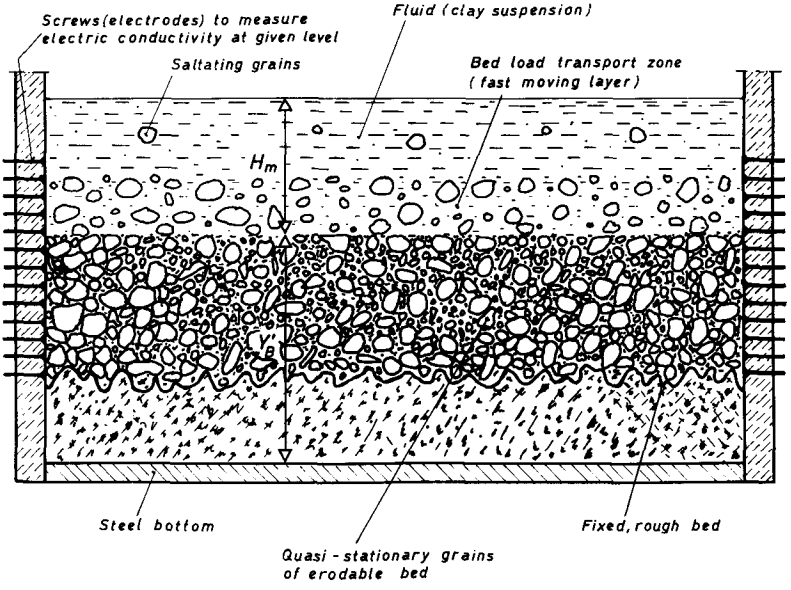


Fig. 3.14 : Scematic sketch of flume cross-section illustrating the method to determine the bed level, i.e. the boundary between the fast moving transport layer and the quasi-stationary zone of the erodable bed.

sediment transport test, the electrical conductivity across the flume (width) was recorded simultanously at six consecutive levels. Examples of such measurements are presented in Fig. 3.15. The sampling frequency was again about 40 Hz, and each measurement lasted about 7 seconds. At a level where grains of the bed load layer were moving fast through the cross-section, the conductivity signal showed marked fluctuations with a frequency of a few Hz. On the other hand there were less frequent and lower amplitude fluctuations (or almost none at all) in the conductivity readings from a level where the bed was quasi-stationary.

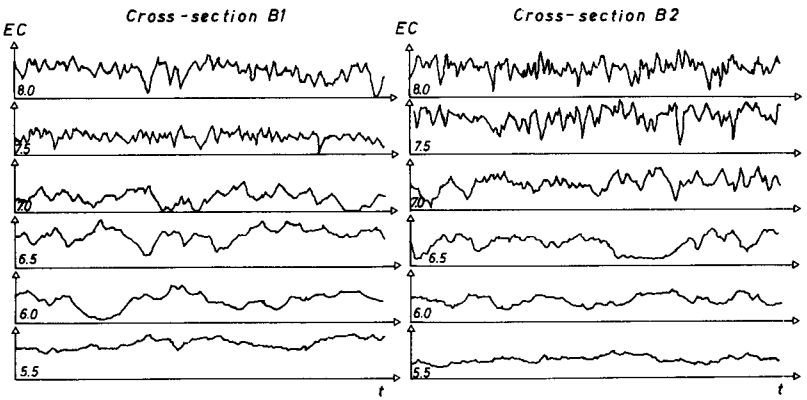


Fig. 3.15 : Example of bed level measurement: Time series of electric conductivity (=EC) readings are shown for the upper (B1) and lower (B2) cross-section of the flume; the numbers on the left indicate the height (in cm) above the flume bottom. (The experimental conditions for this run were: S = 15 %, Q = 30 L/s, $\rho$ = 1.23 g/cm$^3$.) In this case, the bed level $Y'_B$ was taken as 7.0 cm.

First an attempt was made to determine the bed level $Y'_B$ by a numerical analysis of the conductivity readings for each sampled level (e.g. counting number of fluctuations about the mean value, calculating the sum of the absolute amplitude values with respect to the mean value, or by using information from a Fourier transformation). The independent determination of $Y'_B$ was made by visual observation of the bed for tests

with clear water as transporting fluid. The numerical analysis proved to be successful for (only) about 90 % of the cases. So it was finally decided to definitely determine the bed level by visual judgement of the conductivity curves.

### 3.5.6 **Fluid density**

Prior to each experiment the density of the clay suspension was determined by taking a sample of one liter from the flow at the end of the flume. For the lower clay concentrations the density could be measured with a hydrometer. Samples taken in periodic intervalls showed almost no variation in the density over two or three hours. Therefore the density was usually determined once before each test.

At clay concentrations above about 4 % by volume the shear strength of the suspension was so large that the hydrometer no longer moved freely in the fluid. Therefore the density had to be calculated by measuring the volume and weight of a sample.

### 3.5.7 *Rheological parameters*

For each set of experimental runs (for which the fluid density remained practically constant), at least one sample (of 1 liter) of the clay suspension was taken. The samples were then analysed with a viscometer, which allows to determine the shear stress in a fluid as a function of the shear rate. An example of the measurements is shown in Fig. 3.16.

The principle of a rotational viscometer is shown schematically in Fig. 3.17. The fluid is sheared between two cylinders at a given shear rate; from the applied torque, which is measured, the corresponding shear stress can be calculated. In the present analysis, a "Rheomat 30" (manufactured by Contraves AG) was used as a viscometer. With this instrument the clay suspension was sheared in a 1.8 mm wide gap between two concentric cylinders. The shear rate was increased continously and automatically in one minute from 0 to 650 1/s and decreased at the same rate. This comparatively short measuring time (the shortest one available on the instrument) avoided that the rheologic properties changed

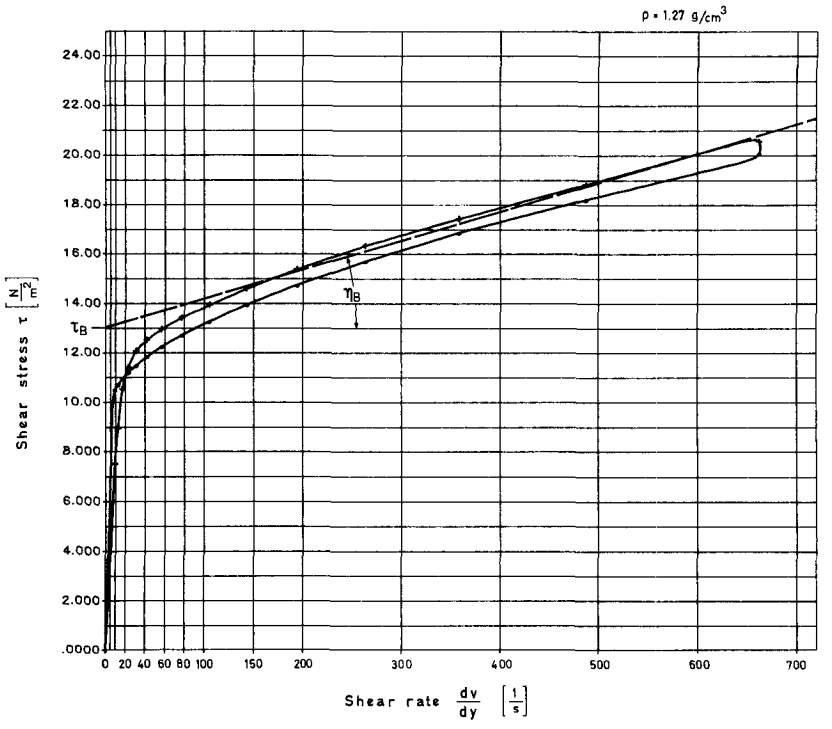


Fig. 3.16 : Example of rheologic behaviour of clay suspension obtained from measurement with a viscometer; the Bingham shear stress $\tau_B$ and the Bingham viscosity $\eta_B$ can be determined from the above diagram.

due to the settling of clay particles during the analysis. If a sample was left undisturbed for three or four minutes, a redetermination of the rheological curve indicated already a decrease in the Bingham shear stress $\tau_B$ and in the Bingham viscosity $\eta_B$. With increasing shear rates, measured shear stresses were generally higher than with decreasing shear rates (s. also the two slightly shifted curves in Fig. 3.16). This behaviour is commonly observed with clay suspensions, and it is associated with the fact that the arrangement of the plate-like particles also depends on the stress history.

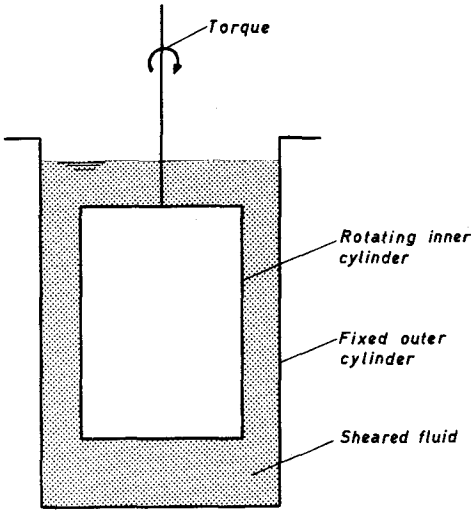


Fig. 3.17 : Schematic cross section through rotational viscometer. From the applied torque the shear stress can be calculated which is necessary to maintain a given shear rate.

The straight line that approximates the true rheologic behaviour (s. Fig. 3.16) was positioned so, that it matched the curve at shear rates above about 150 1/s. For in this region the measured lines are already rather straight; furthermore, it was not known a priori which range of shear rates would be most representative for the experiments to be performed.

## 3.6 Equilibrium transport conditions

The flume slope and the flow rate were set before starting each test. The third independent parameter, the fluid density, was given by the actual concentration of the clay suspension (in the flume) after remixing the suspension in the circuit.

In the case of the flow resistance experiments without any sediment transport, about 12 to 20 sets of measurements were performed for each test. A measurement consisted of a flow depth determination at two cross-sections (B1 and B2) and of a velocity measurement for the upper and lower reach of the flume ($V_1$ and $V_2$; s. Fig. 3.7).

In the case of the sediment transport experiments, the bed level was also determined, apart from recording the fluid surface level and measuring the mean velocity.

Equilibrium transport conditions require that the flow of the sediment-fluid mixture is steady and uniform. The following criteria were used to check whether this requirement was satisfied: The fluid surface slope should be approximately equal to the flume slope; the (mixture) flow depth should be about the same at both measuring cross-sections (implying that also the movable bed slope is equal to the flume slope); and the velocities in the upper and lower flume reach should not differ much from each other. The equilibrium transport conditions for each test had to be found by trial and error. The sediment feeding rate was first set arbitrarily or by trend extrapolation of previous results. If the gravel input was too small, the movable bed was quickly scoured, beginning downstream of the adjustable roughness elements, and the erodable bed was washed down the flume. On the other hand, if there was too much sediment input, the bed aggraded and the bed slope increased. Once the equilibrium conditions were established, the movable bed had reached a quasi steady state, and a set of measurements could be made.

To determine average values for each test, only those measurements were considered for which both the fluid surface and the bed level at the upstream cross-section did not differ by more than about 10 mm from their corresponding values at the downstream cross-section. In general, the velocity measurements which were used in the final analysis did not differ by more than 5 % between the upper and lower flume reach, except for extreme flow conditions; with the highest clay concentrations, successful application of the salt velocity technique became more and more difficult.

## 3.7 Reproduction of some tests of Smart and Jaeggi

In order to ensure that the sediment transport experiments performed by Smart and Jäggi (1983) could serve as reference conditions, some of their tests with bed material No. IV were reproduced with the slightly modified experimental setup. The reproduction of some earlier experiments also allowed to check the new measuring techniques described above.

The six tests which were reproduced are shown in Table 3.3 together with the corresponding tests of Smart and Jäggi. The tests which were chosen to cover mainly the higher transport domain of their test series. Table 3.3 also includes the experimental values obtained and gives the relative deviation between both sets of measurements.

| | | meas. Smart/Jäggi | | | meas. by author | | | rel. deviation | | |
|---|---|---|---|---|---|---|---|---|---|---|
| S | Q | $G_B$ | h | V | $G_B$ | h | V | $\Delta G_B$ | $\Delta h$ | $\Delta V$ |
| [%] | [L/s] | [kg/s] | [cm] | [m/s] | [kg/s] | [cm] | [m/s] | [%] | [%] | [%] |
| 10 | 10 | 0.84 | 5.0 | 1.07 | 0.98 | 4.40 | 1.07 | 17 | -12 | 0 |
| 15 | 10 | 2.30 | 4.8 | 1.18 | 2.78 | 4.85 | 1.17 | 21 | 1 | 9 |
| 15 | 15 | 4.08 | 6.0 | 1.57 | 4.34 | 6.22 | 1.54 | 6 | 4 | -2 |
| 15 | 20 | 5.83 | 7.6 | 1.96 | 5.97 | 7.00 | 1.81 | 2 | -8 | -8 |
| 20 | 30 | 14.91 | 8.5 | - | 13.02 | 8.15 | 2.30 | -13 | -4 | |

Table 3.3 : Comparison between selected tests of Smart/Jäggi (mat. IV) and experiments repeated by the author.

Another possibility to compare the quality of the experimental results, is to plot the measured values against the calculated ones (s. Fig. 3.18). The bed load transport rate $q_B$ was computed with a new equation presented in section 4.6.1 (equ. 4.19), since the Smart/Jäggi equation was found to underpredict the higher transport rates. Equation (2.82) was used to calculate the mixture flow depth $H_m$ (the fluid flow

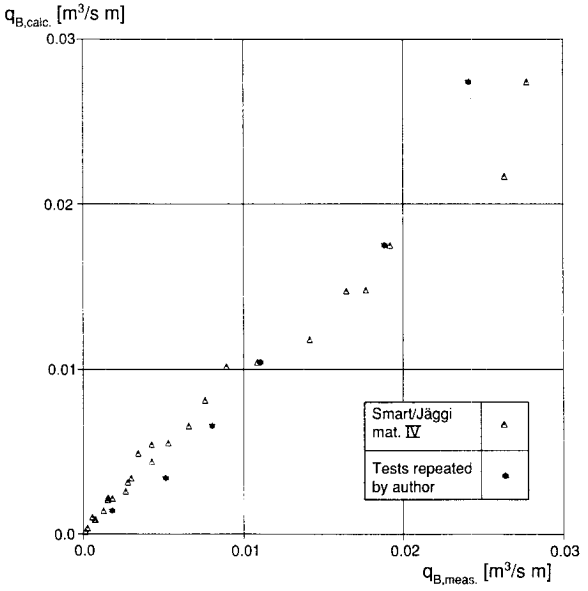


Fig. 3.18 (a)

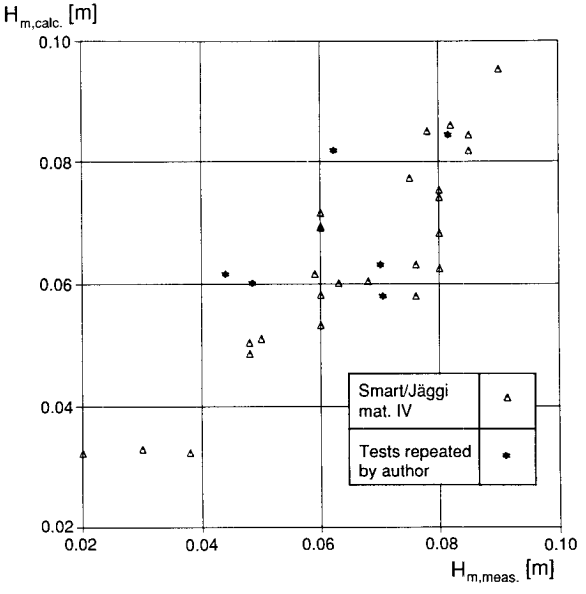


Fig. 3.18 (b)

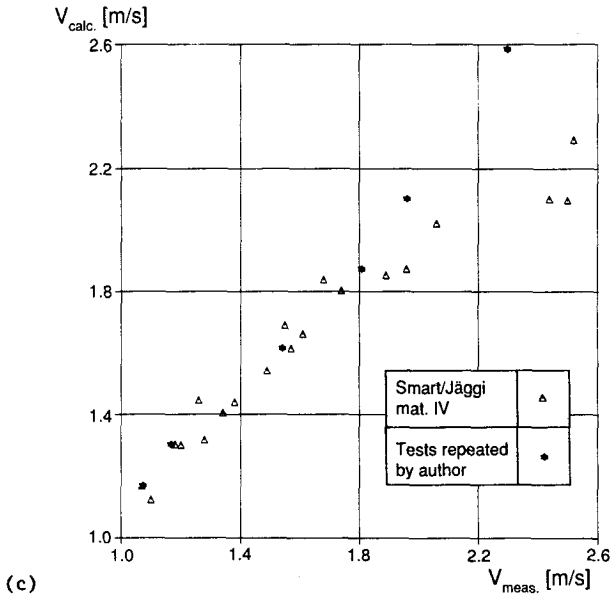


Fig. 3.18 : Comparison of tests repeated by the author with the Smart/Jäggi tests with material IV, shown as calculated against measured values: (a) bed load transport rates, (b) mixture flow depth, (c) mean fluid (water) velocity.

depths as inferred from the flow rate and velocity measurements were considered to be more reliable), and the mean water velocity V was computed using the iterative procedure described in Smart and Jäggi (1983).

It can be seen that the values measured by the author are generally within about +/- 10 % of the calculated ones, and they indicate about the same amount of scatter as the values obtained by Smart and Jäggi. The measured velocities by the author are somewhat smaller than the ones of Smart and Jäggi; this could be due to the fact that they let the salt solution fall into the flow surface from a flat plate while the author injected the solution in the middle of the flow cross section from one

tube or several smaller tubes. Thus the mixing in the first case might not have been sufficient (at higher velocities) to prevent that the major part of the solution travelled with the faster moving upper fluid layers. While the bed load transport rates obtained by the author are close to the calculated ones, the (new) measured depth values appear to be somewhat smaller than the calculated ones.

# 4 RESULTS AND ANALYSIS

## 4.1 Methods used in data analysis

### 4.1.1 Correction for sidewall friction

The flow depth in the steep flume of 20 cm width varied between 2 cm and 10 cm. It was therefore necessary to apply a sidewall correction to account for that part of the energy loss which is due to friction of the fluid along the flume walls.

A procedure originally proposed by H.A. Einstein (1936) was adapted by Smart and Jäggi (1983) to determine the effect of the sidewall influence. The flow cross section is divided into a part where the flow acts on the bed, and into two parts where the flow acts on the sidewalls; the three areas are separated by straight lines (Fig. 4.1a). Assuming equal mean velocities in all three subareas, the following relationship can be used:

$$R_w = \left(\frac{V}{k_w S^{0.5}}\right)^{1.5} \qquad (4.1)$$

where $R_w$ is the hydraulic radius belonging to one sidewall flow subarea $F_w$, and $k_w$ is the Strickler value characterising the flume wall material. The total area can be expressed by (Fig. 4.1b):

$$H \cdot B = (h_r\ B) + (2\ R_w\ H) \qquad (4.2)$$

where H denotes the measured flow depth, $h_r$ is the reduced flow depth corrected for sidewall influence, and B is the flume width. Combining equs. (4.1) and (4.2), $h_r$ is determined as:

$$h_r = H - 2\left(\frac{V}{k_w S^{0.5}}\right)^{1.5} \frac{H}{B} \qquad (4.3)$$

The reduced flow rate, $q_r$, acting on the bed is calculated accordingly as:

$$q_r = q - V\,(H - h_r) \qquad (4.4)$$

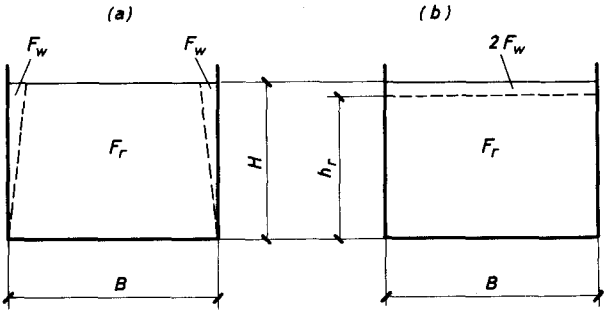


Fig. 4.1 : Sidewall correction procedure applied to the steep flume experiments. The trapezoidal subarea (a), which represents the flow section acting on the bed, is replaced by a rectangular section (b).

Smart and Jäggi examined the influence of the choice of the flume wall Strickler coefficient $k_w$ on the difference between calculated and measured bed load transport rates. Apart from their main experiments in a flume of 20 cm width they also performed some comparative tests in a narrower flume of 10 cm width. They concluded that the choice of the $k_w$ value was important for the 10 cm flume, but not important in the case of the 20 cm flume. For their main experiments they chose a $k_w$ value of 110 $m^{1/3}/s$. Since a similar flume (with 20 cm width) was used in the present study, the same Strickler coefficient was adopted for the sidewall correction procedure.

### 4.1.2 **Regression analysis**

A computer program was applied to perform a regression analysis with the measured parameters or combinations thereof. The logarithmic values of the considered parameters were used in the computational procedure of the implemented standard multiple linear regression analysis. Information on the statistical procedure can be found in Draper and Smith (1966).

To judge the quality of a regression equation, the same method was applied as described in Smart and Jäggi (1983). The correlation coefficient r is obtained as:

$$r = \frac{\Sigma(X_c - \bar{X}_c)(X_m - \bar{X}_m)}{[\Sigma(X_c - \bar{X}_c)^2(X_m - \bar{X}_m)^2]^{0.5}} \qquad (4.5)$$

where $X_c$ denotes the calculated (predicted) value and $X_m$ the measured value; the bars indicate mean values over the total number of observations, N. The standard error $S_E$ is defined as the standard deviation divided by the mean value:

$$S_E = \frac{[\Sigma(X_c - X_m)^2]^{0.5}}{(N-1)^{0.5}\,\bar{X}_m} \qquad (4.6)$$

It should be noted that r and $S_E$ are calculated with linear, and not with logarithmic values. Using these statistical parameters in the analysis of the present experiments, the results were directly comparable to those obtained in the (reference) study of Smart and Jäggi.

## 4.2 Rheology of clay suspension

Before performing the main experiments a few preliminary test were carried out in a smaller flume apparatus. One objective of these tests was to check how well the Opalit clay suspension could be recirculated in a flume system.

Samples of the clay suspension of various concentrations were taken during these tests and analysed with a viscometer (as described in sec. 3.5.7). From the viscometric measurements the Bingham parameters $\tau_B$ and $\eta_B$ were determined. The same procedure was applied to the samples obtained during the experiments in the main flume. The relation between the Bingham parameters and the clay concentration of the suspension is presented in Fig. 4.2 and 4.3.

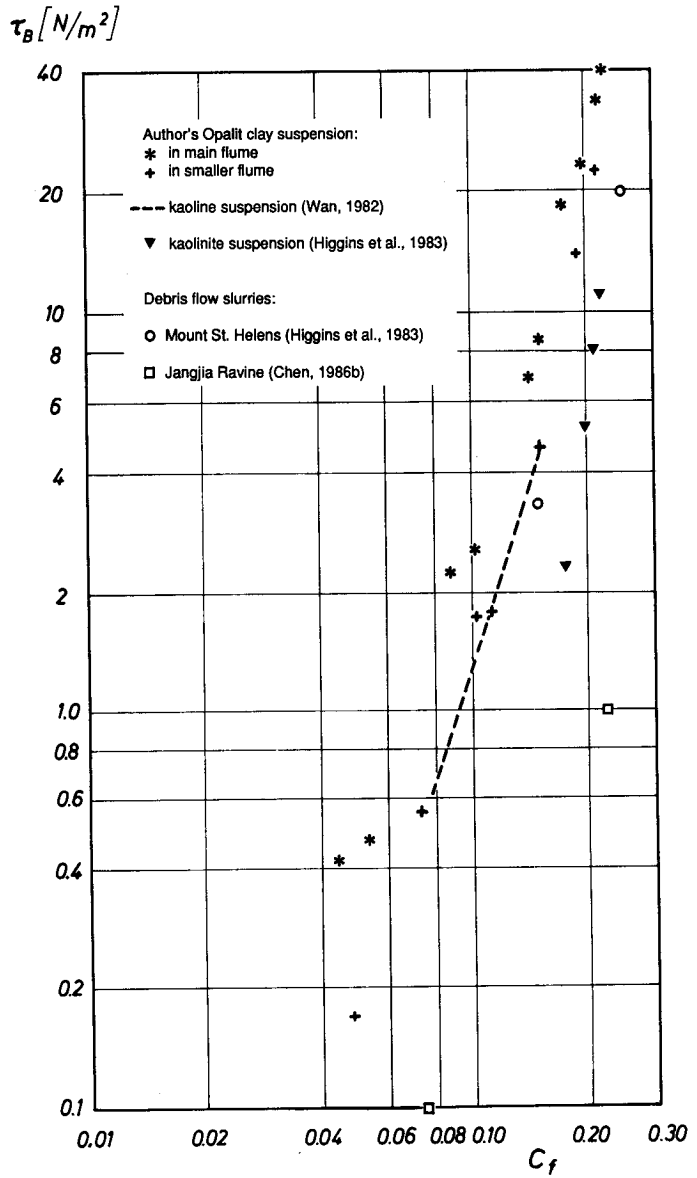


Fig. 4.2 : Relation between Bingham yield stress $\tau_B$ and volume concentration $C_f$ of fine material suspensions; measurements of this study are shown together with data from other sources.

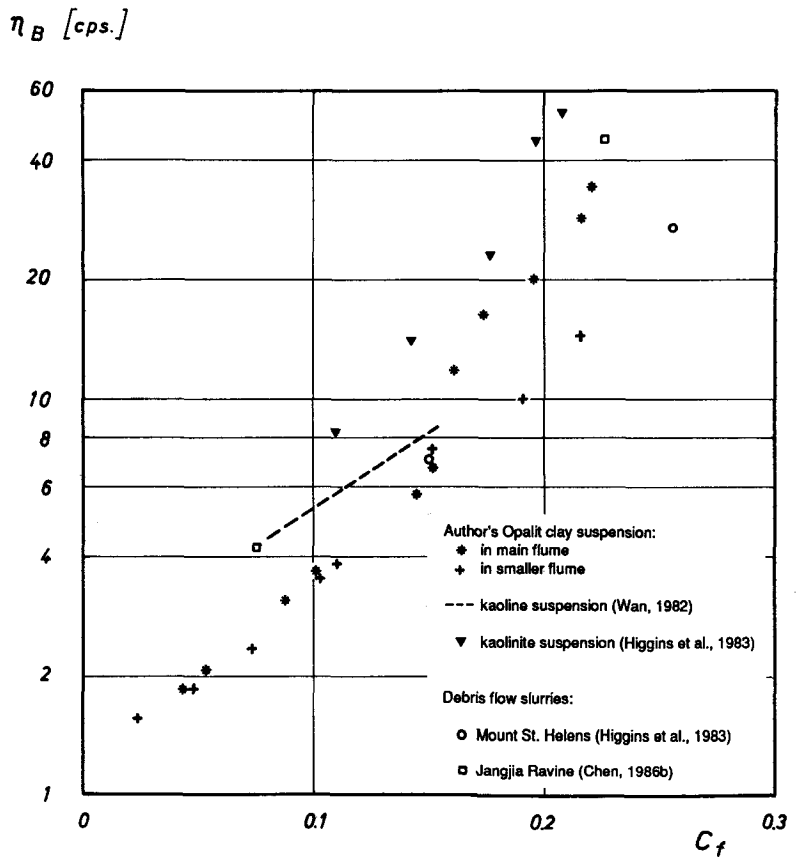


Fig. 4.3 : Relation between Bingham viscosity $\eta_B$ and volume concentration $C_f$ of fine material suspensions; measurements of this study are shown together with data from other sources.

It can be seen from Fig. 4.2 that the samples from the main flume apparatus show a larger $\tau_B$ value than those from the smaller flume for a given clay concentration. This fact can be explained by the relatively much larger fluid volume present in the main flume system; a bigger portion of the added clay material settled out in the dead zones of the system and was not resuspended during the experiments. Thus the samples from the main flume contained a larger fraction of the very fine particles of the Opalit clay.

Fig. 4.2 further shows that in this study, $\tau_B$ is approximately proportional to $C_t^3$; this proportionality is also indicated by the dashed line, which represents measurements made by Wan (1982).

The data points from the main flume apparatus in Fig. 4.3 seem to indicate a discontinuity at a clay concentration of about 15%. A break of a few months occurred at this concentration level because a special slurry pump had to be installed in the system. At the end of this period a substantial part of the coarser clay particles had settled into the dead zones, resulting in a new suspension containing more very fine particles than before. For a clay concentration up to 15%, the data from the two flume systems show that the Bingham viscosity of the Opalit suspension seems to be less sensitive to particle composition than the Bingham yield stress.

In both figures, the data points representing samples of mudflow material from the Mount St. Helens lie relatively close to values obtained in experimental studies. Regarding the samples from debris flow slurries in the Jangjia Ravine (China), the Bingham yield stress is clearly lower than for the other data points shown.

It may be noted that for the Bingham type approximation, the straight line in the rheological diagrams (e.g. Fig. 3.16) was fitted at shear rates above about 100 $s^{-1}$ for most of the data shown in the above figures; no information in this respect was available for the Jangjia Ravine data.

## 4.3 Flow resistance of clay suspension on a fixed rough bed, without sediment transport

In order to examine the flow behaviour of the Opalit suspension without any interference by transported bed load grains, velocity- and depth- measurements were made for the flow of the suspension over a fixed, rough flume bed. The rough bed was made up of the same gravel as that used in the sediment transport tests (s. section 3.4 for grain size characteristics). For each of the examined clay concentration levels,

Ci, twelve combinations of flow rate and flume slope were considered. A list with all performed measurements is given in Appendix I.

Summarised, the fluid flow rate was varied between 10 l/s and 40 l/s, and the slope was set between 5% and 20%. The range of the examined clay concentration levels is shown in Table 4.1, together with the corresponding Bingham parameters; the figures represent mean values for a given clay concentration level. Also shown is the effective viscosity (which depends on the flow conditions).

| Symbol/Ci | $\rho$ [g/cm$^3$] | $C_f$ [%] | $\tau_B$ [N/m$^2$] | $\eta_B$ [cps] | $\mu_{e2}$ [cps] |
|---|---|---|---|---|---|
| △ $H_2O$ | 0.998 | 0.0 | 0.0 | 1.02 | 1 |
| ✱ C1 | 1.078 | 4.7 | 0.44 | 1.93 | 5 - 10 |
| ◇ C2 | 1.165 | 10.0 | 2.82 | 3.60 | 25 - 55 |
| + C3 | 1.238 | 14.4 | 7.29 | 5.92 | 60 - 140 |
| ● C4 | 1.324 | 19.6 | 23.6 | 20.0 | 180 - 400 |
| Y C5 | 1.365 | 22.1 | 40.8 | 34.3 | 250 - 1800 |

Table 4.1 : Experimental range of clay concentration levels (for experiments without sediment transport), shown with the corresponding Bingham parameters $\tau_B$ and $\eta_B$. The effective viscosity $\mu_{e2}$ was calculated according to equ. (2.40); it depends on the flow conditions.

It may be mentioned that the velocity measurement by the salt tracer technique became unreliable for flows which were at transition between the turbulent and laminar regimes (some tests at the levels C4 and C3); this was indicated by relatively large differences in the values V and q/H. At the highest clay concentration level, application of the salt velocity technique was no longer possible. For all these experiments the velocity determined as q/H was used to calculate f, $Re_2$ and $Re_B$ (s. also Appendix I).

Jäggi (1983) proposed a new flow resistance equation for a sediment transporting flow over a movable bed at smaller relative depths $h/d_{90}$, because many conventional formulae tend to overpredict the velocities in the range $5 < h/d_{90} < 20$. His equation is given as:

$$\frac{V}{v^*} = 2.5 \left[1 - \exp\left(-\frac{\alpha_1 h}{d_{90} S^{0.5}}\right)\right]^{0.5} \ln\left(\frac{12.27\ h}{\beta_1\ d_{90}}\right) \qquad (4.7)$$

where the coefficients $\beta_1$ and $\alpha_1$ depend on the grain size distribution, the packing and the shape of the bed material. For their steep channel bed load transport tests, Smart and Jäggi (1983) determined $\alpha_1 = 0.05$ and $\beta_1 = 1.5$.

The results of the flow resistance measurements with the clay suspension are presented in Fig 4.4 in terms of the resistance coefficient $c = V/v^*$ as a function of the relative flow depth $h/d_{90}$; note that the flow depth corrected for sidewall influence, $h_r$, was used to determine $v^*$ and $h/d_{90}$ for the experimental data. Equ. (4E4) and the Nikuradse equation for open channel flow, equ. (2.53), are included for comparison.

It can be seen from Fig. 4.4 that most of the data points show no significant change in flow resistance with increasing clay concentration level Ci. The data points with 5% slope and the largest flow rate (or relative depth) indicate some variation of c. At the highest clay concentration level (C5), the experimental results show a trend for c, at a given slope, to become independent of the parameter $h/d_{90}$; this is an indication that the roughness elements no longer dominate the flow behaviour.

The comparison with equ. (4.7) shows that the flow resistance (at steep slopes) is smaller in a flow over a fixed bed than in a flow over a mobile bed. This conclusion is in agreement with a study by Zagni and Smith (1976) who found that the friction factor for turbulent flow over a permeable bed is higher (by about a factor 1.5 to 2) than for a flow over an impermeable bed with the same roughness elements. Further, the macrostructure of the particles on the fixed bed might have been still somewhat more regular than the natural arrangement on a mobile bed.

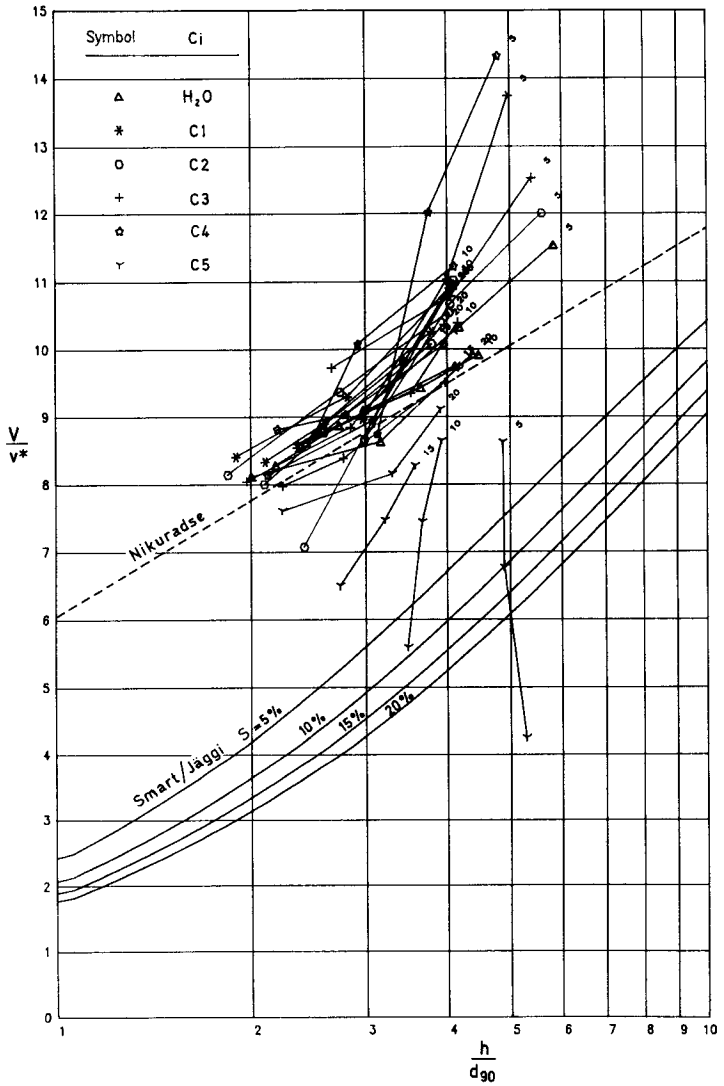


Fig. 4.4 : Flow resistance measurements of clay suspension flows over a fixed rough bed without sediment transport, in terms of the resistance coefficient c = V/v* as a function of the relative flow depth $h/d_{90}$; data points with equal slope and for a given clay concentration level are connected by straight lines. The Nikuradse equation (with $k_s = d_{90}$) and the equation used by Smart and Jäggi (with $\alpha_1 = 0.05$ and $\beta_1 = 1.5$) are shown for comparison.

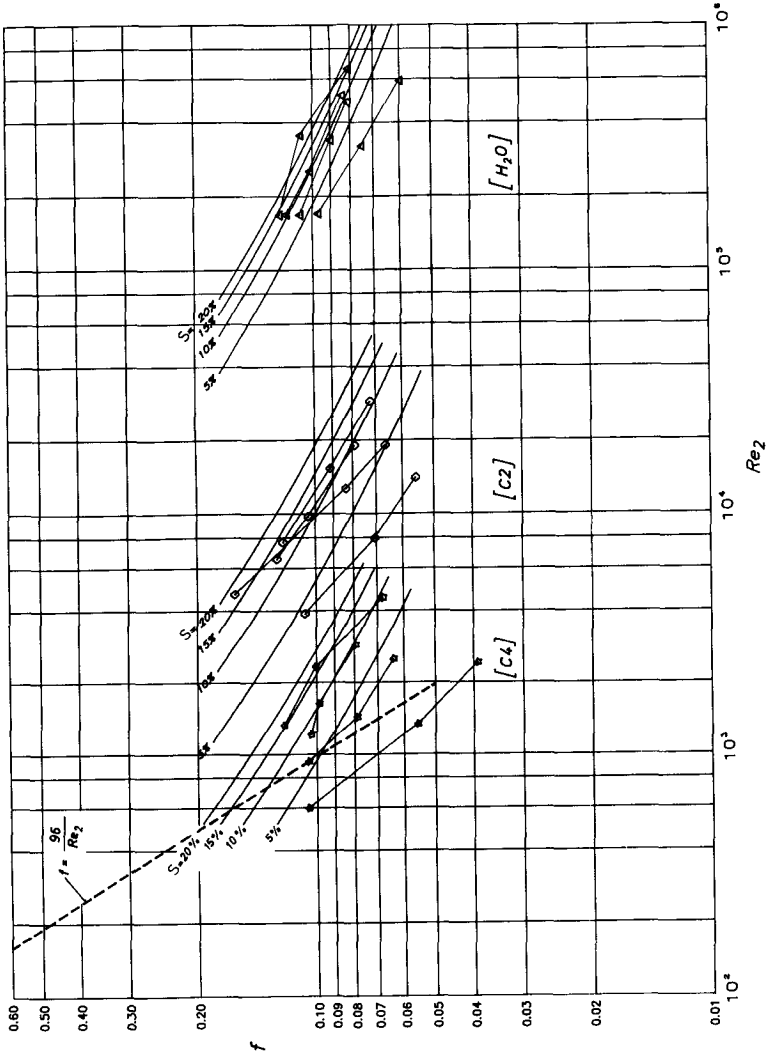


(a)

Fig. 4.5 : Flow resistance measurements of clay suspension flows on a fixed rough bed without sediment transport, in terms of the friction factor f vs. the Reynolds number $Re_2$; data points with equal slope are connected by straight lines. The smooth lines represent f values calculated with the Colebrook equation (with $k_s = d_{90}$). Also shown is the relationship for laminar Newtonian flow, f = 96/Re, in a rectangular channel. (a) Data points for $H_2O$, C2 and C4, (b) data points for C1, C3 and C5.

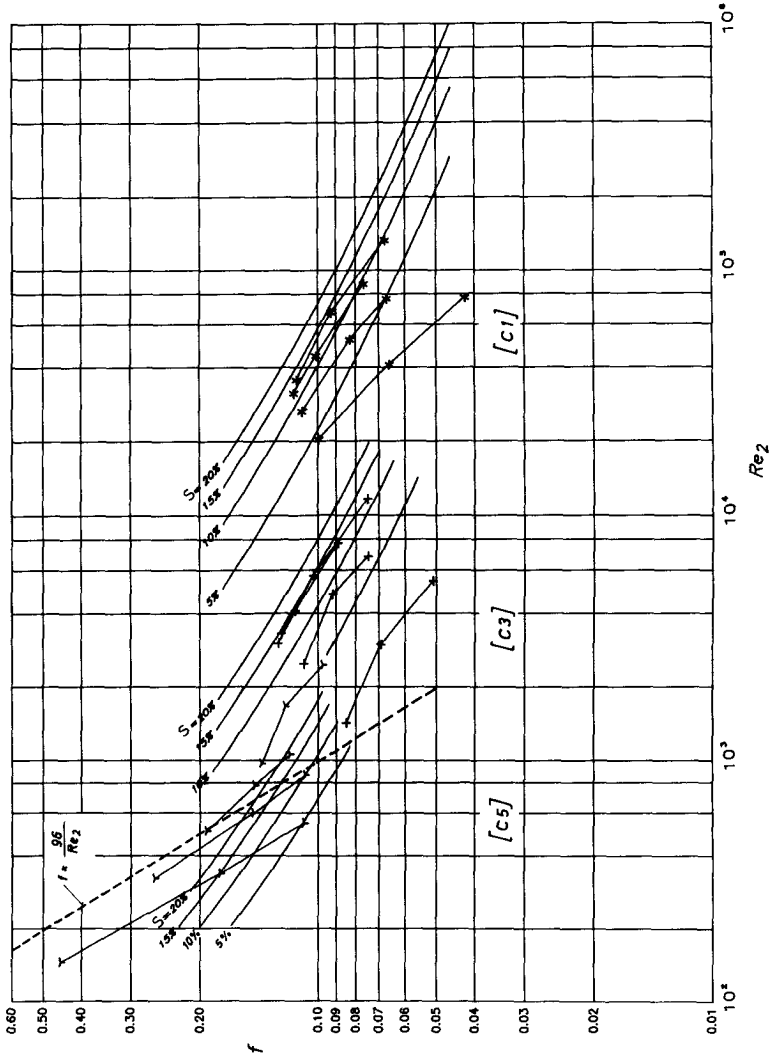
[C1]
[C3]
[C5]
S=20%
15%
10%
5%
f = 96/Re2
Re2
f
0.60
0.50
0.40
0.30
0.20
0.10
0.09
0.08
0.07
0.06
0.05
0.04
0.03
0.02
0.01
10⁶
10⁵
10⁴
10³
10²

Fig. 4.5 (b)

To illustrate the effect of the increasing viscosity on the flow resistance with increasing clay concentration, the experimental results are presented in a Moody type diagram. In Fig. 4.5 (a) and (b) the friction factor f is plotted as a function of the Reynolds number $Re_2$ (as defined by equ. 2.42a). Again the reduced flow depth $h_r$ (corrected for sidewall influence) was used to determine f and $Re_2$ for the experimental data points.

The flow resistance values predicted by the Colebrook equation (2.52) are also shown in Fig. 4.5. For a given clay concentration level, the effective viscosity $\mu_{e2}$ was determined with the Bingham parameters of Table 4.1, which allowed one to calculate the Reynolds number $Re_2$. Not much information is available to decide which representative grain size should be taken for $k_s$ at small relative flow depths. Kamphuis (1974) performed flow resistance measurements with a fixed rough bed, and determined $k_s$ for different values of $h/d_{90}$. He suggested to use $k_s \simeq 2d_{90}$ for larger relative depths ($h/d_{90} >\simeq 15$); a few experimental points in the range $2 < h/d_{90} < 10$ indicate that $k_s$ is approximately equal to $0.5d_{90} \cdots 1.5d_{90}$. A mean value of $k_s \simeq d_{90}$ was used to calculate f with the Colebrook equation in Fig. 4.5.

According to Fig. 4.5 the transition from turbulent to laminar flow occurs at a critical Reynolds number $Re_2$ between about 500 and 1500. The change in $Re_2$ with increasing clay concentration seems to be reasonably well reproduced by using the Colebrook equation in combination with the effective viscosity $\mu_{e2}$.

To determine the limit below which viscous effects begin to take place, the experimental results are presented in another form in Fig. 4.6, plotting the values $[1/\sqrt{f} - 2\cdot\log(h_r/d_{90})] = B_s'$ on the ordinate and $Re_2^*$ on the abscissa (analogous to Fig. 2.2). It is seen that for $Re_2^* >\simeq 10$, $B_s'$ is approximately constant implying that no viscosity influence can be detected; in this region the following relation can be given:

$$\frac{1}{\sqrt{f}} - 2 \log \left(\frac{h_r}{d_{90}}\right) \simeq 2.4 \qquad (4.8)$$

The above equation may be transformed into:

$$\frac{1}{\sqrt{f}} \simeq 2 \log \left(\frac{12\ h_r}{0.76\ d_{90}}\right) \qquad (4.9)$$

Comparing equ. (4.9) with the Nikuradse equation (2.53), it follows that a mean value of $k_s \simeq 0.76 \cdot d_{90}$ would best describe the conditions of the clay suspension experiments.

It is further noted from Fig. 4.6 that $B_s'$ does not change below $Re_2^* \simeq 54$ (corresponding to $v^* k_s/\nu_{e2} \simeq 70$). This value marks the upper limit of the hydraulically transitional region in Newtonian flows; in this region, an increase of $B_s'$ occurs for flows over uniform sand roughness, while $B_s'$ should gradually decrease in the case of a nonuniform sand roughness (Rouse, 1960). There are only two data points for the clay concentration level C4 which may indicate an increase in $B_s'$.

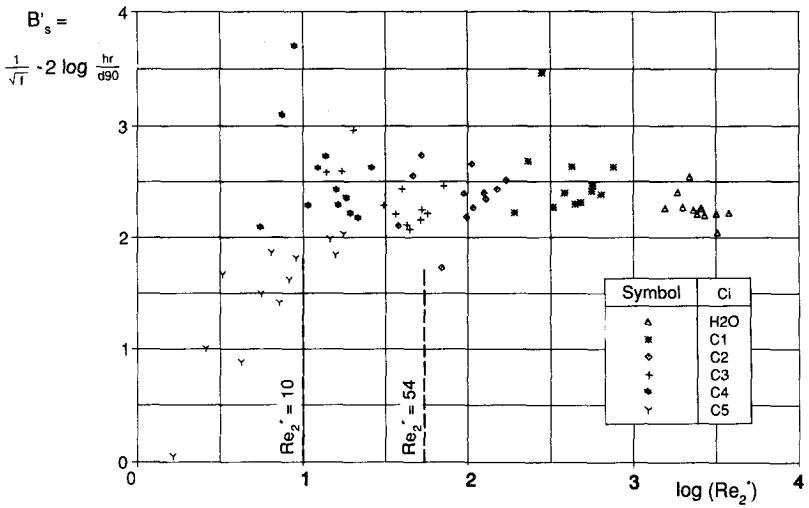


Fig. 4.6 : Flow resistance data shown in terms of the parameters $B_s' = [1/\sqrt{f} - 2 \cdot \log(h_r/d_{90})]$ and $Re_2^*$, for the clay suspension flows over a fixed rough bed.

The transition from turbulent to laminar flow can also be judged using the criterion for Bingham fluids developed by Hanks (1963) for pipe flow and adopted by Naik (1983) for open channel flow. The critical conditions at transition were calculated using equs. (2.43) and (2.44); the corresponding curve is shown in Fig. 4.7, together with the experimental results for the three higher clay concentration levels C3, C4 and C5 (using the reduced flow depth $h_r$). In Fig. 4.7, all those experiments which indicated turbulent flow are grouped together, while those which were laminar or at transition are marked with a different symbol. However, it was difficult to judge from visual observation whether a flow was already laminar or only in a transitional stage. At the more viscous flows, the formation of a plug flow could be observed in the middle of the flume, the plug becoming broader with decreasing turbulence intensity. In these cases, the flow behaviour was classified as transitional in Fig. 4.7, although this may not be evident from Fig. 4.5. Data from preliminary experiments in a smaller flume (with 5 cm width) is also included in Fig. 4.7.

The experimental data shown in Fig. 4.7 seems to support the theoretical criterion for the transition between laminar and turbulent flow of a Bingham fluid in an open channel. It may be noted that the data points marked "laminar or transition" in Fig. 4.7 all have a Reynolds number $Re_2$ smaller than approximately 1500 which is about the upper limit for the critical value of $Re_2$ as predicted from Fig. 4F4. Thus it appears justified to use the effective viscosity $\mu_{e2}$ together with conventional formulae developed for Newtonian fluids.

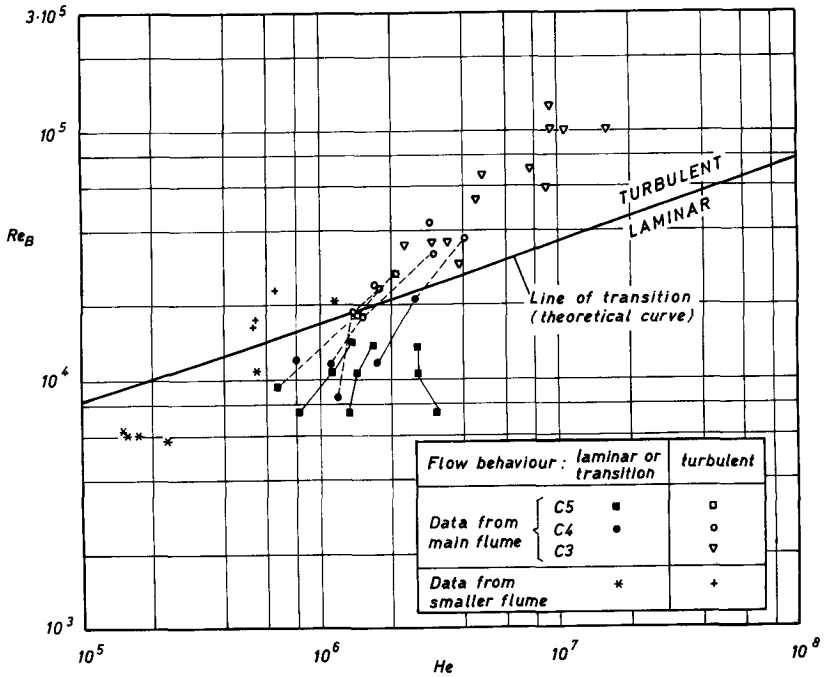


Fig. 4.7 : Experimental results obtained at the higher concentration levels, shown in terms of the Bingham Reynolds number $Re_B$ and the Hedstroem number He; the data points are grouped in tests with turbulent flow, and in those with transitional or laminar flow. The theoretical line of transition was calculated with equs. (2.43) and (2.44).

## 4.4 **Bed load transport experiments**

Similar to the tests without bed load transport on a fixed rough bed, experiments were performed at five different clay concentration levels (Ci). At each level, the fluid flow rate was varied between 10 and 30 L/s, and the slope was set between 7% and 20%. A list with all performed

measurements is given in Appendix II. The range of the examined clay concentration levels is shown in Table 4.2, together with the corresponding Bingham parameters $\tau_B$ and $\eta_B$ and the effective viscosity $\mu_{e2}$.

| Symbol/Ci | $\rho$ [g/cm³] | $C_f$ [%] | $\tau_B$ [N/m²] | $\eta_B$ [cps] | $\mu_{e2}$ [cps] |
|---|---|---|---|---|---|
| △ $H_2O$ | 0.998 | 0.0 | 0.0 | 1.02 | 1 |
| ✳ C1 | 1.072-<br>1.096 | 4.4-<br>5.8 | 0.43-<br>0.67 | 1.87-<br>2.17 | 10 - 15 |
| ◇ C2 | 1.141-<br>1.160 | 8.6-<br>9.7 | 2.20-<br>2.77 | 3.00-<br>3.33 | 35 - 65 |
| + C3 | 1.201-<br>1.246 | 12.2-<br>14.9 | 4.31-<br>8.55 | 4.35-<br>6.74 | 100 - 200 |
| ✿ C4 | 1.257-<br>1.293 | 15.6-<br>17.8 | 12.8-<br>20.1 | 11.2-<br>16.2 | 200 - 450 |
| Y C5 | 1.356-<br>1.363 | 21.6-<br>22.0 | 33.6-<br>40.8 | 28.8-<br>34.3 | 800 - 1000 |

Table 4.2 : Experimental range of clay concentration levels Ci for the sediment transport tests, shown with corresponding Bingham parameters $\tau_B$ and $\eta_B$. The effective viscosity $\mu_{e2}$ was calculated according to equ. (2.40). The symbols of this table are also used in the following figures.

The experimental results clearly indicate a change in the bed load transport rate with increasing clay concentration of the suspension. Fig. 4.8 shows the change of the ratio $q_B/q_{B,H2O}$ with increasing fluid density $\rho$. For a given slope and flow rate, $q_B$ increases with $\rho$ up to the concentration level C3 or C4, and then decreases again at higher fluid densities. While an increase in $q_B$ may be expected with a decrease in the solid-fluid density ratio s, the decrease in $q_B$ with increasing clay concentration is not likely to be associated with the changing fluid density; this decrease is more likely to be a viscosity effect.

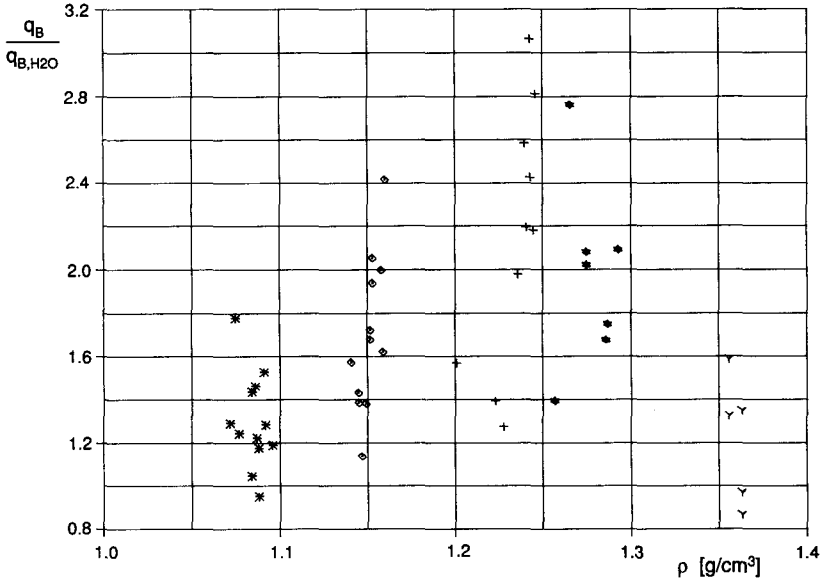


Fig. 4.8 : Ratio of the bed load transport rate measured in the clay suspension to the value obtained in clear water, $q_B/q_{B,H2O}$, as a function of the density $\rho$ of the clay suspension.

In Fig. 4.9 the ratio $q_B/q_{B,H2O}$ is plotted against the particle Reynolds number $Re_2^*$, which accounts for the change in fluid viscosity with increasing clay concentration; $Re_2^*$ is defined as $v^*d_{90}\rho/\mu_{e2}$. It can be observed that there is an increase in $q_B$ with decreasing $Re_2^*$ (or increasing clay concentration) down to a critical value of $Re_2^*$, below which the bed load transport capacity of the flow clearly decreases again. At critical conditions the value of $Re_2^*$ is about 10 to 15.

For open channel flow, the thickness of the laminar (viscous) sublayer, $\delta$, is given as (Yalin, 1977): $\delta = 11.6\nu/v^* = 11.6(\eta/\rho)/v^*$. This implies that in a flow with $Re^* \simeq 12$, the laminar sublayer is of the same magnitude as the equivalent sand roughness $k_s$. It is assumed that the relationship for $\delta$ is also valid in the case of the clay suspension, using the effective viscosity $\mu_{e2}$. With regard to the critical value of $Re_2^*$ shown in Fig. 4.9, this means that the thickness of the laminar

sublayer is of the order of the grain size of the transported bed material. Thus it appears that once the flow around the grains becomes laminar, the bed load transport capacity starts to decrease, for otherwise equal flow conditions.

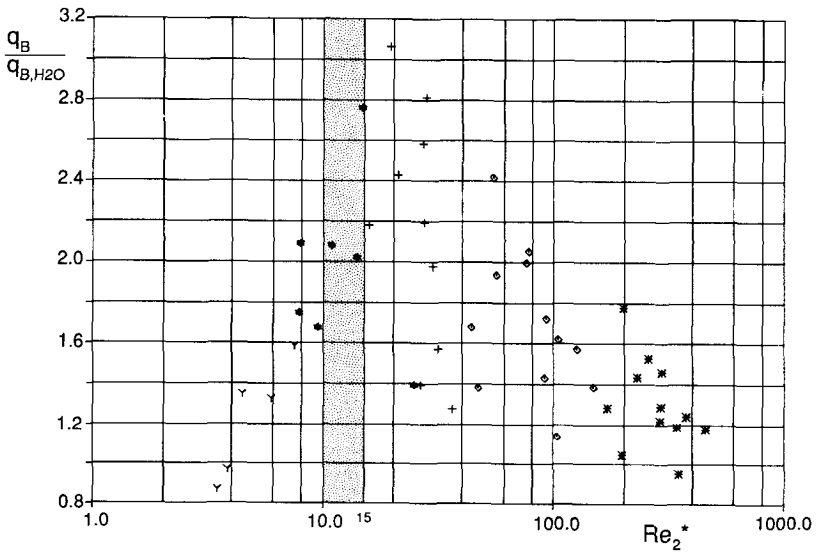


Fig. 4.9 : Ratio of the bed load transport rate measured in the clay suspension to the value obtained in clear water, $q_B/q_{B,H2O}$, as a function of the grain Reynolds number $Re_2^*$.

Also other experimental studies show an increase in $q_B$ with a decrease in the density ratio s (s. sec. 2.3.1.2); in these studies the viscosity of the fluid did not change. It is therefore reasonable to assume that at least a part, if not all of the increase in the ratio $q_B/q_{B,H2O}$ is due to the increasing density of the clay suspension. Some additional tests were carried out in a smaller flume apparatus (with a width of 5 cm), using a cellulose solution so as to change only the viscosity but not the density of the fluid. The results of these qualitative experiments indicated a decrease of the ratio $q_B/q_{B,H2O}$ with increasing fluid viscosity.

The change in flow resistance with increasing clay concentration is depicted in Fig. 4.10, where the friction factor f is plotted against the Reynolds number $Re_2$. Both f and $Re_2$ were determined with the measured fluid velocity , V, and the mixture flow depth corrected for sidewall influence, $h_{r,m}$. A slight increase in f is observed with increasing clay concentration (i.e. decreasing $Re_2$), followed by a slight decrease. This behaviour is qualitatively similar to the change in $q_B$ with increasing clay concentration levels. A decrease in f, however, occurs already at the level C3, while $q_B$ still increases at the same clay concentration level.

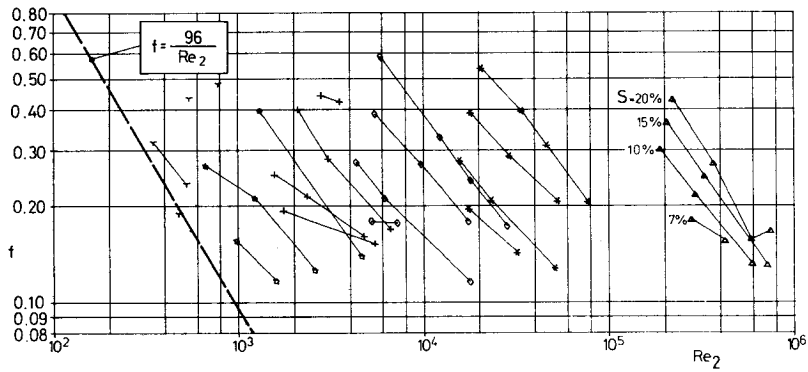


Fig. 4.10: Flow resistance measurements of clay suspension flows with bed load transport. The friction factor f is shown as a function of the Reynolds number $Re_2$; data points with equal slope are connected by straight lines. Also given is the relationship for laminar Newtonian flow, f = 96/Re, in a rectangular channel.

## 4.5 Case I: Thickness of laminar sublayer is smaller than grain size

In the following analysis only those experiments were considered for which an increase in $q_B$ was observed with respect to the $q_B$ value measured at the next lower clay concentration level (with a lower fluid density). Thus 12 individual experiments were available for each of the

levels H20 (data taken from Smart and Jäggi), C1, C2; 10 tests at the level C3; and 4 experiments at the level C4 (s. also Appendix II). This resulted in a total number of 50 tests which were treated as a homogeneous data group. This data set is labelled RI in the following sections.

It can be inferred from Fig. 4.10 that there was no significant change in flow resistance with increasing clay concentration, despite the very pronounced change in the bed load transport rate. This is also confirmed by Fig. 4.11a and b, where the change of the corrected mixture flow depth, $h_{r,m}$, and of the fluid velocity, V, respectively, are shown as a function of the density factor (s-1). There is a tendency for only a slight increase in both $h_{r,m}$ and V with increasing suspension concentration (i.e. decreasing values of s-1).

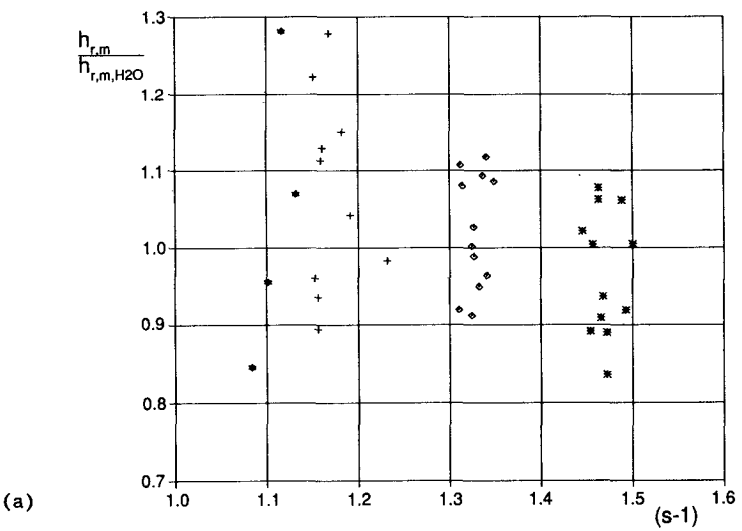


(a)

Fig. 4.11: Variation of flow parameters measured for the clay suspension with bed load transport, as a function of the density factor (s-1): (a) ratio of the corrected mixture flow depth to the corresponding clear water value, $h_{r,m}/h_{r,m,H2O}$, and (b) ratio of the the fluid velocity to the corresponding clear water value, $V/V_{H2O}$.

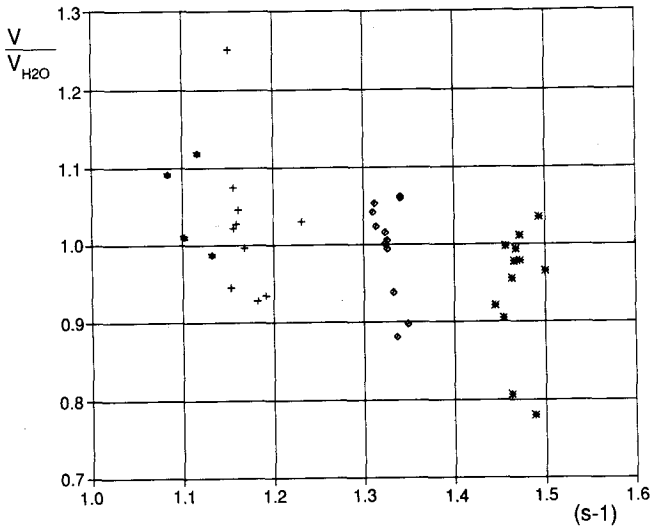


Fig. 4.11 (b)

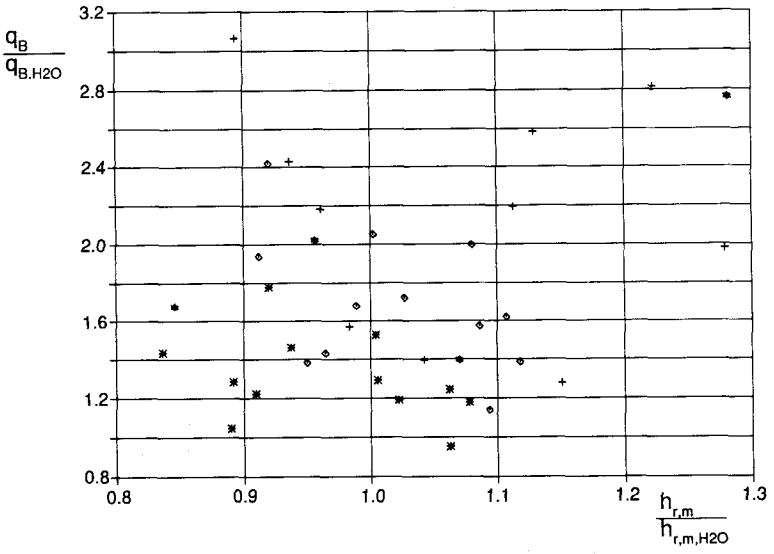


Fig. 4.12: Ratio of the bed load transport rate measured in the clay suspension to the value obtained in clear water, $q_B/q_{B,H2O}$, as a function of the ratio of the corresponding (corrected) mixture flow depths, $h_{r,m}/h_{r,m,H2O}$.

Considering Fig. 4.11a, it may be expected that the change in $q_B$ is not associated with a change in the flow depth. This is in fact confirmed by Fig. 4.12 which shows the ratio $q_B/q_{B,H2O}$ as a function of the ratio $h_{r,m}/h_{r,m,H2O}$; no correlation can be recognised between the two parameters.

In previous studies on bed load transport at steep slopes it was found that $q_B$ is proportional to the flow rate q (s. sec. 2.3). In Fig. 4.13 the ratio $q_B/q_r$ is plotted against the density factor (s-1) for the experimental results of this study; $q_r$ denotes the reduced flow rate corrected for sidewall influence. It is seen that there is generally a stronger than a linear dependence of $q_B/q_r$ on the factor (s-1). It is further observed that the slope is an additional parameter determining the value of the ratio $q_B/q_r$.

A regression analysis was performed to obtain an equation of the form:

$$q_B = B_2 \, q_r^{e1} \, S^{e2} \, (s-1)^{e3} \tag{4.10}$$

where $B_2$ is a constant. The resulting exponent e1 was very close to 1.0, confirming the findings of other studies. It was decided to fix the value e1 = 1.0, with the advantage that equ.(4.10) is then dimensionally correct. Another regression analysis yielded the equation:

$$q_B = \frac{25.2}{(s-1)^{2.0}} \, q_r \, S^{2.3} \qquad \begin{matrix} r^2 = 0.964 \\ S_E = 14.9\% \end{matrix} \tag{4.11}$$

A comparison between the measured $q_B$ values and those calculated by equ. (4.11) is shown in Fig. 4.14.

To check the influence of neglecting the conditions at initiation of motion, a critical slope $S_{cr}$ was determined similarly as described by Smart and Jäggi (1983):

$$S_{cr} = \theta_c \, (s-1) \, d_m \, / \, h_m \tag{4.12}$$

They calculated the Shields parameter $\theta_c$ according to a procedure developed by Iwagaki and Tsuchiya (1959), which basically accounts for the change in $\theta_c$ at particle Reynolds numbers below about 400; at higher

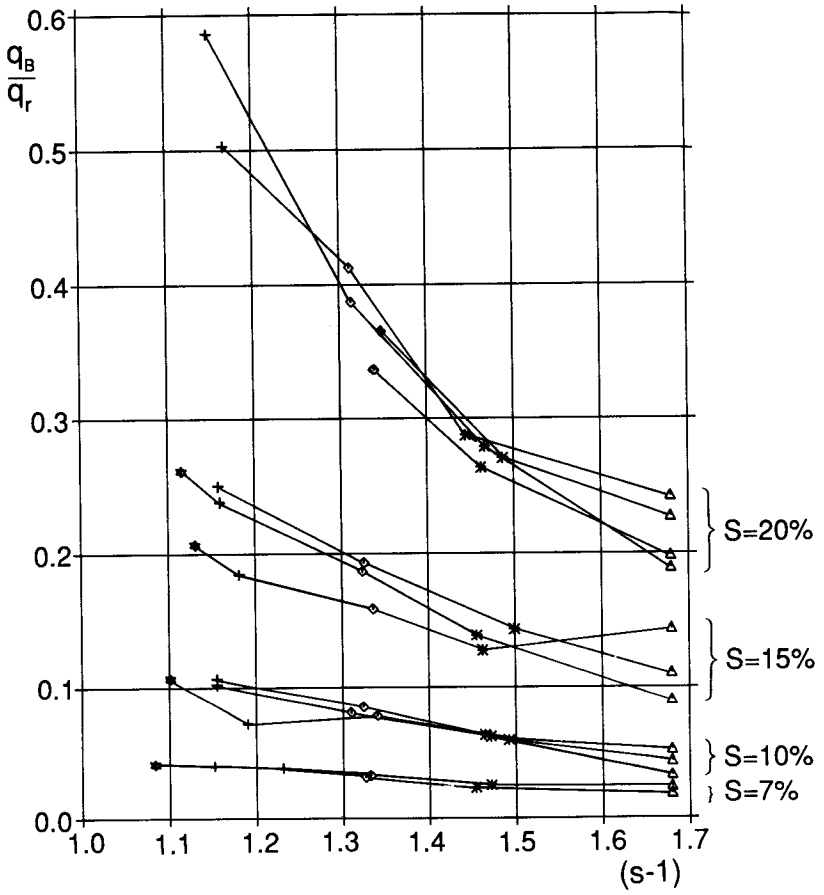


Fig. 4.13: Ratio of bed load transport rate to corrected fluid discharge, $q_B/q_r$, in function of the density factor (s-1), showing the slope S as additional parameter; data points with equal flow rate in the flume (Q) and equal slope are connected by a straight lines.

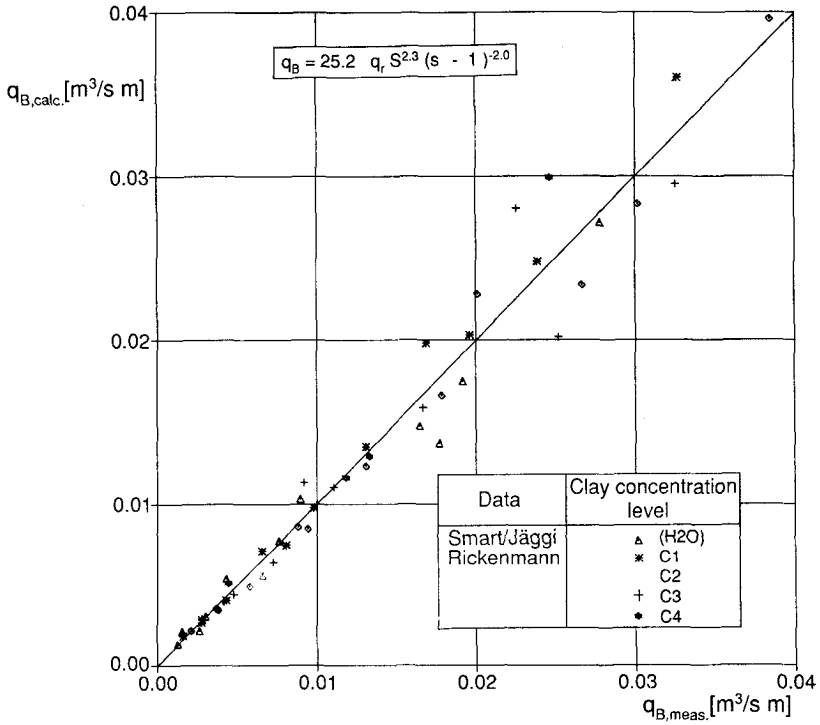


Fig. 4.14: Comparison between measured bed load transport rates, $q_{B,meas.}$, and those calculated, $q_{B,calc.}$, using equ. (4.11).

values of $Re^*$ the Shields parameter has a constant value of about 0.05, while $\theta_c$ assumes a minimum of about 0.03 at an $Re^*$ value of about 10. Daido (1971) extended the above theory to incorporate the effects of a Bingham fluid (clay suspension) on the critical dimensionless shear stress at initiation of motion, $\theta_c$. In the present analysis, Daido's (1971) procedure was used to determine appropriate $\theta_c$ values for the experimental conditions. These $\theta_c$ values were then reduced for the slope effect with the equation of Stevens et al. (1976) (equ. 2.105) to obtain the $\theta_c'$ values which were used in equ. (4.12) to compute $S_{cr}$.

Using now the term $(S - S_{cr})$ instead of S alone, another regression analysis resulted in the equation:

$$q_B = \frac{16.7}{(s-1)^{1.6}} q_r (S - S_{cr})^{2.1} \qquad \begin{matrix} r^2 = 0.959 \\ S_E = 15.9\% \end{matrix} \qquad (4.13)$$

The quality of the correlation is practically the same for equ. (4.13) and equ. (4.11). However, the introduction of the critical slope $S_{cr}$ changes the exponent of the density factor (s-1) markedly. It is noted that for most of the experiments $S > 7 \cdot S_{cr}$, i.e. the flow conditions were clearly above critical conditions for beginning of transport.

According to dimensional analysis (Yalin, 1977), bed load transport relationships may be expressed in terms of the dimensionless parameters $\Phi_B$ and $\theta$, and possibly other parameters. In the present study, the Froude number Fr and the density factor (s-1) were chosen as additional dimensionless parameters. In the bed load transport equation of Smart and Jäggi, equ. (2.83), the factor $cS^{0.6}$ appears, which is very close to $Fr = cS^{0.5}$. Low (1989) showed that the density factor (s-1) should also appear in equ. (2.83) as additional parameter; this may also be expected when comparing equ. (4.13) with the Smart/Jäggi equ. (2.82) or (2.82b). Therefore the following alternative parameter set was used:

$$\Phi_B = \phi(\theta, \theta_c, Fr, s-1) \qquad (4.14)$$

A regression analysis performed with these parameters yielded the following relationships:

$$\Phi_B = \frac{2.9}{(s-1)^{0.5}} \theta_m^{1.5} Fr^{1.1} \qquad (4.15)$$

$$\Phi_B = \frac{3.9}{(s-1)^{0.4}} (\theta_m - \theta_{cr})^{1.5} Fr^{0.8} \qquad (4.16)$$

$$\Phi_B = \frac{3.6}{(s-1)^{0.5}} \theta_m^{0.5} (\theta_m - \theta_{cr}) Fr^{0.9} \qquad (4.17)$$

In all three equations, both $\theta_m$ and Fr were determined with the corrected mixture flow depth, $h_{r,m}$, and $\theta_{cr}$ was calculated according to the procedure of Daido (1971), and then corrected for the slope effect with the relation of Stevens et al. (1976), as described above. It

should be noted, however, that the assumption of a constant $\theta_{cr}$ value, for example 0.05, does not greatly affect the correlation equations. (Note that $\theta > \simeq 7 \cdot \theta_{cr}$.)

One may argue that a regression analysis between $\Phi_B$ and $\theta_m$ leads to a spurious correlation because the density factor (s-1), which was varied during the experiments, is contained in both $\Phi_B$ and $\theta_m$. Therefore, the quality of the correlation was also checked between the measured transport rates ($q_{B,meas.}$) and those calculated ($q_{B,calc.}$) with a transformed version of equs. (4.15) to (4.17). This resulted in the following correlation parameters:

| $q_{B,calc.} = \Phi_{B,calc.}[g(s-1)d_m^3]^{0.5}$ | $r^2$ | $S_E$ |
|---|---|---|
| with equ. (4.15) | 0.967 | 15.0% |
| with equ. (4.16) | 0.975 | 13.0% |
| with equ. (4.17) | 0.972 | 13.9% |

It can be concluded that there is a similar quality of correlation with both parameter sets ($q_B$, $q_r$, S, $S_{cr}$, s-1) and ($\Phi_B$, $\theta_m$, $\theta_{cr}$, Fr, s-1). From the point of view that the experimental determination of the flow rate Q (and thus $q_r$) is more reliable than the measurement of the flow depth H (and thus $h_{r,m}$) and the fluid velocity V, a better correlation might be expected when using the first parameter set. But this first set does not include any parameter describing the flow behaviour (except through the term $S_{cr}$, the influence of which is however small), whereas the second set contains the flow parameters $h_{r,m}$ and V. It is also interesting that the exponent of the density factor (s-1) is less sensitive to the inclusion of $\theta_{cr}$ in equs. (4.15) to (4.17) than of $S_{cr}$ in equs. (4.11) and (4.13).

## 4.6 Comparison and analysis with further data

### 4.6.1 Experiments of Smart and Jaeggi

In the analysis of their steep flume data, Smart and Jäggi (1983) compared their findings with the experiments of Meyer-Peter and Müller and concluded that the bed load transport rate can be predicted by a common expression for both data sets (s. sec. 2.3.2).

During the analysis for the present study it was found that a difference exists in comparison to the procedure that lead to the bed load transport euqation of Smart and Jäggi (1983). To adjust their steep flume data for sidewall friction they used the Einstein procedure as described in section 4.1.1 . For the bed load transport regression analysis, however, they used a fictitious mean velocity (=q/H) derived from the measured flow rate Q and mixture flow depth H. If a significant part of the flow cross section is occupied by transported bed material, this velocity is lower than the effective fluid velocity (which in fact was measured and cannot be derived from the mixture flow depth). Thus their reduced flow rates $q_r$ are higher (for the steeper slope conditions) than if these values are determined with the measured fluid velocities. But it should be pointed out that this peculiarity did only affect the bed load transport equation (2.81). In the other parts of their analysis they used measured values (not corrected for sidewall influence), and in the verification calculations that followed the development of the necessary equations, they used the measured fluid velocity in the sidewall correction procedure.

Their data set includes 77 bed load transport experiments and is labelled SJ henceforth. Four types of bed material were used in their experiments: Two with a relatively uniform grain size distribution (mat. II and IV), and two consisting of a mixture of grain sizes (mat. I and III). These two classes are marked with different symbols in the following figures.

In this study their bed load transport data was reanalysed using the measured fluid velocities in the sidewall correction procedure. It is seen in Fig. 4.15 that a systematic deviation of the bed load transport rates calculated with the Smart/Jäggi equation (2.81) exists for the

higher transport intensity region. From Fig. 4.15 it may be estimated that the higher measured transport rates are systematically underpredicted by about 20% to 30%. In fact, these differences can also be detected from the results of the verification calculations presented in Smart and Jäggi (1983). Equ. (2.81) is rewritten here, using the term $S_{cr}$ instead of $\theta_c$:

$$q_B = \frac{4}{(s-1)} \left(\frac{d_{90}}{d_{30}}\right)^{0.2} q_r \, S^{0.6} \, (S - S_{cr}) \qquad (2.81b)$$

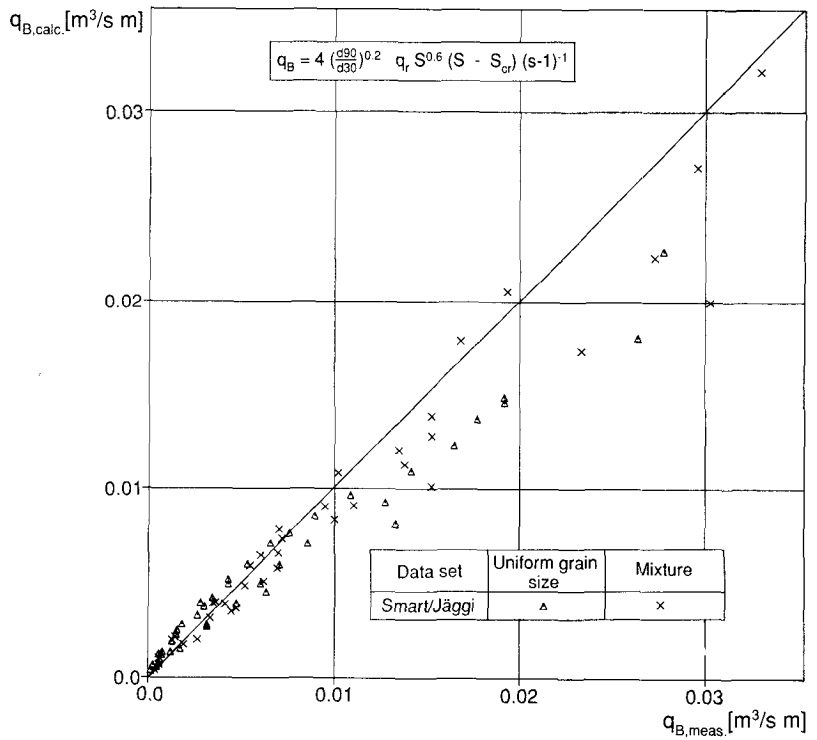


Fig. 4.15 : Bed load transport rates of Smart and Jäggi, comparison between measured values, $q_{B,meas.}$, and those calculated with equ. (2.81), $q_{B,calc.}$ (using the measured fluid velocities in the sidewall correction procedure).

Another difference results from the simplified transformation of equ. (2.81) into an equation in terms of $\Phi_B$ and $\theta$, because the the (fluid) flow rate q should be substituted by V and $h_f$, and not by V and $h_m$. The correct transformed form of equ. (2.81) is equ. (2.83); the simplified form given in Smart and Jäggi (1983), omitting the factor $h_f/h_m$ or $\theta_f/\theta_m$, is:

$$\Phi_B = \frac{4}{(s-1)} \left(\frac{d_{90}}{d_{30}}\right)^{0.2} S^{0.6} \; c \; \theta_m^{0.5} \; (\theta_m - \theta_c) \qquad (4.18)$$

Bed load transport rates $q_B$ were calculated with equ. (4.18) for the Smart/Jäggi data to estimate the resulting deviation (the corrected mixture flow depth, $h_{r,m}$, was used to determine $\theta_m$). It can be seen from Fig. 4.16 that the calculated values systematically overpredict the measured transport rates by about 50% at the highest transport intensities.

It may be noted that the first difference (resulting in an underprediction of transport rates) partly compensates for the second difference which would otherwise lead to an even stronger overprediction of the transport rates. However, it should be pointed out that the bed load transport rates predicted by the equations of Smart and Jäggi only deviate substantially from the measured ones for slopes steeper than 10% to 15%, within the given range of experimental conditions. The validity of both equations is not affected by the differently applied sidewall correction in the lower slope ranges where the bed load grain concentrations are relatively small.

A new regression analysis was performed with the Smart/Jäggi data, which yielded the equations:

$$q_B = \frac{9.4}{(s-1)} \left(\frac{d_{90}}{d_{30}}\right)^{0.2} q_r \; S \; (S - S_{cr}) \qquad \begin{matrix} r^2 = 0.958 \\ S_E = 20.5\% \end{matrix} \qquad (4.19)$$

$$q_B = \frac{8.1}{(s-1)} \left(\frac{d_{90}}{d_{30}}\right)^{0.2} q_r \; (S - S_{cr})^{1.9} \qquad \begin{matrix} r^2 = 0.958 \\ S_E = 20.4\% \end{matrix} \qquad (4.20)$$

$$q_B = \frac{11.0}{(s-1)} \left(\frac{d_{90}}{d_{30}}\right)^{0.2} q_r \; S^{2.1} \qquad \begin{matrix} r^2 = 0.955 \\ S_E = 21.2\% \end{matrix} \qquad (4.21)$$

It is again noted that for the majority of the data points $S > 5 \cdot S_{cr}$, i.e. conditions clearly above beginning of transport. As found for the clay suspension data, the equs. (4.19) to (4.21) show that the inclusion of the term $S_{cr}$ does not greatly affect the quality of the correlations.

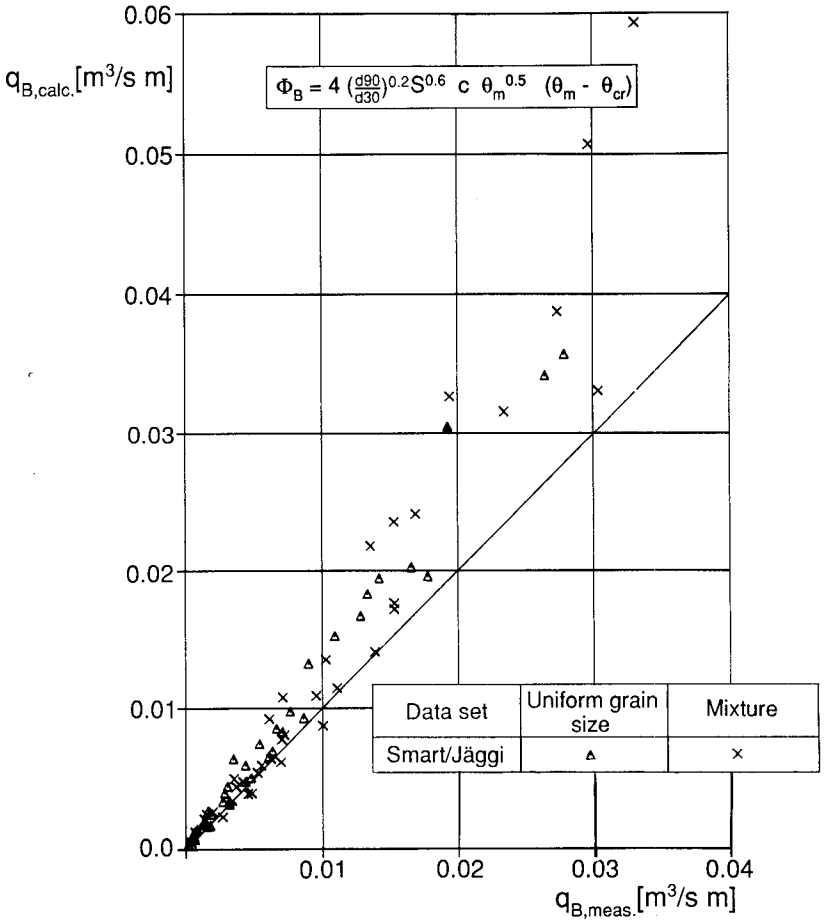


Fig. 4.16 : Bed load transport rates of Smart and Jäggi, comparison between measured values, $q_{B,meas.}$, and those calculated with equ. (4.18), $q_{B,calc.}$.

It is observed that the exponent of the slope factor is now higher than in equ. (2.81b) of Smart/Jäggi, for which the statistical parameters are also given for comparison:

$$q_B = \frac{4}{(s-1)} \left(\frac{d_{90}}{d_{30}}\right)^{0.2} q_r \, S^{0.6} \, (S - S_{cr}) \qquad \begin{matrix} r^2 = 0.952 \\ S_E = 29.3\% \end{matrix} \quad (2.81b)$$

The difference in the exponent might be expected to be due to the differently applied sidewall correction procedure. To check this effect, a comparative regression analysis was made, using the measured flow rates q and ignoring any sidewall effect; the resulting equation is:

$$q_B = \frac{7.2}{(s-1)} \left(\frac{d_{90}}{d_{30}}\right)^{0.2} q \, S^{0.90} \, (S - S_{cr}) \qquad \begin{matrix} r^2 = 0.956 \\ S_E = 27.3\% \end{matrix} \quad (4.17b)$$

It is noted that the exact exponent of S in equ. (4.17) is 0.95 but it was rounded to 1.0 (adjusting the constant correspondingly). The comparison shows that the effect of including a sidewall correction is not very pronounced.

The different exponent in equ. (4.17) and equ. (2.81b) must therefore have another reason. It is presumably due to the fact that Smart and Jäggi wanted to establish a single relationship for both their steep flume data and the experiments of Meyer-Peter and Müller (s. also section 4.6.2).

Comparing the new equations for the Smart/Jäggi data set (SJ) with the relations obtained for the data set of the author (RI), it is recognised that the exponent of the slope factor is not much different, but that there is stronger dependence upon the density factor in the formulae for the clay suspension data. In Fig. 4.17 the measured bed load transport rates of the RI data set are compared with those predicted by equ. (4.20); the $q_B$ values for the higher concentrations levels are seen to be systematically underpredicted, which is due to the exponent of the density factor (s-1).

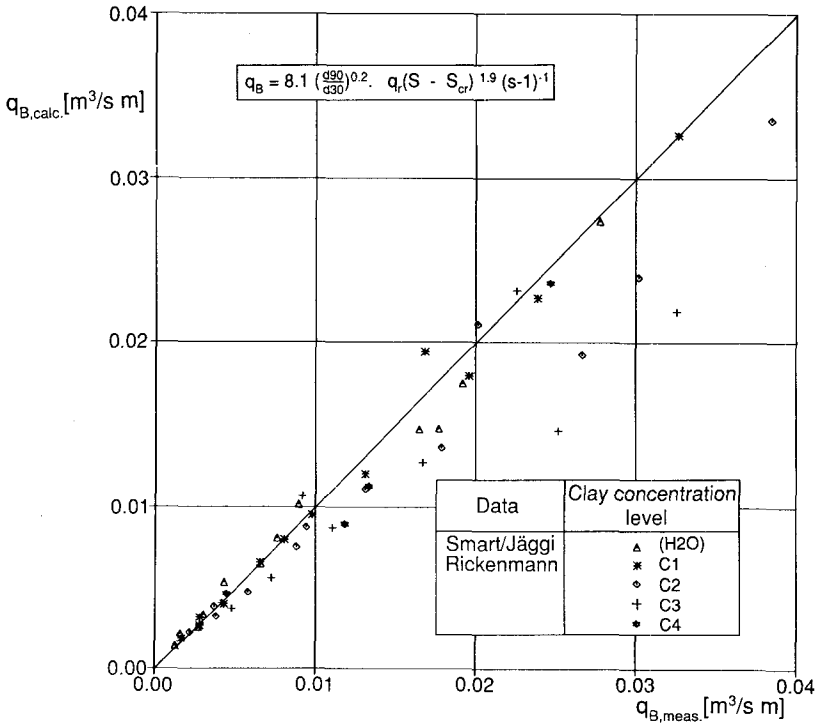


Fig. 4.17 : Comparison between measured bed load transport rates, $q_{B,meas.}$, with those predicted by equ. (4.20), $q_{B,calc.}$, for the new experiments.

Since the density factor (s-1) did not vary in the Smart/Jäggi tests it was decided to fix the exponent at -1.6, the value obtained for the clay suspension data. Another regression analysis was then performed with both data sets SJ and RI, with the resulting formula:

$$q_B = \frac{13.0}{(s-1)^{1.6}} \left(\frac{d_{90}}{d_{30}}\right)^{0.2} q_r (S - S_{cr})^{2.0} \qquad \begin{matrix} r^2 = 0.956 \\ S_E = 19.5\% \end{matrix} \qquad (4.22)$$

The correlation coefficient $r^2$ and the standard error $S_E$ are similar to the values for equ. (4.20). In Fig. 4.18 the measured bed load transport

rates are compared with those predicted by equ. (4.22); it is seen that there is no systematic deviation for both data sets.

If the conditions at initiation of motion are neglected, the following regression equation is obtained for the SJ and RI data sets:

$$q_B = \frac{17.3}{(s-1)^{2.0}} \left(\frac{d_{90}}{d_{30}}\right)^{0.2} q_r \, S^{2.1} \qquad \begin{matrix} r^2 = 0.949 \\ S_E = 20.9\% \end{matrix} \qquad (4.23)$$

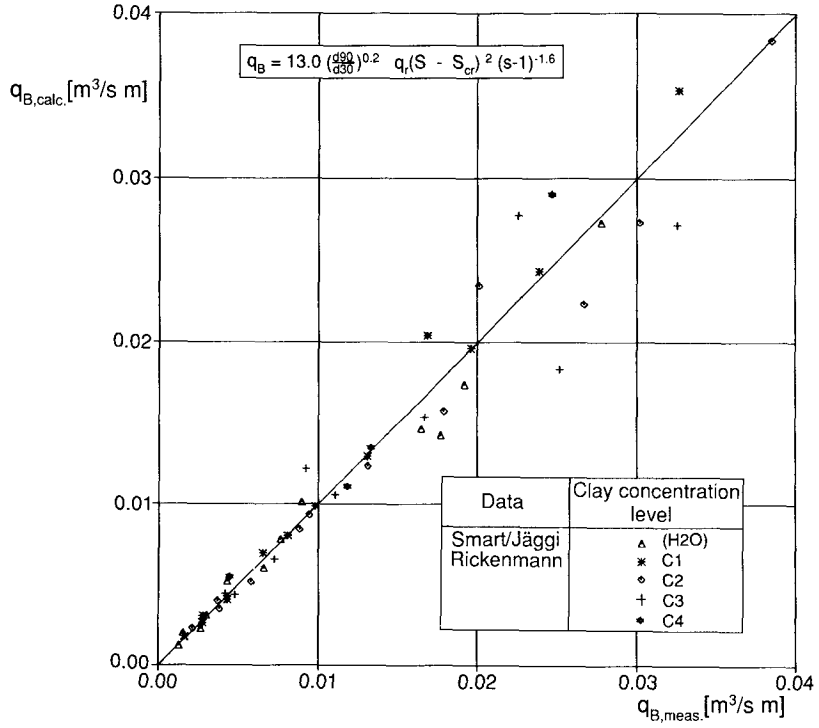


(a)

Fig. 4.18 : Comparison between measured bed load transport rates, $q_{B,meas.}$, and those predicted by equ. (4.22), $q_{B,calc.}$, for (a) the clay suspension data and (b) the Smart/Jäggi data.

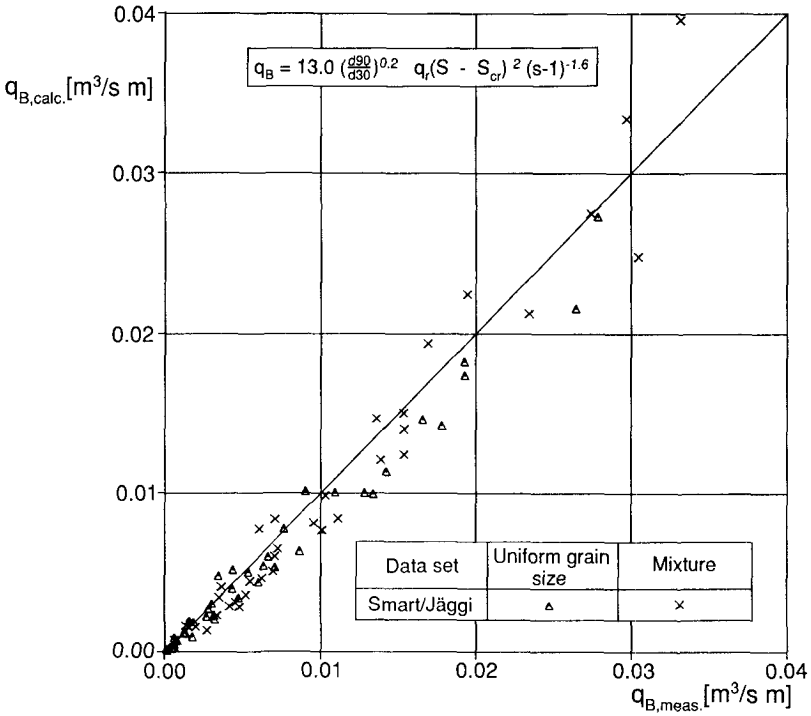


Fig. 4.18 (b)

Equation (4.23) has the practical advantage that it only requires the knowledge of the slope, the flow rate, the grain size characteristics, and the fluid-solid density ratio s. But no information is needed on the flow depth, in contrast to the formulae where the critical slope term $S_{cr}$ is included.

In section 2.3.3 it was shown that the conditions at beginning of bed load transport may as well be expressed by a critical discharge, the determination of which does also not require a knowledge of the flow depth. Since the constant in equ. (2.111) is partly based on the Smart/Jaggi tests, this relation shall be used here:

$$q_{cr} = 0.065 \, (s-1)^{1.67} \, g^{0.5} \, d_{50}^{1.5} \, S^{-1.12} \qquad (2.111)$$

Another regression analysis was performed with the data sets SJ and RI, using the parameter set ($q_B$, $q_r$-$q_{cr}$, S, s-1), where $q_{cr}$ was calculated with equ. (2.111); the resulting equation is:

$$q_B = \frac{12.6}{(s-1)^{1.6}} \left(\frac{d_{90}}{d_{30}}\right)^{0.2} (q_r - q_{cr})\, S^{2.0} \qquad \begin{matrix} r^2 = 0.951 \\ S_E = 20.1\% \end{matrix} \qquad (4.24)$$

Since critical conditions at transport begin have only a weak effect on calculated $q_B$ values for the steep flume data under consideration ($q_r > 6 \cdot q_{cr}$ for most of the data), there is practically no difference in the performance of equs. (4.24) and (4.22); both formulae show a similar quality of correlation.

In steep torrents with a very rough bed, the critical discharge at beginning of transport might be underestimated by equ. (2.111). It may be more appropriate in this case to use equ. (2.113) which was developed to judge the stability of steep block ramps.

### 4.6.2 Experiments of Meyer-Peter and Mueller

The comprehensive data set of the bed load transport experiments performed by Meyer-Peter and Müller (labelled MPM data set below) is given in Smart and Jäggi (1983). [1] Most of the 137 experiments were carried out with ordinary quartz grains as bed material. Coal ($\sigma$ = 1.25 g/cm³) was used as lightweight sediment in twelve tests, and baryt ($\sigma$ = 4.22 g/cm³) as heavy sediment in eight tests. Meyer-Peter and Müller (1948) had shown that their formula adequately accounts for a change in the grain-fluid density ratio $s = \sigma/\rho$. This is also true for the simplified form of their equation, given by Yalin (1977), equ. (2.67) (s. section 2.3.1.2, analysis of Low, 1989).

Low (1989) demonstrated that the Smart/Jäggi formula (equ. 2.83 with $\theta_f/\theta_m = 1$, i.e. small bed load concentrations, = equ. 4.18) does not correctly predict bed load transport rates for varyng s values (s. sec.

---

1) In Smart and Jaeggi (1983), the transport rate $G_B$ [g/s] should be divided by a factor of 10 for the 17 experiments with $d_{90}$ = 4.00 mm, which have a circle as symbol.

2.3.1.2). This can also be seen from Fig. 4.19(a) where $q_B$ values were calculated by equ. (2.82) for all MPM experiments with a mean grain diameter of 5.21 mm (N = 40), having a uniform grain size distribution, including the coal and baryt runs. The data points with s = 1.25 and with s = 4.22 plot systematically away from the line of perfect agreement. Fig. 4.19(b) shows the same data but with $q_B$ values computed by a modified formula, equu. (4.25), which is presented below.

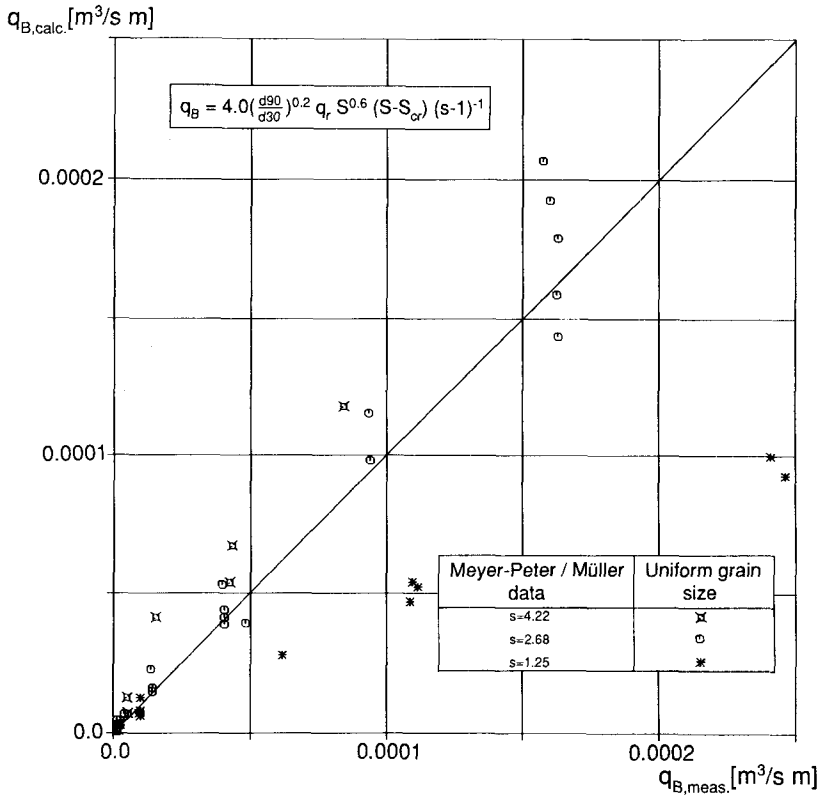


Fig. 4.19 (a)

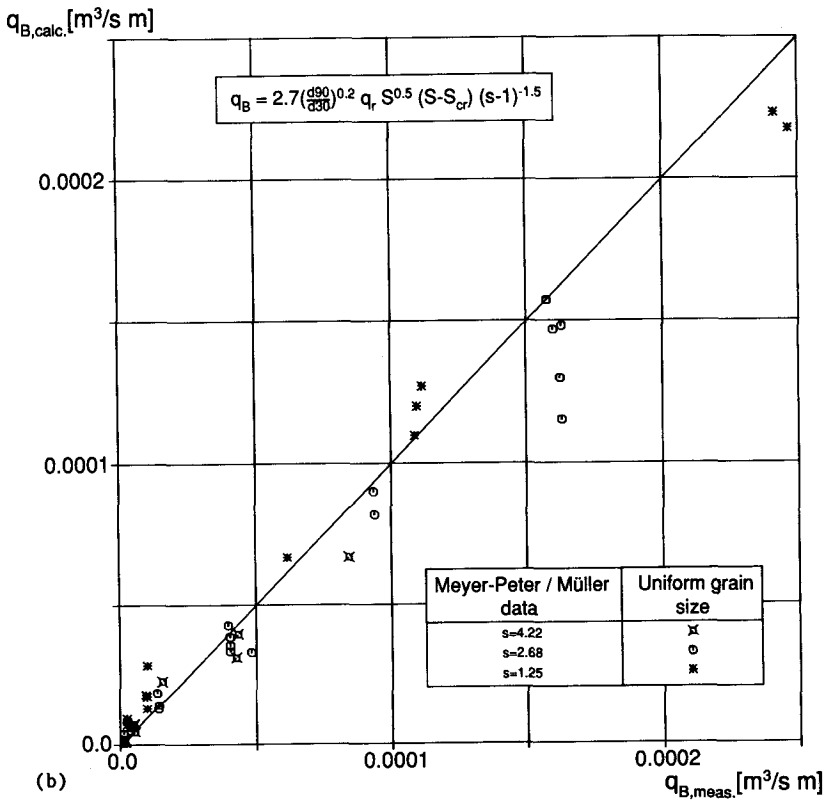


Fig. 4.19 : Bed load transport rates of selected experiments by Meyer-Peter and Müller (N = 40), comparison between measured values, $q_{B,meas.}$, and those calculated, $q_{B,calc.}$, (a) with equ. (2.83 or 4.18) and (b) with equ. (4.25).

An analysis was performed with a subdata set of the coal, baryt and some of the quartz grain experiments of the MPM data. A better agreement between predicted and measured bed load transport rates was found if the exponent of the density factor (s-1) in equ. (2.83 or 4.18) was put to -1.5 instead of -1.0. This modification is also confirmed by the study of Low (1989).

A new regression analysis was performed for the MPM data set only, and the exponent of the density factor (s-1) was fixed at -1.5. The following equation best fitted the data set:

$$q_B = \frac{2.7}{(s-1)^{1.5}} \left(\frac{d_{90}}{d_{30}}\right)^{0.2} q_r \, S^{0.5} \, (S - S_{cr}) \qquad \begin{matrix} r^2 = 0.960 \\ S_E = 45.9\% \end{matrix} \qquad (4.25)$$

$S_{cr}$ was calculated by equ. (4.12), and a constant $\theta_c = 0.047$ was used, a mean value for the MPM experiments. Smart and Jäggi gave the correlation parameters for equ. (2.82) applied to the MPM data set as: $r^2 = 0.97$, $S_E = 66\%$, and for the original formula developed by Meyer-Peter and Müller (1948) as: $r^2 = 0.92$, $S_E = 72\%$. It appears that the standard error $S_E$ is further reduced by using equ. (4.25).

Equ. (4.25) can be transformed into a relationship in terms of the dimensionless parameters ($\Phi_B$, $\theta$, Fr, s-1):

$$\Phi_B = \frac{2.7}{(s-1)^{0.5}} \left(\frac{d_{90}}{d_{30}}\right)^{0.2} \theta_r^{0.5} \, (\theta_r - \theta_{cr}) \, Fr \qquad (4.26)$$

where again a constant value $\theta_{cr} = 0.047$ was used. (Note that at the lower slopes no distinction between $\theta_f$ and $\theta_m$ is necessary). Equ. (4.26) is confirmed by a separate regression computation using the dimensionless parameters. The performance of equ. (4.26) applied to the MPM data set is illustrated in Fig. 4.20. It may be seen that the relative error between measured and calculated bed load transport rates decreases with increasing transport intensity. As for the SJ data, the MPM experiments performed with a uniform bed material and with a mixture of grain sizes, respectively, are marked by different symbols.

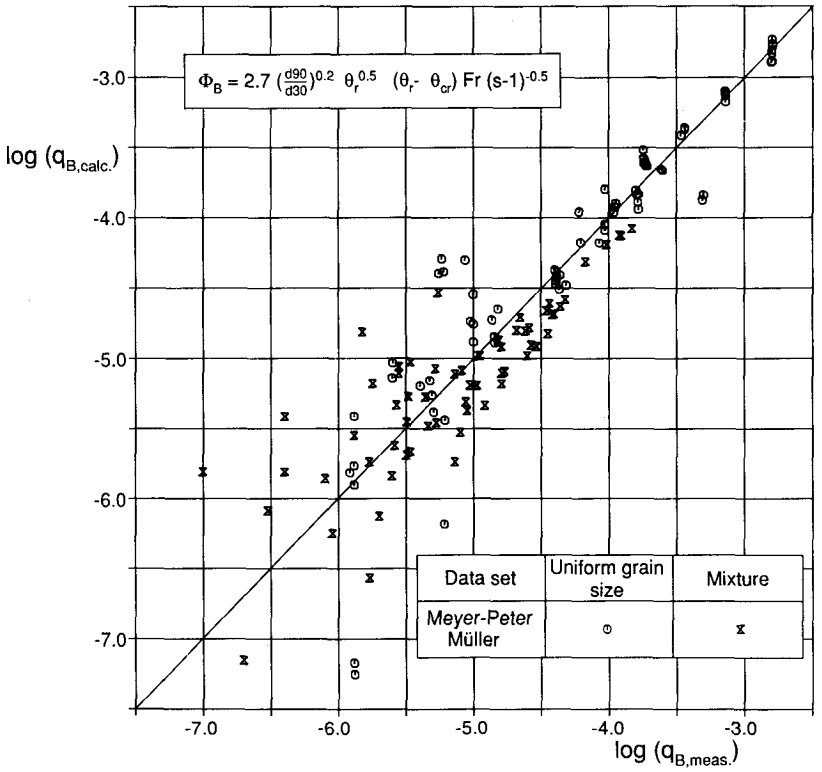


Fig. 4.20 : Bed load transport rates of the Meyer-Peter and Müller data set (N = 137), comparison between measured values, $q_{B,meas.}$, and those calculated with equ. (4.26), $q_{B,calc.}$.

If the exponent of the density factor is adjusted in the original equation (2.81) of Smart and Jäggi (1983) from -1.0 to -1.5, the formula can be transformed to (using s = 1.68):

$$q_B = \frac{5.2}{(s-1)^{1.5}} \left(\frac{d_{90}}{d_{30}}\right)^{0.2} q_r\, S^{0.6}\, (S - S_{cr}) \qquad (4.27)$$

Comparing equ. (4.27) with equ. (4.25) it is seen that there is only a difference in the constant and in the slope factor; this difference is tabulated below for some slope values within the range of the MPM experiments:

| | in equ. (4.25): $2.7 \cdot S^{0.5}$ | in equ. (4.27): $5.2 \cdot S^{0.6}$ | Δ[%] |
|---|---|---|---|
| S = 0.02 | 0.382 | 0.497 | 30 |
| S = 0.01 | 0.270 | 0.328 | 21 |
| S = 0.002 | 0.121 | 0.125 | 3 |
| S = 0.001 | 0.0854 | 0.0824 | -4 |

It is observed that the maximum difference at a slope of 2% is about 30% (which is still within the calculated standard error for equ. 2.25). It is noted, that equ. (4.27) shows a stronger slope dependence, because it was developed by Smart and Jäggi to also predict the steep flume data. However, an equation based on the Smart/Jäggi data only, equ. (4.19), is seen to be even more dependent on the slope (factor S instead of $S^{0.6}$). Thus the exponent of S in equ. (4.27 or 2.81) appears to be a compromise for both the low and steep slope data.

The difference in the slope factor S suggests that in terms of the parameter set ($q_B$, $q_r$, S, $S_{cr}$, s-1) two separate equations should be used to predict transport rates for low and steep slopes. Thus a better agreement between measured and predicted values is obtained than in the case of one equation covering both slope ranges. It should be noted that in view of the scatter between predicted and measured values, the Smart/Jäggi formula, equ. (2.81 or 4.27), is equally valid as equ. (4.25) over the whole range of the MPM data set but their equation tends to underpredict the higher transport rates of the SJ and RI data sets (i.e. at slopes steeper than about 10%).

If equ. (4.26) is compared with the corresponding formula obtained for the clay suspension data, equ. (4.16), a remarkable similarity is recognised. A similar equation also results from an analysis of the Smart/Jäggi data set. In Fig. 4.21 all three data sets obtained at the same hydraulic laboratory (MPM, SJ and RI), including a total number of 252 experiments, are plotted in terms of $\Phi_B$ vs. $\Theta_r$ (determined with $h_{r,m}$ for the SJ and RI data). It may also be inferred from this figure that a common analysis of all experimental results is promising.

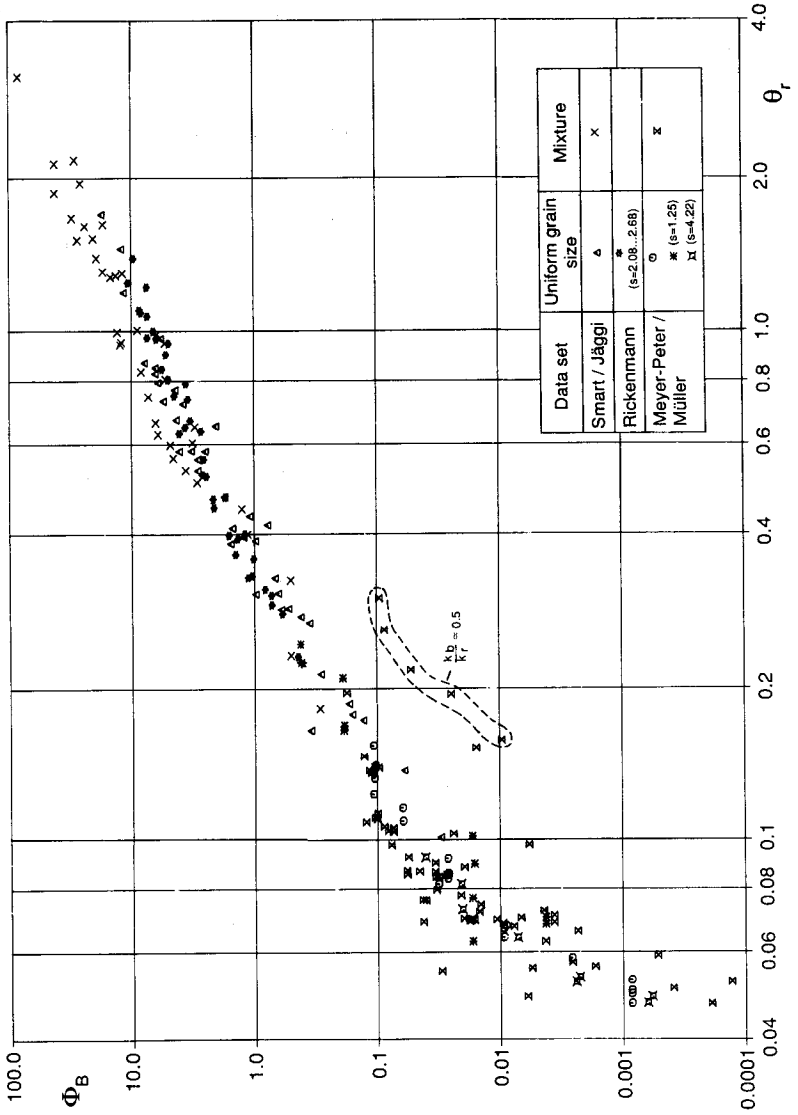


Fig. 4.21 : Experimental results of the three bed load transport data sets MPM, SJ and RI (N= 252), in terms of the parameters $\Phi_B$ and $\theta$. The term $k_b/k_r$ represents the ratio of grain friction to total friction (including form drag); the average value for the MPM data is about 0.85, five tests with an exceptionally low ratio are marked in the figure.

The following bed load transport formula was obtained from a regression analysis with the data shown in Fig. 4.21:

$$\Phi_B = \frac{3.1}{(s-1)^{0.5}} \left(\frac{d_{90}}{d_{30}}\right)^{0.2} \theta_r^{0.5} \left(\theta_r - \theta_{cr}\right) Fr^{1.1} \qquad (4.28)$$

where $h_{r,m}$ was used to determine $\theta_r$ for the steep flume data (SJ and RI). Again, the correlation parameters are given in terms of $q_{B,meas.}$ and $q_{B,calc.} = \Phi_{B,calc.}[g(s-1)d_m^3]^{0.5}$ : $r^2 = 0.961$ and $S_E = 34.8\%$.

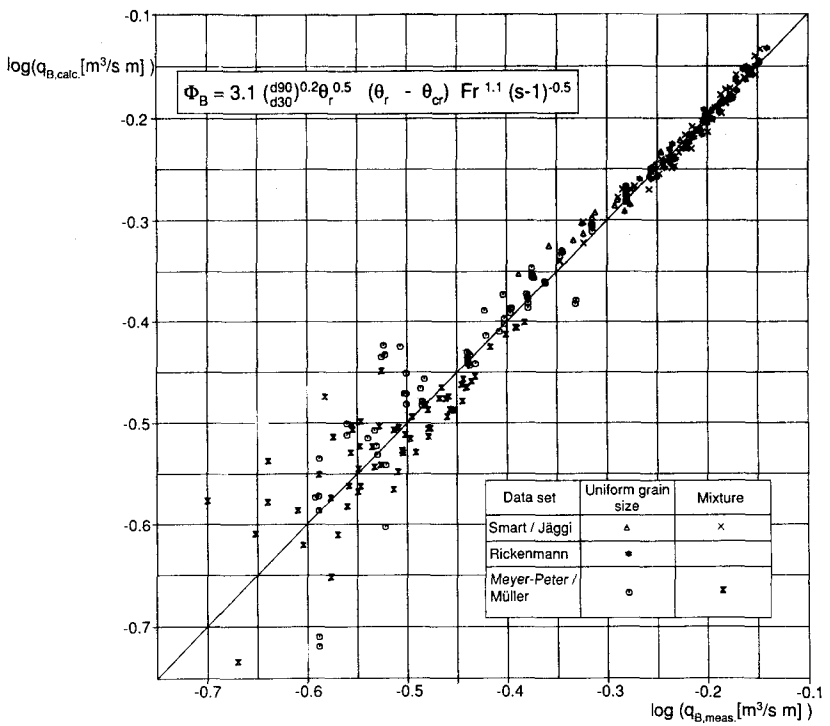


Fig. 4.22 : Comparison between measured bed load transport rates, $q_{B,meas.}$, and those predicted by equ. (4.28), $q_{B,calc.}$, for the three data sets MPM, SJ and RI. Note that logarithmic values are used to cover the whole experimental range in the same figure.

A comparison between measured transport rates and those calculated with equ. (4.28) is shown in Fig. 4.22. For ease of comparison, the performance of equ. (4.28) is also shown in linear plots separatly for the steep flume data in Fig. 4.23.

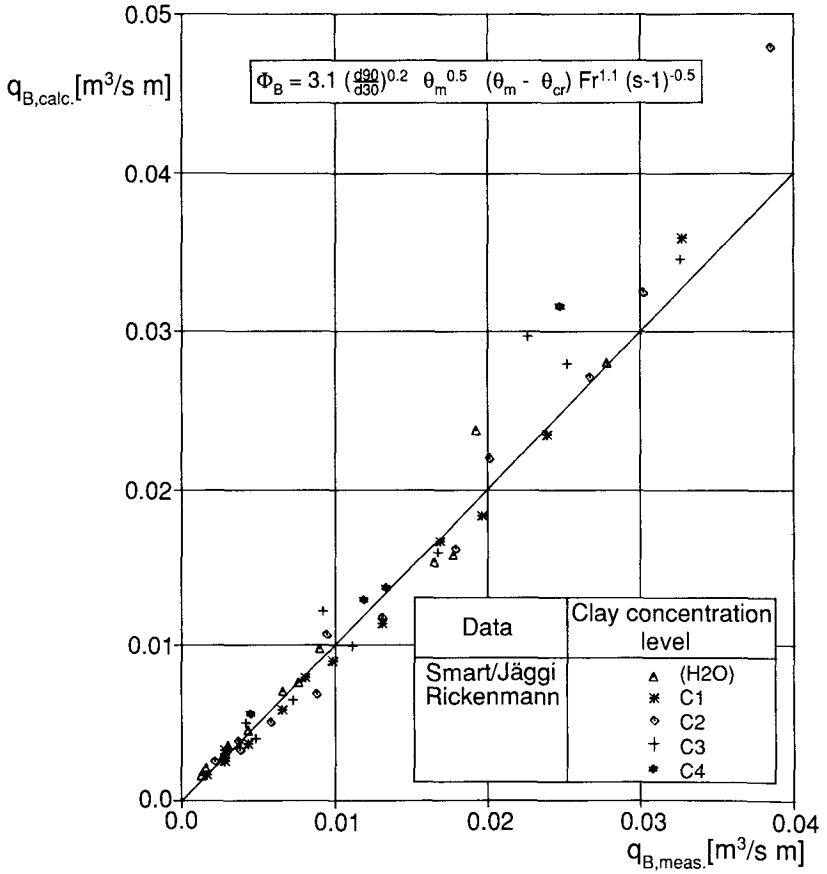


(a)

Fig. 4.23 : Comparison between measured bed load transport rates, $q_{B,meas.}$, and those predicted by equ. (4.28), $q_{B,calc.}$, shown in a linear scale for (a) the clay suspension data and (b) the Smart/Jäggi data.

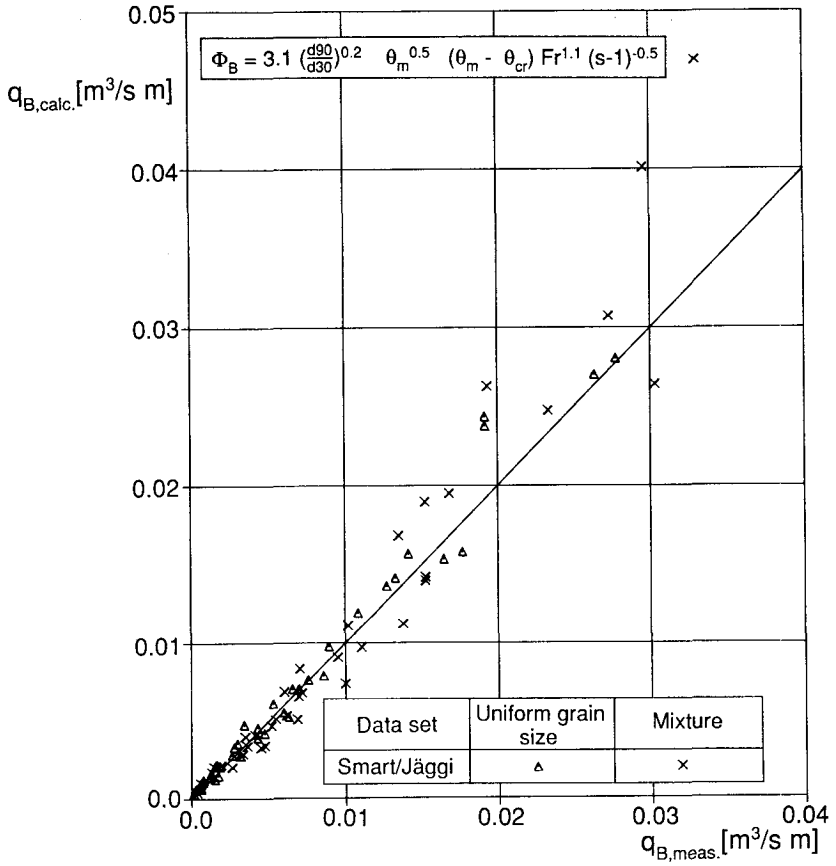


Fig. 4.23 (b)

## 4.7 **Summary of bed load transport formulae**

The following tables summarise the bed load transport equations that were determined above. Note that the correlation parameters $r^2$ and $S_E$ are always given in terms of $q_{B,calc.}$ versus $q_{B,meas.}$, also if the equation is presented in a $\Phi_B$ form.

| RI data set (N = 50): | | $r^2$ | $S_E$[%] |
|---|---|---|---|
| $q_B = \frac{25.2}{(s-1)^{2.0}} q_r S^{2.3}$ | ..(4.11) | 0.964 | 14.9 |
| $q_B = \frac{16.7}{(s-1)^{1.6}} q_r (S - S_{cr})^{2.1}$ | ..(4.13) | 0.959 | 15.9 |
| $\Phi_B = \frac{3.9}{(s-1)^{0.4}} (\theta_m - \theta_{cr})^{1.5} Fr^{0.8}$ | ..(4.16) | 0.975 | 13.0 |
| $\Phi_B = \frac{3.6}{(s-1)^{0.5}} \theta_m^{0.5} (\theta_m - \theta_{cr}) Fr^{0.9}$ | ..(4.17) | 0.972 | 13.9 |
| **SJ data set (N = 77):** | | $r^2$ | $S_E$[%] |
| $q_B = \frac{9.4}{(s-1)} (\frac{d_{90}}{d_{30}})^{0.2} q_r S (S - S_{cr})$ | ..(4.19) | 0.958 | 20.5 |
| $q_B = \frac{8.1}{(s-1)} (\frac{d_{90}}{d_{30}})^{0.2} q_r (S - S_{cr})^{1.9}$ | ..(4.20) | 0.958 | 20.4 |
| $q_B = \frac{11.0}{(s-1)} (\frac{d_{90}}{d_{30}})^{0.2} q_r S^{2.1}$ | ..(4.21) | 0.955 | 21.2 |
| **MPM data set (N = 137):** | | $r^2$ | $S_E$[%] |
| $q_B = \frac{2.7}{(s-1)^{1.5}} (\frac{d_{90}}{d_{30}})^{0.2} q_r S^{0.5} (S - S_{cr})$ | ..(4.25) | 0.960 | 45.9 |
| $\Phi_B = \frac{2.7}{(s-1)^{0.5}} (\frac{d_{90}}{d_{30}})^{0.2} \theta_r^{0.5} (\theta_r - \theta_{cr}) Fr$ | ..(4.26) = (4.25) | | |

Table 4.3 : Summary of bed load transport equations developed independently for the clay suspension data (RI), the Smart/Jäggi data (SJ) and the Meyer-Peter/Müller data (MPM).

Table 4.3 shows the bed load transport equations developed independently for the data sets RI, SJ and MPM.

In Table 4.4 the new formulae are listed which were developed for a combination of the data sets RI, SJ, and MPM. They are compared to the original formula of Smart and Jäggi, for which the influence of the density factor was adjusted, equ. (4.27). It is recognised that those equations valid only for the steep flume data (equ. 4.22, 4.24, 4.23) or the one valid for the low slope data only (equ. 4.26 = 4.25) show a better performance in their corresponding range of application than any of the formula that is based on all data sets (equ. 4.28 and 4.27). It is further observed that equ. (4.28) has generally smaller standard errors $S_E$ than equ. (4.27).

It is recommended that the first three equations are only applied within a slope range 5% <= S <≃ 25 %, while equ. (4.26 or 4.25) should be used only in the range 0.1 % <≃ S <≃ 2%.

It has also been checked how well the proposed equations perform for a subdata set containing only experiments with an essentially uniform bed material and those with a mixture of grain sizes. The correlation parameters calculated for these subdata sets are given in Table 4.5. It is noted that both subdata sets of the Smart/Jäggi experiments are best predicted with the first three equations.

| Data set: | RI (N = 50) | | SJ (N = 77) | | RI + SJ (N = 115) | | MPM (N = 137) | | RI + SJ + MPM (N = 252) | |
|---|---|---|---|---|---|---|---|---|---|---|
| | $r^2$ | $S_E$ | $r^2$ | $S_E$ | $r^2$ | $S_E$ | $r^2$ | $S_E$ | $r^2$ | $S_E$ |
| $q_B = \frac{13.0}{(s-1)^{1.6}} (\frac{d_{90}}{d_{30}})^{0.2} q_f (S - S_{cr})^{2.0}$ ...(4.22) | 0.954 | 16.8 | 0.957 | 21.3 | 0.956 | 19.5 | | | | |
| $q_B = \frac{12.6}{(s-1)^{1.6}} (\frac{d_{90}}{d_{30}})^{0.2} (q_f - q_{cr}) S^{2.0}$ ...(4.24) | 0.943 | 18.6 | 0.957 | 20.6 | 0.950 | 20.3 | | | | |
| $q_B = \frac{17.3}{(s-1)^{2.0}} (\frac{d_{90}}{d_{30}})^{0.2} q_f S^{2.1}$ ...(4.23) | 0.952 | 18.4 | 0.954 | 22.2 | 0.949 | 20.9 | | | | |
| $\Phi_B = \frac{3.1}{(s-1)^{0.5}} (\frac{d_{90}}{d_{30}})^{0.2} \theta_r^{0.5} (\theta_r - \theta_{cr}) Fr^{1.1}$ ...(4.28) | 0.970 | 18.9 | 0.948 | 30.5 | 0.959 | 25.4 | 0.962 | 61.8 | 0.961 | 34.8 |
| $\Phi_B = \frac{2.7}{(s-1)^{0.5}} (\frac{d_{90}}{d_{30}})^{0.2} \theta_r^{0.5} (\theta_r - \theta_{cr}) Fr$ ...(4.26) | | | | | | | 0.960 | 45.9 | | |
| $q_B = \frac{5.2}{(s-1)^{1.5}} (\frac{d_{90}}{d_{30}})^{0.2} q_f S^{0.6} (S - S_{cr})$ ...(4.27) | 0.910 | 29.4 | 0.951 | 28.9 | 0.930 | 29.9 | 0.965 | 72.8 | 0.957 | 43.5 |

Table 4.4: Comparison of bed load transport formulae for various combinations of the data sets of the author (RI), of Smart and Jäggi (SJ), and of Meyer-Peter and Müller (MPM). The correlation coefficient squared, $r^2$, and the standard error, $S_E$, were determined between measured and calculated values of $q_B$.

| Data set: | SJ | | | | MPM | | | |
|---|---|---|---|---|---|---|---|---|
| | Uniform g.s. (N = 40) | | Mixtures (N = 37) | | Uniform g.s. (N = 74) | | Mixtures (N = 63) | |
| | $r^2$ | $S_E$ | $r^2$ | $S_E$ | $r^2$ | $S_E$ | $r^2$ | $S_E$ |
| $q_B = \frac{13.0}{(s-1)^{1.6}} \left(\frac{d_{90}}{d_{30}}\right)^{0.2} q_r (S - S_{cr})^{2.0}$ ...(4.22) | 0.977 | 21.7 | 0.957 | 20.8 | | | | |
| $q_B = \frac{12.6}{(s-1)^{1.6}} \left(\frac{d_{90}}{d_{30}}\right)^{0.2} (q_r - q_{cr}) S^{2.0}$ ...(4.24) | 0.976 | 19.4 | 0.954 | 20.8 | | | | |
| $q_B = \frac{17.3}{(s-1)^{2.0}} \left(\frac{d_{90}}{d_{30}}\right)^{0.2} q_r S^{2.1}$ ...(4.23) | 0.969 | 23.0 | 0.952 | 21.4 | | | | |
| $\Phi_B = \frac{3.1}{(s-1)^{0.5}} \left(\frac{d_{90}}{d_{30}}\right)^{0.2} \theta_r^{0.5} (\theta_r - \theta_{cr}) Fr^{1.1}$ ...(4.28) | 0.977 | 18.7 | 0.938 | 34.5 | 0.958 | 48.5 | 0.924 | 61.1 |
| $\Phi_B = \frac{2.7}{(s-1)^{0.5}} \left(\frac{d_{90}}{d_{30}}\right)^{0.2} \theta_r^{0.5} (\theta_r - \theta_{cr}) Fr$ ...(4.26) | | | | | 0.956 | 35.7 | 0.924 | 74.2 |
| $q_B = \frac{5.2}{(s-1)^{1.5}} \left(\frac{d_{90}}{d_{30}}\right)^{0.2} q_r S^{0.6} (S - S_{cr})$ ...(4.27) | 0.973 | 35.1 | 0.948 | 24.7 | 0.962 | 57.2 | 0.920 | 59.6 |

Table 4.5: Comparison of bed load transport formulae for the subdata sets with nearly uniform bed material and with mixtures of grain sizes; experiments of Smart and Jäggi (SJ), and of Meyer-Peter and Müller (MPM). The correlation coefficient squared, $r^2$, and the standard error, $S_E$, were determined between measured and calculated values of $q_B$.

## 4.8 Flow resistance and other aspects of the grain-fluid mixture

It is seen from Fig. (4.10) that the friction factor did not significantly change with increasing clay concentration. In the previous sections it is shown that the bed load transport behaviour is essentially the same as for the clear water case, if the flow around the grains is not laminar ($Re_2^* \leq \approx 15$). For these conditions, the fluid velocity slightly increased with increasing clay concentration, because the higher bed load transport rates brought about a slight increase in the mixture flow depth (Fig. 4.12).

In Fig. 4.24 the flow resistance coefficient $c = V/v*$ is shown as a function of the relative depth $h/d_{90}$. The data points of the clay suspension tests were determined with the corrected mixture flow depth $h_{r,m}$; they are compared in Fig. 4.24 with equ. (4.7) used by Smart and Jäggi (1983). There is a similar agreement with the calculated values as found by Smart/Jäggi for their experimental results. In general, a slight tendency can be observed that the experiments with the higher transport rates (especially C2 and C3 tests with $S \geq \approx 15$ %) show a somewhat higher flow resistance (smaller c value) than those experiments with smaller transport rates.

To compare the fluid velocities measured in the clay suspension experiments (data set RI) with those of the Smart/Jäggi tests, the flow resistance equation used in their study, equ. (4.7), was applied to both data sets. Calculated and measured values are depicted in Fig. 4.25. It appears that the two data sets may be analysed together. In general, the predicted velocities are somewhat larger than the measured ones; this was already noted by Smart and Jäggi.

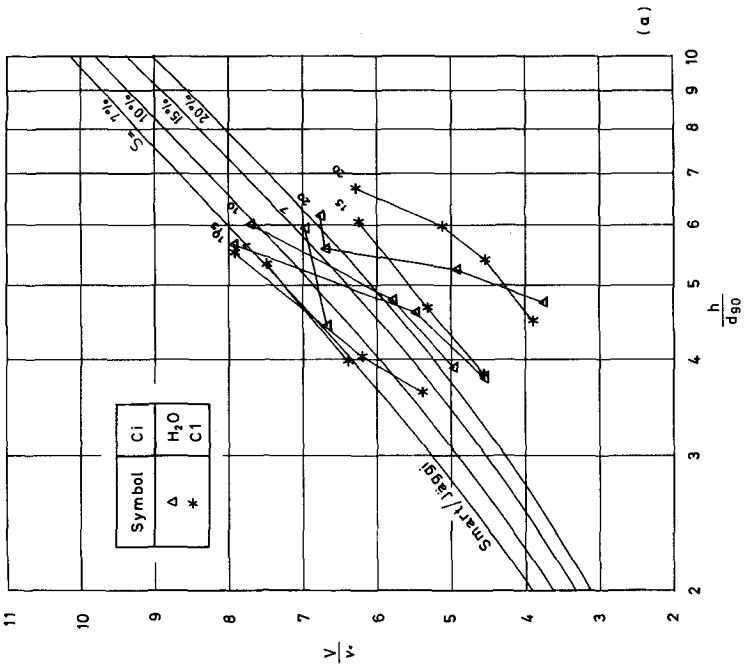


(a)

Fig. 4.24 : Comparison of data from clay suspension experiments with the flow resistance equation (4.7) used by Smart and Jäggi, shown in terms of $V/v^*$ vs. $h/d_{90}$; data points with equal slope are connected by straight lines. The concentration levels (Ci) are: (a) $H_2O$ (mat. IV of SJ) and C1, (b) C2 and C3, (c) C4 and C5.

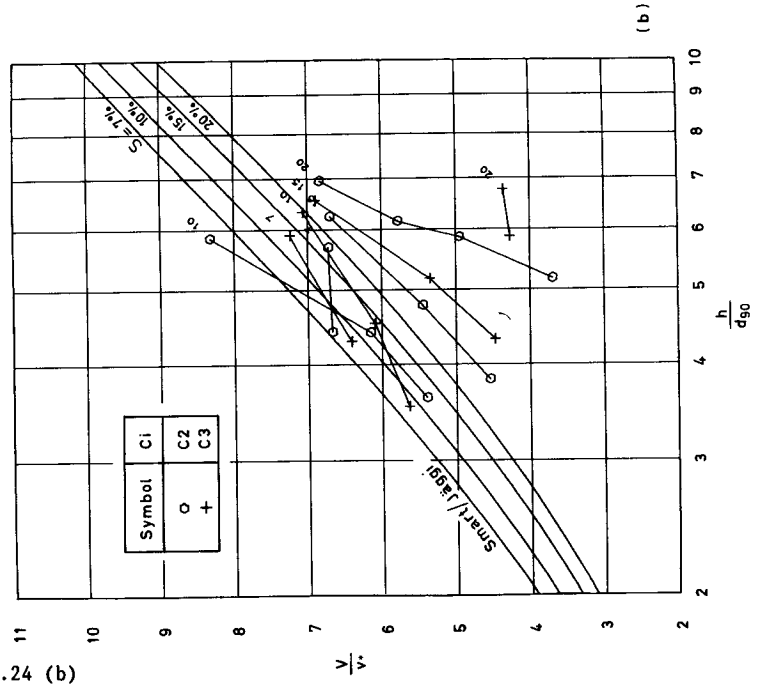


Fig. 4.24 (b)

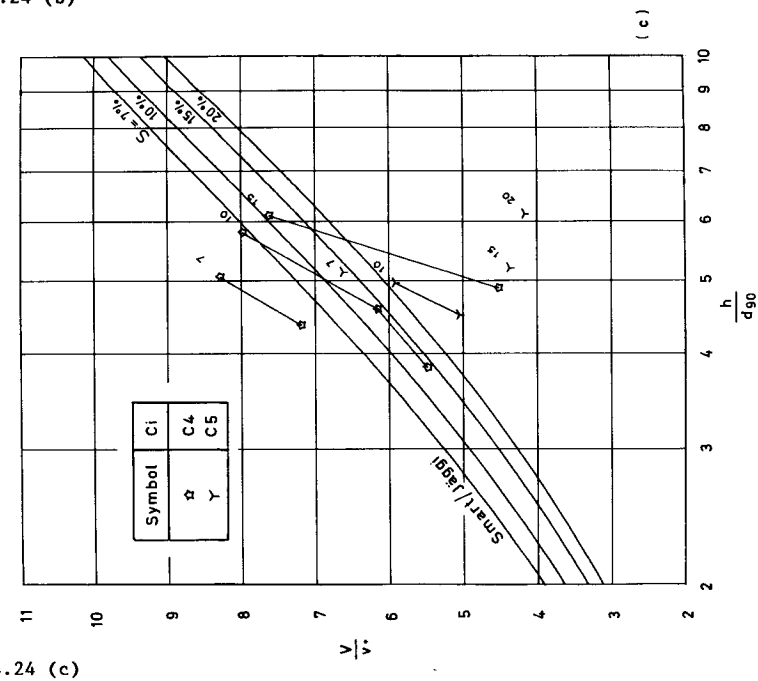


Fig. 4.24 (c)

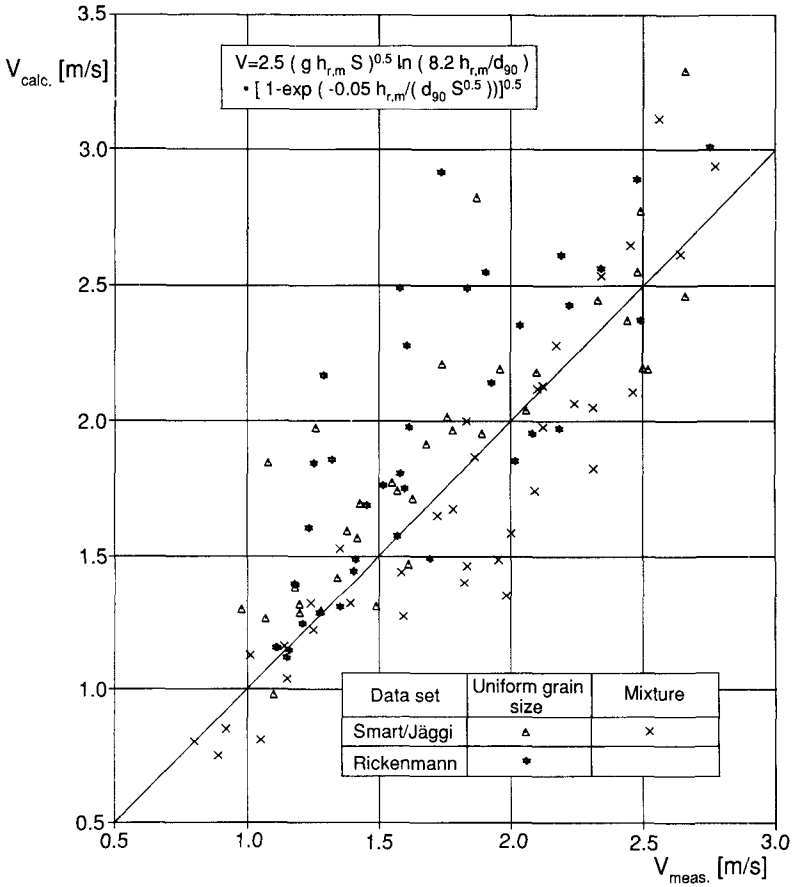


Fig. 4.25 : Comparison between measured fluid velocites, $V_{meas.}$, and those calculated with equ. (4.7), $V_{calc.}$, for the data sets SJ and RI.

The correlation parameters for the data shown in Fig. 4.25 were determined between measured and calculated (with equ. 4.7) velocities as: $r^2$ = 0.68 and $S_E$ = 20%. (It may be noted that a slightly better correlation results for the SJ data set alone: $r^2$ = 0.74 and $S_E$ = 17%.) A regression analysis was performed to obtain equations with dimensionless parameters in the form of:

$$\left(\frac{8}{f}\right)^{0.5} = 1.50 \frac{1}{S^{0.29}} \left(\frac{h_{r,m}}{d_{90}}\right)^{0.5} \tag{4.29}$$

and

$$\frac{V}{(gd_{90})^{0.5}} = 2.14\, S^{0.30} \left[\frac{q_r}{(gd_{90}^3)^{0.5}}\right]^{0.5} \tag{4.30}$$

In terms of $V_{meas.}$ versus $V_{calc.}$ the corresponding correlation parameters are: $r^2 = 0.68$, $S_E = 16.5\%$ with equ. (4.29), and $r^2 = 0.88$, $S_E = 10.8\%$ with equ. (4.30). Since both equations are based on a limited experimental conditions, they might not be applicable at relative depths $h/d_{90}$ larger than about 20.

The performance of equ. (4.29) is illustrated in Fig. 4.26; a similar scatter of the data points as on Fig. (4.25) can be observed. Accordingly, equ. (4.29) and equ. (4.7) show similar agreement between measured and predicted velocities. However, the first relationship has a much simpler form and is thus easier to apply.

Equ. (4.30) was developed as an alternative form because it allows to determine the fluid velocity as a function of the design discharge, without requiring the knowledge of the flow depth, which is difficult to estimate in a steep torrrent.

The performance of equ. (4.30) with the data on which it is based is shown in Fig. 4.27 (a). It may be noted that generally slightly higher velocities were measured for the case with a bed material with a wide grain size distribution. This might be due to a smoothening effect of the finer particles lying between the coarser grains on the stationary bed. It may also be noted that in general $d_{90}$ is taken as a measure of an average, characteristic grain size of the armour layer; if there are many fine particles present near the bed surface, this approximation might become inadequate.

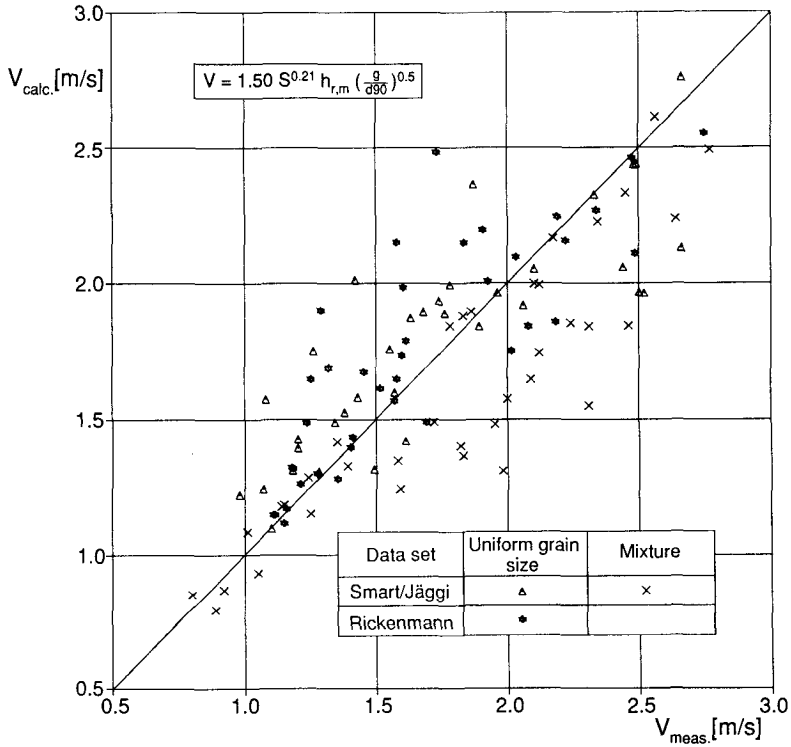


Fig. 4.26 : Comparison between measured fluid velocites, $V_{meas.}$, and those calculated with equ. (4.29), $V_{calc.}$, for the data sets SJ and RI.

The flow resistance measurements for the clay suspension without sediment transport were used to check how well equ. (4.30) would apply to flows over a rigid bed without sediment transport. It is seen from Fig. 4.27 (b) that the measured velocities systematically deviate from the predicted ones by about 16% on the average (the corresponding correlation between measured and predicted velocities was calculated as: $r^2 = 0.96$). While the form of equ. (4.30) is confirmed by the independent data set, the constant should be a bit higher than 2.14. But it is not unexpected that there is no unique constant for the two cases, i.e. for a sediment transporting flow over a mobile, permeable bed and for a fluid flow over a fixed, impermeable bed (s. also section 4.3).

Theoretically, the knowledge of the increase in the flow depth due to transported bed load grains should allow to compute the mean grain velocity $U_B$, if the fictitious fluid depth (q/V or $q_r$/V) is known:

$$\frac{q}{V} + \frac{q_B}{U_B} = H_m \qquad (4.31a)$$

or

$$\frac{q_r}{V} + \frac{q_B}{U_B} = h_{r,m} \qquad (4.31b)$$

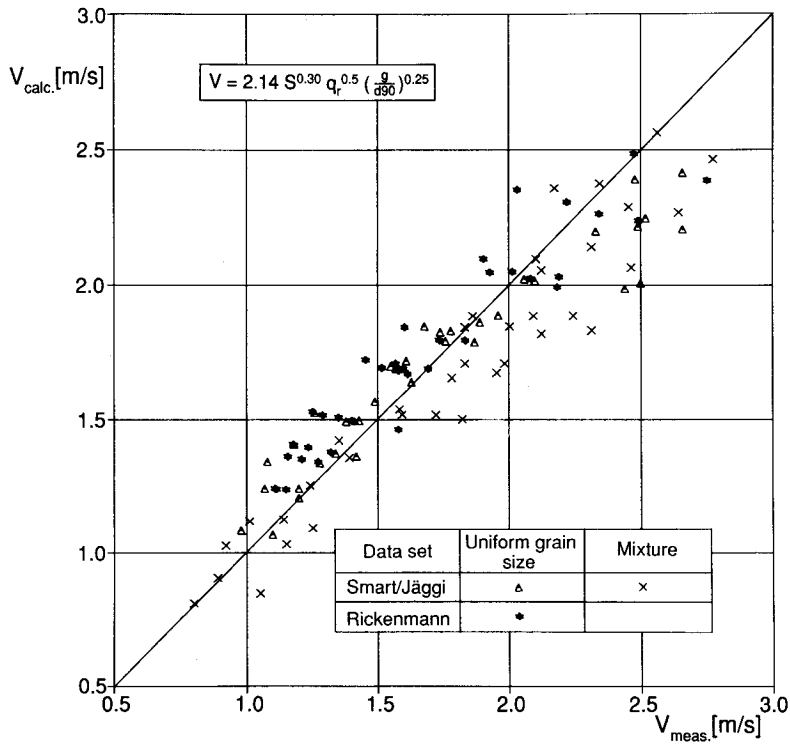


(a)

Fig. 4.27 : Comparison between measured fluid velocites, $V_{meas.}$, and those calculated with equ. (4.30), $V_{calc.}$, for (a) the sediment transport tests (SJ and RI) and (b) the clay suspension experiments with a fixed rough bed.

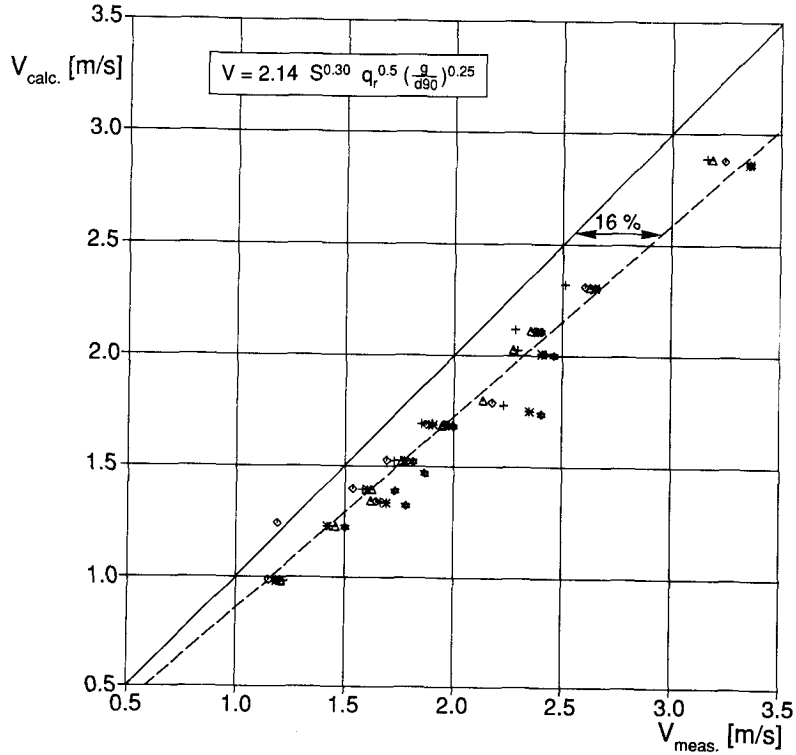


Fig. 4.27 (b)

Because of limited accuracy of the measurements (particularly of the mixture flow depth $H_m$, and to a lesser extent of the fluid velocity V), application of equ. (4.31a) or (4.31b) to the steep flume data results in negative grain velocities $U_B$ for some experiments. A regression equation was therefore proposed by Smart and Jäggi (1983) to determine smoothed values for $H_m$:

$$\frac{H_f}{H_m} = \frac{q/V}{H_m} = 1 - 1.41\ S^{1.14}\ \Phi_B^{0.18} \qquad (4.32)$$

A combined analysis of the data sets SJ and RI showed that the constant 1.41 in equ. (4.32) should be replaced by the term 2.37/(s-1) to account for the change in $\Phi_B$ with increasing clay suspension concentration:

$$\frac{H_f}{H_m} = 1 - \frac{2.37}{(s-1)} S^{1.14} \Phi_B^{0.18} \qquad (4.33)$$

An alternative equation was devloped from both data sets using the depths values corrected for sidewall influence ($h_{r,f}$ and $h_{r,m}$) and the ratio $q_B/q_r$ instead of the terms $\Phi_B$ and (s-1):

$$\frac{h_{r,f}}{h_{r,m}} = 1 - 1.64\, S^{0.42} \left(\frac{q_B}{q_r}\right)^{0.63} \qquad (4.34)$$

with $r^2 = 0.70$ and $S_E = 13\%$. It is noted that the correlation parameters for equ. (4.33) and (4.34) are practically the same. A comparison between measured and calculated depths ratios is shown in Fig. 4.28a for equ. (4.33), and in Fig. 4.28b for equ. (4.34).

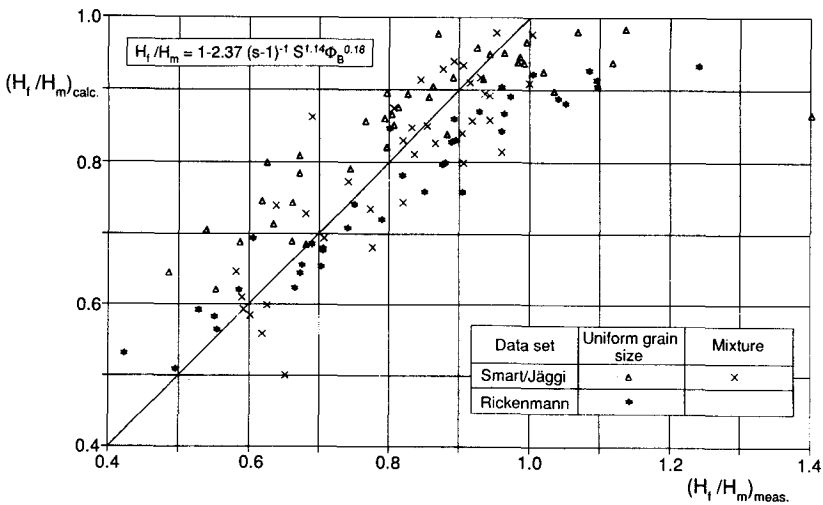


(a)

Fig. 4.28 : Ratio of fictitious fluid flow depth to mixture flow depth: Comparison between measured and predicted values, calculated (a) with equ. (4.33) and (b) with equ. (4.34). (It may be noted that measured values > 1.0 were not used in the regression analysis, because theoretically the ratio should be $\leq 1.0$.)

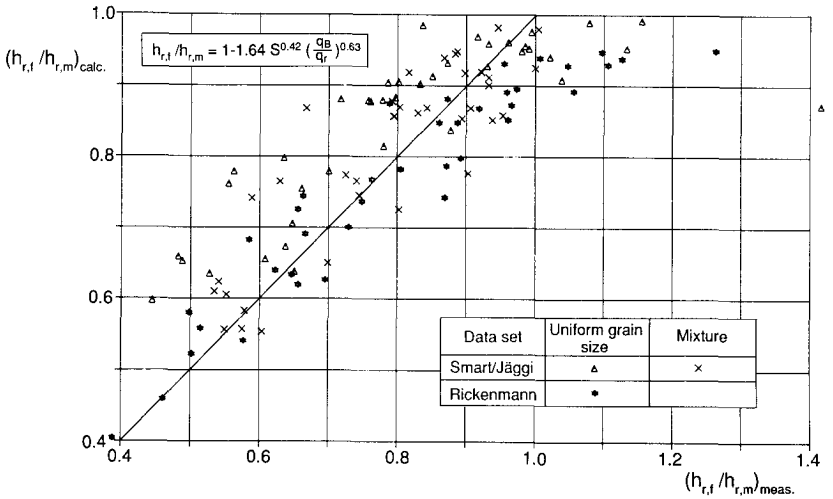


Fig. 4.28 (b)

It was decided to use equ. (4.31b) in combintion with equ. (4.34) to determine a mean grain velocity and a mean bed load concentration (by volume) of the moving grains for each experiment. First, the smoothed mixture flow depth was calculated as:

$$h_{r,m,calc.} = \frac{q_r/V}{1 - 1.64\ S^{0.42}(q_B/q_r)^{0.63}} \tag{4.35}$$

and then the mean grain velocity, $U_B$, was obtained as:

$$U_B = \frac{q_B}{h_{r,m,calc.} - (q_r/V)} \tag{4.36}$$

Since the fluid and the grains do not move with the same (mean) velocity, the bed load volume concentration $C_{v,B}$ is not simply given by the ratio $q_B/q$; it is defined as that part of the cross section which is occupied by the transported grains, and it was calculated as:

$$C_{v,B} = 1 - \frac{q_r/V}{h_{r,m,calc.}} \tag{4.37}$$

Comparative calculations were also made using equ. (4.33) instead of equ. (4.34) but this was not found to greatly affect the results presented below. The effect of an increasing clay concentration (of the suspension) on the calculated $U_B$ and $C_{v,B}$ values was examined using the procedure described above. The change in the mean grain velocity is shown in Fig. 4.29 as a function of the density factor (s-1). It is observed that $U_B$ increases slightly with a decrease in (s-1), similarly to the change of $h_{r,m}$ and V with clay concentration shown in Fig. 4.11a and Fig. 4.11b, respectively. The change in the mean bed load concentration is illustrated in Fig. 4.30 as a function of (s-1). The increase of the bed load concentration with decreasing clay concentration is much more pronounced than the change of $U_B$ in the previous figure.

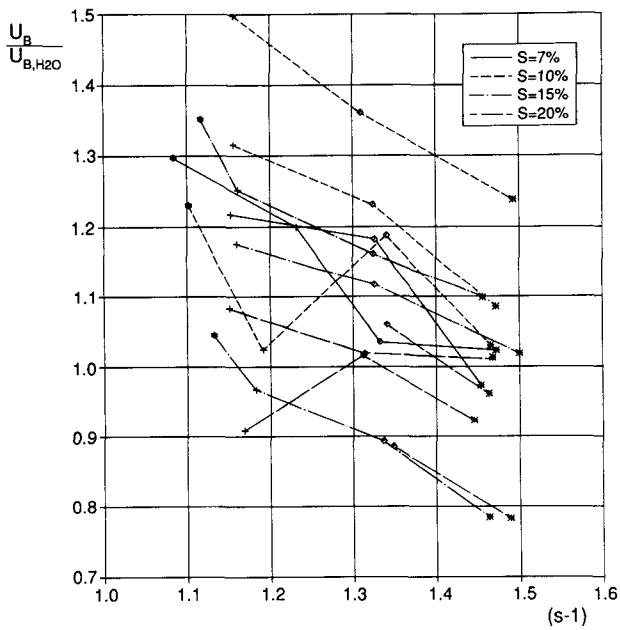


Fig. 4.29 : Ratio of mean bed load grain velocity in clay suspension to corresponding value in clear water, $U_B/U_{B,H2O}$, as a function of the density factor (s-1); experimental points with equal slope and flow rate are connected by straight lines.

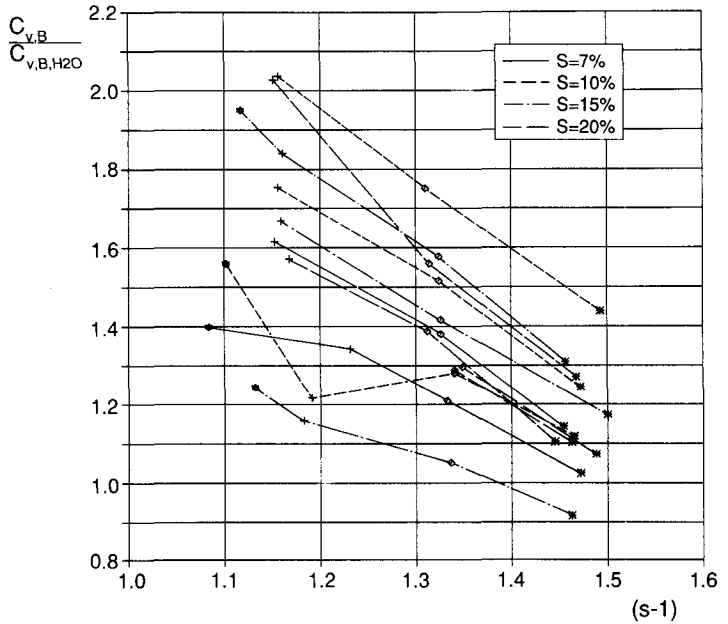


Fig. 4.30 : Ratio of mean bed load concentration (by volume) in clay suspension to corresponding value in clear water, $C_{v,B}/C_{v,B,H2O}$, as a function of the density factor (s-1); experimental points with equal slope and flow rate are connected by straight lines.

Calculated mean grain velocities for the clay suspension experiments are shown in Fig. 4.31 as a function of the shear velocity (determined with $h_{r,m}$). The data points with 7% slope were omitted from the figure for clarity, and because the calculated velocities are somewhat more vague for these experiments with relatively large errors between mixture flow depth and fictitious fluid flow depth. In Fig. 4.31 there is an almost linear dependence of $U_B$ on the shear velocity; it is further evident that the $U_B$ values depend also on the flume slope.

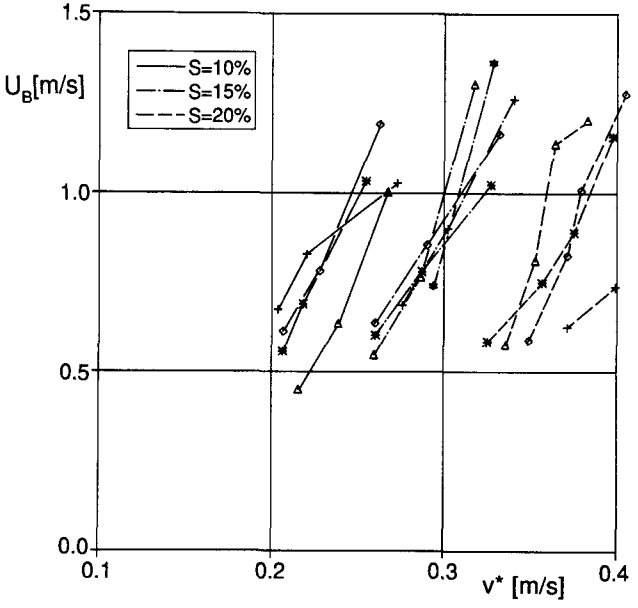


Fig. 4.31 : Mean velocity of bed load grains, $U_B$, as a function of the shear velocity, v*, for the clay suspension data; experimental points with equal slope and flow rate are connected by straight lines.

## 4.9 Case II: Laminar flow around bed load grains

In this section only those experiments of the clay suspension data are considered for which the fluid showed a higher viscosity. It can be seen in Fig. 4.9 that the bed load transport rate decreased with increasing clay concentration below a particle Reynolds number $Re_2^*$ of 10 to 15. The physical meaning of this critical value of $Re_2^*$ is that the flow around the bed load grains was laminar in the experiments with $Re_2^*$ $\leq\approx$ 10 (s. sec. 4.4).

The criterion used to separate experiments belonging to case I and case II is also described in sec. 4.5. A decrease in the bed load transport rate $q_B$ with respect to the corresponding value at the next lower concentration level was observed for the following tests (s. also Appendix II): For three experiments at the level C4 and for all 5 tests performed at the highest clay concentration level C5. All these experiments belong to the case II category.

It may be mentioned that the velocity measurements were not reliable for the experiments at the level C5, because the mixing of the salt solution within the viscous clay suspension was not sufficient. As an approximation, the corresponding velocities measured at level C4 were used to calculate the friction factor f and the Reynolds number $Re_2$ for the C5 experiments (used in Fig. 4.10).

For the case II experiments, Fig 4.9 shows that the ratio $q_B/q_{B,H2O}$ is related to the logarithm of the corresponding $Re_2^*$ values. The decrease in $q_B$ may also be examined with respect to the maximum transport rate (for the same flow rate and flume slope) observed at the level C3, $q_{B,C3}$. This new ratio, $q_B/q_{B,C3}$, is plotted against the logarithm of $Re_2^*$ in Fig. 4.32, and against the viscosity change, $\mu_{e2}/\mu_{e2,C3}$, in Fig. 4.33. (The correlation coefficient squared is for the line in Fig. 4.32: $r^2 = 0.81$, and for the line in Fig. 4.33: $r^2 = 0.89$.) It may be noted that $q_B/q_{B,C3}$ can also be related to linear values of $Re_2^*$ but then a worse correlation results.

Comparing the shear rates for the case II experiments with the corresponding values for the C3 tests, the difference is seen to be less than 15%. It can therefore be concluded that the decrease in the bed load transport rate is mainly due to the increase in the fluid viscosity.

It can be hypothesised that the decrease in $q_B$ is, at least partly, due to a change in the critical shear stress for initiation of motion which increases for $Re_2^*$ values below about 10. The relation for $\theta_c$ given in Yalin and Karahan (1979), equ. (2.107), was used (with $Re_2^*$ instead of $Re^*$) to determine $S_{cr}$ with equ. (4.12); then $q_B$ was calculated with equ. (4.22). The $q_B$ values calculated for the C4 tests (case II) were smaller than the $q_B$ values for the corresponding C3 experiments. But for the C5 tests, all calculated $q_B$ values were larger than the corresponding

values for the C3 experiments. But it is questionable, whether an equation such as equ. (4.22) may be applied to the case II experiments (with $Re_2^*$ values below 10) where the viscous influence should not be neglected; it cannot be decided therefore whether the $\theta_c$ values are correctly determined by equ. (2.107).

The increase in $\theta_c$ was also calculated with the relationship proposed by Wan (1982) for Bingham fluids, equ. (2.108). However, the computed $\theta_c$ values were larger than the measured $\theta$ values, and thus no bed load transport rates could be determined.

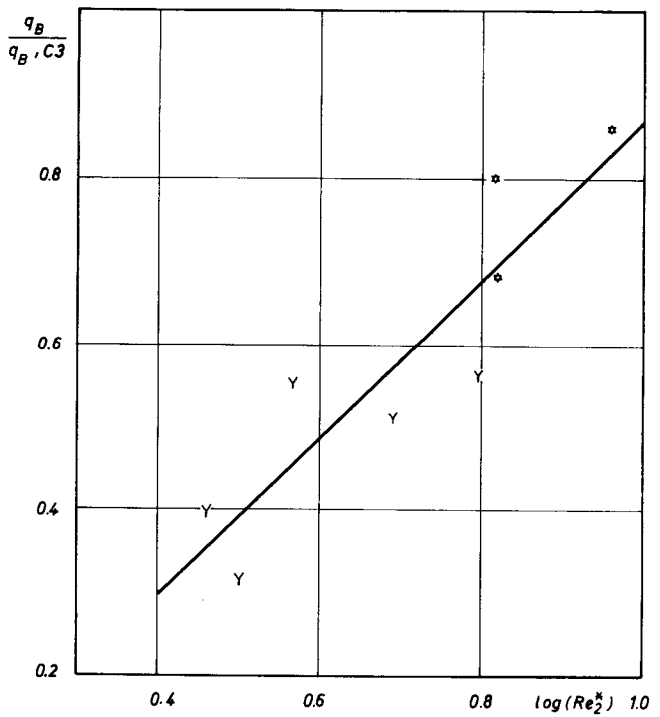


Fig. 4.32 : Ratio of bed load transport rate for case II experiments to the corresponding value at level C3, as a function of the grain Reynolds number $Re_2^*$ (logarithmic values).

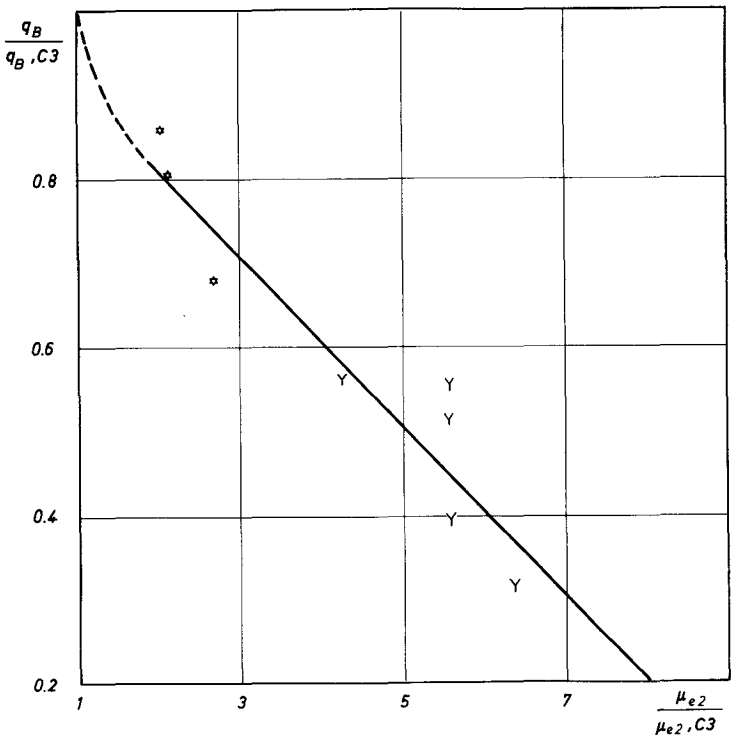


Fig. 4.33 : Ratio of bed load transport rate for case II experiments to the corresponding value at level C3, as a function of the respective ratio of the effective viscosities, $\mu_{e2}/\mu_{e2,C3}$.

# 5 DISCUSSION

## 5.1 Bed Load Transport

Note that in this section only those experiments (case I) of the author are considered, for which viscous effects were found not to be important.

### Form of proposed equations

Based on the steep flume experiments with both clear water (Smart and Jäggi, 1983) and the clay suspension (tests of this study), a new bed load transport formula, equ. (4.22), has been developed in terms of the following parameters:

$$q_B = \phi\ (q_r,\ S,\ S_{cr},\ s\text{-}1,\ d_{90}/d_{30}) \qquad (5.1)$$

Using the same parameters, a similar relationship, equ. (4.25), has been established for the low slope experiments of Meyer-Peter and Müller (1948; data given in Smart and Jäggi, 1983). Comparing equ. (4.25) with equ. (4.19), it is evident that the exponent of the slope factor is different for the two data sets. This suggests that two different formula for the two slope ranges will give better predictions than one common equation. Therefore, the density adjusted version of the original Smart/Jäggi equation (4.27) shows a larger scatter between predicted and measured transport rates than any of the formulae developed only for a limited data range (s. Table 4.4, section 4.7).

Many bed load transport equations based on the tractive force concept can be expressed with the dimensionless parameters $\Phi_B$ and $\theta$ (Graf, 1971; Yalin, 1977). Choosing the additional parameters given below:

$$\Phi_B = \phi\ (\theta,\ \theta_{cr},\ Fr,\ s\text{-}1,\ d_{90}/d_{30}) \qquad (5.2)$$

a more universal formula, equ. (4.28), has been proposed which predicts bed load transport rates reasonably well for both the low slope and the

steep slope data analysed in this study. It should be pointed out that in a relation of the form of (5.2), two parameters are included which describe the flow "behaviour" ($\theta$ and Fr), whereas no such parameter is contained in (5.1). It is therefore not surprising that equ. (4.28) can be applied to a wider range of conditions than any equation of the form of (5.1). When comparing equ. (4.28) and (4.27) in Table 4.4 (section 4.7), it should be remembered that that the experimental determination of $\theta$ in the steep flume situation is clearly less accurate than that of q; despite that fact equ. (4.28) shows a better overall performance.

Based on dimensional analysis, Yalin (1977) proposed equ. (2.93) as a general form of a bed load transport relation. If the term representing viscosity influences is neglected, and if the parameter h/d is replaced by Fr, using the "bridge relation" $Fr = c[(s-1)\cdot\theta\cdot d/h]^{0.5}$ (Yalin, 1977), then the following relationship is obtained from equ. (2.93):

$$\Phi = \phi[\theta, Fr, s-1] \qquad (5.3)$$

The use of the Froude number implies that the bed load transport rates depend also on the flow resistance. It is noted that relation (5.2) is of a similar form, except for the additional inclusion of the grain size distribution parameter $d_{90}/d_{30}$.

Comparison with other formulae

The entire data set used in this study is replotted in Fig. 5.1. Also shown are the three bed load transport equations of Meyer-Peter and Müller (in the simplified version given by Yalin, 1977), equ. (2.67), of Bagnold (1956; with an average value of $b \approx 4$ for $d > \approx 0.5$ mm), equ. (2.97), and of Luque and van Beek (1976), equ. (2.69). It is seen from Fig. 5.1 that equ. (2.67) predicts an upper limit of the Meyer-Peter/Müller data; this is not surprising since any effects of (bed) form drag and sidewall friction were neglected in the derivation of equ. (2.67) from the original version of Meyer-Peter and Müller (1948). The general tendency of Bagnold's equation is to overpredict the low slope data, and to underpredict the steep slope data. The formula of Luque and van Beek is based on lower shear intensity data ($\theta \leq 0.06$) but there is fair agreement with the presented data up to $\theta \approx 0.4$. It may be noted that this value of $\theta$ is an approximate limit above which bed load con

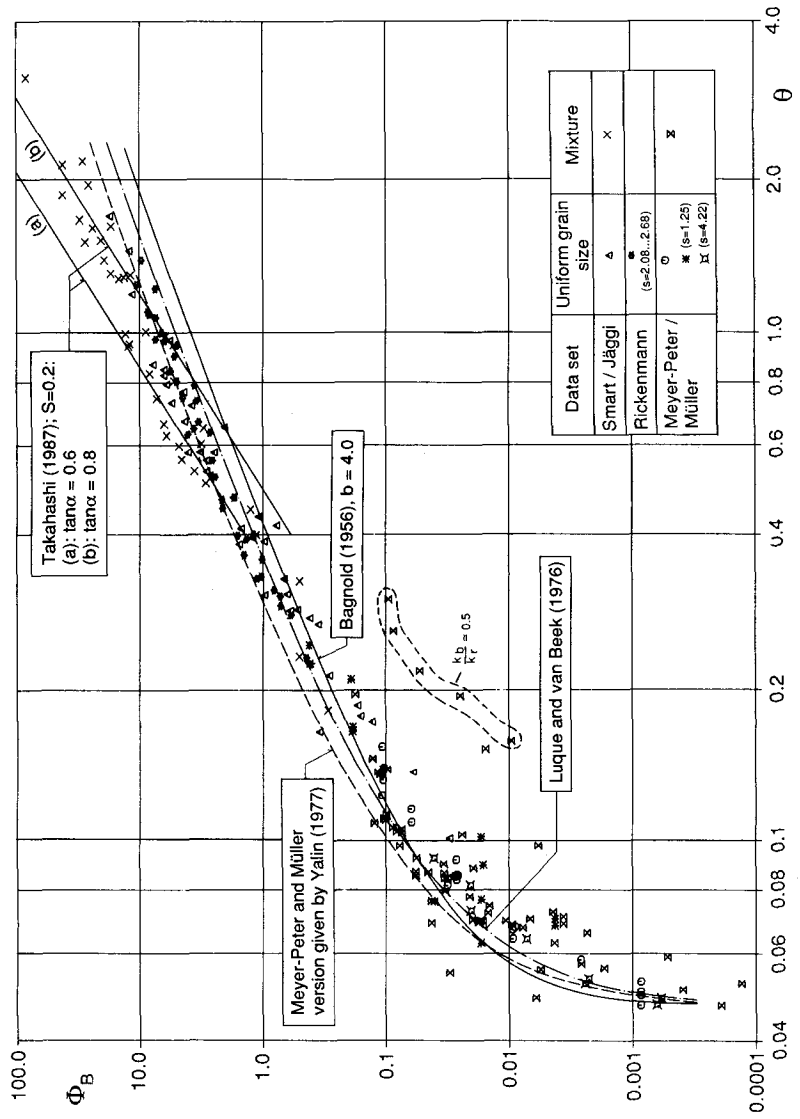


Fig. 5.1 : Reproduction of Fig. 4.21 showing the three data sets used in the present study, in terms of the dimensionless parameters $\Phi_B$ and $\theta$. Also shown are three bed load transport formulae developed from lower slope data, and an equation proposed by Takahashi (1987) for "immature" debris flow conditions.

centrations (in the steep flume tests) were no longer negligible, i.e. the transport layer occupied more than about 10% of the flow depth.

Inclusion of the Froude number

In many bed load transport equations based on the tractive force concept, $\Phi_B$ is given as a function of $\theta$ and $\theta_c$. In equ. 2.83, Smart and Jäggi included the factor $c \cdot S^{0.6}$, which is very close to the Froude number $Fr = c \cdot S^{0.5}$. Bridge and Dominic (1984) compared several data sets concerning bed load transport rates for flows over plane beds. They developed an equation in terms of the parameters ($\Phi_B$, $\theta$, $\theta_c$), equ. 2.101, and concluded that the value of the factor ($a/\tan\alpha$) in their relationship should increase from lower stage to upper stage plane beds by about a factor of 2, on the average. There are a number of bed load transport equations similar to equ. (2.101), but they have a constant instead of ($a/\tan\alpha$), probably because they are based on limited data sets. In his analysis of steep flume tests, Daido (1983) proposed that the "constant" $B_2$ in his equation (2.86) may be a function of the Froude number in general. A flow resistance coefficient and a slope factor is also included in a formula (equ. 2.85) presented by Takahashi (1987) to predict transport rates in flows at steep slopes.

Thus it appears that the Froude number may be an important parameter to predict bed load transport rates in flows over plane beds for both the subcritical and supercritical flow regime.

The role of the Froude number in the experiments of Meyer-Peter and Müller was discussed by Smart and Jäggi (1983). For the majority of the tests, Fr was below or close to 1.0; in a few experiments Fr was as high as 1.7. The mainly observed bed forms included plane beds and dunes of various forms, while ripples were present only in very few tests. To account for additional friction due to bed forms, Meyer-Peter and Müller (1948) had introduced the factor $(k_b/k_r)^{1.5}$ in their original bed load transport equation; $k_s$ denotes the Strickler k value for the total bed resistance, and $k_r$ the corresponding value for grain friction only. Thus the factor $k_b/k_r$ represents a correction factor to reduce the shear stress in account of form drag losses. Smart and Jäggi demonstrated that their factor $c \cdot S^{0.6}$ has a similar effect on the calculated $\Phi_B$ values as the factor $(k_b/k_r)^{1.5}$ in the original Meyer-Peter/Müller equation.

However, it should be noted that there were only a few experiments with a high form roughness (the tests with ripples, where $k_b/k_r \approx 0.5$); the mean value of the ratio $k_b/k_r$ was about 0.85.

It was also shown by Mantz and Emmett (1985) that a flow resistance coefficient may be required to predict sediment transport rates (at lower slopes), if no other correction for form drag losses is included. They presented numerous field measurements on bed load transport, using Bagnold's (1966) stream power parameters $i_B$ and $(\omega - \omega_c)$; where $i_B$ is the bed load transport rate by immersed of solids per unit width, $\omega = \tau_o \cdot V$ is the stream power and $\omega_c$ the critical value of $\omega$ at initiation of motion. For a given value of $(\omega - \omega_c)$, the bed load transport rates $i_B$ were shown to be about an order of magnitude larger, if the friction factor f decreased by about 50%.

Effect of a change in the grain - fluid density ratio

The influence of a change in the density ratio s on $q_B$ was studied by Low (1989). From an analysis of his experiments with lightweight sediment he found that $q_B$ should be proportional to $d \cdot v^{*2}/W^5$. He argued that the shear velocity v* (or the mean flow velocity V) may be considered as a measure of the flow strength, while the fall velocity W can be looked at as a measure of the resistance of the grains to motion. For his experimental conditions, he showed W to be a function of the factor $[gd(s-1)]^{0.5}$, and found that the relation $\Phi_B \sim \theta^3$ does also correctly account for the density effect. He further demonstrated that several bed load transport formulae in terms of ($\Phi_B$, $\theta$ and $\theta_c$) adequately account for a change in the density factor (s-1). This is independently confirmed by the experiments of Luque and van Beek (1976); their data, including varying values of s, is well described by a transport equation using the parameters ($\Phi_B$, $\theta$ and $\theta_c$), equ. (2.69). According to the analysis of Low, a correct reproduction of the density effects requires that the ratio of the shear velocity to the fall velocity is correctly represented.

Low (1989) proposed to include a modified density factor (s-1) in the Smart/Jäggi equation (2.83). In the present study, this modification was confirmed in the analysis of a subset of the Meyer-Peter/Müller experi-

ments, where the density ratio s was varied. It appears that the inclusion of the Froude number $Fr = V/(gh)^{0.5}$ requires the additional factor $(s-1)^{-0.5}$, which accounts for the change in fall velocity.

The regression analysis of the clay suspension data resulted in a similar dependence of $\Phi_B$ on (s-1), (s. equ. 4.15 to 4.17). For this data set (case I experiments), the calculated fall velocity at the concentration level C4 is about 25% of the corresponding clear water value. In a Newtonian fluid, viscosity begins to affect the fall velocity in the hyraulically transitional regime. From the analysis of the clay suspension flow over a fixed rough bed, viscous effects were found to become important only at $Re_2^* \lesssim 10$ (s. sec. 4.3). Interestingly, a distinct change in the bed load transport behaviour was found in the clay suspension tests at $Re_2^* \approx 10$; in the region $Re_2^* \gtrsim 10$, transport rates can be well predicted by an equation which includes the density factor (s-1) but no viscosity term.

Brühl (1976) studied the hydraulic transport of sand in pipes. He found that the pressure gradient is reduced (i.e. the transport capacity increased) if he used a slurry with fines as transporting fluid instead of clear water. In analysing his results, he calculated the pressure gradient with existing methods developed for the clear water case. In these methods, the fall velocity of the transported solids appears explicitly as a parameter. By adequately accounting for the change in the density factor (s-1) and in the fall velocity W, he obtained fair predictions for the slurry data. This again suggests that a correct representation of the effects of W is a necessary requirement to describe the (bed load) transport in the case of a varying solid-fluid density ratio s.

Equations for steep flume data

For the Meyer-Peter/Müller data, the density factor $(s-1)^{-1.5}$ in equ. (4.25) is equivalent to the density factor $(s-1)^{-0.5}$ in equ. (4.26), which can be shown by transforming one form of the equation into the other. But for the steep flume situation with high bed load concentrations, a formula in terms of the parameter set (5.2) cannot be easily transformed into the parameter set (5.1), because the flow rate can no longer be expressed as the product of the (mixture) flow depth

and the fluid velocity. The regression analysis of the clay suspension data (RI) resulted in similar exponents for the density factor (s-1) as for the low slope data. However, if the term $S_{cr}$ is neglected in parameter set (5.1), there is a dependence on $(s-1)^{-2.0}$ in equ. (4.11) and in equ. (4.23):

$$q_B = \frac{17.3}{(s-1)^{2.0}} \left(\frac{d_{90}}{d_{30}}\right)^{0.2} q_r \, S^{2.1} \qquad (4.23)$$

It is interesting that both Mizuyama and Shimohigashi (1985), and Chee (1988) proposed from steep slope experiments with varying s values that $q_B$ should depend on $(s-1)^{-2.0}$. In fact, the bed load transport formula of Mizuyama and Shimohigashi is very similar to the above equation:

$$q_B = A' \, q \, S^2 \, \frac{1}{(s-1)^2} \qquad (2.66)$$

Mizuyama (1981) earlier presented a similar equation obtained from steep flume tests with clear water as transporting fluid:

$$q_B = 5.5 \, q \, S^2 \qquad (2.87)$$

It is not known whether a correction for sidewall effects was applied to the experimental data that lead to either equ. (2.66) or (2.87).

In order to compare the steep flume data used in this study with these two formulae, a regression calculation was made with the data sets RI and SJ, fixing the factor $S^2$; the result is:

$$q_B = 14.4 \left(\frac{d_{90}}{d_{30}}\right)^{0.2} q_r \, S^{2.0} \, \frac{1}{(s-1)^{2.0}} \qquad r^2 = 0.94 \quad S_E = 21.5\% \qquad (5.4)$$

If the grain size distribution factor $(d_{90}/d_{30})^{0.2}$ is to be neglected, it should be replaced by the value 1.05 according to Smart and Jäggi (1983). Comparing equ. (5.4) with equ. (2.66), this results in A' = 15.1 for the data of this study. Mizuyama and Shimohigashi (1985) gave A' = 20 for the case of clear water, and A' = 25 for the tests performed with a fine material suspension. If equ. (2.87) is transformed into a relationship of the form of equ. (2.66), the corresponding constant A' =

15.5 is obtained (using s = 1.68). Thus it can be concluded that the steep flume data used in this study (data sets RI and SJ) and the one used by Mizuyama (1981) result in very similar bed load transport formulae. No explanation could be given by Mizuyama (1988) as to why the experiments with a fine material slurry (in the study with Shimohigashi) lead to a different value for the constant A'.

Effect of increasing clay concentration on grain transport

In the clay suspension experiments (RI data set), the same slope and flow rate combinations were used for all clay concentration levels (Ci). According to equ. (4.11), the bed load transport rate can be described by the three parameters q, S and (s-1). Therefore, the effect of (s-1) on $q_B$ or related parameters is easily seen on appropriate diagrams. Considering Fig. 4.29 and Fig. 4.30, it is observed that the increase in $q_B$ with a decrease in (s-1) is mainly due to an increase in the mean bed load concentration ($C_{v,B}$), while there is a much weaker increase in the mean transport velocity of the grains ($U_B$).

It is seen from Fig. 4.31 that the calculated mean grain velocity $U_B$ depends on the shear velocity in an approximately linear way. This is in agreement with the empirical relationship for the velocity of single grains $U_b$ found by Luque and van Beek (1976), equ. (2.71), and also with the theoretical equation (2.98) for the mean velocity of bed load grains proposed by Bridge and Dominic (1984). A linear dependence of $U_b$ on v* was also observed by Abbott and Francis (1977); they further showed that $U_b$ was slightly higher for smaller grain densities $\sigma$ (or smaller values of s, since $\rho$ was constant). In Fig. 4.31 there seems to be a similar tendency for the data from the tests with 10% and 15% slope, whereas the data points with 20% slope show no clear grouping.

It is also observed from Fig. 4.31 that the mean grain velocity $U_B$ is not only a function of v* but also of the slope. A higher shear velocity is required for a steeper slope to result in the same $U_B$ value. Since the bed load concentration are clearly higher at steeper slopes, grain to grain interactions may be expected to become more important, possibly resulting in an increased loss of grain momentum.

General flow characteristics

In the steep flume tests of Smart and Jäggi (1983), the bed forms present were flat beds and antidunes; for the tests with mat. IV (used as reference conditions) there were only flat beds. In the clay suspension experiments, flat beds also existed at the lowest clay concentration level; no direct observation was possible for the tests with a denser suspension. However, some indication was obtained from the operation of the flume system: With increasing suspension concentration it was found easier to adjust the upstream roughness elements to establish equilibrium transport conditions; the bed stability seemed to be less influenced by slightly varying conditions at the flume entrance.

White (1987) presented a criterion to delineate the occurrence of different bed forms. The dimensionless unit stream power $U_E$ is rearranged here as:

$$U_E = \frac{V\ S\ \nu^{1/3}}{g^{2/3}\ d\ (s-1)^{1/3}} \qquad (5.5)$$

White proposed that for flat beds and antidunes $U_E$ should be greater than 0.02. This criterion is satisfied for the clay suspension experiments (using $\nu = \mu_{e2}/\rho$). It is interesting that the value of $U_E$ increases with a decrease in (s-1) and with an increase in $\nu$. For the clay suspension experiments, a stabilising effect on the bed forms under consideration may therefore be expected.

Kresser (1964) established the following criterion for a minimum flow velocity above which there should be suspended load: $V \geq 360 \cdot g \cdot d$. For the clay suspension experiments this would require a velocity of about 6 m/s; this value was clearly not reached. But a number of grains certainly moved in saltation as was observed by Smart and Jäggi in their clear water experiments.

To distinguish between bed load and suspended load, another criterion is given by Bagnold (1966): If $W/v^* \geq 0.8$, then only a negligible part of the sediment is supposed to be carried as suspended load. According to this criterion some tests at the concentration level C3 and all experiments at the levels C4 and C5 should have carried a non-negligible part of grains in suspension (if $\mu_{e2}$ is used to calculate W). However,

Murphy and Aguirre (1985) suggested that suspended load and bed load can only be distinguished, if effects of the fluctuating fluid forces are considered, apart from the trajectory length and height of the grains which can be obtained from mean flow parameters.

The maximum packing concentration (by volume) $C_*$ for a static gravel layer is between 0.63 and 0.74 (O'Brien and Julien, 1984). For the clay suspension experiments with 20% slope, the calculated mean bed load grain concentrations ($C_{v,B}$) range between 30% and 55% by volume. If the "packing" concentration in the transport layer is assumed to be about 0.60 (in a sheared layer it must be less than $C_*$), it results that this layer occupied more than half of the total (mixture) flow depth. In other words, the transport layer had a thickness of several grain diameters while the "clear" fluid layer above was only a few grain diameters thick. Thus it seems questionable whether a suspended load should be defined for the given flow and transport conditions.

At the higher transport rates it was observed by Smart and Jäggi (1983) in their tests that the grains close to the grain surface moved in a suspended like manner because inter-particle contact prevented saltating particles from returning to the bed. They also noted then a tendency towards a more uniform mixing of water and grains. These conditions may be termed debris-flow-like sediment transport. In the case of the clay suspension experiments this corresponds to type 1 debris flow as defined by Davies (1988) (s. Table 1.2, section 1.3).

The role of the Froude number was discussed by Smart and Jäggi (1983) with respect to the Meyer-Peter/Müller experiments; it may be looked at as an indicator for friction losses other than grain friction. In the steep flume tests the bed forms were flat beds and antidunes, and bed load transport rates were generally large. Therefore, bed form drag may be considered negligible in comparison to the part of the flow energy required to transport the grains. The dimensionless shear stress $\theta_m$ is a measure of the flow strength at the bottom of the flowing grain-fluid mixture. However, in the steep flume tests the transport layer extended over more than half the (mixture) flow depth. Therefore, the use of $\theta_m$ alone may not be sufficient to predict bed load transport rates. The Froude number (or the fluid velocity) may be looked at as a measure of the forces acting on the grains within the flow. Since both Fr and $q_B$ increased with slope and flow rate, it seems reasonable to use Fr as an

additional parameter to predict bed load transport rates at steep slopes.

Comparison with stream power approach

Putting $Fr^{1.1} \approx Fr$ and considering conditions with $\theta >> \theta_c$, equ. 4.28 simplifies to:

$$\Phi_B = \frac{B_3}{(s-1)^{0.5}} \theta^{1.5} Fr \qquad (5.6)$$

This equation can be rearranged in terms of the stream power approach:

$$i_B = B_3 \omega S^{0.5} \qquad (5.7)$$

Bagnold (1973) postulated that the work rate performed by the transported solids is equal to the available power (stream power) times an efficiency factor. If the effects of an appreciable gravity slope cannot be neglected, the following relationship can be given according to Bagnold (1973), to express the maximum bed load transport efficiency:

$$i_B = \frac{1}{(\tan\alpha - \tan\beta)} \omega \qquad (5.8)$$

where the first factor on the right hand side is the efficiency factor. Many attempts were made to determine the angle of internal friction for the dynamic case of bed load transport. Bridge and Dominic (1984) summarised values proposed in the literature: A range of $\tan\alpha = 0.4 \ldots 0.7$ was found by various authors for inertial grain shearing conditions ($G^2 > 1500$), while $\tan\alpha = 0.75$ was proposed by Bagnold (1954) for macroviscous conditions ($G^2 < 100$). It was concluded by Bridge and Dominic that $\tan\alpha$ should also increase with increasing bed shear stress (in the inertial region).

The steep flume data (sets SJ and RI) are shown in Fig. 5.2 in terms of the stream power parameters. Also shown are two lines defining the 100% efficiency according to Bagnold (1973), equ. (5.8); both lines were determined for the steepest slope of 20%, line (A) represents the case of inertial shearing (with $\tan\alpha = 0.4$) and line (B) the case of macroviscous shearing (with $\tan\alpha = 0.75$). It is noted that the flows of

the clay suspension experiments performed at the clay concentration C3 approached the limit of viscous grain shearing ($Re_2^* \approx 10$; s sec. 2.1.3). The largest bed load transport rates were measured at the level C3, and it is interesting that the corresponding points in Fig. 5.2 lie close to the 100% efficiency line (B).

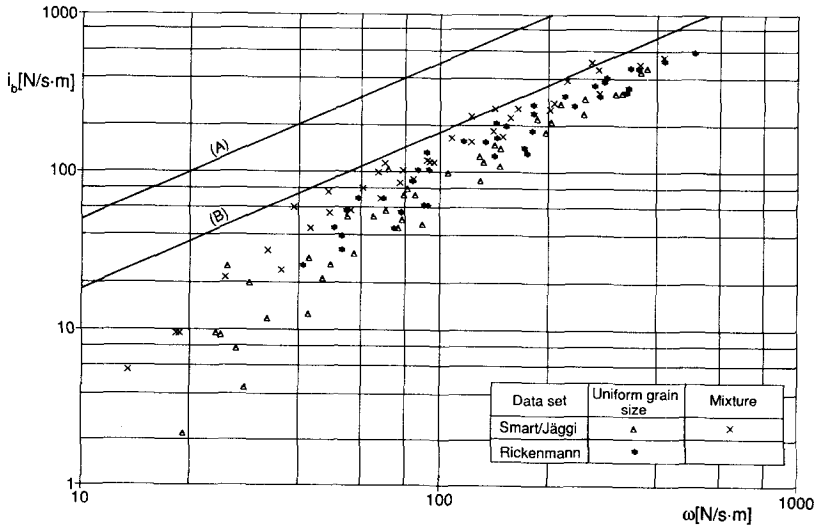


Fig. 5.2 : Experimental data from steep flume tests (data sets SJ and RI), shown in terms of the bed load transport rate by immersed weight per unit width, $i_B$, and the stream power, $\omega = \tau_o \cdot V$. The straight lines represent the 100% efficiency relationship, equ. (5.8), for a slope of 20% and (A) for inertial grain shearing ($\tan\alpha = 0.4$) and (B) for viscous grain shearing ($\tan\alpha = 0.75$), respectively.

## $\Phi_B$ - $\theta$ relationships for high shear stresses

Yalin (1977) demonstrated that many bed load transport formulae predict the proportionality relation $\Phi_B \sim \theta^{3/2}$ at high shear stresses. This same result is also obtained from equ. (4.28) and (4.26), for constant Fr and s. If the thickness of the transport layer is small with

respect to the total flow depth and if a flow over a plane bed is considered, then Fr may have no influence on $\Phi_B$. In Fig. 5.1, the simplified Meyer-Peter/Müller equation (2.67) is seen to predict $\Phi_B$ values within the range defined by the steep flume data. A correlation calculation with the data sets SJ and RI gives:

$$\Phi_B = 8\ (\theta_r - \theta_{cr})^{1.5} \qquad r^2 = 0.87,\ S_E = 37\%$$

However, as is also seen from Fig. 5.1, the steep flume experiments alone define a relationship in terms of $(\theta-\theta_c)$ with an exponent somewhat higher than 1.5; a regression computation results in:

$$\Phi_B = 8.9\ (\theta_r - \theta_{cr})^{1.9} \qquad r^2 = 0.94,\ S_E = 39\% \qquad (5.9)$$

Takahashi (1987) defined an "immature" debris flow as a flow with a clear water layer and a transport layer underneath, in which dispersive forces between the grains dominate. According to Takahashi, some of the Smart/Jäggi tests fall within the category of immature debris flows. Based on experiments with quartz sand in water, he gave a critical concentration within the transport layer as $0.4C_*$ below which the grains cannot disperse throughout the flow depth. Assuming a value of $C_* = 0.75$ for the steep flume experiments, the critical concentration would be about 0.30. However, larger concentrations (defined with respect to the total depth, and not to the thickness of the transport layer) were determined for some of the steep flume tests. For the clay suspension experiments there was no indication that the grains were transported in significant concentrations within the upper fluid layer; this is concluded from the conductivity readings of the bed level measurements, and from several checks by holding one hand into the muddy grain-fluid mixture.

Considering the mode of transport, it may be concluded that some of the steep flume tests (SJ and RI data) were in the regime of Takahashi's immature debris flows, although calculated bed load concentrations are not quite in agreement with the values proposed by Takahashi. The bed load transport equation proposed by Takahashi (1987), equ. (2.89b), is shown in Fig. 5.1 for comparison with the steep flume data; the values $\tan\beta = 0.20$ (S = 20%), $C_* = 0.65$, $\theta_c = 0.05$ were used to determine the

lines (a) with $\tan\alpha = 0.6$, and (b) with $\tan\alpha = 0.8$. It was noted by Takahashi (1987) that his equ. (2.85), which is similar to the Smart/Jäggi equation, is also valid for immature debris flows.

According to Takahashi's (1987) equ. (2.89b), $\Phi_B$ should depend on $\theta^{2.5}$ at high shear stresses ($\theta >> \theta_c$). This is a somewhat stronger dependence than suggested by equ. (5.9), which was fitted to the steep flume data. Hanes and Bowen (1985) theoretically developed an equation for intense bed load transport, defining a transport layer zone dominated by grain collisions and a saltation zone where both grain and fluid stresses are important. Their results also lead to the conclusion that $\Phi_B$ may become proportional to $\theta^{2.5}$ at high shear stresses.

## 5.2 Flow resistance

Analysis of a Bingham fluid with Newtonian formulae

It is shown in section 4.2 that the clay suspension used in the experiments can be characterised as a Bingham fluid. The tests without sediment transport are analysed in section 4.3. The analysis suggests that the flow characteristics can be reasonably well described by using an effective viscosity $\mu_{e2}$ (defined by equ. (2.40)) in combination with flow resistance formulae developed for Newtonian fluids.

The flow resistance of a laminar flow of a Newtonian fluid is given by:

$$f = K_{lam}/Re \tag{5.10}$$

where for pipe flow, $K_{lam} = 96$ is a constant. It is seen in Fig. 4.5 that the data points in the laminar flow region lie below the theoretical relationship for Newtonian pipe flow. Straub et al. (1958) noted that the channel geometry is an important factor determining the value of $K_{lam}$ in the above equation. They showed theoretically how $K_{lam}$ varies for a rectangular channel with the aspect ratio (W/h). For the experimental conditions of the data shown in Fig. 4.5, $K_{lam}$ would be expected to assume a value between 60 and 77. This is in good agreement with the

lines defined by the data in Fig. 4.5. Zhang et al. (1980) also analysed the flow of a Bingham fluid using $\mu_{e2}$ and $Re_2$; for experiments made in a rectangular channel, they found that a value of $K_{lam} = 84$ fitted their laminar flow data the best. Kozicki and Tiu (1967) presented a theoretical analysis of the laminar flow of Non-Newtonian fluids, and they demonstrated that the aspect ratio has an influence on the flow of a Bingham fluid through a rectangular channel.

With regard to the transition from the turbulent flow of the clay suspension to laminar flow, the hydraulically smooth turbulent flow region seems to be hardly detectable for the given flow conditions. According to Fig. 4.6 no viscous effects on the flow resistance could be detected in the region $Re_2^* >\simeq 10$ (which corresponds to hydraulically transitional or rough turbulent flow for a Newtonian fluid). A plug flow zone already started to form, however, for a few flows in this region, extending from the middle of the flow surface out- and downwards; this is a characteristic feature of a Bingham fluid. In the region $Re_2^* <\simeq 10$, the flows should be first in the hydraulically smooth turbulent regime, before changing to laminar flow (according to Newtonian fluid mechanics). According to the experimental results, some flows (at steep slopes, with small depths) appeared to have become laminar with increasing visosity, without a clear notion of hydraulically smooth turbulent flow (Fig. 4.5 and Fig. 4.6). This particularity could be explained by the fact, that there is not only a growing viscous sublayer at the bottom, but also a (laminar) plug flow zone near the surface, increasing with increasing Bingham yield stress; if the (relative) depth is small, the two laminar zones may soon merge with growing viscous effects in a Bingham fluid, and may thus confine the hydraulically smooth turbulent region somewhat.

The fact that any viscous effects may be neglected in the region $Re_2^* >\simeq 10$, is also supported by the analysis of the bed load transport experiments: A bed load transport formula was developed which describes equally well both clear water data and clay suspension tests with $Re_2^*$ values down to about 10.

Steep flume data with bed load transport; comparison with other data and flow resistance equations

In the combined analysis (sec. 4.8) with the experiments of Smart and Jäggi (1983), only those bed load transport tests with the clay suspension are considered for which viscous effects may be neglected ($Re_2^* \geq\simeq 10$).

In the analysis of their steep flume experiments, Smart and Jäggi (1983) proposed to apply a logarithmic flow resistance formula, equ. (4.7). In another study, Jäggi (1983) had found that velocities tend to be overpredicted by Nikuradse type equations for lower relative flow depths and steeper slopes in flows over mobile gravel beds. He therefore introduced a correction factor to account for form drag losses. This correction is a function of the slope and of grain characteristics; it is given by the term in square brackets in equ. 4.7.

Recently, Griffiths (1989) presented an approach to predict the flow resistance in gravel channels with mobile beds. Similarly to the correction of Jäggi (1983), he suggested to divide the total energy slope or friction factor, f, into a part representing pure grain friction, f', and a part accounting for form drag, f''; the part f'' can be due to either bed form drag or viscous drag on transported grains. He calculated the flow resistance due to grain friction, f', with a Nikuradse type equation:

$$\frac{1}{\sqrt{f'}} = 2.12 + 2.03 \log\left(\frac{h}{d_m}\right) \tag{5.11}$$

Using the data sets of Meyer-Peter/Müller and of Smart/Jäggi, he determined $f'' = f - f'$, where f is given by the experimental values. He then showed how the ratio f''/f' varied with total dimensionless bed shear stress, $\theta$, and relative depth, h/d. He found that different patterns should exist for the subcritical and the supercritical flow regime. For the supercritical case Griffith (1989) gave the relation:

$$f = f' \left(1 + \exp\left[\frac{-0.066}{\theta^{0.455}}\left(\frac{h}{d_m}\right)^{1.30}\right] \left(\frac{\theta-\theta_c}{\theta_c}\right)\right) \tag{5.12}$$

The procedure of Griffiths (1989) was applied to the steep flume data (SJ and RI), and a comparison between calculated and measured velocities

is shown in Fig. 5.3. It may be noted that there is a systematic deviation between $V_{meas.}$ and $V_{calc.}$ for the clay suspension data with increasing velocity. This may be due to the fact that the relatively high transport rates in these tests result in a too high a factor $(\theta-\theta_c)/\theta_c$ in equ. (5.12).

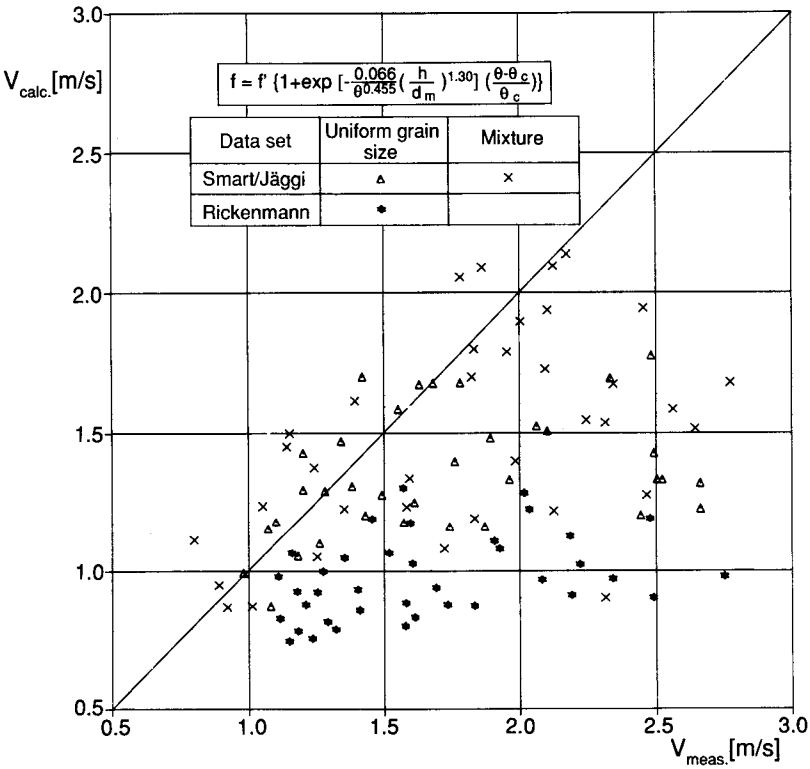


Fig. 5.3 : Comparison between measured velocities, $V_{meas.}$, and those calculated according to Griffiths (1989), $V_{calc.}$, for the steep flume data.

It may be noted that according to Yalin (1977), the validity of the logarithmic velocity distribution in open channel flow is questionable at relative flow depths below about 6 to 7. For this case, measured velocity profiles indicate a deviation from the logarithmic distribution

at the bottom layer. Kamphuis (1974) stated that it may be doubtful to use the equivalent sand roughness $k_s$ as a measure of flow resistance for relative depths below about 10.

Bathurst et al. (1982b) reported on a study about bedforms and flow resistance in steep gravel bed channels. For flume slopes between 3% and 9%, bed load transport was generally initiated at Froude numbers above 1. For a flow with constant discharge, and only minor variations in depth and velocity, they found the flow resistance coefficient $c = (8/f)^{0.5}$ to decrease with increasing slope and bed load transport. Since the bed forms changed from plane bed to antidunes and then weak antidunes, they concluded that the increase in resistance is due to grains in transport. On the other hand, for flows with no or little bed load transport, c was shown to be mainly related to the relative depth.

A similar conclusion was drawn by Cao (1985). He obtained flow resistance measurements from experiments with a mobile gravel bed, with varying bed load transport rates. He presented his data in a plot of c versus the parameter $V/(gd_{50})^{0.5}$, called grain Froude number or sediment mobility number. In such a plot, c is seen to decrease with increasing sediment concentration in the flow, at a given value of the sediment mobility number. The same behaviour was shown to apply to data taken from Cooper and Peterson (1969), and to the data of Smart and Jäggi (1983).

A tendency towards an increase in flow resistance (decrease in c) with increasing transport rates (at a given relative depth $h/d_{90}$) can be inferred from the clay suspension experiments at slopes steeper than about 10 % (s. Fig. 4.24). To judge from the steep flume data, a decrease in c with increasing $q_B$ already at moderate slopes (with weaker transport rates) must appear somewhat doubtful.

Bathurst (1985) reported on a study on the flow resistance of gravel and boulder-bed rivers with slopes between 0.4% and 4%. The relative depths of the examined flows varied between 0.6 and 11.5, and all flows were subcritical. No sediment transport occurred in these flows. He presented his data in diagrams in terms of c versus $h/d_{84}$, together with field and laboratory data from other sources with $h/d_{84} < 50$, including also flows with sediment transport. In the region of the sediment transporting flows (approximately defined by $h/d_{84} \geq 5$), the envelope of the

available data shows that c may vary by about as much as a factor of 2 for a given value of $h/d_{84}$. If the steep flume data of this study is plotted in a similar diagram it is clearly seen that the relative depth alone cannot explain the variation of c.

In a study on the hydraulics of torrents, Meunier (1988) performed a regression analysis with the field data given by Bathurst (1985), and presented the following equation:

$$V = \frac{3.9}{(d_{84})^{0.56}} S^{0.289} h \tag{5.13}$$

for which he determined the correlation coefficient squared as $r^2 = 0.87$. Putting $(d_{84})^{0.56} \simeq (d_{90})^{0.5}$ and substituting $3.9 = 1.25 \cdot g^{0.5}$, a dimensionally correct version of equ. (5.13) can be obtained which can then be transformed into:

$$(\frac{8}{f})^{0.5} = \frac{1.25}{S^{0.21}} (\frac{h}{d_{90}})^{0.5} \tag{5.14}$$

Interestingly, this formula is very similar to equ. (4.29). Both equations are of the form:

$$(\frac{8}{f})^{0.5} = m' (\frac{h}{d})^{0.5} \tag{5.15}$$

where m' is a function of the slope. Equ. (5.14) and equ. (4.29) are compared in Table 5.1, where the corresponding values for m' are given for the different slope values.

For the slope range of this study, equ. (4.29) is seen to predict velocities about 40% to 60% higher than those calculated with equ. (5.14). However, it is not this difference that is surprising but rather the fact that both equations are of very similar form although one was developed from subcritical flows over a rigid bed while the other applies to a supercritical, bed load transporting flow over a mobile bed.

| Slope S | Steep flume data of this study, equ. (4.29) $m_1'$ | Bathurst (1985) data, analysis by Meunier (1988), equ. (5.14) $m_2'$ | $\frac{m_1'}{m_2'}$ |
|---|---|---|---|
| 0.01 | 5.7 | 3.3 | 1.73 |
| 0.05 | 3.6 | 2.3 | 1.57 |
| 0.10 | 2.9 | 2.0 | 1.45 |
| 0.15 | 2.6 | 1.86 | 1.40 |
| 0.20 | 2.4 | 1.75 | 1.37 |

Table 5.1 : Comparison of flow resistance formulae, derived from steep flume data and field observations by Bathurst, respectively.

From steep flume experiments classified as "immature" debris flows, Takahashi (1987) derived the empirical expression:

$$(\frac{8}{f})^{0.5} = 1.5\ (\frac{h}{d})^{0.56} \qquad (5.16)$$

where d probably refers to $d_m$ (no exact definition is given). Putting $(h/d)^{0.56} \simeq (h/d_m)$, equ. (5.16) is again of the same form as equ. (5.15). The following formula is obtained from a regression of the steep flume data (SJ and RI), using $d_m$ instead of $d_{90}$:

$$(\frac{8}{f})^{0.5} = \frac{0.45}{S^{0.27}}\ (\frac{h}{d_m})^{0.5} \qquad (5.17)$$

for which the correlation parameters between $V_{meas.}$ and $V_{calc.}$ are: $r^2$ = 0.66 and $S_E$ = 18%. The factor $m_3' = 0.45/S^{0.27}$ is compared with Takahashi's constant 1.5 in Table 5.2, for slope values at which "immature" debris flows may occur.

| Slope S | Steep flume data of this study, equ. (5.17) $m'_3$ | $\frac{m'_3}{1.5}$ |
|---|---|---|
| 0.10 | 2.3 | 1.53 |
| 0.15 | 0.82 | 1.40 |
| 0.20 | 0.87 | 1.30 |
| 0.25 | 0.92 | 1.22 |

Table 5.2 : Comparison of a flow resitance equation from this study with a formula developed by Takahashi (1987) for intense bed load transport conditions, equ. (5.16), for which $m' = 1.5$.

It is observed from Table 5.2 that the equation developed from the steep flume data of this study (equ. 5.17) predicts velocities that are 20% to 50% higher than those calculated with Takahashi's (1987) formula (equ. 5.16) for intense bed load transport conditions. It cannot be decided whether this difference is a result of different measuring techniques, or whether it is caused by different flow conditions.

In conclusion, it may be noted that there is still a considerable scatter between predicted and measured velocities for the steep flume experiments of this study, irrespective of which approach is used to calculate the flow resistance. It is therefore recommended to use the flow resistance equation given by Smart and Jäggi (1983), equ. (4.7), if the fluid velocity is to be estimated as a function of the mixture flow depth (and the slope). On the other hand, if the flow rate is given or assumed (as in the design case), it is more reliable to use equ. (4.30), in a slope range between 5% and 20% (s. also sec. 6.2), or equ. (5.20, presented below) in a slope range between 5% and 50%.

Comparison with Takhashi's debris flow velocity equation

Based on the concept of dispersive stresses between the moving grains, Takahashi (1978) developed an equation for the mean velocity of a quasi-steadily moving debris flow front (integrated form of equ. 2.12, section 2.1.3). Replacing concentration and density terms together with grain shearing coefficients by one single parameter A*, the following expression is obtained (Takahashi, 1978):

$$\frac{U/(gd)^{0.5}}{[q^2/(gd^3)]^{0.3}} = A^* (\sin\beta)^{0.2} \qquad (5.18)$$

where U is the mean velocity of the moving grains and q is the fluid discharge per unit with. Takahashi plotted his experimental results in terms of the nondimensional velocity (given by the left-hand side of equ. 5.18) *vs.* the bed slope $\tan\beta$. As predicted by equ. (5.18), there is only a slight dependence on $\tan\beta$ in his figure. From his diagram (Fig. 9, Takahashi, 1978), it can be determined that $A^* \approx 1.3$. Using this experimental value for the parameter A*, equ. (5.18) can be transformed into:

$$U = 1.3\ (\sin\beta)^{0.2}\ q^{0.6}\ g^{0.2}\ /\ d^{0.4} \qquad (5.19)$$

Comparing this relation with the empirical equ. (4.30) derived in this study, a remarkable similarity is evident. In fact, Fig. 5.4 shows very good agreement for the steep flume data between measured and calculated fluid velocities; putting $\sin\beta \approx \tan\beta = S$, $d \approx d_{90}$ and $U = V$, equ. (5.19) becomes:

$$V = 1.3\ S^{0.2}\ q^{0.6}\ g^{0.2}\ /\ d_{90}^{0.4} \qquad \begin{matrix} r^2 = 0.79 \\ S_E = 13.9\ \% \end{matrix} \qquad (5.20)$$

where the reduced discharges $q_r$ were used to compute the statistical parameters $r^2$ and $S_E$. Interestingly the fluid velocity of a bed load transporting flow at slopes $0.05 <= S <= 0.20$ may be predicted by the same formula as the velocity of the front of a debris flow. The corresponding debris flow experiments of Takahashi (1978) cover a slope range $0.17 <= S <= 0.47$.

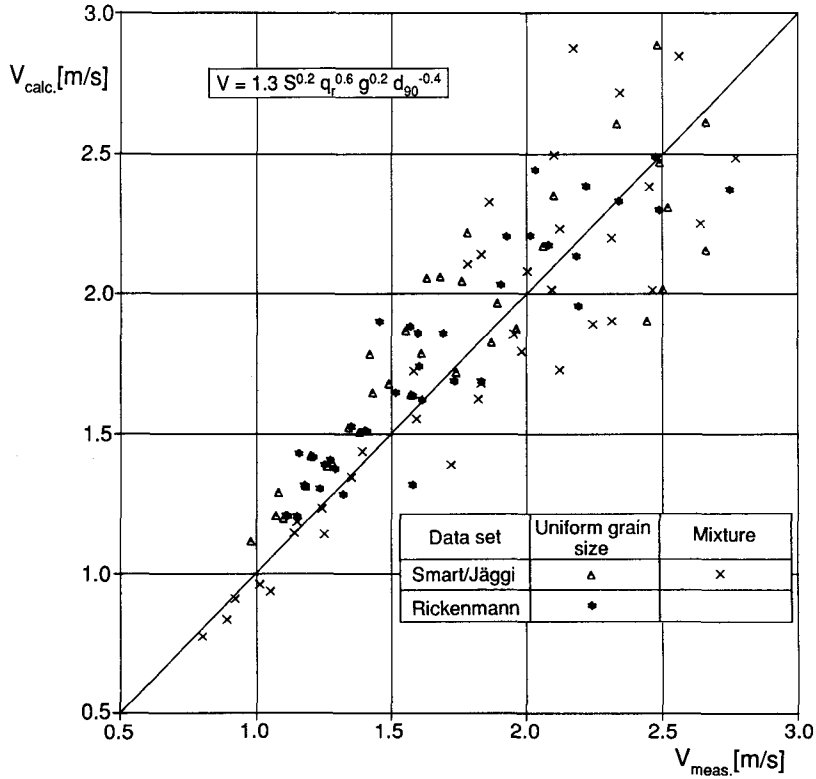


Fig. 5.4 : Comparison between measured velocities, $V_{meas.}$, and those calculated with equ. (5.20), $V_{calc.}$, for the steep flume data.

Analysis of clay suspension experiments

Increasing clay concentrations in the suspension used by the author produced an interesting result: For a given slope and flow rate, the bed load transport rates increased considerably with increasing fluid density, particularly at steeper slopes (Fig. 4.13). This change was associated with only a minor increase in flow depth and in flow velocity (Fig. 4.11), implying that the flow resistance did not significantly change (Fig. 4.10). It can be concluded that the fluid velocity is largely determined by the slope and the flow rate. Since these two

parameters also determine the bed load transport rates (s. for example equ. 4.23), any effects of a bed load on the fluid velocity could be implicitly accounted for by q and S. This may explain the rather good performance of equ. (4.30), in which the fluid velocity is related to the slope, the flow rate and a characteristic grain size.

Equ. (4.30) is based on flume tests with relatively high bed load transport rates. Somewhat larger velocities were measured for the flows over a fixed rough bed without sediment transport (for the same values of q and S); however, the velocities were found to be only about 16% higher on the average for the case of a rigid bed (s. Fig. 4.27). A closer examination of Fig. 4.27a and b reveals the following trend: For lower values of q and S (imlying weaker transport rates), the measured velocities are smaller in the movable bed case while for larger values of q and S they seem to approach those of the rigid bed case.

As a rough approximation, it is proposed that the turbulent flow in a steep rough channel is mainly governed by the slope and the flow rate and the fluid density. For a given q and S, larger depths were observed for the flows over a movable bed than for the flows over a fixed bed. These larger flow depths (or shear velocities) are associated with the space required for the transported grains. The only minor change in fluid velocity suggests that the adjustement of the (mixture) flow depth could be the primary mechanism by which the flow supplies the energy required for grain movement. It may be hypothesised therefore that the fluid - grain mixture is a self - regulating system, adjusting flow depth and transport rates in such a way that the fluid velocity is not greatly affected, but instead is largely determined by the slope and flow rate.

## 5.3 Effects of high fine material concentrations; implications for field situation

### Effect of increasing viscosity

At clay concentrations $C_f$ above about 16%, a decrease in the bed load transport rates was observed with further increasing $C_f$ values (s. also

Appendix II). This decrease was found to be associated with a grain Reynolds number $Re_2^*$ below about 10 (Fig. 4.9) which implies that the thickness of the laminar sublayer, $\delta$, is greater than the grain size, d.

A similar conclusion can be drawn based on a study about the hydraulic transport of solids in pipes by A.D. Thomas (1979a,b). The transport capacity of solids can be expected to decrease if $\delta > \simeq d$; then, according to equ. (2.80), the critical gradient at deposition increases linearly with increasing fluid viscosity. Interestingly, a linear decrease in bed load transport rates with increasing viscosity $\mu_{e2}$ of the clay suspension is suggested by the case II experiments of this study (Fig. 4.33).

Negative lift forces may be an explanation for this decrease. Based on experiments, Davies and Samad (1979) found the lift forces to decrease with decreasing particle Reynolds numbers; they measured negative values for $Re^* < \simeq 5$. Similar experimental results were reported by Coleman (1967).

It is noted that the case II experiments of this study were in the hydraulically smooth turbulent regime. For a given pressure gradient in pipe flow, A.D. Thomas (1979b) concluded that the transport capacity should be smaller in laminar than in turbulent flow. Since the flow resistance increases strongly in laminar flow with increasing viscosity, larger flow depths will result in open channel flows (for a given flow rate), implying an increase in shear stress. With increasing viscosity, the bed load transport rate is expected to decrease; however, a part of the grains may then be transported in "suspension" (not supported by turbulence but due to a very small settling velocity), and the total load was found to be increased in laminar flow (sec. 2.3.1). It is difficult to predict what the combined effect will be on the bed load transport capacity in laminar open channel flow. Experimental evidence (Bradley, 1986a; Wan and Song, 1987) suggests that the total transport capacity may be considerably higher in laminar flow.

At steeper slopes, a mechanism called "autosuspension" may become important (Bagnold, 1962). When the the bed slope is higher than the ratio $W/U_B$, then the gravity component of the moving grains contributes enough energy to maintain the grains in "suspension". Using calculated settling velocities (W = 0.75 m/s in clear water, W $\simeq$ 0.14 m/s at

concentration level C4) and mean grain velocities ($U_B$), this mechanism seems possible for the steepest slopes at the the clay concentration levels C3 and C4.

Scaling considerations

In the case II experiments, the bed load transport rates decreased by about a factor of 3; this decrease is assumed to be a result of a corresponding viscosity increase by about the same factor (s. also Fig. 4.33). The effective viscosity $\mu_{e2}$ is given as:

$$\mu_{e2} = \eta_B + \frac{\tau_B h}{2\,V} \tag{2.40}$$

For the given "mean" shear rates ($2 \cdot V/h$) and fluid properties of the case II tests, it can be concluded that $\mu_{e2}$ is mainly determined by the Bingham yield stress $\tau_B$ because the Bingham viscosity $\eta_B$ accounts for less than 10% of the right hand side of equ. (2.40). Therefore, the effective viscosity may be approximated in this range as:

$$\mu_{e2} \approx \frac{\tau_B h}{2\,V} \tag{5.21}$$

The experimental flows in the turbulent regime can be scaled to the field situation according to Froude scaling. If the length scale is defined as $h_R = h_{Nature}/h_{Model}$, then the velocity scale is $V_R = (h_R)^{0.5}$. Given the same $\tau_B$ value in the model and in nature and using equ. (5.21), the viscosity scale becomes: $(\mu_{e2})_R = (h_R)^{0.5}$. This allows the scale of the grain Reynolds number $Re_2^*$ to be determined:

$$(Re_2^*)_R = \frac{(h_R)^{0.5}\, h_R}{(h_R)^{0.5}} = h_R \tag{5.22}$$

Considering a field situation with the same fluid and flow properties, it can thus be concluded that $Re_2^*$ will be greater in nature, despite a larger effective viscosity $\mu_{e2}$. At the same fine material concentration in the flow, somewhat smaller values of the Bingham parameters can be expected in the field situation because of a smaller proportion of very fine particles. Therefore, higher fine material concentrations will be

required in nature to produce a critical grain Reynolds number $Re_2^*$ below 10. This conclusion is in general agreement with a critical value of $C_f \approx 30\%$ suggested by Davies (1988) above which a flow in nature might be in the macroviscous regime (i.e. have $Re_2^* \lesssim 10$); this value of $C_f$ was estimated by Davies based on field data concerning the Bingham parameters of fine material suspensions.

Wide grain size distribution

It should be pointed out, however, that the field situation is complicated by the very wide grain size distribution of the material available for transport, in the case of flood conditions in a torrent catchment. Viscous effects will influence the transport of smaller particles already in a less concentrated slurry of fine material. With increasing fine material concentrations in the flow, the small particles may soon become transported in suspension, while intermediate sized grains might be deposited when the flow around them becomes laminar. It may also be noted in this context that the grain size distribution parameter $d_{90}/d_{30}$ assumed a maximum value of 8.5 in the experiments of Smart and Jäggi (1983). It is recommended to use only values of roughly $d_{90}/d_{30} \lesssim 10$ in the proposed bed load transport equations.

Pulsing behaviour of debris flows

Three mechanisms were proposed by Takahashi (1981) for the initiation of a debris flow: (a) a landslide from a hillslope may transform into a debris flow, (b) at sufficiently steep slopes ($> \approx 27\%$) and with large bed shear stresses, material deposited in a channel bed may be mobilized and eventually form a debris flow, (c) accumulation of debris material from the sideslopes can cause a temporary dam to be built up in the channel, and a debris flow may be initiated when this dam breaks.

It was noted by Davies (1988) that a temporary blockage of large grains can occur in a uniform flow of a grain - fluid mixture in a steep, narrow channel. He further pointed out that the development of roll waves may cause the pulsing of a debris flow; the critical Froude number for the occurrence of roll waves is much smaller in laminar than in turbulent flow. Based on field data, Davies showed that the limiting

conditions developed for clear water flows, also apply generally for debris flow conditions. Recently, Savage (1989) demonstrated theoretically that the critical Froude number for the occurrence of roll waves decreases with increasing cohesion, viscosity and particle interaction.

In the light of the experimental results of this study, the pronounced decrease of the bed load transport rate in macroviscous flow may also be seen as an element enhancing the instability of a uniform flow. In the range of fine material concentrations $C_f$ between 20% and 50%, the Bingham yield stress $\tau_B$ increases strongly with $C_f$ (sec. 2.2.1). The transition to macroviscous flow may be expected to occur in this concentration range (Davies , 1988). For a given flow rate in a torrent, a local input of fine material might thus cause a sudden decrease in bed load transport capacity, causing a part of the grains to be deposited. If such events are frequent and/or large enough, the deposited material could form a temporary dam. In contrast to direct deposition of material from the sideslopes, a partial or full blockage of the flow might therefore also be caused by a change in flow properties.

# 6 SUMMARY AND CONCLUSIONS

## 6.1 Summary

In a debris flow, big boulders and stones are transported in a slurry of finer material, which typically consists of a mixture of sand, silt and clay particles. It has been shown that these slurries often show a Bingham type rheological behaviour, which is different from that of a Newtonian fluid such as clear water.

The objective of this study was to investigate the transport of coarse bed material in a slurry of fine material. This mode of transport may be expected in the transition region between a "normal" flood with clear water and approximately uniform flow on the one side, and the unsteady, pulsing debris flow on the other side. In the experiments, a clay suspension of various concentrations was recirculated in a 20 cm wide and 5 m long flume. For slopes ranging from 7% to 20% and for flow rates between 10 l/s and 30 l/s, the equilibrium bed load transport rates were determined. A rather uniform gravel mixture with a mean diameter of 1 cm was used as bed material. The clay suspension showed increasing non-Newtonian characteristics with increasing concentration. Its rheological behaviour was approximated as a Bingham fluid. The maximum density of the suspension was about 1.36 g/cm$^3$ (corresponding to a volume concentration of 22%), and the maximum effective viscosity (defined analogous to the Newtonian viscosity) reached 1800 cps.

In the hydraulically rough turbulent or transitional regime ($Re_2^* \gtrsim 10$), no viscous effects on the bed load transport rates could be detected. However, the decrease in the grain - fluid density ratio brought about a marked increase in bed load transport rates with increasing clay concentration, by as much as a factor of 3 as compared to the clear water case. According to a study by Low (1989) it appears that this change can be correctly predicted if the ratio of the shear velocity to the fall velocity is adequatly represented in a bed load transport formula; if viscosity effects can be neglected, the density factor (s-1) may be substituted for the fall velocity. A regression analysis of the present experiments showed that the observed bed load transport rates

can be fairly well predicted by an adequate inclusion of the density factor. For a given slope and flow rate, the calculated mean bed load concentrations increased considerably with increasing clay concentration while there was only a minor increase in the corresponding mean grain velocities.

A regression analysis of the bed load transport measurements (with the clay suspension) resulted in a relationship in terms of $q_B = \phi(q_r, S, S_{cr}, s-1)$. A reanalysis was made of the steep flume experiments of Smart and Jäggi (1983), using a slightly different procedure in the data preparation. The resulting equations were of a very similar form, and therefore a formula could be derived which applies to both data sets; a grain size distribution parameter, $d_{90}/d_{30}$, was also included in the form as proposed by Smart and Jäggi. A separate regression analysis was performed with the Meyer-Peter and Müller (1948) bed load transport experiments which were carried out at lower slopes (data given in Smart and Jäggi, 1983). The exponent of the slope factor was found to be different, and it was therefore concluded that the steep and low slope data should be described by two separate equations in the $q_B(q)$ - form.

In a second step, a more general relationship was developed in terms of the parameters $\Phi_B = \phi(\theta, \theta_c, Fr, s-1, d_{90}/d_{30})$. The resulting bed load transport formula can be applied to all three data sets considered (Meyer-Peter/Müller, Smart/Jäggi and author). This relationship appears to be valid over a wider range of conditions than an equation in terms of the first parameter set, because it also contains parameters describing the flow behaviour (i.e. $\theta$ and Fr). It should however be pointed out that the role of the Froude number is different for the low and steep slope case. For the Meyer-Peter/Müller experiments, in which bed forms were noted, Fr can be considered as a measure of that part of the (total) flow resistance which is due to bed forms and is thus not available for bed load transport. In the case of the steep flume experiments (of Smart/Jäggi and of the author), antidunes and plane beds were present; they caused probably not much form drag. In the tests with high Froude numbers, bed load grain concentrations were so large that several grain layers were in motion, occupying a considerable part of the total flow depth. Since $\theta$ is only a measure for the shear stress at the interface to the quasi-stationary bed, the Froude number may in this case be a measure for the velocity of the upper, faster moving grain layers.

In the hydraulically smooth turbulent regime ($Re_2^* \lesssim 10$), the bed load transport rates decreased with increasing clay concentration. This decrease was found to be linearly related to the increase of the fluid viscosity. No bed load tests could be carried out in the laminar flow regime.

To study the effect of the increasing non-Newtonian properties with increasing clay concentration (i.e. increasing Bingham yield stress and Bingham viscosity) on the flow, additional experiments were performed with the suspension flowing over a fixed rough bed without any sediment transport. The flow resistance analysis indicated that Newtonian formulae can still be used if an adequate viscosity is defined, such as the effective visosity $\mu_{e2}$. No viscous effects could be detected in the hydraulically transition region, which is in agreement with the analysis of the bed load transport tests. The hydraulically smooth turbulent regime appears to "obscured" by the formation of a plug flow. This is a zone with no shearing between adjacent fluid layers, extending from the flow surface downwards; with increasing Bingham yield stress of the fluid, this zone occupies increasing proportions of the flow cross-section. When it merges with the viscous sublayer, the flow becomes laminar.

As noted by Smart and Jäggi (1983), the flow resistance of the sediment transporting flows cannot be determined by the relative depth alone. Including a slope dependent correction term, their formula reduces the available (energy) slope in order to account for additional resistance due to transported grains. However, there is still a large scatter between predicted and calculated velocities, which can be only partly attributed to inaccurate depth measurements. An alternative equation for the fluid velocity was developed as a function of the flow rate, the slope and a characteristic grain size. A theoretical equation was proposed by Takahashi (1978) to describe the velocity of a debris flow front; introducing an experimentally determined parameter, this formula becomes very similar to the one of the author. If applied to the steep flume data of this study, it shows even a better performance than the author's equation. It is therefore recommended to use this semi-theoretical formula if the velocity is to be calculated as a function of the flow rate.

## 6.2 Recommended calculation procedure

The equations presented in this study allow the unknown parameters of a bed load transporting flow to be estimated. In engineering applications, usually either (A) the flow rate or (B) the mixture depth is given to calculate the other required parameters; in both cases, the slope and the grain size characteristics can be obtained in the field, while an appropriate value for the fluid density has probably to be assumed.

Different equations were developed to determine the unknown parameters of the grain-fluid flow. If one particular set of formulae is used, the quality of the predicted parameters will not be the same whether the calculations are made for case (A) or (B). It is therefore proposed to use two different sets of equations, which should give best estimates of the unknown parameters for each of the two cases. The two recommended calculation procedures are presented in the following figures.

If two out of the three parameters (q, V, $h_f$) are known, then the fluid flow is determined. In the case (A), q is given, and the calculation according to Fig. 6.1 results in a similar agreement between predicted and measured mixture flow depths, as when applying the iterative procedure given in Smart and Jäggi (1983). In the case (B), however, the computations are based on a parameter which characterises the flow of the grain - fluid mixture. Then, two fluid flow parameters have to be calculated, s. Fig. 6.2, and the agreement between predicted and measured q values is not as good as in case (A) for $h_m$. Since it is the fluid flow rate that largely determines the flow of the mixture, a different quality of the results can be expected, depending on the applied procedure.

It is pointed out that the procedure (A) should only be applied to a slope range between 5% and 20%, because the bed load transport equation (4.24) was derived from the steep flume data. It has been shown that an equation of the form of (5.1) is less general than one in terms of (5.2). Furthermore, the velocity formula (5.20) is based on steep flume experiments that cover a limited range of relative flow depths.

Procedure (B), on the other hand, may be used both for steep and low slope situations (slope range 0.2 % <= S <= 20 %). The bed load transport equation (4.28) was developed from the Meyer-Peter/Müller and the steep flume data. The logarithmic flow resistance formula (4.7) can be applied generally; the correction factor in square brackets becomes unity for low slope values and for large relative flow depths. Also, no distinction between the mixture depth and the fluid depth is necessary at low slopes and low bed load concentrations, i.e. equ. (4.23) and (4.34) can be omitted for slopes less than about 5 %.

In a torrent situation, procedure (A) can be used if the the flow section of check dams or if an artificial channel on the fan are to be designed according to a maximum flood discharge. The procedure may be further applied to estimate transported sediment volumes during a flood event if a hydrograph is known or determined from rainfall intensity data.

A typical application of procedure (B) is given, when the (mixture) flow depth at a defined cross-section can be determined from flood marks but no information is available on the flow rate. Of course, one has to be sure that these flood marks are due to a more or less steady uniform flow and were not caused by a debris flow.

In both procedures, it is assumed that there is a full, unlimited supply or availability of bed material. This requirement might not be satisfied particularly in situations where an armour layer of coarse material is not yet broken up. In this case, equ. (2.113) may be used instead of equ. (2.111). But it should be remembered that the bed load transport rates calculated by either of the two procedures give values corresponding to the (maximum) transport capacity.

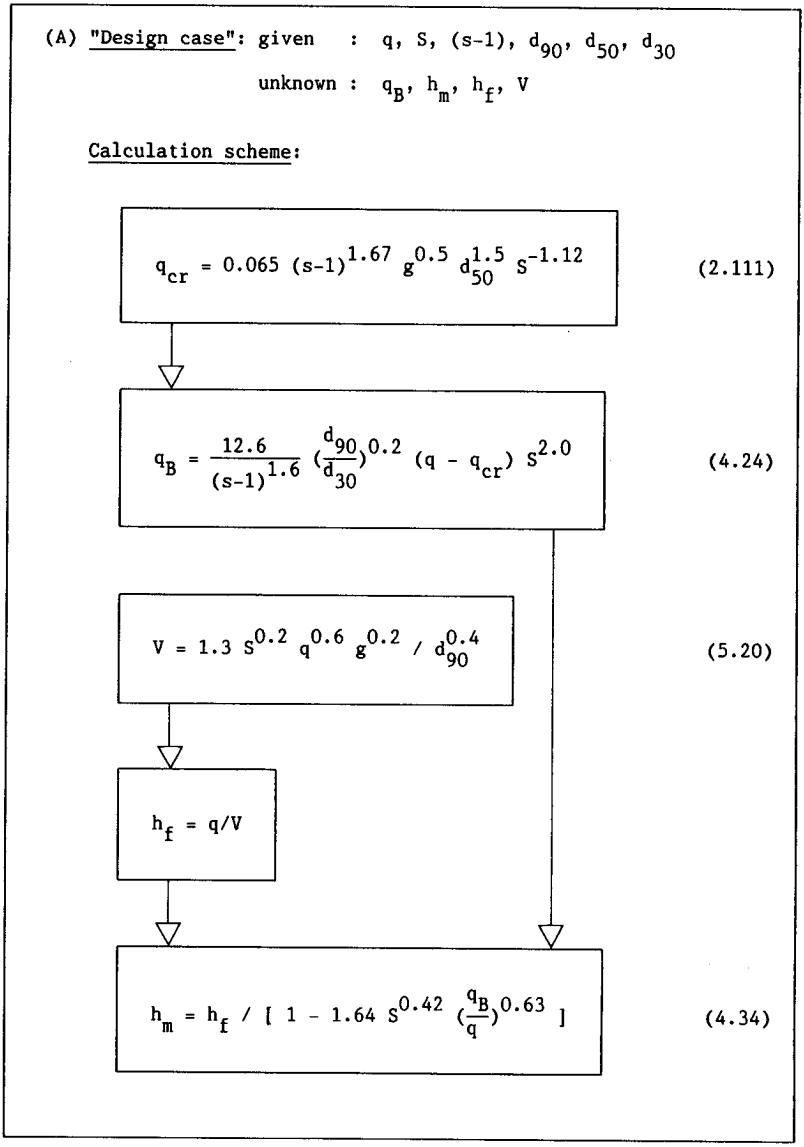


Fig. 6.1 : Proposed calculation procedure for the "design case" (A). Recommended range of application: 5 % <= S <= 20 %, $q \geq \approx 5 \cdot q_{cr}$, $h_m/d_{90} \leq \approx 20$. (A sidewall correction procedure may be applied additionally.)

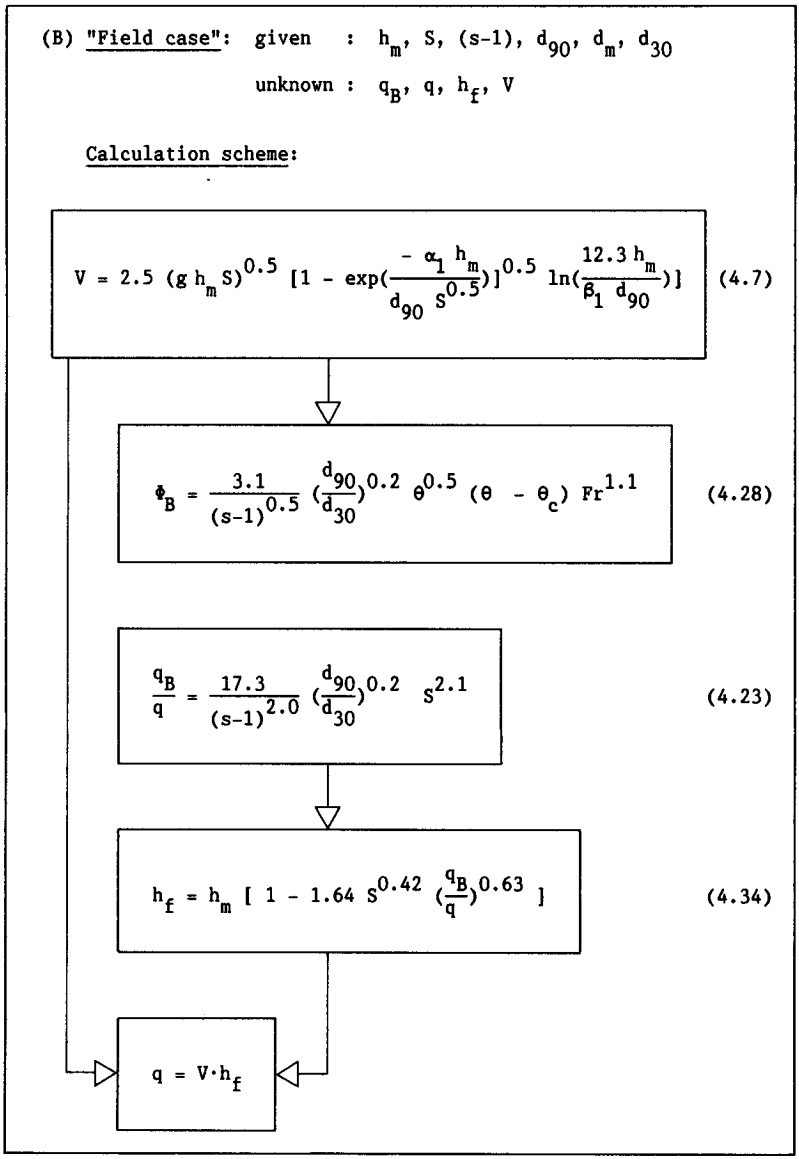


Fig. 6.2 : Proposed calculation procedure for the "field case" (B). Recommended range of application: 0.2 % <= S <= 20 %; $\alpha_1$ = 0.05 and $\beta_1$ = 1.5 for S >= 5 %; equ. (4.23) and equ. (4.34) can be omitted for S < 5 % (then $h_f \approx h_m$); $d_m$ >≈ 1 mm. (A sidewall correction procedure may be applied additionally.)

## 6.3 Example calculation

Consider a channel reach in a torrent, where the following information on slope and grain size characteristics is given:

$S = 0.15$
$d_{90} = 0.50$ m
$d_{50} \simeq d_m = 0.15$ m
$d_{30} = 0.04$ m ;

assume $\rho = 1.15$ t/m³, with $\sigma = 2.65$ t/m³ --> $(s-1) = 1.30$ ;
since $d_{90}/d_{30} = 12.5$, take maximum recommended value of 10.

a) In the first case, the fluid discharge shall be given as $q = 3.5$ m³/s.m, and procedure (A) can be applied:

(2.111) $q_{cr} = 0.065 \cdot 1.30^{1.67} \cdot 9.81^{0.5} \cdot 0.15^{1.5} / 0.15^{1.12}$
$= 0.153$ m³/s.m

(4.24) $q_B = 12.6 \cdot 10^{0.2} \cdot (3.5 - 0.153) \cdot 0.15^{2.0} / 1.30^{1.6}$
$= 0.985$ m³/s
$= 2610$ kg/s

(5.20) $V = 1.3 \cdot 0.15^{0.2} \cdot 3.5^{0.6} \cdot 9.81^{0.2} / 0.45^{0.4}$
$= 4.10$ m/s

$h_f = q / V$
$= 0.854$ m

(4.34) $h_m = 0.854 / [1 - 1.64 \cdot 0.15^{0.42} \cdot (0.985/3.5)^{0.63}]$
$= 1.28$ m

b) In the second case, it is assumed that the mixture flow depth has been measured as $h_m = 1.4$ m, and procedure (B) can be applied:

(4.7) $V = 2.5 \cdot (9.81 \cdot 1.4 \cdot 0.15)^{0.5} \cdot [1 - \exp(\frac{-0.05 \cdot 1.4}{0.45 \cdot (0.15)^{0.5}})]^{0.5} \cdot \ln(\frac{12.3 \cdot 1.4}{1.5 \cdot 0.45})$
$= 3.84$ m/s

$$\theta = h_m \cdot S \,/\, [(s-1)\cdot d_m] = 1.4\cdot 0.15 \,/ [1.30\cdot 0.15] = 1.08$$

$$Fr = V \,/\, (g\, h_m)^{0.5} = 3.84 \,/\, (9.81\cdot 1.4)^{0.5} = 1.04$$

assume $\theta_c = 0.05$

(4.28) $$\Phi_B = 3.1\cdot 10^{0.2}\cdot 1.08^{0.5}\cdot (1.08 - 0.05)\cdot 1.04^{1.1} \,/\, 1.30^{0.5}$$
$$= 4.78$$

$$q_B = \Phi_B \cdot [g(s-1)d_m^3]^{0.5} = 4.78\cdot [9.81\cdot 1.30\cdot 0.15^3]^{0.5}$$
$$= 0.996 \text{ m}^3/\text{s}$$
$$= 2640 \text{ kg/s}$$

(4.23) $$q_B/q = 17.3\cdot 10^{0.2}\cdot 0.15^{2.1} \,/\, 1.30^{2.0}$$
$$= 0.30$$

(4.34) $$h_f = 1.4\cdot [1 - 1.64\cdot 0.15^{0.42}\cdot 0.30^{0.63}]$$
$$= 0.916 \text{ m}$$

$$q = V\cdot h_f = 3.84\cdot 0.916$$
$$= 3.52 \text{ m}^3/\text{s.m}$$

In comparison, it is observed that procedure (A) predicts a slightly higher fluid velocity and a lower mixture depth than procedure (B), at about the same flow rate and bed load transport rate. This is not surprising, because different sets of equations are used. It may be noted that a sidewall correction could be included in both procedures.

## 6.4 Suggestions for further research

In this study, the effect of an increasing fluid density and viscosity on the bed load transport capacity in flows at steep slopes has been examined. Little is still known about how flows carrying a heavy sediment load can become unsteady and eventually turn into a pulsing debris flow. The following aspects of sediment transporting flows in steep channels should be studied further:

- How does the bed load transport capacity change from the hydraulically smooth turbulent regime to the laminar regime ?

- A wide grain size distribution can considerably affect the rheological properties of the slurry. What will the effect be on bed load and suspended load transport rates, particularly in the transition region between turbulent and laminar flow ?

- According to the theoretical analysis of Savage (1989), roll waves are more likely to occur in laminar flows and fluids with a high cohesion (or Bingham yield stress) than in turbulent water flows. The stability of such flows should also be studied experimentally.

- In order to gain a better understanding of the mechanics of these flows, further attempts should be made to measure velocity profiles both of the fluid and the grains, or to track the paths of individual particles.

- If heavily sedimented uniform flows at steep slopes appear to become easily unstable because of the inherent mechanical characteristics, it would be interesting to study the effect of disturbances such as slug inputs of debris material at different positions along a channel. For in the field situation, failures of sideslopes may be an important factor to trigger a flow instability. The effect of a varying channel geometry on the flow stability could also be examined.

- More experiments should be performed with flows over a mobile bed at slopes steeper than about 25%. Under these conditions, small shear stresses are already sufficient to destabilise a loose bed down to considerable depths; the theoretical analysis of Takahashi (1981) suggests that the whole layer of loose material may start to move en masse. Similar conditions are indicated by observations made by Smart and Jäggi (1983) at flume slopes of 25%. Such experiments will have to be carefully designed because the "erosion" depth will be very sensitive to the shear strength of the bed (underground) material. Recently, Tanigushi et al. (1988), reported on an experimental study concerning the erosion capacity of a debris flow front at a slope of 40%.

REFERENCES

**Abbott, J.E. and Francis, J.R.D.** (1977):
"Saltation and suspension trajectories of solid grains in a water stream", Phil. Trans. Royal Soc. London, Vol. 284 A.

**Abdel-Rahman, N.M.** (1963):
"The effect of flowing water on cohesive beds", Ph.D. thesis No. 3263, ETH Zürich.

**Ackerman, N.L. and Shen, H.** (1979):
"Rheological characteristics of solid-liquid mixtures", AIChE Journal, Vol. 25, No. 2.

**Ansley, R.W. and Smith, T.N.** (1967):
"Motion of spherical particles in a Bingham plastic", AIChE Journal, Vol. 13, No. 6.

**Ashida, K. and Bayazit, M.** (1973):
"Initiation of motion and roughness of flows in steep channels", Proc. 15th IAHR Congress, Istanbul, Turkey, Vol. 1.

**Ashida, K. , Miyamoto, K. and Kanda, M.** (1987):
"Characteristics of hyperconcentrated flows", Proc. 22nd IAHR Congress, Lausanne, Switzerland, Techn. Session A.

**Bagnold, R.A.** (1954):
"Experiments on a gravity-free dispersion of large solid spheres in a Newtonian fluid under shear", Proc. Royal Soc. London, Vol. 225A.

**Bagnold, R.A.** (1955):
"Some flume experiments on large grains but little denser than the transporting fluid, and their implications", Proc. Inst. Civil Engrs., London, 4(3).

**Bagnold, R.A.** (1956):
"The flow of cohesionless grains in fluids", Phil. Trans. Royal Soc. London, 249A.

**Bagnold, R.A.** (1962):
"Auto-suspension of transported sediment; turbidity currents", Proc. Royal Soc. London, 265A.

**Bagnold, R.A.** (1966):
"An approach to the sediment transport problem from general physics", U.S. Geol. Survey Prof. Paper 422-I.

**Bagnold, R.A.** (1973):
"The nature of saltation and of 'bed-load' transport in water", Proc. Royal Soc. London, Vol. 332 A.

**Bathurst, J.C.** (1985):
"Flow resistance estimation in mountain rivers", ASCE, J.Hydr.Eng., Vol. 111, No. 4.

**Bathurst, J.C., Graf, W.H. and Cao, H.H.** (1982a):
"Initiation of sediment transport in steep channels with coarse bed material", Proc. Euromech 156: Mechanics of sediment transport, Istanbul.

**Bathurst, J.C., Graf, W.H. and Cao, H.H.** (1982b):
"Bedforms and flow resistance in steep gravel-bed rivers", Proc. Euromech 156: Mechanics of sediment transport, Istanbul.

**Bathurst, J.C., Cao, H.H. and Graf, W.H.** (1984):
"The data from the EPFL study on hydraulics and sediment transport in a steep flume", EPFL, Lausanne.

**Bathurst, J.C., Graf, W.H. and Cao, H.H.** (1987):
"Bed load discharge equations for steep mountain rivers", in: Sediment transport in gravel bed rivers, eds. Thorne, Bathurst, Hey, John Wiley and Sons.

**Beverage, J.P. and Culbertson, J.K.** (1964):
"Hyperconcentrations of suspended sediment", ASCE, J.Hydr.Div., Vol. 90, No. HY6.

**Bingham, E.C.** (1922):
"Fluidity and plasticity", McGraw-Hill, New York.

**Bradley, J.B.** (1986):
"Hydraulics and bed material transport at high fine suspended sediment concentrations", Ph. D. Dissertation, Colorado State Univ., Fort Collins, Colorado.

**Bradley, J.B. and McCutcheon, S.C.** (1987):
"Influence of large suspended-sediment concentrations in rivers", in: Sediment transport in gravel bed rivers, eds. Thorne, Bathurst, Hey, John Wiley and Sons.

**Brauer, H.B.** (1971):
"Grundlagen der Einphasen- und Mehrphasenströmungen", Verlag Sauerländer, Aarau und Frankfurt.

**Bridge, J.S. and Domonic, D.F.** (1984):
"Bed load grain velocities and sediment transport rates", Water Res. Res., Vol. 20, No. 4.

**Brühl, H.** (1976):
"Einfluss von Feinststoffen in Korngemischen auf den hydraulischen Feststofftransport in Rohrleitungen", Mitt. des Franzius-Instituts für Wasserbau und Küsteningenieurwesen der Tech. Univ. Hannover, Heft 43.

**Caldwell, D.H. and Babbitt, H.E.** (1941):
"Flow of muds, sludges, and suspensions in circular pipe", Industrial and Engineering Chemistry, 33, 2.

**Cao, H.H.** (1985):
"Résistance hydraulique d'un lit de gravier mobile à pente raide; étude expérimentale", thèse No. 589, EPFL, Lausanne.

**Cao, R., Chen, S., Lu, W. and Ren, X.** (1983):
"The law of hydraulic resistance in density current with hyperconcentration", Proc. 2nd Int. Symp. on River Sedimentation, Nanjing, China (in Chinese with English abstract).

**Chee, S.P.** (1988):
"Models and scale effects related to erosion of granular dams", Proc. int. symp. on Modelling soil-water structure interactions, Kolkman et al. (eds.), Balkema, Rotterdam.

**Chen, C.** (1983):
"On frontier between rheology and mudflow mechanics", Proc. of the Hydraulics Division Speciality Conference on "Frontiers in Hydraulic engineering", ASCE, Massachusetts Institute of Technology, Cambridge, Mass.

**Chen, C.** (1986a):
"Bingham plastic of Bagnold's dilatant fluid as a rheological model of debris flow?", 3rd Int. Symp. on River Sedimentation, Univ. of Mississippi.

**Chen, C.** (1986b):
"Chinese concepts of modeling hyperconcentrated streamflow and debris flow", 3rd Int. Symposium on River Sedimentation, Univ. of Mississippi.

**Chen, C.** (1988a):
"Generalized viscoplastic modeling of debris flow", ASCE, J.Hydr.Eng., Vol. 114, No. 3.

**Chen, C.** (1988b):
"Generalized solutions for viscoplastic debris flow", ASCE, J.Hydr.Eng., Vol. 114, No. 3.

**Chu, J.** (1983):
"Basic characteristics of sediment-water mixture with hyperconcentration", Proc. 2nd int. symp. on river sedimentation, Beijing, China, Vol. 1.

**Colby, B.R.** (1964):
"Practical computations of bed material discharge", ASCE, J.Hydr.Div., Vol. 90, No. HY2.

**Coleman,N.L.** (1967):
"A theoretical and experimental study of drag and lift forces acting on a sphere resting on a hypothetical stream bed", Proc. 12th IAHR Congress, Fort Collins, USA, Vol. 3.

**Cooper, R.H. and Peterson, A.W.** (1969):
"A review of data from sediment transport experiments", Rep. No. HY-1969-ST2, Dept. of Civil Eng., Univ. of Alberta.

**Costa, J.E.** (1984):
"Physical geomorphology of debris flows", Developments and applications of geomorphology (eds. Costa and Fleisher), Springer-Verlag, Berlin and Heidelberg.

**Daido, A.** (1971):
"On the occurrence of mud-debris flow", Bull. Disaster Prevention Research Institute, Kyoto Univ., Vol. 21, Part 2.

**Daido, A.** (1983):
"Incipient motion and bed load of sediment in steep channel", 10th IAHR Congress, Moscow, Soviet Union, Vol. VII.

**Davies, T.R.H.** (1985):
"Mechanics of large debris flows", Proc. int. symp. on erosion, debris flow and disaster prevention, Tsukuba, Japan.

**Davies, T.R.H.** (1986):
"Large debris flows: a macroviscous phenomenon", Acta Mechanica, Vol. 63.

**Davies, T.R.H.** (1988):
"Debris Flow Surges - A Laboratory Investigation", Mitt. Nr. 96 der Versuchsanstalt für Wasserbau, Hydrologie und Glaziologie, ETH Zürich.

**Davies, T.R.H. and Samad, M.F.A.** (1978):
"Fluid Dynamic Lift on a Bed Particle", ASCE, J.Hydr.Div., Vol.104, HY8.

**Davies, T.R.H. and Jäggi, M.N.R.** (1981):
"Precise Laboratory Measurement of Flow Resistance", Proc. 19th IAHR Congress, New Dehli, India.

**Dodge, D.W. and Metzner, A.B.** (1959):
"Turbulent flow of non-Newtonian systems", A.I.Ch.E. Jour., Vol. 5, No. 2.

**Drake, T.G. and Shreve, R.L.** (1986):
"High-speed motion pictures of nearly steady, uniform, two-dimensional, inertial flows of granular materials", Jour. Rheology, Vol. 30.

**Draper, N.R. and Smith, H.** (1966):
"Applied regression analysis", John Wiley and Sons, New York.

**Du, R., Kang Z., and Zhang S.** (1986):
"On the Classification of Debris Flow in China", Third int. Symp. on River Sed., Mississippi, USA.

**Einstein, H.** (1966):
"Die Scherfestigkeit kohäsiver Böden in Abhängigkeit vom Lagerungszustand und von der Materialart", Diss. ETH Nr. 3811, (= Mitt. der Versuchsanstalt für Wasserbau und Erdbau Nr. 71), Zürich.

**Einstein, H.A.** (1934):
"Der hydraulische oder Profilradius", Schweiz. Bauzeitung, No. 8.

**Einstein, H.A.** (1950):
"The bed-load function for sediment transportation in open channel flows", U.S. Dept. of Agriculture, Techn. Bull. No. 1026.

**Einstein, H.A. and Abdel-Aal, F.M.** (1972):
"Einstein bed load function at high sediment rates", ASCE, J.Hydr.Div., Vol. 98, No. HY1.

**Einstein, H.A. and Chien, N.** (1953):
"Transport of sediment mixture with large ranges of grain sizes", U.S. Army Corps of Eng., M.R.D. Sediment Series, No. 2.

**Einstein, H.A. and Chien, N.** (1955):
"Effects of heavy sediment concentration near the bed on velocity and sediment distribution", Univ. of Berkley, California.

**Engelund, F. and Fredsoe, J.** (1976):
"A sediment transport model for straight alluvial channels", Nordic Hydrology 7.

**Fan, J. and Dou, G.** (1980):
"Sediment transport mechanics (including hyperconcentration transportation)", Proc. Int. Symp. Riv. Sed., Beijing, China.

**Fei, X.** (1981):
"Bingham yield stress of sediment-water mixture with hyperconcetration", Jour. Sediment Research, Beijing, China, No. 3.

**Fei, X.** (1983):
"Grain composition and flow properties of heavily concentrated suspensions", Proc. 2nd int. symp. on river sedimentation, Nanjing, China, Vol. 1.

**Graf, W.H.** (1971):
"Hydraulics of sediment transport", McGraw-Hill, New York.

**Grim, R.E.** (1968):
"Clay mineralogy", 2nd ed., McGraw-Hill, New York.

**Griffiths, G.A.** (1989):
"Form resistance in gravel channels with mobile beds", ASCE, J.Hydr.Eng., Vol. 115, No. 3.

**Gupta, S.N. and Mishra, P.** (1974):
"Turbulent flow of inelastic non-Newtonian fluids in pipes", Indian Jour. of Technology, Vol. 12.

**Gust, G.** (1976):
"Observations on turbulent-drag reduction in a dilute suspension of clay in sea-water", J. Fluid Mech., Vol. 75, Part 1.

**Hampton, M.A.** (1975):
"Competence of fine-grained debris flow", Jour. Sedimentary Petrology, Vol. 45.

**Hanes, D.M.** (1986):
"On the use of grain-flow dynamics to model intense bedload sediment transport", ASCE Spec. Conf. on advances in aerodynamics, fluid mechanics, and hydraulics, Minneapolis.

**Hanes, D.M. and and Bowen, A.J.** (1985):
"A granular-fluid model for steady intense bed-load transport", J. Geophys. Res., Vol. 90, No. C5.

**Hänger, M.** (1979):
"Geschiebetransport in Steilgerinnen. Pilotstudie für feste und glatte Sohle und Gefälle von 3 bis 30%", Mitt. Nr. 38 der Versuchsanstalt für Wasserbau, Hydrologie und Glaziologie, ETH Zürich.

**Hanks, R.W.** (1963):
"The laminar-turbulent transition for fluids with a yield stress", A.I.Ch.E. Journal, Vol. 9, No. 3.

**Hanks, R.W. and Dadia, B.H.** (1971):
"Theoretical analysis of the turbulent flow of non-Newtonian slurries in pipes", Am. Soc. Chem. Eng. Jour., Vol. 17, No. 3.

**Henderson, F.M.** (1966):
"Open channel flow", MacMillan Publ. Co., New York.

**Hong, R.-J., Karim, M.R. and Kennedy, J.F.** (1984):
"Low-temperature effects on flow in sand-bed streams", ASCE, J.Hydr.Eng., Vol. 110, No. 2.

**Howard, C.D.D.** (1963):
"Flow of clay-water suspensions", ASCE, J.Hydr.Div., Vol. 89, No. HY5.

**Ikeda, S.** (1982):
"Incipient motion of sand particles on side slopes", ASCE, J.Hydr.Div., Vol. 108, No. HY1.

**Innes, J.L.** (1984):
"Debris flows", Progress in Physical Geography.

**Iverson, R.M. and Denlinger, R.P.** (1987):
"The physics of debris flows - a conceptual assessment", Proc. Symp. on Erosion and Sedimentation in the Pacific Rim, Corvallis, IAHS Publ. No. 165.

**Iwagaki, Y. and Tsuchiya, Y.** (1959):
"An analysis of the stable cross section of a stream channel", Bull. Disaster Prevention Research Institute, Kyoto Univ., No. 29.

**Jäggi, M.N.R.** (1983):
"Alternierende Kiesbänke", Diss. ETH Nr. 7208, Zürich (= Mitt. Nr. 62 der Versuchsanstalt für Wasserbau, Hydrologie und Glaziologie der ETH).

**Johnson, A.M.** (1965):
"A model for debris flow", Pennsylvania State Univ., unpublished Ph.D. Dissertation.

**Johnson, A.M.** (1970):
"Physical processes in geology", Freeman Cooper and Co.

**Johnson, A.M. and Rodine, J.R.** (1984):
"Debris Flow", Chapter 8 in "Slope Instability", ed. D. Brunsden and D.B.Prior, John Wiley and Sons.

**Julien, P.Y. and Lau, Y.** (1988):
Discussion of "Simple model of sediment-laden flows" by Parker and Coleman (1986); ASCE, J.Hydr.Eng., Vol. 114, No. 2.

**Kahr, G.** (1989):
personal communication

**Kamphuis, J.W.** (1974):
"Determination of sand roughness for fixed beds", J.Hydr.Res., Vol. 12, No. 2.

**Kang, Z. and Zhang, S.** (1980):
"A preliminary analysis of the characteristics of debris flow", Proc. Int. Symp. on River Sedimentation, Beijing, China (in Chinese with English abstract).

**Kikkawa, W. and Fukuoka, S.** (1969):
"The characteristics of flow with wash load", Proc. 13th IAHR Congress, Tokyo, Japan, Vol. 2.

**Kozicki, W. and Tiu, C.** (1967):
"Non-Newtonian flow through open channels", Canadian J. Chem. Eng., Vol. 45.

**Kresser, W.** (1964):
"Gedanken zur Geschiebe- und Schwebstofführung der Gewässer", Oesterreichische Wasserwirtschaft, 16. Jhg., Heft 1 und 2.

**Krieger, I.M. and Dougherty, T.J.** (1959):
"A mechanism for non-Newtonian flow in suspensions of rigid spheres", Trans. Soc. of Rheology, Vol. 3.

**Kurdin, R.D.** (1973):
"Classification of mudflows", Soviet Hydrology: Selected Papers, Issue No. 4.

**Lau, Y.L.** (1987):
Discussion of "Low temperature effects on flow in sand-bed streams" by Hong et al. (1984), ASCE, J.Hydr.Eng., Vol. 113, No. 1.

**Lanzendorf, W.** (1984):
"Zum Bewegungsverhalten von Feststoffpartikeln im Bereich der laminaren Unterschicht einer Rohrströhmung", Mitt. des Leichtweiss-Instituts für Wasserbau, Techn. Univ. Braunschweig, Heft 83.

**Lin, C. and Sun, M.** (1983):
"A remark on the shields diagram", 2nd Int. Symp. on River Sedimentation, China (in Chinese with English abstract).

**Low, H.S.** (1989):
"Effect of sediment density on bed-load transport", ASCE, J.Hydr.Eng., Vol. 115, No. 1.

**Luque, R.F. and van Beek, R.** (1976):
"Erosion and transport of bed-load sediment", IAHR, J.Hydr.Res., Vol. 14, No. 2.

**Mantz, P.A.** (1977):
"Incipient transport of fine grains and flakes by fluids - extended Shields diagram", ASCE, J.Hydr.Div., Vol. 103, No. HY6.

**Mantz, P.A. and Emmett, W.W.** (1985):
"Analysis of United States Geological Survey sediment transport data for some California streams", Proc. Euromech 192: Transport of suspended solids in open channels, Neubiberg.

**Meyer-Peter, E. and Mueller, R.** (1948):
"Formulas for bed-load transport", 2nd meeting IAHSR, Stockholm, Sweden.

**McTigue, D.F.** (1982):
"A nonlinear constitutive model for granular materials: application to gravity flow", J. of Applied Mechanics, ASME, Vol. 49(2).

**Mills, S.V.** (1983):
"An experimental study of the rheology of mudflows", M.S. thesis, College of Eng., Washington State Univ.

**Mizuyama, T.** (1977):
"Bedload transport in steep channels", Ph.D. Dissertation, Kyoto Univ.

**Mizuyama, T.** (1981):
"An intermediate phenomenon between debris flow and bed load transport", Symp. on Erosion and Sed. Transp., Pacific Rim, Christchurch, New Zealand.

**Mizuyama, T.** (1988):
written communication

**Mizuyama, T. and Shimohigashi, H.** (1985):
"Influence of fine sediment concentration on sediment transport rates", Jap. Civil Eng. Jour. 27-1, 1985 (in Japanese).

**Moshev, V.V.** (1979):
"Viscosity relationship for heavily filled suspensions", Fluid mechanics - Soviet research, Vol. 8, No. 2.

**Murphy, P.J. and Aguirre, E.J.** (1985):
"Bed load or suspended load", ASCE, J.Hydr.Eng., Vol. 111, No. 1.

**Naik, B.** (1983):
"Mechanics of Mudflow treated as the Flow of a Bingham Fluid", Ph.D. Thesis, Washington State University, USA.

**O'Brien, J.S. and Julien, P.Y.** (1984):
"Physical properties and mechanics of hyperconcentrated sediment flows", Proc. Specialty Conference on Delineation of Landslides, Flashfloods and Debris Flow Hazards in Utah, Logan, Utah.

**O'Brien, J.S. and Julien, P.Y.** (1986):
"Rheology of non-Newtonian fine sediment mixtures", ASCE, Speciality Conference on advances in aerodynamics, fluid mechanics, and hydraulics, Minnesota.

**Parker, G. and Coleman, N.L.** (1986):
"Simple model of sediment laden flows", ASCE, J.Hydr.Eng., Vol. 112, No. 5.

**Pierson, T.C. and Costa, J.E.** (1984):
"A rheological classification of subaerial sediment-water flows", Abstracts with Programs, 97th Annual Meeting GSA, Vol. 16, No. 6.

**Quian, Y., Yang W., Zhao W., Cheng X., Zhang L., Xu W.** (1980)
"Basic Characteristics of Flow with Hyperconcentration of Sediment", Int. Symp. on River Sed., Beijing, China.

**Richardson, E.V. and Julien, P.Y.** (1986):
"Bedforms, fine sediments, washload and sediment transport", 3rd Int. Symp. on River Sedimentation, Univ. of Mississippi.

**Rouse, H.** (1960):
"Elementary mechanics of fluids", John Wiley and Sons, London.

**Rubey, W.W.** (1933):
"Settling velocities of gravel, sand and silt particles", American J. of Science, 5th Series, Vol. 25(148).

**Savage, S.B.** (1989):
"Flow of granular materials", in: Theoretical and Applied Mechanics, eds. Germain, Piau, Caillerie, Elsevier, Amsterdam.

**Schoklitsch, A.** (1950):
"Handbuch des Wasserbaus", 2. Auflage, Springer Verlag, Wien.

**Shen, S. and Xie, S.** (1985):
"Structure mode and rheologic property of mud debris flow", Int. Symp. on Erosion, Debris Flow and Disaster Prevention, Tsukuba, Japan.

**Shields, A.** (1936):
"Anwendung der Aehnlichkeitsmechanik und der Turbulenzforschung auf die Geschiebebewegung", Mitt. d. Preuss. Vers.anst. für Wasserbau und Schiffbau, Berlin, Nr. 26.

**Simons, D.B., Richardson, E.V. and Haushild, W.L.** (1963):
"Some effects of fine sediment on flow phenomena", U.S.G.S. Water-Supply Paper 1498-G.

**Smart, G.M.** (1984):
"Sediment transport formula for steep channels", ASCE, J.Hydr.Eng., Vol. 110, No. 3.

**Smart, G.M., and Jaeggi, M.** (1983):
"Sediment Transport on Steep Slopes", Mitt. Nr. 64 der Versuchsanstalt für Wasserbau, Hydrologie und Glaziologie, ETH Zürich.

**Stevens, M.A., Simons, D.B. and Lewis, G.L.** (1976):
"Safety factors for riprap protection", ASCE, J.Hydr.Div., Vol. 104, No. HY8.

**Stiny, J.** (1910):
"Die Muren", Verlag der Wagner'schen Universitätsbuchhandlung, Innsbruck.

**Straub, L.G., Silberman, E. and Nelson, H.C.** (1958):
"Open-channel flow at small Reynolds numbers", ASCE, Transactions, Vol. 123.

**Syanozhetsky, T.G.V., Beruchashvili, G.M. and Kereselidze, N.B.** (1973):
"Hydraulics of rapid turbulent and quasilaminar (structural) mud-streams in deformed beds with abrupt slopes", Proc. 15th IAHR Congress, Istanbul, Turkey, Vol. 1.

**Tang, C.** (1981):
"Formula for the Bingham limit shear stress in sediment-water mixture", Jour. of Sediment Research, Beijing, China, No. 2.

**Takahashi, T.** (1978):
"Mechanical characteristics of debris flow", ASCE, J.Hydr. Div., Vol. 104, No. HY8.

**Takahashi, T.** (1980):
"Debris flow on prismatic open channel", ASCE, J.Hydr.Div., Vol. 106, No. HY3.

**Takahashi, T.** (1981):
"Debris flow", Ann. Rev. Fluid Mech., Vol. 13. (1987):
"High velocity flow in steep erodible channels", 22nd IAHR Congress, Lausanne, Switzerland, Techn. Session A.

**Taniguchi, Y., Takahashi, T. and Sassa, K.** (1988):
"Determination of the sheared thickness of torrent sediment deposit by debris flow", Interpraevent, Graz, Austria, Vol. 2.

**Thomas, A.D.** (1979a):
"Predicting the deposit velocity for horizontal turbulent pipe flow of slurries", Int. J. Multiphase Flow, Vol. 5.

**Thomas, A.D.** (1979b):
"The role of laminar/turbulent transition in determining the critical deposit velocity and the operating pressure gradient for long distance slurry pipelines", Proc. 6th Int. Conference on the Hydraulic Transport of Solids in Pipes, BHRA Fluid Engineering, Cranfield, Bedford, England.

**Thomas, D.G.** (1961):
"Laminar flow properties of flocculated suspensions", A.I.Ch.E. Jour., Vol. 7, No. 3.

**Thomas, D.G.** (1963a):
"Non-Newtonian suspensions, Part I: Physical properties and laminar transport characteristics", Ind. and Eng. Chemistry, Vol. 55, No. 11.

**Thomas, D.G.** (1963b):
"Non-Newtonian suspensions, Part II: Turbulent transport characteristics", Ind. and Eng. Chemistry, Vol. 55, No. 12.

**Torrance, B.Mck.** (1963):
South African Mechanical Engineer, Vol. 13, p. 89.

**Tsubaki, T., Hashimoto, H. and Suetsugi, T.** (1982):
"Grain stresses and flow properties of debris flow", Proc. Jap. Soc. of Civ. Eng., Vol. 317 (in Japanese; a condensed version appeared in Trans. of Jap. Soc. of Civ. Eng., Vol. 14).

**VanDine, D.F.** (1984):
Debris flows and debris torrents in the Southern Canadian Cordillera", Can. Geotech. Jour., Vol. 22.

**van Rijn, L.C.** (1983):
"Sediment transportation in heavy sediment-laden flows", Proc. 2nd Int. Symp. on River Sedimentation, Nanjing, China.

**Wan, Z.** (1982):
"Bed Material Movement in Hyperconcentrated Flow", Ser. Paper 31, Inst. Hydrodyn., T.U. Denmark, Lyngby.

**Wan, Z. and Song, T.** (1987):
"The effect of fine particles on vertical concentration distribution and transport rate of coarse particles", Proc. 22nd IAHR Congress, Lausanne, Switzerland, Techn. Session A.

**Wang, S. and Zhang, R.** (1987):
"A new equation of bed load transport", Proc. 22nd IAHR Congress, Lausanne, Switzerland, Techn. Session A.

**Ward, T.J.** (1986):
Discussion of "Sediment Transport Formula for Steep Channels" by G.M. Smart, ASCE, J.Hydr.Eng., Vol.112, No.10.

**Ward, T. and O'Brien, J.S.** (1981):
"Hydraulic and rheologic modelling of mud and grain flows", Proc. Erosion and sediment transport in Pacific Rim Steeplands, IAHS Publ. No. 132, Christchurch, New Zealand.

**White, W.R.** (1987):
"Engineering aspects of fluvial morphology", Proc. 22nd IAHR Congress, Lausanne, Switzerland, Techn. Session A.

**Whittaker, J, and Jäggi, M.N.R.** (1986):
"Blockschwellen", Mitt. Nr. 91 der Versuchsanstalt für Wasserbau, Hydrologie und Glaziologie, ETH Zürich.

**Willi, W.** (1965):
"Zur Frage der Sohlenerosion bei grossen Gefällen", Mitt. Nr. 68 der Versuchsanstalt für Wasserbau und Erdbau, ETH Zürich.

**Wilson,K.C.** (1966):
"Bed-load transport at high shear stress", ASCE, J.Hydr.Div., Vol. 92, No. HY6.

**Wilson, K.C.** (1984):
"Analysis of contact-load distribution and application to deposition limit in horizontal pipes", Journal of Pipelines, Vol. 4.

**Wilson, K.C.** (1986):
"Analysis of bed-load motion at high shear stress", ASCE, J.Hydr.Eng., Vol. 113, No. 1.

**Wilson, K.C. and Judge, D.G.** (1976):
"New techniques for the scale-up of pilot plant results to coal slurry pipelines", Int. Symp. on Freight Pipelines, Washington.

**Woo, H.** (1985):
"Sediment transport in hyperconcentrated flows", Ph.D. Dissertation, Colorado State Univ.

**Yalin, M.S.** (1977):
"Mechanics of sediment transport", 2nd ed., Pergamon Press, Oxford.

**Yalin, M.S. and Karahan, E.** (1979):
"Inception of sediment transport", ASCE, J.Hydr.Div., Vol. 105, No. HY11.

**Yang, C.T.** (1979):
"Unit stream power equations for total load", Jour. of Hydrology, Vol. 40, No. 1/2.

**Yang, W. and Zhao, W.** (1983):
"An experimental study of the resistance to flow with hyperconcentration in rough flumes", Proc. 2nd Int. Symp. on River Sedimentation, Nanjing, China (in Chinese with English abstract).

**Yano, K. and Daido, A.** (1965):
"Fundamental study on mud-flow", Bull. Disaster Prevention Research Institute, Kyoto Univ., Vol. 14, Part 2.

**Zhang, H., Ren, Z., Jiang, S., Sun, D. and Lu, N.** (1980):
"Settling of sediment and the resistance to flow at hyperconcentrations", Proc. Int. Symp. on River Sedimentation, Beijing, China (in Chinese with English abstract).

**Zagni, F.E. and Smith, K.V.H.** (1976):
"Channel Flow over permeable beds of graded spheres", ASCE, J.Hydr.Div., Vol. 102, No. HY2.

## LIST OF SYMBOLS

| | |
|---|---|
| $A$ | dimensional constant |
| $A'$ | constant in Mizuyama and Shimohigashi's (1985) bed load transport equation |
| $A^*$ | parameter in velocity equation for debris flow front |
| $A_{cs}$ | area of the flow cross section |
| $A_o$ | parameter in the flow resistance equation proposed by Naik (1983) |
| $A_s$ | shape factor in the flow resistance equation proposed by Naik |
| $A_1$, $A_2$, $A_3$, $A_4$, $A_5$ | constants in the flow resistance equations proposed by Torrance (1963) (pipe flow) |
| $A_6$, $A_7$, $A_8$ | constants in the flow resistance equations proposed by Yang and Zhao (1983) |
| $B$ [m] | flume width |
| $B'$ | "intrinsic" viscosity (constant) |
| $B_s$, $B_s'$ | nondimensional parameter in the logarithmic velocity law |
| $B_1$ | constant in Daido's (1983) bed load transport equation |
| $C_D$ | drag coefficient $=( 4(\sigma-\rho)gd/3\rho W^2 )$ |
| $C_o$ | grain concentration at the bed |
| $C_f$ | volume concentration of fine material |
| $C_s$ | volume concentration of solids (grains) |
| $C_{sfw}$ | weight concentration of fine particles smaller than 0.025 mm |
| $C_{v,B}$ | (calculated) volume concentration of bed load grains |
| $C_1$ | parameter that depends on depth, concentration, sediment size and boundary roughness |
| $C_*$ | maximum possible packing concentration of particles |
| Ci | clay concentration level |
| Fr | Froude number $=( V/(gh)^{1/2} )$ |
| G | dimensionless grain flow parameter $=( \sigma d^2 T/\lambda\eta^2 )$ |
| $G_B$ [$kg_{force}/s$] | sediment feeding rate |
| H [m] | measured flow depth |

| | | |
|---|---|---|
| $H_f$ | [m] | fictitious fluid flow depth =( q/V ) |
| $H_m$ | [m] | measured mixture flow depth |
| $\frac{\Delta H}{L}$ | | change in the pressure gradient (pipe flow) |
| He | | Hedstroem number =( $\rho\tau_B 16h^2/\eta_B^2$ ) |
| $J_d$ | | critical gradient at deposition, for case $\delta<d$ (pipe flow) |
| $J_d^*$ | | critical gradient at deposition, for case $\delta>\approx d$ (pipe flow) |
| K | | factor accounting for the interaction of the colliding particles (usually taken as $K=1/C_*$) |
| K′ | | constant in Wan's (1982) equ. for $\theta_c$ |
| $K_1$, $K_3$, $K_4$, $K_5$, $K_6$, $K_8$, $K_{10}$, $K_{11}$ | | dimensional constants, and |
| $K_2$, $K_7$, $K_9$ | | constants, in empirical equations for Bingham parameters |
| N | | number of observations |
| P | [N/m²] | dipersive pressure |
| Q | [L/s] | flow rate in the flume |
| R | [m] | hydraulic radius |
| $R_B$ | [m] | hydraulic radius corrected for side wall influence |
| $R_w$ | [m] | hydraulic radius belonging to sidewall subarea |
| Re | | Reynolds number =( $4VR\rho/\eta_w$ ) or ( $4Vh\rho/\eta_w$ ) |
| $Re_B$ | | Bingham Reynolds number =( $4Vh\rho/\eta_B$ ) |
| $Re_2$ | | Reynolds number defined with the effective viscosity $\mu_{e2}$ =( $4Vh\rho/\mu_{e2}$ ) |
| $Re^*$ | | particle Reynolds number =( $v^*d\rho/\eta$ ) |
| $Re_2^*$ | | particle Reynolds number defined with the effective viscosity $\mu_{e2}$ =( $v^*d\rho/\mu_{e2}$ ) |
| $Re_k^*$ | | roughness Reynolds number =( $v^*k_s\rho/\eta$ ) |
| $Re_B^*$ | | roughness Reynolds number defined with the Bingham viscosity =( $v^*k_s\rho/\eta_B$ ) |
| $Re_k^{*\prime}$ | | roughness Reynolds number as defined by Naik (1983) =( $v^*k_s\rho(1-a')/\eta_B$ ) |
| $Re_1$ | | universal Reynolds number as defined by Ansley and Smith (1967) =( $\rho W^2/[\eta_B W/d + \tau_B \pi 7/24]$ ) |
| S | [%, -] | slope (=tanβ) |
| $S_{cr}$ | [%, -] | critical slope value at initiation of motion |

| | | |
|---|---|---|
| $S_E$ | [%] | standard error |
| T | [N/m²] | shear stress acting between different grain layers |
| $T_{yy}$ | [N/m²] | total shear stress |
| $T_{yx}$ | [N/m²] | normal stress |
| U | [m/s] | mean velocity of debris flow front |
| $U_b$ | [m/s] | average velocity of a single particle |
| $U_B$ | [m/s] | average velocity of bed load grains |
| V | [m/s] | average fluid velocity |
| $V_d$ | [m/s] | critical deposit velocity, for the case $\delta<d$ (pipe flow) |
| $V_d^*$ | [m/s] | critical deposit velocity, for the case $\delta>\approx d$ (pipe flow) |
| W | [m/s] | particle settling velocity |
| W' | [N/m²] | immersed weight of grains moving over a unit bed area |
| $Y_f$ | | Yield factor $=( 2\tau_B/\rho V^2 )$ |
| $a_i$ | | constant |
| $a_j$ | | constant |
| $a_v$ | | constant |
| a' | | ratio between Bingham yield and bed shear stress $=( \tau_B/\tau_o )$ |
| $a'_c$ | | critical value of a' at laminar - turbulent transition |
| b | | constant in Bagnold's (1956) bed load transport equation |
| c | | flow resistance coefficient defined as $c=V/v*$ |
| c' | [N/m²] | cohesion |
| d | [m] | grain size |
| $d_m$ | [m] | mean grain size |
| $d_{30}$ | [m] | characteristic grain size, than which 30% of the material by weight is finer |
| $d_{50}$ | [m] | characteristic grain size, than which 50% of the material by weight is finer |
| $d_{90}$ | [m] | characteristic grain size, than which 90% of the material by weight is finer |
| $\frac{du}{dy}$ | [1/s] | grain velocity gradient perpendicular to the flow direction |

| | | |
|---|---|---|
| $\frac{dv}{dy}$ | [1/s] | fluid velocity gradient (shear rate) perpendicular to the flow direction |
| f | | Darcy-Weisbach friction factor $=( 8\tau_o/\rho V^2 )$ |
| f' | | Darcy-Weisbach friction factor, part due to grain roughness |
| f'' | | Darcy-Weisbach friction factor, part due to form drag |
| g | | acceleration due to gravity |
| h | [m] | flow depth |
| $h_r$ | [m] | (reduced) flow depth corrected for sidewall influence |
| $h_{r,f}$ | [m] | fictitious fluid flow depth in flow of grain-fluid mixture $=( q_r/V )$, corrected for sidewall influence |
| $h_{r,m}$ | [m] | mixture flow depth (including space occupied by moving grains), corrected for sidewall influence |
| $i_B$ | [N/s.m] | bed load transport rate by immersed weight of solids per unit width $=( q_B g(\sigma-\rho) )$ |
| k | | slope parameter in Mizuyama's (1977) bed load transport equation |
| k' | | slope parameter in Takahashi's (1977) bed load transport equation |
| $k_b$ | [$m^{1/3}/s$] | Strickler coefficient for bed (grain and form drag) |
| $k_r$ | [$m^{1/3}/s$] | Strickler coefficient due to grain roughness only |
| $k_w$ | [$m^{1/3}/s$] | Strickler coefficient for flume walls |
| $k_s$ | [m] | equivalent sand roughness |
| $\frac{k_s}{h}$ | | relative roughness |
| l | [m] | Prandtl's mixing length |
| m | | parameter in Yalin's (1977) bed load transport equation |
| n | | fluid or flow behaviour index (empirical constant) |
| p | [$N/m^2$] | pressure |
| $p_n$ | [$N/m^2$] | normal stress |
| q | [$m^3/s.m$] | volumetric water or fluid discharge per unit width |
| $q_{cr}$ | [$m^3/s.m$] | critical flow discharge at beginning of bed load transport |
| q* | | dimensionless water or fluid discharge $=( q/[g^{1/2}d^{3/2}] )$ |
| $q_B$ | [$m^3/s.m$] | volumetric bed load transport rate per unit width |

| | | |
|---|---|---|
| $q_t$ | [m³/s.m] | volumetric transport rate per unit width of bed load and suspended load |
| r | | correlation coefficient (between measured and calculated values) |
| s | | ratio between grain and fluid density =( $\sigma/\rho$ ) |
| t | [s] | time |
| u | [m/s] | local grain velocity |
| v | [m/s] | local fluid velocity |
| v* | [m/s] | shear velocity =( $[ghS]^{1/2}$ ) |
| $v^*_c$ | [m/s] | shear velocity at initiation of motion |
| x | [m] | coordinate in flow direction |
| y | [m] | coordinate perpendicular to the flow direction, measured upwards from the bed |
| y' | [m] | coordinate measured downwards from the flow surface |
| $y_n$ | [m] | distance from the boundary of the effective fluid thrust on the bed load grains |
| $y_1$ | [m] | rougness height |
| z | | parameter in Yalin's (1977) bed load transport equation |
| $\alpha$ | | dynamic angle of internal friction |
| $\alpha'$ | | angle of internal friction |
| $\alpha_s$ | | static angle of internal friction |
| $\alpha_1$ | | coefficient in flow resistance formula of Smart and Jäggi (1983) |
| $\beta$ | | slope angle |
| $\beta_1$ | | coefficient in flow resistance formula of Smart and Jäggi (1983) |
| $\delta$ | [m] | thickness of laminar (viscous) sublayer |
| $\eta$ | [kg/m.s] | dynamic fluid viscosity |
| $\eta_B$ | [kg/m.s] | Bingham viscosity |
| $\eta_r$ | | relative viscosity of a suspension = $\eta_s/\eta$ or $\eta_s/\eta_w$ |
| $\eta_s$ | [kg/m.s] | dynamic viscosity of a suspension |
| $\eta_w$ | [kg/m.s] | dynamic viscosity of water |

$\theta_*$ dimensionless bed shear stress parameter $=( [(\theta-\theta_c)\theta^{1/2}]^{2/3} )$

$\theta$ dimensionless bed shear stress $=( \tau_o/\rho g(s-1)d_m ) \quad =( hS/(s-1)d_m )$

$\theta_c$ critical value of $\theta$ at initiation of motion

$\theta_{cr}$ critical value of $\theta$ at initiation of motion, used in data analysis

$\theta_f$ dimensionless bed shear stress defined with the fictitious fluid depth (used in data analysis) $=( h_{r,f}S/(s-1)d_m )$

$\theta_m$ dimensionless bed shear stress in grain-fluid mixture (used in data analysis) $=( h_{r,m}S/(s-1)d_m )$

$\theta_r$ dimensionless bed shear stress, corrected for sidewall influence $=( h_rS/(s-1)d_m )$ or $=( h_{r,m}S/(s-1)d_m )$

$\theta_{sc}$ critical dimensionless bed shear stress for initiation of motion at steep slopes (modified definition)

$\theta'_c$ critical dimensionless bed shear stress for initiation of motion at steep slopes (corrected Shields parameter)

$\Theta$ dimensionless bed shear stress used by Bagnold (1956) $=( \theta/\cos\beta )$

$\Theta_c$ dimensionless critical bed shear stress used by Bagnold (1956) $=( \theta_c/\cos\beta )$

$\kappa$ von Karman constant

$\kappa'$ von Karman constant as modified by the presence of grains

$\lambda$ linear grain concentration $=( 1/[(C_*/C_s)^{1/3}-1] )$

$\mu_1$ consistency index (dimensional parameter)

$\mu_2$ cross-consistency index (dimensional parameter)

$\mu_{e2}$ [kg/s.m] effective viscosity $=( \eta_B + \tau_B h/2V )$

$\mu'_{e2}$ [kg/s.m] effective viscosity $=( \eta_B/[1-1.5(\tau_B/\tau_o)+0.5(\tau_B/\tau_o)^3] )$

$\nu$ [$m^2/s$] kinematic viscosity

$\nu'$ [$m^2/s$] eddy viscosity (also called 'turbulent' viscosity)

$\rho$ [$kg/m^3$] fluid density

$\sigma$ [$kg/m^3$] grain density

$\tau$ [$N/m^2$] shear stress in the fluid

$\tau_c$ [$N/m^2$] critical shear stress at incipient motion

$\tau_o$ [$N/m^2$] fluid shear stress at the bed $=( g\rho Sh )$

| | | |
|---|---|---|
| $\tau'$ | [N/m²] | total shear stress (caused by fluid and grains) |
| $\tau_B$ | [N/m²] | Bingham (yield) stress |
| $\tau_{B,c}$ | [N/m²] | critical Bingham stress at non-settling conditions |
| $\Phi_B$ | | dimensionless bed load transport rate $=( q_B/[g(s-1)d_m^3]^{1/2} )$ |
| $\Phi_t$ | | dimensionless sediment transport rate $=( q_t/[g(s-1)d_m^3]^{1/2} )$ |
| $\Phi_{*B}$ | | dimensionless bed load transport rate $=( q_B/b[g(s-1)d_m^3\cos\beta]^{1/2} )$ |
| $\Phi_{*t}$ | | dimensionless sediment transport rate $=( q_t/b[g(s-1)d_m^3\cos\beta]^{1/2} )$ |
| $\phi$ | | general function in bed load transport relationships |
| $\omega$ | [N/s.m] | stream power $=( V\tau_o ) = ( V\rho g h_{r,m} S )$ |

Leer - Vide - Empty

# APPENDIX

## I : Experimental results of clay suspension flows without sediment transport

Note: The fixed rough bed consisted of gravel particles glued to the flume bottom, with the same grain size characteristics as for the bed material used in the sediment transport tests.

Columns (1) to (7) refer to measured parameters, columns (8) to (14) give derived parameters.

a: In these tests, a velocity measurement by the salt tracer technique was not reliable (C3, C4) or not possible at all (C5); the velocity determined as $V = Q/(B \cdot H)$ was used here.

| | (1) | (2) | (3) | (4) | (5) | (6) | (7) | (8) | (9) | (10) | (11) | (12) | (13) | (14) |
|---|---|---|---|---|---|---|---|---|---|---|---|---|---|---|
| Ci | S | Q [l/s] | V [m] | H [cm] | $\tau_B$ [N/m$^2$] | $\eta_B$ [cps] | $\rho$ [g/cm$^3$] | $h_r$ [cm] | $\frac{h_r}{d90}$ | c | f | $\mu_{e2}$ [cps] | $Re_2$ [$\cdot 10^2$] | $Re^*_2$ |
| H2O | 0.05 | 10.0 | 1.20 | 4.01 | 0.00 | 1.02 | 0.998 | 3.58 | 2.98 | 9.09 | 0.0969 | 1.0 | 1685.95 | 1555.4 |
| | 0.05 | 20.0 | 1.62 | 6.02 | 0.00 | 1.02 | 0.998 | 5.01 | 4.18 | 10.31 | 0.0752 | 1.0 | 3170.77 | 1840.6 |
| | 0.05 | 40.0 | 2.13 | 9.38 | 0.00 | 1.02 | 0.998 | 6.99 | 5.83 | 11.53 | 0.0602 | 1.0 | 5843.38 | 2174.5 |
| | 0.10 | 10.0 | 1.46 | 3.19 | 0.00 | 1.02 | 0.998 | 2.92 | 2.43 | 8.61 | 0.1079 | 1.0 | 1663.87 | 1986.5 |
| | 0.10 | 20.0 | 1.95 | 5.04 | 0.00 | 1.02 | 0.998 | 4.37 | 3.64 | 9.42 | 0.0901 | 1.0 | 3341.10 | 2432.0 |
| | 0.10 | 30.0 | 2.27 | 6.44 | 0.00 | 1.02 | 0.998 | 5.37 | 4.47 | 9.90 | 0.0816 | 1.0 | 4776.74 | 2694.7 |
| | 0.15 | 10.0 | 1.63 | 2.83 | 0.00 | 1.02 | 0.998 | 2.62 | 2.18 | 8.28 | 0.1168 | 1.0 | 1666.40 | 2305.5 |
| | 0.15 | 15.0 | 1.95 | 3.63 | 0.00 | 1.02 | 0.998 | 3.28 | 2.73 | 8.86 | 0.1019 | 1.0 | 2496.10 | 2578.4 |
| | 0.15 | 30.0 | 2.63 | 5.83 | 0.00 | 1.02 | 0.998 | 4.94 | 4.12 | 9.74 | 0.0843 | 1.0 | 5080.84 | 3166.2 |
| | 0.20 | 10.0 | 1.76 | 2.58 | 0.00 | 1.02 | 0.998 | 2.41 | 2.01 | 8.11 | 0.1216 | 1.0 | 1659.17 | 2551.0 |
| | 0.20 | 20.0 | 2.35 | 4.24 | 0.00 | 1.02 | 0.998 | 3.80 | 3.17 | 8.62 | 0.1076 | 1.0 | 3499.43 | 3205.2 |
| | 0.20 | 40.0 | 3.18 | 6.29 | 0.00 | 1.02 | 0.998 | 5.26 | 4.38 | 9.92 | 0.0814 | 1.0 | 6555.33 | 3771.5 |
| C1 | 0.05 | 10.0 | 1.18 | 3.98 | 0.47 | 1.92 | 1.079 | 3.56 | 2.97 | 8.96 | 0.0997 | 9.0 | 202.47 | 190.4 |
| | 0.05 | 20.0 | 1.69 | 5.86 | 0.47 | 1.92 | 1.079 | 4.81 | 4.01 | 11.02 | 0.0659 | 8.6 | 408.37 | 231.3 |
| | 0.05 | 40.0 | 2.35 | 8.45 | 0.47 | 1.92 | 1.079 | 5.97 | 4.97 | 13.74 | 0.0424 | 7.9 | 767.35 | 280.9 |
| | 0.10 | 10.0 | 1.42 | 3.08 | 0.47 | 1.92 | 1.079 | 2.83 | 2.36 | 8.53 | 0.1099 | 6.6 | 262.89 | 326.9 |
| | 0.10 | 20.0 | 1.98 | 4.79 | 0.47 | 1.92 | 1.079 | 4.14 | 3.45 | 9.82 | 0.0829 | 6.8 | 517.82 | 381.8 |
| | 0.10 | 30.0 | 2.41 | 6.03 | 0.47 | 1.92 | 1.079 | 4.94 | 4.11 | 10.94 | 0.0669 | 6.7 | 760.98 | 422.8 |

cont.

| | (1) S | (2) Q | (3) V | (4) H | (5) $\tau_B$ | (6) $\eta_B$ | (7) $\rho$ | (8) $h_r$ | (9) $\frac{h_r}{d90}$ | (10) c | (11) f | (12) $\mu_{e2}$ | (13) $Re_2$ | (14) $Re^*_2$ |
|---|---|---|---|---|---|---|---|---|---|---|---|---|---|---|
| | 0.15 | 10.0 | 1.60 | 2.72 | 0.47 | 1.92 | 1.079 | 2.52 | 2.10 | 8.33 | 0.1154 | 5.6 | 310.96 | 444.2 |
| | 0.15 | 15.0 | 1.90 | 3.44 | 0.47 | 1.92 | 1.079 | 3.12 | 2.60 | 8.89 | 0.1013 | 5.8 | 443.75 | 480.7 |
| | 0.15 | 30.0 | 2.65 | 5.38 | 0.47 | 1.92 | 1.079 | 4.55 | 3.79 | 10.24 | 0.0763 | 6.0 | 873.87 | 562.6 |
| | 0.20 | 10.0 | 1.77 | 2.44 | 0.47 | 1.92 | 1.079 | 2.27 | 1.89 | 8.40 | 0.1134 | 4.9 | 352.98 | 554.5 |
| | 0.20 | 20.0 | 2.39 | 3.78 | 0.47 | 1.92 | 1.079 | 3.38 | 2.81 | 9.28 | 0.0928 | 5.2 | 664.73 | 636.0 |
| | 0.20 | 40.0 | 3.36 | 5.90 | 0.47 | 1.92 | 1.079 | 4.85 | 4.04 | 10.89 | 0.0675 | 5.3 | 1323.62 | 751.7 |
| C2 | 0.05 | 10.0 | 1.15 | 3.99 | 2.92 | 3.62 | 1.165 | 3.59 | 2.99 | 8.65 | 0.1069 | 49.3 | 38.97 | 37.6 |
| | 0.05 | 20.0 | 1.64 | 5.87 | 2.92 | 3.62 | 1.165 | 4.86 | 4.05 | 10.65 | 0.0705 | 46.8 | 79.68 | 46.2 |
| | 0.05 | 40.0 | 2.18 | 9.10 | 2.92 | 3.62 | 1.165 | 6.72 | 5.60 | 11.99 | 0.0556 | 48.7 | 140.02 | 52.1 |
| | 0.10 | 10.0 | 1.19 | 3.09 | 2.51 | 3.55 | 1.163 | 2.90 | 2.41 | 7.05 | 0.1607 | 34.1 | 46.95 | 68.9 |
| | 0.10 | 20.0 | 1.97 | 4.76 | 2.51 | 3.55 | 1.163 | 4.12 | 3.44 | 9.79 | 0.0835 | 29.8 | 126.48 | 94.1 |
| | 0.10 | 30.0 | 2.42 | 6.02 | 2.51 | 3.55 | 1.163 | 4.92 | 4.10 | 11.00 | 0.0661 | 29.1 | 190.28 | 105.4 |
| | 0.15 | 10.0 | 1.54 | 2.70 | 2.92 | 3.62 | 1.165 | 2.52 | 2.10 | 7.99 | 0.1254 | 27.5 | 65.48 | 97.7 |
| | 0.15 | 15.0 | 1.87 | 3.42 | 2.92 | 3.62 | 1.165 | 3.11 | 2.59 | 8.76 | 0.1044 | 27.8 | 97.31 | 107.3 |
| | 0.15 | 30.0 | 2.61 | 5.36 | 2.92 | 3.62 | 1.165 | 4.55 | 3.79 | 10.06 | 0.0790 | 29.1 | 189.69 | 124.2 |
| | 0.20 | 10.0 | 1.69 | 2.36 | 2.92 | 3.62 | 1.165 | 2.21 | 1.84 | 8.13 | 0.1210 | 22.7 | 76.88 | 128.4 |
| | 0.20 | 20.0 | 2.38 | 3.68 | 2.92 | 3.62 | 1.165 | 3.29 | 2.74 | 9.35 | 0.0914 | 23.8 | 152.95 | 149.0 |
| | 0.20 | 40.0 | 3.24 | 5.82 | 2.92 | 3.62 | 1.165 | 4.84 | 4.03 | 10.53 | 0.0722 | 25.4 | 288.02 | 169.6 |

| | (1) S | (2) Q | (3) V | (4) H | (5) $\tau_B$ | (6) $\eta_B$ | (7) $\rho$ | (8) $h_r$ | (9) $\frac{h_r}{d90}$ | (10) c | (11) f | (12) $\mu_{e2}$ | (13) $Re_2$ | (14) $Re^*_2$ |
|---|---|---|---|---|---|---|---|---|---|---|---|---|---|---|
| C3 | 0.05 | 10.0[a] | 1.22 | 3.59 | 8.65 | 6.70 | 1.250 | 3.20 | 2.66 | 9.71 | 0.0848 | 136.3 | 14.27 | 13.8 |
| | 0.05 | 20.0[a] | 1.66 | 5.90 | 8.65 | 6.70 | 1.250 | 4.87 | 4.06 | 10.77 | 0.0690 | 134.9 | 30.01 | 17.2 |
| | 0.05 | 40.0[a] | 2.23 | 8.89 | 8.65 | 6.70 | 1.250 | 6.47 | 5.39 | 12.52 | 0.0510 | 132.6 | 54.45 | 20.2 |
| | 0.10 | 10.0 | 1.43 | 3.09 | 6.60 | 5.46 | 1.227 | 2.83 | 2.36 | 8.58 | 0.1086 | 79.7 | 24.97 | 30.8 |
| | 0.10 | 20.0 | 1.90 | 4.84 | 6.60 | 5.46 | 1.227 | 4.22 | 3.52 | 9.34 | 0.0917 | 82.3 | 47.90 | 36.4 |
| | 0.10 | 30.0 | 2.30 | 6.00 | 6.60 | 5.46 | 1.227 | 4.99 | 4.16 | 10.37 | 0.0743 | 82.1 | 68.45 | 39.7 |
| | 0.15 | 10.0 | 1.58 | 2.89 | 6.95 | 5.75 | 1.237 | 2.68 | 2.24 | 7.96 | 0.1263 | 69.4 | 30.27 | 42.5 |
| | 0.15 | 15.0 | 1.85 | 3.66 | 6.95 | 5.75 | 1.237 | 3.33 | 2.77 | 8.37 | 0.1142 | 74.3 | 41.07 | 44.2 |
| | 0.15 | 30.0 | 2.51 | 5.56 | 6.95 | 5.75 | 1.237 | 4.77 | 3.97 | 9.49 | 0.0888 | 76.4 | 77.63 | 51.5 |
| | 0.20 | 10.0 | 1.73 | 2.53 | 6.95 | 5.75 | 1.237 | 2.36 | 1.97 | 8.03 | 0.1241 | 61.0 | 33.18 | 52.4 |
| | 0.20 | 20.0 | 2.28 | 3.79 | 6.95 | 5.75 | 1.237 | 3.41 | 2.84 | 8.83 | 0.1027 | 67.7 | 56.99 | 56.8 |
| | 0.20 | 40.0 | 3.16 | 5.68 | 6.95 | 5.75 | 1.237 | 4.76 | 3.97 | 10.35 | 0.0747 | 63.9 | 116.44 | 70.9 |
| C4 | 0.05 | 10.0[a] | 1.18 | 4.20 | 23.60 | 20.00 | 1.324 | 3.76 | 3.13 | 8.73 | 0.1050 | 394.2 | 5.98 | 5.5 |
| | 0.05 | 20.0[a] | 1.78 | 5.58 | 23.60 | 20.00 | 1.324 | 4.50 | 3.75 | 12.01 | 0.0555 | 317.6 | 13.37 | 7.4 |
| | 0.05 | 40.0[a] | 2.41 | 8.27 | 23.60 | 20.00 | 1.324 | 5.75 | 4.79 | 14.32 | 0.0390 | 302.1 | 24.26 | 8.8 |
| | 0.10 | 10.0[a] | 1.50 | 3.31 | 23.60 | 20.00 | 1.324 | 3.01 | 2.51 | 8.74 | 0.1047 | 256.6 | 9.35 | 10.6 |
| | 0.10 | 15.0[a] | 1.87 | 4.00 | 23.60 | 20.00 | 1.324 | 3.51 | 2.92 | 10.06 | 0.0790 | 241.7 | 14.33 | 12.2 |
| | 0.10 | 30.0[a] | 2.46 | 6.06 | 23.60 | 20.00 | 1.324 | 4.92 | 4.10 | 11.21 | 0.0637 | 255.9 | 25.10 | 13.6 |

| | (1) S | (2) Q | (3) V | (4) H | (5) $\tau_B$ | (6) $\eta_B$ | (7) $\rho$ | (8) $h_r$ | (9) $\frac{h_r}{d90}$ | (10) c | (11) f | (12) $\mu_{e2}$ | (13) $Re_2$ | (14) $Re^*_2$ |
|---|---|---|---|---|---|---|---|---|---|---|---|---|---|---|
| | 0.15 | 10.0 | 1.73[a] | 2.87 | 23.60 | 20.00 | 1.324 | 2.64 | 2.20 | 8.80 | 0.1033 | 199.5 | 12.13 | 15.7 |
| | 0.15 | 15.0 | 2.00[a] | 3.73 | 23.60 | 20.00 | 1.324 | 3.35 | 2.79 | 9.01 | 0.0986 | 217.7 | 16.32 | 16.2 |
| | 0.15 | 30.0 | 2.66[a] | 5.62 | 23.60 | 20.00 | 1.324 | 4.75 | 3.96 | 10.05 | 0.0793 | 231.0 | 28.92 | 18.2 |
| | 0.20 | 10.0 | 1.82[a] | 2.74 | 23.60 | 20.00 | 1.324 | 2.55 | 2.12 | 8.12 | 0.1212 | 185.5 | 13.21 | 19.1 |
| | 0.20 | 20.0 | 2.40[a] | 4.14 | 23.60 | 20.00 | 1.324 | 3.70 | 3.08 | 8.92 | 0.1004 | 201.5 | 23.34 | 21.2 |
| | 0.20 | 40.0 | 3.36[a] | 5.92 | 23.60 | 20.00 | 1.324 | 4.87 | 4.06 | 10.88 | 0.0676 | 190.8 | 45.41 | 25.7 |
| C5 | 0.05 | 10.0 | 0.75[a] | 6.69 | 40.80 | 34.30 | 1.365 | 6.34 | 5.28 | 4.22 | 0.4482 | 1770.1 | 1.46 | 1.6 |
| | 0.05 | 15.0 | 1.14[a] | 6.53 | 40.80 | 34.30 | 1.365 | 5.88 | 4.90 | 6.74 | 0.1759 | 1081.5 | 3.40 | 2.6 |
| | 0.05 | 20.0 | 1.46[a] | 6.83 | 40.80 | 34.30 | 1.365 | 5.85 | 4.87 | 8.61 | 0.1080 | 852.7 | 5.46 | 3.3 |
| | 0.10 | 10.0 | 1.13[a] | 4.43 | 40.80 | 34.30 | 1.365 | 4.17 | 3.48 | 5.56 | 0.2588 | 791.1 | 3.24 | 4.2 |
| | 0.10 | 15.0 | 1.54[a] | 4.85 | 40.80 | 34.30 | 1.365 | 4.40 | 3.67 | 7.42 | 0.1452 | 616.3 | 6.01 | 5.5 |
| | 0.10 | 20.0 | 1.86[a] | 5.37 | 40.80 | 34.30 | 1.365 | 4.71 | 3.93 | 8.63 | 0.1075 | 552.5 | 8.64 | 6.4 |
| | 0.15 | 10.0 | 1.42[a] | 3.50 | 40.80 | 34.30 | 1.365 | 3.29 | 2.74 | 6.47 | 0.1908 | 505.2 | 5.06 | 7.1 |
| | 0.15 | 15.0 | 1.77[a] | 4.21 | 40.80 | 34.30 | 1.365 | 3.85 | 3.21 | 7.45 | 0.1442 | 477.5 | 7.82 | 8.2 |
| | 0.15 | 20.0 | 2.07[a] | 4.80 | 40.80 | 34.30 | 1.365 | 4.29 | 3.57 | 8.26 | 0.1173 | 456.0 | 10.65 | 9.0 |
| | 0.20 | 10.0 | 1.74[a] | 2.87 | 30.00 | 26.00 | 1.340 | 2.68 | 2.23 | 7.59 | 0.1389 | 257.0 | 9.72 | 14.3 |
| | 0.20 | 20.0 | 2.27[a] | 4.39 | 30.00 | 26.00 | 1.340 | 3.96 | 3.30 | 8.14 | 0.1208 | 287.7 | 16.72 | 15.6 |
| | 0.20 | 30.0 | 2.76[a] | 5.41 | 30.00 | 26.00 | 1.340 | 4.70 | 3.91 | 9.09 | 0.0968 | 281.3 | 24.69 | 17.4 |

cont.

## II : Experimental results of clay suspension flows with bed load transport

### II.1 : Case I experiments

Note: Columns (1) to (8) refer to measured parameters, columns (9) to (26) give derived parameters.

The experimental results labelled $H_2O$ were taken from Smart and Jäggi (1983).

b: No velocity was measured in this experiment; the velocity calculated by Smart and Jäggi was used here.

| Ci | (1) S | (2) Q [l/s] | (3) V [m/s] | (4) H [cm] | (5) $G_B$ [kg/s] | (6) $\tau_B$ [N/m$^2$] | (7) $\eta_B$ [cps] | (8) $\rho$ [g/cm$^3$] |
|---|---|---|---|---|---|---|---|---|
| H2O | 0.07 | 15.0 | 1.28 | 5.90 | 0.68 | 0.00 | 1.02 | 0.998 |
| | 0.07 | 25.0 | 1.55 | 8.20 | 1.42 | 0.00 | 1.02 | 0.998 |
| | 0.10 | 10.0 | 1.07 | 5.00 | 0.84 | 0.00 | 1.02 | 0.998 |
| | 0.10 | 15.0 | 1.38 | 6.30 | 1.60 | 0.00 | 1.02 | 0.998 |
| | 0.10 | 30.0 | 2.06 | 6.00 | 3.53 | 0.00 | 1.02 | 0.998 |
| | 0.15 | 10.0 | 1.18 | 4.80 | 2.30 | 0.00 | 1.02 | 0.998 |
| | 0.15 | 15.0 | 1.57 | 6.00 | 4.08 | 0.00 | 1.02 | 0.998 |
| | 0.15 | 30.0 | 2.52 | 8.00 | 9.49 | 0.00 | 1.02 | 0.998 |
| | 0.20 | 10.0 | 1.26 | 6.00 | 4.80 | 0.00 | 1.02 | 0.998 |
| | 0.20 | 15.0 | 1.74 | 6.80 | 8.84 | 0.00 | 1.02 | 0.998 |
| | 0.20 | 20.0 | 2.44 | 7.60 | 10.30 | 0.00 | 1.02 | 0.998 |
| | 0.20 | 30.0 | 2.59[b] | 8.50 | 14.91 | 0.00 | 1.02 | 0.998 |
| C1 | 0.07 | 15.0 | 1.16 | 5.19 | 0.88 | 0.67 | 2.17 | 1.092 |
| | 0.07 | 25.0 | 1.57 | 7.31 | 1.49 | 0.61 | 2.09 | 1.084 |
| | 0.10 | 10.0 | 1.11 | 4.61 | 1.49 | 0.43 | 1.93 | 1.075 |
| | 0.10 | 15.0 | 1.35 | 5.25 | 2.31 | 0.60 | 2.13 | 1.084 |
| | 0.10 | 30.0 | 2.01 | 7.69 | 4.34 | 0.63 | 2.13 | 1.087 |
| | 0.15 | 10.0 | 1.18 | 4.82 | 3.52 | 0.59 | 2.05 | 1.091 |
| | 0.15 | 15.0 | 1.52 | 6.01 | 5.29 | 0.52 | 1.93 | 1.072 |
| | 0.15 | 30.0 | 2.03 | 8.12 | 9.08 | 0.63 | 2.13 | 1.088 |
| | 0.20 | 10.0 | 1.25 | 5.62 | 7.05 | 0.59 | 2.17 | 1.086 |
| | 0.20 | 15.0 | 1.60 | 6.89 | 10.58 | 0.58 | 2.03 | 1.096 |
| | 0.20 | 20.0 | 1.90 | 7.77 | 12.88 | 0.43 | 1.93 | 1.077 |
| | 0.20 | 30.0 | 2.47 | 9.07 | 17.63 | 0.63 | 2.13 | 1.088 |

cont

| | (1) | (2) | (3) | (4) | (5) | (6) | (7) | (8) |
|---|---|---|---|---|---|---|---|---|
| | S | Q | V | H | $G_B$ | $\tau_B$ | $\eta_B$ | $\rho$ |
| | | [l/s] | [m/s] | [cm] | [kg/s] | [N/m$^2$] | [cps] | [g/cm$^3$] |
| C2 | 0.07 | 15.0 | 1.27 | 5.83 | 1.15 | 2.70 | 3.33 | 1.152 |
| | 0.07 | 25.0 | 1.46 | 7.80 | 1.97 | 2.56 | 3.22 | 1.149 |
| | 0.10 | 10.0 | 1.12 | 4.80 | 2.03 | 2.50 | 3.32 | 1.160 |
| | 0.10 | 15.0 | 1.40 | 5.96 | 3.12 | 2.77 | 3.33 | 1.153 |
| | 0.10 | 30.0 | 2.18 | 8.54 | 5.08 | 2.26 | 3.06 | 1.145 |
| | 0.15 | 10.0 | 1.18 | 4.95 | 4.75 | 2.20 | 3.16 | 1.153 |
| | 0.15 | 15.0 | 1.58 | 6.30 | 7.05 | 2.20 | 3.16 | 1.152 |
| | 0.15 | 30.0 | 2.22 | 8.52 | 10.85 | 2.41 | 3.19 | 1.147 |
| | 0.20 | 10.0 | 1.29 | 6.58 | 9.63 | 2.50 | 3.32 | 1.158 |
| | 0.20 | 15.0 | 1.83 | 7.70 | 14.37 | 2.38 | 3.22 | 1.159 |
| | 0.20 | 20.0 | 2.19 | 8.25 | 16.27 | 2.26 | 3.00 | 1.141 |
| | 0.20 | 30.0 | 2.75 | 9.79 | 20.74 | 2.26 | 3.06 | 1.145 |
| C3 | 0.07 | 15.0 | 1.21 | 5.62 | 1.49 | 8.06 | 6.27 | 1.245 |
| | 0.07 | 25.0 | 1.60 | 8.11 | 2.24 | 4.31 | 4.35 | 1.201 |
| | 0.10 | 10.0 | 1.15 | 4.50 | 2.58 | 8.07 | 6.43 | 1.243 |
| | 0.10 | 15.0 | 1.41 | 5.91 | 3.91 | 8.07 | 6.43 | 1.243 |
| | 0.10 | 30.0 | 1.93 | 8.72 | 4.95 | 7.35 | 6.00 | 1.223 |
| | 0.15 | 10.0 | 1.23 | 5.44 | 5.97 | 6.95 | 5.75 | 1.240 |
| | 0.15 | 15.0 | 1.61 | 6.70 | 9.01 | 8.14 | 6.74 | 1.241 |
| | 0.15 | 30.0 | 2.34 | 9.04 | 12.20 | 7.75 | 6.37 | 1.228 |
| | 0.20 | 10.0 | 1.58 | 7.46 | 13.56 | 8.55 | 6.10 | 1.246 |
| | 0.20 | 15.0 | 1.73 | 8.69 | 17.55 | 8.14 | 6.74 | 1.236 |
| C4 | 0.07 | 25.0 | 1.69 | 7.06 | 2.39 | 18.60 | 16.20 | 1.286 |
| | 0.10 | 30.0 | 2.08 | 8.15 | 7.18 | 17.60 | 15.70 | 1.275 |
| | 0.15 | 10.0 | 1.32 | 6.21 | 6.38 | 20.10 | 17.50 | 1.266 |
| | 0.15 | 30.0 | 2.49 | 8.53 | 13.32 | 16.20 | 14.80 | 1.257 |

| Ci | (1) S | (2) Q [l/s] | (9) $q_B$ [$\cdot 10^{-3} m^3/s$] | (10) $q_r$ [$m^3/s$] | (11) $q_{cr}$ [$m^3/s$] | (12) $S_{cr}$ | (13) (s-1) |
|---|---|---|---|---|---|---|---|
| H2O | 0.07 | 15.0 | 1.27 | 0.0676 | 0.0101 | 0.0148 | 1.680 |
| | 0.07 | 25.0 | 2.65 | 0.1093 | 0.0101 | 0.0110 | 1.680 |
| | 0.10 | 10.0 | 1.56 | 0.0471 | 0.0068 | 0.0157 | 1.680 |
| | 0.10 | 15.0 | 2.99 | 0.0681 | 0.0068 | 0.0128 | 1.680 |
| | 0.10 | 30.0 | 6.59 | 0.1249 | 0.0068 | 0.0102 | 1.680 |
| | 0.15 | 10.0 | 4.29 | 0.0474 | 0.0043 | 0.0146 | 1.680 |
| | 0.15 | 15.0 | 7.61 | 0.0684 | 0.0043 | 0.0120 | 1.680 |
| | 0.15 | 30.0 | 17.71 | 0.1210 | 0.0043 | 0.0098 | 1.680 |
| | 0.20 | 10.0 | 8.96 | 0.0469 | 0.0031 | 0.0104 | 1.680 |
| | 0.20 | 15.0 | 16.49 | 0.0672 | 0.0031 | 0.0094 | 1.680 |
| | 0.20 | 20.0 | 19.22 | 0.0795 | 0.0031 | 0.0089 | 1.680 |
| | 0.20 | 30.0 | 27.80 | 0.1233 | 0.0031 | 0.0080 | 1.680 |
| C1 | 0.07 | 15.0 | 1.63 | 0.0699 | 0.0079 | 0.0119 | 1.454 |
| | 0.07 | 25.0 | 2.77 | 0.1101 | 0.0081 | 0.0090 | 1.472 |
| | 0.10 | 10.0 | 2.77 | 0.0469 | 0.0056 | 0.0127 | 1.493 |
| | 0.10 | 15.0 | 4.29 | 0.0692 | 0.0054 | 0.0115 | 1.472 |
| | 0.10 | 30.0 | 8.06 | 0.1278 | 0.0054 | 0.0086 | 1.465 |
| | 0.15 | 10.0 | 6.55 | 0.0472 | 0.0034 | 0.0108 | 1.457 |
| | 0.15 | 15.0 | 9.82 | 0.0685 | 0.0036 | 0.0094 | 1.500 |
| | 0.15 | 30.0 | 16.86 | 0.1321 | 0.0034 | 0.0070 | 1.463 |
| | 0.20 | 10.0 | 13.09 | 0.0469 | 0.0025 | 0.0082 | 1.468 |
| | 0.20 | 15.0 | 19.62 | 0.0682 | 0.0024 | 0.0069 | 1.445 |
| | 0.20 | 20.0 | 23.90 | 0.0883 | 0.0025 | 0.0064 | 1.488 |
| | 0.20 | 30.0 | 32.70 | 0.1240 | 0.0025 | 0.0058 | 1.463 |

cont

| | (1) | (2) | (9) | (10) | (11) | (12) | (13) |
|---|---|---|---|---|---|---|---|
| | S | Q | $q_B$ | $q_r$ | $q_{cr}$ | $S_{cr}$ | (s-1) |
| | | [l/s] | [$\cdot 10^{-3} m^3/s$] | [$m^3/s$] | [$m^3/s$] | | |
| C2 | 0.07 | 15.0 | 2.13 | 0.0679 | 0.0068 | 0.0080 | 1.326 |
| | 0.07 | 25.0 | 3.66 | 0.1119 | 0.0069 | 0.0062 | 1.332 |
| | 0.10 | 10.0 | 3.77 | 0.0468 | 0.0045 | 0.0090 | 1.310 |
| | 0.10 | 15.0 | 5.79 | 0.0681 | 0.0046 | 0.0075 | 1.324 |
| | 0.10 | 30.0 | 9.43 | 0.1208 | 0.0047 | 0.0057 | 1.341 |
| | 0.15 | 10.0 | 8.80 | 0.0471 | 0.0029 | 0.0078 | 1.324 |
| | 0.15 | 15.0 | 13.09 | 0.0677 | 0.0029 | 0.0063 | 1.326 |
| | 0.15 | 30.0 | 20.14 | 0.1269 | 0.0029 | 0.0046 | 1.337 |
| | 0.20 | 10.0 | 17.88 | 0.0462 | 0.0021 | 0.0049 | 1.314 |
| | 0.20 | 15.0 | 26.70 | 0.0647 | 0.0021 | 0.0043 | 1.312 |
| | 0.20 | 20.0 | 30.20 | 0.0828 | 0.0022 | 0.0042 | 1.349 |
| | 0.20 | 30.0 | 38.50 | 0.1144 | 0.0021 | 0.0037 | 1.341 |
| C3 | 0.07 | 15.0 | 2.77 | 0.0689 | 0.0054 | 0.0067 | 1.153 |
| | 0.07 | 25.0 | 4.16 | 0.1078 | 0.0060 | 0.0057 | 1.232 |
| | 0.10 | 10.0 | 4.78 | 0.0467 | 0.0036 | 0.0079 | 1.156 |
| | 0.10 | 15.0 | 7.26 | 0.0679 | 0.0036 | 0.0062 | 1.156 |
| | 0.10 | 30.0 | 9.19 | 0.1275 | 0.0038 | 0.0046 | 1.191 |
| | 0.15 | 10.0 | 11.08 | 0.0465 | 0.0023 | 0.0058 | 1.161 |
| | 0.15 | 15.0 | 16.70 | 0.0667 | 0.0023 | 0.0049 | 1.160 |
| | 0.15 | 30.0 | 22.60 | 0.1222 | 0.0024 | 0.0039 | 1.182 |
| | 0.20 | 10.0 | 25.20 | 0.0430 | 0.0017 | 0.0038 | 1.151 |
| | 0.20 | 15.0 | 32.60 | 0.0648 | 0.0017 | 0.0033 | 1.168 |
| C4 | 0.07 | 25.0 | 4.44 | 0.1077 | 0.0049 | 0.0053 | 1.084 |
| | 0.10 | 30.0 | 13.31 | 0.1246 | 0.0034 | 0.0046 | 1.102 |
| | 0.15 | 10.0 | 11.84 | 0.0453 | 0.0022 | 0.0049 | 1.117 |
| | 0.15 | 30.0 | 24.70 | 0.1195 | 0.0022 | 0.0040 | 1.132 |

| | (1) | (2) | (14) | (15) | (16) | (17) | (18) | (19) |
|---|---|---|---|---|---|---|---|---|
| Ci | S | Q [l/s] | $\Phi_B$ | $\theta$ | $\theta_{cr}$ | Fr | $C_{v,B}$ | $U_B$ [m/s] |
| H2O | 0.07 | 15.0 | 0.290 | 0.213 | 0.045 | 1.77 | 0.044 | 0.524 |
| | 0.07 | 25.0 | 0.606 | 0.285 | 0.045 | 1.85 | 0.052 | 0.692 |
| | 0.10 | 10.0 | 0.358 | 0.268 | 0.042 | 1.57 | 0.073 | 0.451 |
| | 0.10 | 15.0 | 0.682 | 0.329 | 0.042 | 1.83 | 0.087 | 0.636 |
| | 0.10 | 30.0 | 1.506 | 0.413 | 0.042 | 2.44 | 0.098 | 1.004 |
| | 0.15 | 10.0 | 0.981 | 0.389 | 0.038 | 1.76 | 0.163 | 0.549 |
| | 0.15 | 15.0 | 1.740 | 0.475 | 0.038 | 2.12 | 0.185 | 0.767 |
| | 0.15 | 30.0 | 4.053 | 0.582 | 0.038 | 3.07 | 0.220 | 1.306 |
| | 0.20 | 10.0 | 2.047 | 0.652 | 0.034 | 1.68 | 0.294 | 0.578 |
| | 0.20 | 15.0 | 3.770 | 0.720 | 0.034 | 2.20 | 0.344 | 0.814 |
| | 0.20 | 20.0 | 4.393 | 0.766 | 0.034 | 3.00 | 0.341 | 1.139 |
| | 0.20 | 30.0 | 6.359 | 0.847 | 0.034 | 3.03 | 0.326 | 1.205 |
| C1 | 0.07 | 15.0 | 0.443 | 0.230 | 0.039 | 1.69 | 0.050 | 0.510 |
| | 0.07 | 25.0 | 0.728 | 0.304 | 0.039 | 1.98 | 0.053 | 0.708 |
| | 0.10 | 10.0 | 0.723 | 0.291 | 0.037 | 1.70 | 0.105 | 0.559 |
| | 0.10 | 15.0 | 1.126 | 0.329 | 0.038 | 1.96 | 0.108 | 0.691 |
| | 0.10 | 30.0 | 2.120 | 0.452 | 0.039 | 2.50 | 0.109 | 1.035 |
| | 0.15 | 10.0 | 1.731 | 0.474 | 0.034 | 1.75 | 0.213 | 0.603 |
| | 0.15 | 15.0 | 2.560 | 0.561 | 0.035 | 2.04 | 0.218 | 0.782 |
| | 0.15 | 30.0 | 4.450 | 0.746 | 0.035 | 2.41 | 0.202 | 1.024 |
| | 0.20 | 10.0 | 3.450 | 0.734 | 0.030 | 1.72 | 0.373 | 0.586 |
| | 0.20 | 15.0 | 5.210 | 0.898 | 0.031 | 2.01 | 0.380 | 0.752 |
| | 0.20 | 20.0 | 6.250 | 0.965 | 0.031 | 2.27 | 0.366 | 0.891 |
| | 0.20 | 30.0 | 8.630 | 1.100 | 0.032 | 2.79 | 0.360 | 1.159 |

cont

| | (1) | (2) | (14) | (15) | (16) | (17) | (18) | (19) |
|---|---|---|---|---|---|---|---|---|
| | S | Q [l/s] | $\Phi_B$ | $\theta$ | $\theta_{cr}$ | Fr | $C_{v,B}$ | $U_B$ [m/s] |
| C2 | 0.07 | 15.0 | 0.593 | 0.280 | 0.032 | 1.77 | 0.061 | 0.620 |
| | 0.07 | 25.0 | 1.014 | 0.359 | 0.032 | 1.78 | 0.062 | 0.717 |
| | 0.10 | 10.0 | 1.047 | 0.332 | 0.030 | 1.71 | 0.128 | 0.614 |
| | 0.10 | 15.0 | 1.605 | 0.399 | 0.030 | 1.95 | 0.132 | 0.784 |
| | 0.10 | 30.0 | 2.616 | 0.524 | 0.030 | 2.63 | 0.125 | 1.193 |
| | 0.15 | 10.0 | 2.442 | 0.520 | 0.027 | 1.76 | 0.257 | 0.638 |
| | 0.15 | 15.0 | 3.628 | 0.648 | 0.027 | 2.11 | 0.262 | 0.857 |
| | 0.15 | 30.0 | 5.582 | 0.841 | 0.026 | 2.59 | 0.232 | 1.167 |
| | 0.20 | 10.0 | 4.954 | 0.945 | 0.023 | 1.65 | 0.459 | 0.589 |
| | 0.20 | 15.0 | 7.395 | 1.071 | 0.023 | 2.21 | 0.478 | 0.827 |
| | 0.20 | 20.0 | 8.373 | 1.088 | 0.023 | 2.58 | 0.442 | 1.009 |
| | 0.20 | 30.0 | 10.674 | 1.246 | 0.023 | 3.04 | 0.420 | 1.278 |
| C3 | 0.07 | 15.0 | 0.821 | 0.313 | 0.030 | 1.70 | 0.071 | 0.638 |
| | 0.07 | 25.0 | 1.196 | 0.402 | 0.033 | 1.92 | 0.069 | 0.831 |
| | 0.10 | 10.0 | 1.422 | 0.366 | 0.029 | 1.79 | 0.148 | 0.676 |
| | 0.10 | 15.0 | 2.155 | 0.470 | 0.029 | 1.93 | 0.153 | 0.837 |
| | 0.10 | 30.0 | 2.690 | 0.637 | 0.029 | 2.23 | 0.119 | 1.028 |
| | 0.15 | 10.0 | 3.290 | 0.668 | 0.026 | 1.73 | 0.299 | 0.688 |
| | 0.15 | 15.0 | 4.970 | 0.803 | 0.026 | 2.07 | 0.309 | 0.902 |
| | 0.15 | 30.0 | 6.630 | 1.000 | 0.026 | 2.66 | 0.255 | 1.263 |
| | 0.20 | 10.0 | 7.480 | 1.222 | 0.023 | 1.90 | 0.596 | 0.626 |
| | 0.20 | 15.0 | 9.670 | 1.390 | 0.023 | 1.94 | 0.541 | 0.739 |
| C4 | 0.07 | 25.0 | 1.362 | 0.393 | 0.030 | 2.19 | 0.072 | 0.898 |
| | 0.10 | 30.0 | 4.053 | 0.632 | 0.029 | 2.52 | 0.152 | 1.236 |
| | 0.15 | 10.0 | 3.578 | 0.788 | 0.026 | 1.74 | 0.317 | 0.742 |
| | 0.15 | 30.0 | 7.420 | 0.971 | 0.026 | 2.93 | 0.274 | 1.365 |

| | (1) | (2) | (20) | (21) | (22) | (23) | (24) | (25) | (26) |
|---|---|---|---|---|---|---|---|---|---|
| Ci | S | Q [l/s] | $h_r$ [cm] | $\frac{h_r}{d90}$ | c | f | $\mu_{e2}$ [cps] | $Re_2$ [$\cdot 10^2$] | $Re^*_2$ |
| H2O | 0.07 | 15.0 | 5.36 | 4.43 | 6.67 | 0.1797 | 1.0 | 2690.51 | 2276.5 |
| | 0.07 | 25.0 | 7.19 | 5.94 | 6.98 | 0.1644 | 1.0 | 4370.39 | 2635.9 |
| | 0.10 | 10.0 | 4.73 | 3.91 | 4.97 | 0.3242 | 1.0 | 1984.75 | 2555.2 |
| | 0.10 | 15.0 | 5.80 | 4.79 | 5.79 | 0.2390 | 1.0 | 3138.82 | 2829.3 |
| | 0.10 | 30.0 | 7.28 | 6.02 | 7.71 | 0.1346 | 1.0 | 5881.10 | 3169.7 |
| | 0.15 | 10.0 | 4.58 | 3.79 | 4.55 | 0.3872 | 1.0 | 2119.37 | 3079.6 |
| | 0.15 | 15.0 | 5.58 | 4.61 | 5.48 | 0.2665 | 1.0 | 3435.53 | 3398.7 |
| | 0.15 | 30.0 | 6.85 | 5.66 | 7.94 | 0.1270 | 1.0 | 6769.41 | 3766.4 |
| | 0.20 | 10.0 | 5.75 | 4.75 | 3.75 | 0.5685 | 1.0 | 2841.18 | 3984.7 |
| | 0.20 | 15.0 | 6.35 | 5.25 | 4.93 | 0.3292 | 1.0 | 4332.94 | 4187.5 |
| | 0.20 | 20.0 | 6.76 | 5.59 | 6.70 | 0.1782 | 1.0 | 6468.39 | 4320.4 |
| | 0.20 | 30.0 | 7.47 | 6.17 | 6.77 | 0.1748 | 1.0 | 7587.18 | 4541.1 |
| C1 | 0.07 | 15.0 | 4.78 | 3.98 | 6.39 | 0.1958 | 16.0 | 151.13 | 148.4 |
| | 0.07 | 25.0 | 6.40 | 5.33 | 7.48 | 0.1430 | 14.5 | 299.28 | 187.5 |
| | 0.10 | 10.0 | 4.35 | 3.63 | 5.36 | 0.2781 | 10.4 | 199.84 | 257.0 |
| | 0.10 | 15.0 | 4.85 | 4.04 | 6.19 | 0.2085 | 12.9 | 220.24 | 219.9 |
| | 0.10 | 30.0 | 6.62 | 5.52 | 7.90 | 0.1281 | 12.5 | 464.36 | 266.2 |
| | 0.15 | 10.0 | 4.60 | 3.83 | 4.52 | 0.3909 | 13.6 | 174.00 | 250.9 |
| | 0.15 | 15.0 | 5.61 | 4.68 | 5.28 | 0.2874 | 11.6 | 315.71 | 319.9 |
| | 0.15 | 30.0 | 7.28 | 6.07 | 6.21 | 0.2074 | 13.4 | 480.32 | 318.7 |
| | 0.20 | 10.0 | 5.39 | 4.49 | 3.85 | 0.5397 | 14.9 | 197.14 | 285.0 |
| | 0.20 | 15.0 | 6.49 | 5.41 | 4.49 | 0.3964 | 13.8 | 331.19 | 340.8 |
| | 0.20 | 20.0 | 7.18 | 5.98 | 5.07 | 0.3109 | 10.0 | 586.72 | 483.2 |
| | 0.20 | 30.0 | 8.05 | 6.71 | 6.23 | 0.2063 | 12.4 | 700.64 | 419.3 |

cont

| | (1) | (2) | (20) | (21) | (22) | (23) | (24) | (25) | (26) |
|---|---|---|---|---|---|---|---|---|---|
| | S | Q [l/s] | $h_r$ [cm] | $\frac{h_r}{d90}$ | c | f | $\mu_{e2}$ [cps] | $Re_2$ [$\cdot 10^2$] | $Re^*_2$ |
| C2 | 0.07 | 15.0 | 5.30 | 4.42 | 6.67 | 0.1797 | 59.5 | 52.22 | 44.3 |
| | 0.07 | 25.0 | 6.83 | 5.69 | 6.72 | 0.1772 | 63.3 | 72.15 | 47.2 |
| | 0.10 | 10.0 | 4.35 | 3.63 | 5.40 | 0.2746 | 52.1 | 43.21 | 55.2 |
| | 0.10 | 15.0 | 5.29 | 4.41 | 6.15 | 0.2112 | 55.6 | 61.53 | 56.7 |
| | 0.10 | 30.0 | 7.02 | 5.85 | 8.32 | 0.1156 | 39.4 | 178.15 | 91.5 |
| | 0.15 | 10.0 | 4.59 | 3.83 | 4.54 | 0.3874 | 45.9 | 54.45 | 78.3 |
| | 0.15 | 15.0 | 5.73 | 4.78 | 5.44 | 0.2705 | 43.1 | 96.78 | 93.2 |
| | 0.15 | 30.0 | 7.49 | 6.24 | 6.69 | 0.1789 | 43.8 | 173.99 | 104.2 |
| | 0.20 | 10.0 | 6.21 | 5.18 | 3.70 | 0.5857 | 63.5 | 58.44 | 76.4 |
| | 0.20 | 15.0 | 7.03 | 5.86 | 4.94 | 0.3284 | 48.9 | 122.27 | 105.7 |
| | 0.20 | 20.0 | 7.34 | 6.12 | 5.77 | 0.2402 | 40.9 | 179.49 | 127.1 |
| | 0.20 | 30.0 | 8.35 | 6.96 | 6.80 | 0.1732 | 37.4 | 281.61 | 148.9 |
| C3 | 0.07 | 15.0 | 5.15 | 4.29 | 6.43 | 0.1932 | 177.8 | 17.45 | 15.8 |
| | 0.07 | 25.0 | 7.07 | 5.89 | 7.25 | 0.1523 | 99.8 | 54.38 | 31.8 |
| | 0.10 | 10.0 | 4.23 | 3.53 | 5.65 | 0.2510 | 154.8 | 15.62 | 19.6 |
| | 0.10 | 15.0 | 5.43 | 4.53 | 6.11 | 0.2143 | 161.8 | 23.52 | 21.3 |
| | 0.10 | 30.0 | 7.59 | 6.32 | 7.06 | 0.1606 | 150.8 | 47.41 | 26.6 |
| | 0.15 | 10.0 | 5.17 | 4.31 | 4.47 | 0.3997 | 151.3 | 20.91 | 27.1 |
| | 0.15 | 15.0 | 6.21 | 5.18 | 5.34 | 0.2810 | 163.4 | 30.42 | 27.5 |
| | 0.15 | 30.0 | 7.88 | 6.57 | 6.87 | 0.1694 | 136.9 | 66.18 | 36.7 |
| | 0.20 | 10.0 | 7.03 | 5.86 | 4.25 | 0.4437 | 196.7 | 28.09 | 28.2 |
| | 0.20 | 15.0 | 8.12 | 6.77 | 4.34 | 0.4239 | 197.3 | 35.28 | 30.0 |
| C4 | 0.07 | 25.0 | 6.08 | 5.07 | 8.28 | 0.1167 | 350.4 | 15.10 | 9.0 |
| | 0.10 | 30.0 | 6.96 | 5.80 | 7.96 | 0.1261 | 310.0 | 23.83 | 12.9 |
| | 0.15 | 10.0 | 5.87 | 4.89 | 4.49 | 0.3966 | 464.4 | 8.45 | 9.6 |
| | 0.15 | 30.0 | 7.33 | 6.11 | 7.58 | 0.1394 | 253.4 | 36.18 | 19.5 |

## II : Experimental results of clay suspension flows with bed load transport

### II.2 : Case II experiments

Note: Columns (1) to (8) refer to measured parameters, the other columns give derived parameters.

c: In these tests, a velocity measurement by the salt tracer technique was not reliable (C5); as an approximation, the velocity of the corresponding flow at the next lower concentration level (C4 or C3) was used here.

| | (1) | (2) | (3) | (4) | (5) | (6) | (7) | (8) |
|---|---|---|---|---|---|---|---|---|
| | S | Q | V | H | $G_B$ | $\tau_B$ | $\eta_B$ | $\rho$ |
| | | [l/s] | [m/s] | [cm] | [kg/s] | [N/m$^2$] | [cps] | [g/cm$^3$] |
| C4 | 0.07 | 15.0 | 1.36 | 5.83 | 1.20 | 18.60 | 16.20 | 1.287 |
| | 0.10 | 10.0 | 1.16 | 4.90 | 1.76 | 20.10 | 17.50 | 1.293 |
| | 0.10 | 15.0 | 1.43 | 6.00 | 3.35 | 16.20 | 14.80 | 1.275 |
| C5 | 0.07 | 15.0 | 1.36 [c] | 6.85 | 0.59 | 40.80 | 34.30 | 1.363 |
| | 0.10 | 10.0 | 1.16 [c] | 5.75 | 0.81 | 40.80 | 34.30 | 1.363 |
| | 0.10 | 15.0 | 1.43 [c] | 6.50 | 2.17 | 40.80 | 34.30 | 1.363 |
| | 0.15 | 10.0 | 1.32 [c] | 6.60 | 3.06 | 33.60 | 28.80 | 1.356 |
| | 0.20 | 10.0 | 1.58 [c] | 7.80 | 7.65 | 33.60 | 28.80 | 1.356 |

| Ci | (1) S | (2) Q [l/s] | (9) $q_B$ [$\cdot 10^{-3} m^3/s$] | (10) $q_r$ [$m^3/s$] | (13) (s-1) | (14) $\Phi_B$ | (15) $\theta$ |
|---|---|---|---|---|---|---|---|
| C4 | 0.07 | 15.0 | 2.22 | 0.0666 | 1.080 | 0.689 | 0.340 |
| | 0.10 | 10.0 | 3.26 | 0.0463 | 1.070 | 1.017 | 0.430 |
| | 0.10 | 15.0 | 6.22 | 0.0675 | 1.100 | 1.913 | 0.500 |
| C5 | 0.07 | 15.0 | 1.10 | 0.0690 | 0.966 | 0.361 | 0.459 |
| | 0.10 | 10.0 | 1.51 | 0.0460 | 0.966 | 0.496 | 0.561 |
| | 0.10 | 15.0 | 4.03 | 0.0695 | 0.966 | 1.323 | 0.629 |
| | 0.15 | 10.0 | 5.68 | 0.0482 | 0.976 | 1.855 | 0.987 |
| | 0.20 | 10.0 | 14.20 | 0.0484 | 0.976 | 4.637 | 1.564 |

| | (1) | (2) | (20) | (21) | (22) | (23) | (24) | (25) | (26) |
|---|---|---|---|---|---|---|---|---|---|
| Ci | S | Q [l/s] | $h_r$ [cm] | $\frac{h_r}{d90}$ | c | f | $\mu_{e2}$ [cps] | $Re_2$ | $Re^*_2$ |
| C4 | 0.07 | 15.0 | 5.24 | 4.37 | 7.18 | 0.1552 | 374.0 | 9.82 | 7.8 |
| | 0.10 | 10.0 | 4.60 | 3.83 | 5.47 | 0.2678 | 415.7 | 6.64 | 7.9 |
| | 0.10 | 15.0 | 5.50 | 4.58 | 6.15 | 0.2117 | 326.8 | 12.26 | 10.9 |
| C5 | 0.07 | 15.0 | 6.34 | 5.28 | 6.52 | 0.1883 | 985.3 | 4.77 | 3.5 |
| | 0.10 | 10.0 | 5.42 | 4.52 | 5.03 | 0.3161 | 987.5 | 3.47 | 3.8 |
| | 0.10 | 15.0 | 6.08 | 5.07 | 5.86 | 0.2333 | 901.7 | 5.26 | 4.4 |
| | 0.15 | 10.0 | 6.42 | 5.35 | 4.29 | 0.4337 | 845.9 | 5.43 | 5.9 |
| | 0.20 | 10.0 | 7.63 | 6.36 | 4.08 | 0.4797 | 840.1 | 7.78 | 7.5 |

## Curriculum vitae

Born in Zürich on October 11, 1958, I grew up in a village nearby where I visited the primary school. From the age of 12 on I went to a high school in Zürich (Literargymnasium Rämibühl), graduating with a Matura Typus B. During this time I was playing football with a local sport club.

In the following years I studied civil engineering at the Swiss Federal Institute of Technology (ETH) in Zürich, before receiving the Diploma in 1983. During the term holidays I did some practical training with consulting engineers. Outdoor sports and hiking in the mountains had meanwhile become my favourite activities in the leisure time.

Thanks to a scholarship from the ETH I spent one year in Canada at the University of New Brunswick. There I was involved in graduate studies in the field of hydrology, hydraulics and wastewater treatment.

Since October 1984 I am employed as a research engineer at the Laboratory of hydraulics, hydrology and glaciology of the ETH. My main subjects of interest are debris flows and hydraulics of mountain torrents.